Lecture Notes in Civil Engineering

Sunil Kumar
Ajay Kalamdhad
Makarand M. Ghangrekar *Editors*

Sustainability in Environmental Engineering and Science

Select Proceedings of SEES 2019

Springer

Lecture Notes in Civil Engineering

Volume 93

Lecture Notes in Civil Engineering (LNCE) publishes the latest developments in Civil Engineering - quickly, informally and in top quality. Though original research reported in proceedings and post-proceedings represents the core of LNCE, edited volumes of exceptionally high quality and interest may also be considered for publication. Volumes published in LNCE embrace all aspects and subfields of, as well as new challenges in, Civil Engineering. Topics in the series include:

- Construction and Structural Mechanics
- Building Materials
- Concrete, Steel and Timber Structures
- Geotechnical Engineering
- Earthquake Engineering
- Coastal Engineering
- Ocean and Offshore Engineering; Ships and Floating Structures
- Hydraulics, Hydrology and Water Resources Engineering
- Environmental Engineering and Sustainability
- Structural Health and Monitoring
- Surveying and Geographical Information Systems
- Indoor Environments
- Transportation and Traffic
- Risk Analysis
- Safety and Security

To submit a proposal or request further information, please contact the appropriate Springer Editor:

– Mr. Pierpaolo Riva at pierpaolo.riva@springer.com (Europe and Americas);
– Ms. Swati Meherishi at swati.meherishi@springer.com (Asia - except China, and Australia, New Zealand);
– Dr. Mengchu Huang at mengchu.huang@springer.com (China).

All books in the series now indexed by Scopus and EI Compendex database!

More information about this series at http://www.springer.com/series/15087

Sunil Kumar · Ajay Kalamdhad ·
Makarand M. Ghangrekar
Editors

Sustainability in Environmental Engineering and Science

Select Proceedings of SEES 2019

Springer

Editors
Sunil Kumar
Technology Development Centre, Council of Scientific and Industrial Research National Environmental Engineering Research Institute
Nagpur, Maharashtra, India

Ajay Kalamdhad
Department of Civil Engineering
Indian Institute of Technology Guwahati
Guwahati, Assam, India

Makarand M. Ghangrekar
Department of Civil Engineering
Indian Institute of Technology Kharagpur
Kharagpur, West Bengal, India

ISSN 2366-2557 ISSN 2366-2565 (electronic)
Lecture Notes in Civil Engineering
ISBN 978-981-15-6886-2 ISBN 978-981-15-6887-9 (eBook)
https://doi.org/10.1007/978-981-15-6887-9

This Springer imprint is published by the registered company Springer Nature Singapore Pte Ltd.
The registered company address is: 152 Beach Road, #21-01/04 Gateway East, Singapore 189721, Singapore

Convener of the International Conference:

Dr. Sushovan Sarkar (BE, ME, MBA, Ph.D.), Professor and Head, Department of Civil Engineering, Dr. Sudhir Chandra Sur Degree Engineering College (A Flagship Institute under JIS Group, An education Initiatives)

Contents

About the Editors

Dr. Sunil Kumar is a Senior Researcher with more than 20 years of experience in leading, supervising and undertaking research in the broader field of Environmental Engineering and Science with focus on Solid and Hazardous Waste Management. Dr. Kumar is heading Technology Development Centre at CSIR-National Environmental Engineering Research Institute, Nagpur, India. His contributions since inception at CSIR-NEERI in 2000 include 140 refereed journal publications, 04 books and 35 book chapters, 08 Edited volumes and numerous project reports to various governmental and private, local and International academic/research bodies. Dr. Kumar was a Visiting Researcher at University of Calgary, Canada, Hongkong Baptist University Hongkong, United Nations University Germany, etc. He has contributed immensely to the advancement of environmental engineering/ science fields in India in the region and internationally by acting as editor/ editorial member of numerous journals, Expert committee member for revision of Solid Waste Manual in India, organizing workshops/conferences and delivering invited speeches at both Indian and international venues. Dr. Kumar was awarded as Outstanding Scientist in 2011 and 2016 at CSIR-NEERI for his Scientific Excellence in the field of Research & Development in Solid Waste Management. Dr. Kumar was also awarded with the most prestigious award Alexander von Humboldt-Stiftung Jean-Paul-Str.12 D-53173 Bonn, Germany as a Senior Researcher for developing a Global Network and Excellence for more advanced research and technology innovation.

Prof. Makarand M. Ghangrekar is Head, School of Environmental Science and Engineering and PK Sinha Centre for Bioenergy and Chair Professor, Aditya Choubey Centre for Re-Water Research at Indian Institute of Technology Kharagpur. He had been visiting Scientist to Ben Gurion University, Israel and University of Newcastle upon Tyne, UK under Marie Curie fellowship by European Union. He has successfully completed multinational collaborative projects with European Countries and few projects are ongoing. He has guided 19 Ph.D. Research Scholars and more than 50 Master students' projects. He has contributed 179 research papers in journals of international repute, and contributed 39 book

chapters and more than 250 conference papers in India and abroad. He has received recognition of his research contribution by receiving Swachha Bharat Award 2017, Gandhian Young Technology Innovation awards, National Design Award, Best paper Awards by IEI, etc.

Dr. Ajay Kalamdhad is currently working as a Professor in Department of Civil Engineering, Indian Institute of Technology (IIT) Guwahati. He obtained his Bachelors, Masters and PhD in Civil and Environmental Engineering from GEC Jabalpur, VNIT Nagpur and IIT Roorkee respectively. Prior to joining IIT Guwahati in 2009, He was an Assistant Professor at VNIT Nagpur and worked in various projects at RRL, Bhopal (Now AMPRI, Bhopal) and NEERI, Nagpur. In addition to his books on solid waste management, rotary drum composting and metal speciation, Dr Kalamdhad has published more than 170 research papers in acclaimed journals and has presented his work in more than 200 national and international conferences/workshops. He is associated with Indian Public Health Engineers, India, International Solid Waste Association Italy and National Solid Waste Association of India; and serves as a reviewer for 50 international journals. He is a recipient of ISTE- GSITS national award for best research by young teachers of engineering colleges for the year 2012 and IEI Young Engineers Award 2011-2012 in Environmental Engineering discipline from Institute of Engineers India.

Design and Simulation of Vertical Handover Algorithm for Intelligent Transport System Using Analytic Hierarchy Process

Kankan Ghosh and Rabi Adhikary

1 Introduction

The concept of vertical handover was proposed with the development of various wireless technologies, with the simultaneous positioning of UMTS, GPRS, and GSM as cellular networks and their network implementations, including WiMAX, Wi-Fi [1]. Mobile station capable of handling several technologies should be able to navigate freely from one network interface to another, enabling it to maintain its network connection and QoS required by higher level applications. The tool vertical handover is an extremely important capability for future wireless communications, where the integrated network will seek to provide a global broadband access for mobile users belonging to multiple technology groups. However, compared to horizontal handovers, signal strength metrics are sometimes inappropriate and often insufficient to properly trigger vertical handovers: as different networks characterized by different systems. The signal strength of two cells cannot be compared by their performance [2]. In a given location, multiple networks (WLAN, WCDMA or 3G, and WiMAX) may be available, and on the contrary, it may happen that the desired network, through which the vehicle is currently communicating, is not available in a particular region. So, the network needs to be fixed immediately to ensure QoS. It arranges continuity and handover of existing sessions. Vertical handoff can be divided into three stages: network discovery, handoff decision, and handoff execution [3]. The purpose of this paper is to define an efficient user-driven vertical handover process that does not require any changes to the network and protocol architecture and can be easily applied to existing Wi-Fi/WiMAX/3G systems. To this purpose,

K. Ghosh (✉) · R. Adhikary
Pailan Technical Campus, Kolkata, India
e-mail: kankanghosh04@gmail.com

R. Adhikary
e-mail: rabi.kolkata@gmail.com

S. Kumar et al. (eds.), *Sustainability in Environmental Engineering and Science*, Lecture Notes in Civil Engineering 93,
https://doi.org/10.1007/978-981-15-6887-9_1

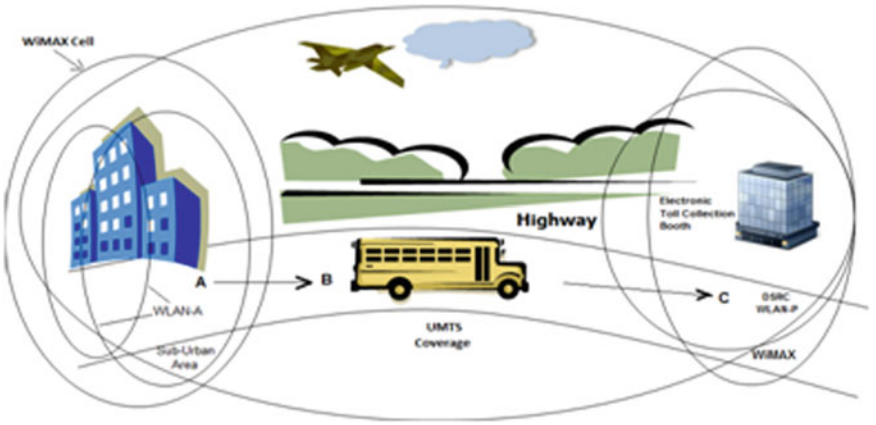

Fig. 1 Pictorial representation of VHO

we first choose the criteria for the performance of the network based on technical and customer requirements. We then propose a novel algorithm which provides automatic handover between the networks and thus increases the performance of the total telecommunication system (Fig. 1).

2 Analytic Hierarchy Process

The analytic hierarchy process (AHP) is a procedure designed to quantify managerial judgments of the relative importance of each of several conflicting criteria used in the decision-making process [4]. The pair-wise comparison on 'n' criteria can be summarized in an ($n \times n$) evaluation matrix 'A' in which every element 'a_{ij}' (where $i, j = 1, 2, \ldots, n$) is the weight of the criteria, as shown:

$$A = \begin{bmatrix} a_{11} & a_{12} & \cdots & \cdots & a_{1n} \\ a_{21} & a_{22} & \cdots & \cdots & a_{2n} \\ \vdots & & \cdots & a_{33} & \cdots \vdots \\ \vdots & \vdots & \vdots & \ddots & \vdots \\ a_{n1} & \cdots & \cdots & \cdots & a_{nn} \end{bmatrix} \quad \text{where } a_{ij} = 1, \text{ for } i = j, \text{ and } a_{ij} = 1/a_{ji} \text{ for } a_{ij} \neq 0 \tag{1}$$

The consistency of judgment needs to be verified through evaluating the consistency ratio (CR). The consistency ratio is:

$$\text{CR} = \text{CI}/\text{RI} \tag{2}$$

where consistency index of comparison matrix CI = $(\lambda_{max} - n)/(n - 1)$, and λ is the Eigen value calculated from the matrix and RI = Random inconsistency. The value of RI is constant, i.e., 0.58 for three alternatives. According to Saaty [5], if the consistency ratio is <10%, then the level of inconsistency is acceptable. It is unique in its ability to deal with intangible attributes and to monitor the consistency with which a decision maker makes his decisions. The process it makes possible to incorporate decision on intangible qualitative criteria alongside tangible quantitative criteria.

3 Design Methodology of Vertical Handover

Analytical hierarchy process or AHP starts by laying out the total hierarchy of the decision-making problem. The hierarchy process is structured from the top (the overall goal of the problem) through the intermediate levels (different criteria on which subsequent levels depend) to the bottom level (the list of alternatives).

Here, in Fig. 2, we discuss three different stages to determine the best network. Each and individual criterion in the lower level of hierarchy is compared with respect to the criteria in the upper level of hierarchy. The criteria in the same level are compared using pair-wise comparison. Figure 3 describes the hierarchy of a decision-making problem.

Once the hierarchy is established, the pair-wise comparison evaluation takes place. All the criteria on the same level of the hierarchy are compared to each of the criterion of the preceding (upper) level. Figure 3 shows that the selection of best

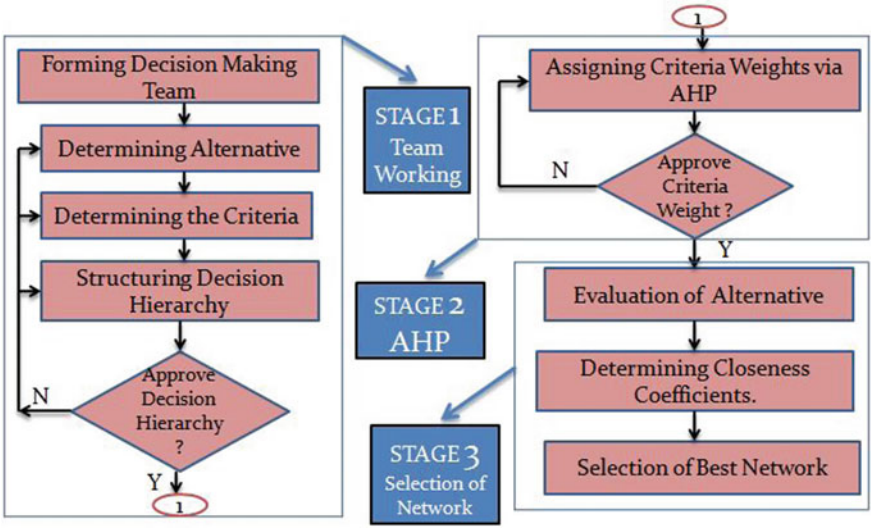

Fig. 2 Flowchart of AHP for vertical handover algorithm

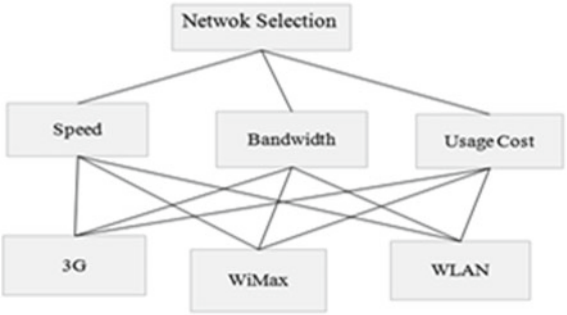

Fig. 3 Hierarchy of criteria for selection of 'best network'

network depends upon the three criteria speed, bandwidth, and data rate. Among the networks 3G, WiMAX, and WLAN, best network is selected. We calculate the closeness coefficient to rank the network. To determine the closeness coefficient, a fuzzy set $\tilde{a}$ in a universe of discourse X is characterized by a membership function $\mu_{\tilde{a}}$, a real number in the interval (0, 1). A triangular fuzzy number $\tilde{a}$ can be defined by a triplet (a_1, a_2, a_3) [6]. The mathematical forms are shown by Eq. (3):

$$\mu_{\tilde{a}} = \begin{cases} 0 & x \leq a_1 \\ \frac{x-a_1}{a_2-a_1} & a_1 < x \leq a_2 \\ \frac{a_3-x}{a_3-a_2} & a_2 < x \leq a_3 \\ 1 & x > a_3 \end{cases} \tag{3}$$

Let $\tilde{a} = (a_1, a_2, a_3)$ and $\tilde{b} = (b_1, b_2, b_3)$ be two triangular fuzzy numbers, then the vertex method is defined to calculate the distance between them, as Eq. (4):

$$d\left(\tilde{a}, \tilde{b}\right) = \sqrt{\frac{1}{3}\left[(a_1 - b_1)^2 + (a_2 - b_2)^2 + (a_3 - b_3)^2\right]} \tag{4}$$

For each criteria at the bottom, set the positive ideal solution and negative ideal solution.

$$d_i^* = \left\{v_1^*, v_2^*, \ldots, v_n^*\right\},\ d_i^- = \left\{v_1^-, v_2^-, \ldots, v_n^-\right\} \tag{5}$$

where d_i^* is the set of positive ideal solutions, v_i^* for all $i = 1, 2, \ldots, n$ is the positive ideal solution to the ith criteria at the bottom. d_i^- is the set of negative ideal solutions, v_i^- for all $i = 1, 2, \ldots, n$ is the negative ideal solution to the ith criteria at the bottom [7].

The closeness coefficient is the distance to the fuzzy positive ideal solution (d_i^*) and the fuzzy negative ideal solution (d_i^-).

Table 1 Computation of d_i^-, d_i^* and CC_i

Networks	d_i^*	d_i^-	$d_i^* + d_i^-$	$CC_i = \frac{d_i^-}{d_i^- + d_i^*}$
WLAN (N1)	1.1428	0.8204	1.9632	0.4178
WiMAX (N2)	1.0859	0.9601	2.046	0.4692
3G (N3)	1.1308	0.8244	1.9552	0.4216

The closeness coefficient (CC_i) for each network is calculated as:

$$CC_i = \frac{d_i^-}{d_i^- + d_i^*} \text{ where } i = 1, 2, \ldots, m. \tag{6}$$

So closeness coefficient is calculated using above formula and is given in Table 1.

The value of closeness coefficient (CC_i) of networks are in the order as follows: N2 > N3 > N1.

So, here the best suitable network is ***WiMAX***.

The ranking order of network is N2 > N3 > N1., i.e., WiMAX > 3G > WLAN.

4 Simulation Results for Voice Application

The model designed in simulink is used to select best network for different speed of vehicle. In this case up to speed of 27 kmph, WLAN network is selected, after 27 kmph, network is handed over from WLAN to 3G, and when the speed of vehicle becomes 60 kmph, the network is handed over to WiMAX. The model is shown in Fig. 4. Performance analysis of three networks on the basis of closeness coefficient and performance index of voice application with respect to vehicle speed. Graphical representation for the choice of networks in case of voice application with respect to closeness coefficient versus speed is shown in Fig. 5.

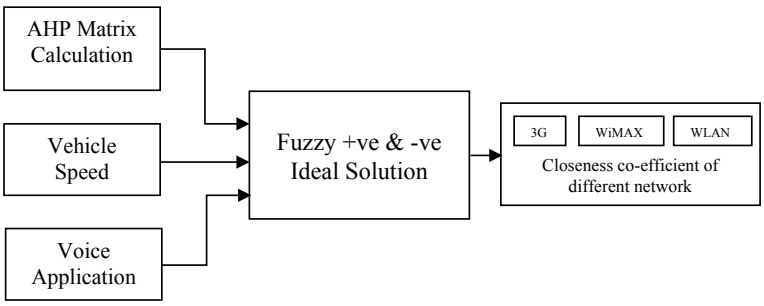

Fig. 4 Block schematic of vertical handover algorithm

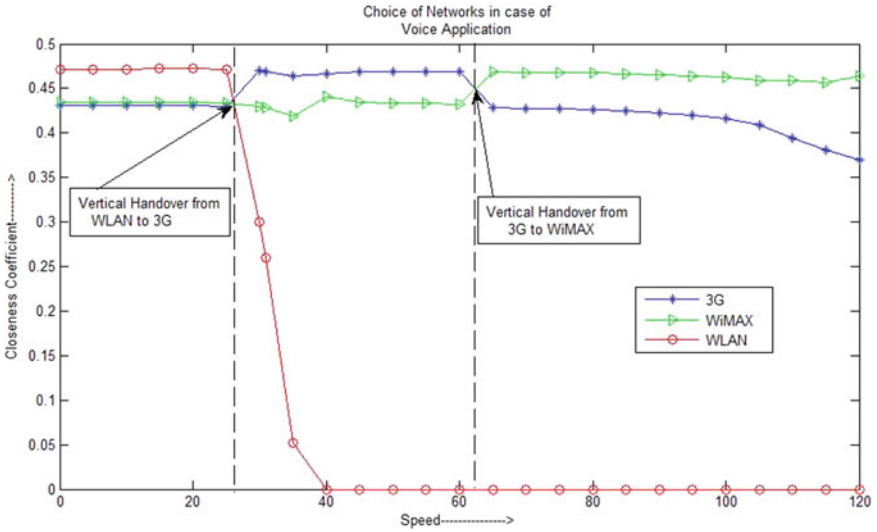

Fig. 5 Simulation graph for handover of networks in case of voice application

From the above graph, we find that weightage of WLAN is maximum at speeds of 0–27 kmph vehicular speed; while that of 3G is the lowest within that range. At speeds of about 27 kmph, the weightage of both 3G and WLAN is almost the same. After 27 kmph, weightage of WLAN decreases and then constant as WLAN cannot support voice communication above vehicular speeds of 27 kmph. Also, beyond 27 kmph, weightage of WiMAX also starts reducing with rise in vehicle speed up to 60 kmph. Handovers take place between WLAN and 3G at about speeds of 28 and 30 kmph, while handover take place between 3G and WiMAX at about speed of 60 and 63 kmph.

5 Conclusion

From the graph, we can say that overall WLAN will be selected for speeds below 27 kmph, whereas 3G is selected between speeds of 27–63 kmph and WiMAX is selected above speeds of 63 kmph. This algorithm, as designed, can be implemented in mobile phones and laptops, so that the appropriate network can be selected whenever the user wants to access the Internet (wireless), when the node is in mobile. However, a limitation of the designed algorithm is that since WiMAX cannot be accessed at vehicle speeds above 150 kmph, this system is limited for speed up to 120 kmph.

References

1. Ray A, Sarkar B, Sanyal S (2008) Outsourcing decision under utopian environment. J. Appl. Account. Res. 9(3):181–191
2. Saaty TL (1987) The analytical hierarchy process—what it is and how it is used. Math. Model. 9:161–176
3. Ray A, Sarkar B, Sanyal S (2009) The TOC-based algorithm for solving multiple constraint resources. IEEE Trans. Eng. Manage. 99:1–9
4. Daia, Z., Fracchiaa, R., Gosteaub, J., Pellatia, P., Viviera, G.: Vertical handover criteria and algorithm in IEEE 802.11 and 802.16 hybrid networks
5. Saaty TL (1986) Exploring optimization through hierarchies and ratio scales. Socio Econ. Plann. Sci. 20(6):355–360
6. Kaufmann A, Gupta MM (1991) Introduction to Fuzzy Arithmetic: Theory and Applications. Van Nostrand Reinhold, New York
7. Yu, Y., Bai, Y.: Application of Interval-Valued AHP and Fuzzy TOPSIS in the Quality Classification of the Heaters (2010)

Particulate Matter Emission Assessment and Future Outlook Through Air Dispersion Model for Sustainable Development Planning in an Inland City in Central Maharashtra, India

Sweta Kumari, Adhikari Srikanth, Ashish Patil, Anirban Middey, Aariz Ahmed, and Navneet Kumar

1 Introduction

The concern of air pollution has materialized in developing countries because of its adverse health impact [1]. Increased quantity of vehicles, decreased road capacity, and less investment in public transportation are the major contributor for extreme urban air pollution [2]. Air quality model (AQM) is a critical part of air pollutant prediction and forecasting that are required for urban air quality management. AQM such as AERMOD is well set up in developing countries where the input data are adequate. Air pollution is severely augmenting in India and other developing countries due to growth of population, urbanization, transportation, and industrialization [3]. Research study has confirmed the interim as well as enduring exposure to PM_{10} is allied with amplified motbidity and mortality impacts [4]. Various actions have been initiated previously to deal with air pollution, i.e., comprehensive inspection of pollutin industries, process development, enhanced energy efficiency, vehicle emission control technology, fuel quality improvement, and enforcement of vehicular exhaust norms. Despite of all this actions, PM_{10} has shown rising trend for megacities like Delhi, Mumbai, Kolkata, and Chennai [5]. The possible reason for PM_{10} might be due to inadequate information on sources and its contribution [6].

S. Kumari · A. Srikanth · A. Patil · A. Middey (✉) · A. Ahmed · N. Kumar
CSIR-National Environmental Engineering Research Institute, Nagpur 440020, India
e-mail: a_middey@neeri.res.in

S. Kumari · N. Kumar
Academy of Scientific and Innovative Research, HRDC Campus, Sector-19, Kamla Nehru Nagar, Gaziabad, Uttar Pradesh 201002, India

A. Srikanth
School of Renewable Energy & Environment, Jawaharlal Nehru Technological University, Kakinada, East Godavari, Andhra Pradesh 533003, India

S. Kumar et al. (eds.), *Sustainability in Environmental Engineering and Science*, Lecture Notes in Civil Engineering 93,
https://doi.org/10.1007/978-981-15-6887-9_2

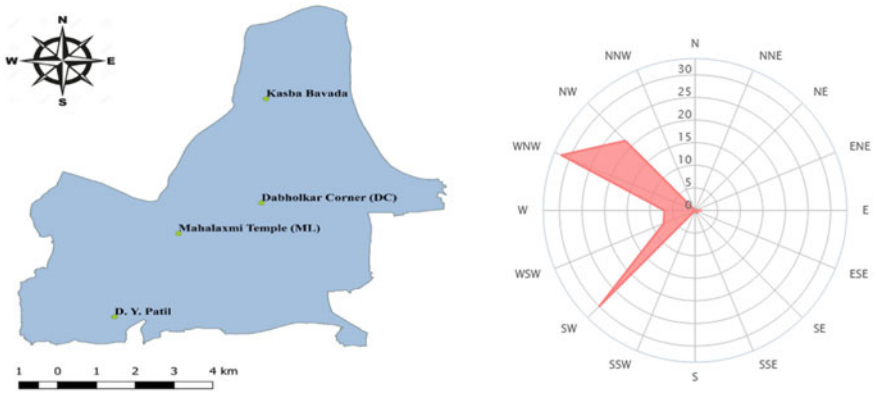

Fig. 1 Study area Kolhapur and wind rose of study area

1.1 Study Area

Kolhapur city is situated at 228 km south to the Pune city. The hottest month is April with average temperature of 29 °C (Max. temperature 35 °C and Min. temperature 24 °C). The coldest month is pace with increasing population in this city. Wind direction distribution (%) in May at Kolhapur (*Source: Windfinder.com*) is shown in the following figure. The study area map and wind rose diagram of the study are has been depicted in Fig. 1.

2 Methodology

2.1 Emission Inventory

Gross emission inventory of different sources of air pollution has been prepared for 10–15 km radial distance from center of Kolhapur city (120 km). The base year 2018 is taken for most of the source data collection. This emission inventory is used to estimate/extrapolate total emissions for the whole of the city for next 5 years. The source-wise emissions are estimated based on activity data and source-wise emission factor for particulate matter (PM_{10} and $PM_{2.5}$). These emission factors are obtained from published documents of CPCB, ARAI, and AP-42 USEPA.

Emission inventory has been prepared in terms particulate matter (PM_{10}, $PM_{2.5}$). Source categories and types of sources of air pollution in Kolhapur are presented in Table 1.

Table 1 Source categories and types of sources of air pollution

Source category	Types of sources
Area sources	• Domestic cooking • Bakeries • Crematoria • Hotels and restaurants • Open eat outs • Open burning (refuse/biomass/tire, etc., burning) • Paved and unpaved roads • Construction/demolition/alteration activities for buildings • Roads, flyovers • Waste incinerators • DG sets
Point sources	• Large-scale industries foundry, distilleries, textile, sugar, etc. • Medium-scale industries • Small-scale industries • five industrial areas
Line sources	• 2 wheelers (Scooters, motorcycles, mopeds) • 4 wheelers (Gasoline, diesel,) • Light commercial vehicles (LCVs) • Trucks (Trucks, min-trucks, multi-axle trucks) • Buses (Diesel)

2.2 Dispersion Modelling

In the present study, an air dispersion modelling using AERMOD has been performed to see the present scenario of particulate matter as well as a prediction for upcoming five years scenario. The dominant emissions of particulate matter, (both PM_{10} and $PM_{2.5}$), are ascribed to growing industrial activity in foundry, vehicular traffic, stone crushing units, and construction projects as well as commercial and infrastructure development including road construction, etc.

2.3 Ambient Air Quality Monitoring at Receptor

The air quality monitoring was performed for PM_{10} and $PM_{2.5}$ in order to validate the dispersion modeling with ground truthing. Total of four sites have been selected based on the different categories, i.e., kerb site, commercial site, residential site, and control site. Air quality monitoring was conducted for 10 days 24 h basis with Quartz and PTFE filter paper.

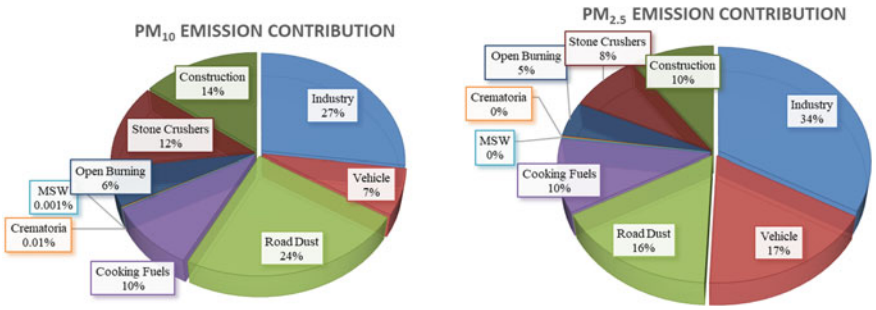

Fig. 2 Source contribution to the PM_{10} and $PM_{2.5}$ emissions

3 Result

3.1 Emission Inventory

From the source emission inventory of the city, it has been found that the major sources of PM_{10} are industry (27%), road dust (24%), construction (14%), stone crusher (12%), cooking fuels (10%), vehicle (7%), open burning (6%), crematoria (0.001%), and municipal solid waste (0.01%) in decreasing order. While the main contributing sources for $PM_{2.5}$ were found as industry (34%), vehicle (17%), road dust (16%), construction (10%), cooking fuels (10%), stone crusher (8%), open burning (5%) in decreasing order. The results obtained in this study reveal that the major source for both pollutants varies slightly in their input. Emission sources and their contribution to particulate matter pollution are shown in Fig. 2.

3.2 Disperssion Modelling

The dispersion of PM_{10} has shown the highest level concentration of 97.22 $\mu g/m^3$ which has found in core area of city. As the pollutant dispersed outwards the city, the concentration goes down with minimum concentration value of 0.97 $\mu g/m^3$. The PM_{10} disperssion has been depicted in Fig. 3, while the dispersion of $PM_{2.5}$ has shown the highest level concentration of 62.0 $\mu g/m^3$ which has found in core area of city. As the pollutant dispersed outwards the city the concentration goes down with minimum concentration value of 0.5 $\mu g/m^3$. The $PM_{2.5}$ disperssion has been depicted in Fig. 4.

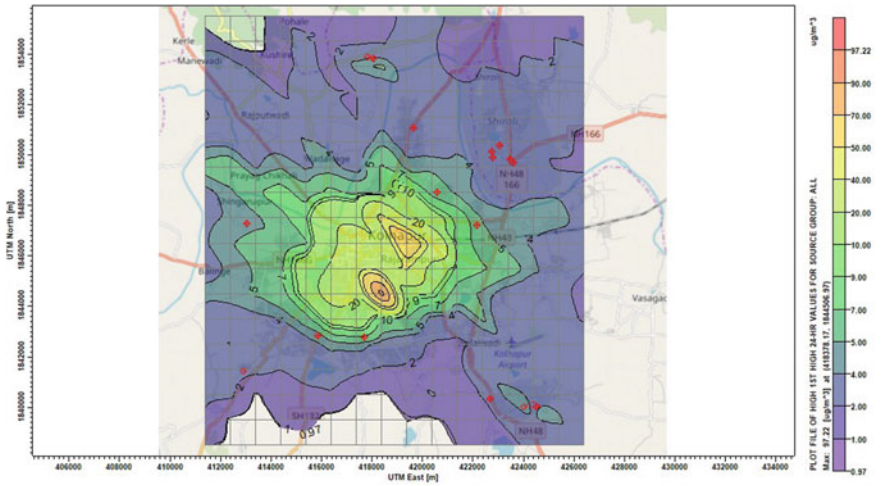

Fig. 3 Illustration of PM_{10} disperssion in Kolhapur region through dispersion modelling

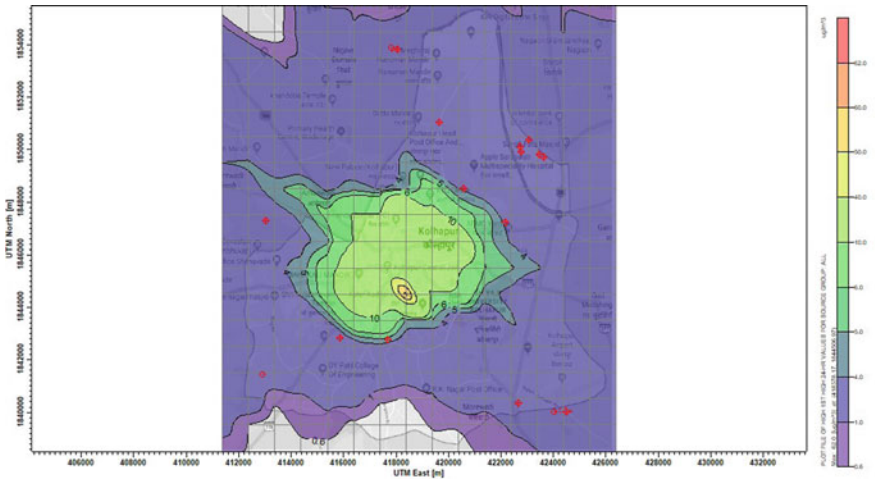

Fig. 4 Illustration of $PM_{2.5}$ disperssion in Kolhapur region through dispersion modelling

3.3 Monitoring

The monitoring of air quality has shown the highest concentration of PM_{10} at site I (kerb site) of 111 $\mu g/m^3$ followed by site II (commercial site) with concentration of 92 $\mu g/m^3$. Site III (residential) and site IV (control) have shown PM_{10} concentration of 78 $\mu g/m^3$ and 53 $\mu g/m^3$, respectively. The $PM_{2.5}$ showed maximum value of

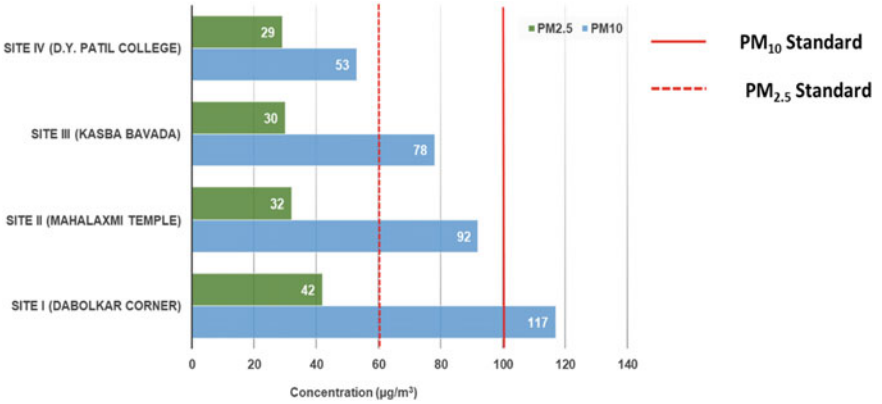

Fig. 5 PM_{10} and $PM_{2.5}$ ground-level concentration at selected monitoring sites

42 µg/m^3 at site I(kerb site) followed by site II (commercial site) with value of 32 µg/m^3. The site III (residential) and site IV (control) show the $PM_{2.5}$ value of 30 µg/m^3 and 29 µg/m^3, respectively. The bar diagram representing the value of PM_{10} $PM_{2.5}$ has been depicted in Fig. 5.

4 Discussion

4.1 Point Source Mitigation Action Plan

A range of air pollution control system needs to adopted to mitigate the emission from point source. The control technologies recommended for the industries within city impact zone, include fuel substitution, changes in production process, and pollution abatement through flue gas treatment, etc., to reduce the ambient concentrations of pollutants.

4.2 Area Sources

Busy urban areas with commercial activities, which give rise to pollution from area sources, surround city. Unpaved roads re-suspension dust is due to vehicle movements, domestic/residential burning, crematoria's, solid waste burning, etc., which form the major contributors of area sources. Paving the unpaved roads can help in reducing the road dust emission. Construction and demolition are another sources of particulate matter which can be reduced by stringent enforcement of C&D rule, 2016. Few cooking fuels are also responsible for increase in particulate matter, i.e.,

firewood, crop residue, cow dung cake, coal, and kerosene. The burning of such fuels in domestic as well as in restaurants should be monitored and reduced by distributing cleaner fuel. The open burning of garbage and litters should be strictly prohibited. Therefore, LPG and biogas facility provision is to be increased from current 65% scenario to 70% by 2019, to 75% by 2020, and to 80% by 2021 to achieve the targets proposed in strategic plan. Furthermore, the slum area, open burning from dumpsite and crematoria has also contributed in air pollution. There are sentiments involved in the activities that are carried out in crematorium. Still all crematoria should be provided with efficient pyres and chimneys with bag filters for release of emissions through stacks at appropriate height. Further, a study involving usage of NG burners in a closed furnace like electrical crematoria may be explored as substitute to existing practices. This will require participation of social organizations for increasing the awareness about need to change from the traditional methods. Concept like Green Crematoria should be explored. It has been observed that the unaccounted or mismanaged waste from SWM system, often are reported into road side/slum areas open burning cases. As city is receiving 60MT of solid waste per day, proper collection and disposal practices should be adopted on daily basis so that opening burning cases are not reported. Fast track steps for scientific SW management. Refuse of all types are burning from certain localities slum areas where auxiliary and small scale industries are located should restricted. This practice needs to be stopped by planning of dumping till sanitary landfills are made.

4.3 Line Sources

Since city has large network of roads and busy urban areas, with roads running all around its periphery, a synchronized auto traffic signal system needs to be provided at all the intersection around the monument, for better and smooth flow of vehicles with minimum halt period.

The pollution from autoexhaust is the most important causative factor in busy congested roads. Therefore, the traffic on the roads around the city should be minimal with complete ban on heavy traffic. Commercial vehicles, particularly autos, school/other buses, taxis, and buses were found quite old. Adoption of regular inspection and maintenance program for these vehicles are suggested in order to meet emission norms. Ban of old commercial vehicles may be promulgated.

Implementation of the expert committee recommendations on Auto Fuel policy (August 2002) with respect to different categories of vehicles should be ensured.

The continued growth in the future demographic profile of the automobile is inevitable. Thus, it becomes imperative to control the autoemissions at source. The best strategy is proper maintenance and tuning of the carburetor of the gasoline-powered vehicles which can ensure low CO and HC levels. PUC system needs to be upgraded with latest state-of-the-art technology.

5 Conclusion

Emission inventory of the city shows maximum source contribution of industry, road dust, stone crusher, cooking fuels, vehicles, open burning, and crematoria.

The projected ground-level concentration (GLC) using the dispersion model reveals the appalling future scenario if the present situation is not tackled with proper mitigation measures and controls. Dispersion of PM_{10} and $PM_{2.5}$ shows hotspot regions for particular meteorological condition. Site-specific mitigation measure is also possible from this study.

Ground truthing with ambient air quality measurement at receptor locations shows similarity with forecasted GLC from air dispersion model (ADM).

This study suggests different action plan management deal with air pollution with bottom-up approach. This study will be helpful in air quality management, health management and urban planning of Kolhapur city.

References

1. Nandasena YL, Wickremasinghe AR, Sathiakumar N (2010) Air pollution and health in Sri Lanka: a review of epidemiologic studies. BMC Public Health 10:300. https://doi.org/10.1186/1471-2458-10-300
2. Silva CB, Saldiva PH, Amato-Lourenço LF, Rodrigues-Silva F, Miraglia SG (2012) Evaluation of the air quality benefits of the subway system in São Paulo, Brazil. J Environ Manage 101:191–196. https://doi.org/10.1016/j.jenvman.2012.02.009
3. Aneja VP, Schlesinger WH, Erisman JW, Behera SN, Sharma M, Battye W (2012) Reactive nitrogen emissions from crop and livestock farming in India. Atmos Environ 47:92–103. ISSN 1352-2310, https://doi.org/10.1016/j.atmosenv.2011.11.026
4. Rabl A (2006) Analysis of air pollution mortality in terms of life expectancy changes: relation between time series, intervention, and cohort studies. Environ Health 5:1. https://doi.org/10.1186/1476-069X-5-1
5. CPCB (Central Pollution Control Board) (2013) Annual Report 2011–2012. http://cpcb.nic.in/upload/AnnualReports/AnnualReport_43_AR_2011-12_English.pdf
6. Gargava P, Rajagopalan V (2016) Source apportionment studies in six Indian cities—drawing broad inferences for urban PM10 reductions. Air Qual Atmos Health 9:471–481. https://doi.org/10.1007/s11869-015-0353-4

Assessment on Prevention of Groundwater Contamination

Aishik Sett, Tuhin Nayak, and Madhusmita Mishra

1 Introduction

Groundwater is the water present below the surface of the Earth in soil pore spaces. It contains soil humidity, frozen soil, immovable water in very low permeability bedrock. Groundwater may provide lubrication which helps in the movement of faults. Groundwater is recharged from the surface via water cycle and can be discharged from the surface of the Earth in the form of springs. Groundwater is used for agricultural, municipal, etc., by people across the globe. Hydrogeology defines the study of the distribution and movement of groundwater.

Groundwater pollution (also called groundwater contamination) occurs when pollutants are released to the ground and seeps deep into groundwater. This occurs naturally for the presence of a minor and unwanted constituent, contaminant, or impurity in the groundwater. The causes of groundwater pollution include

- Naturally-occurring
- On-site sanitation systems
- Sewage and sewage sludge
- Fertilizers and pesticides
- Commercial and industrial leaks.

The different methods that can be used to prevent groundwater contamination are:

A. Sett (✉) · T. Nayak · M. Mishra
Dr. Sudhir Chandra Sur Degree Engineering College, 540 Dumdum Road, Kolkata 700074, India
e-mail: aishiksett@gmail.com

T. Nayak
e-mail: nayaktuhin@gmail.com

M. Mishra
e-mail: madhusmita.mishra@dsec.ac.in

S. Kumar et al. (eds.), *Sustainability in Environmental Engineering and Science*, Lecture Notes in Civil Engineering 93,
https://doi.org/10.1007/978-981-15-6887-9_3

- Groundwater quality monitoring: Groundwater quality monitoring programs play a major role in preventing groundwater contamination. It have been implemented regularly in many countries around the world. Groundwater quality must be regularly monitored across the aquifer to determine the quality of the water. Effective groundwater monitoring should be carried out by a specific objective such as a specific contaminant of concern. It can be achieved by checking the contaminant levels and comparing to the World Health Organization (WHO) guidelines for drinking water quality.
- Locating on-site sanitation systems: The health effects of toxic chemicals arise after a long time exposure are higher as compared to health from chemicals. Thus, the quality of the groundwater at source plays an important component in controlling whether pathogens may be present in the final drinking water. Some of the conditions for safe siting are:
  - Aquifer type
  - Groundwater flow direction
  - Impermeable layers
  - Slope and surface drainage
- Educating the farmers about the proper use of pesticides and fertilizers
- Limited use of chemicals by industries.

The options for remediation of contaminated groundwater can be grouped by:

- Removal of the pollutants to prevent them from further contamination of groundwater.
- Removing the pollutants from the aquifer itself.
- Remediating the aquifer by detoxifying the contaminants at the location of the aquifer (in situ).
- Treating the groundwater at the point of its usage
- Abandoning the use of this aquifer's groundwater and finding an alternative source of water.

2 Illustrations

2.1 Groundwater: Its Contamination, Pollution, and Its Prevention in India. By Kunjlata Lal, Assistant Professor, Dept. of Education Ranchi Women's College, Ranchi, Jharkhand [5]

2.1.1 Background

The journal describes and marks the major contaminants like arsenic, fluoride, nitrate, heavy metals, phosphates from human activities such as domestic sewage, agricultural practices, and industrial effluents. In addition, landfills, septic tanks, leaky underground gas tanks, overuse of pesticides, and fertilizers have a major role in the underground contamination.

2.1.2 Proposed Methods/Recommendations

The Ministry of Environment, Forest, and Climate should make a minimum standard of quality for lakes, rivers, and underground water, the state government is encouraged to make special teams for checking these heavy metals around the states, and the quality check has been done on a regular basis to help protect the ecosystem and human health. In addition, the author proposed along with the standards if one found guilty for contamination of the water body, then they should be fined.

2.1.3 Conclusions

Since this contamination is a worldwide issue, it will be better if actions are taken from the government, and this journal proposes the same, I accept the methods of prevention by the author to some extent, but the people should be educated in an effective manner about the hazards before talking harsh actions. In addition, the author has not suggested a proper method, which could have been taken care within the society rather than pushing every task to the government.

2.2 Groundwater Arsenic Contamination in Bangladesh: Causes, Effects, and Remediation

AUTHORS

1. MD. SAFIUDDIN

DEPARTMENT OF CIVIL AND ENVIRONMENTAL ENGINEERING

FACULTY OF ENGINEERING, UNIVERSITY OF WINDSOR

WINDSOR, ONTARIO, N9B 3P4 CANADA

2. MD. MASUD KARIM

ENGCONSULT LIMITED

21 QUEEN STREET EAST, SUITE 201

BRAMPTON, ONTARIO, L6Y 2N4 CANADA [1]

2.2.1 Background

Bangladesh is currently suffering from serious arsenic contamination on their groundwater, according to statistics, 59 out of 64 districts are suffering from arsenic contamination, the 75 million people are at risk of the health hazards, and nearly 24 million are potentially exposed.

The causes of arsenic contamination

Bangladesh has a vast thickness of alluvial and deltaic sediments, which has favored the arsenic contamination. Most of the arsenic contamination occurs from younger sediments derived from the Ganges Basin. The excess use of underground water causes the creation of a zone of aeration in clayey and peaty sediments containing arseno-pyrite. Under the aerobic condition, these minerals decompose and releases arsenic that mobilizes to the subsurface water.

Remediation

The authors in the remediation proposed that the groundwater can be extracted, filtered, and distributed over long municipality operated water pipelines. In addition, the addition of proper sewage and water disposal system can help prevent the soil contamination, as later on downpour, these gets dissolved and precipitate to groundwater, thus causing contamination.

According to the author, the best way of prevention of groundwater contamination is enriching the natural river and underground aquifers, this will flush any contaminant in the groundwater, also will fill the void, creating an anaerobic condition, so that arseno-pyrite does not decompose.

2.2.2 Proposed Methods/Recommendations

The authors suggested the formation of a research group, consisting of hydrologist, geo-chemist, and public health expert and generated data for the sources and causes of the arsenic contamination; data from the research group be used to develop proper projects to prevent further groundwater contamination.

In addition, they suggested that implementation of a comprehensive water distribution system along with an efficient monitoring system provides potable water and prevents future arsenic contaminations.

Effective sewage disposal system was deployed nation-wide, with proper guidelines of disposal to those who deal with arsenic wastes.

In addition, proper annual arsenic use in agriculture is required, and the data will be used to find the long-term and short-term environmental impact of arsenic, thus limiting any overuse of the arsenic in agriculture.

2.2.3 Conclusions

The authors proposed methods based on the natural cause of arsenic contamination, the alluvial and deltaic sediments containing large quantities of it. Since, a natural cause can never be eliminated. The author suggested active remedies to purify the water on consumption, thus the area that require immediate purification, the author suggest a team of expert to examine the groundwater quality in every district. Due to human activities, arsenic contamination is beyond natural recoveries, and proposed few methods like a sewage canal dedicated for disposal of any hazardous chemicals, this canal should also be supplied to the agricultural field which generate the most groundwater contamination. I accept their method which covers the government or non-profit organization that assists to examine the water quality and also suggest the farmers to change their methods for reduction of arsenic contamination. But according to the data, the reduction of groundwater causes the arseno-pyrites to produce salts which contaminate the already low quantity groundwater,and the author has not taken any action how to reduce consumption of groundwater or to enrich the aquifers.

2.3 Groundwater Pollution and Remediation

BY ABEL O. TALABI*, TOSIN J. KAYODE

DEPARTMENT OF GEOLOGY, EKITI STATE UNIVERSITY, ADO-EKITI, NIGERIA [6]

2.3.1 Background

According to the authors, the causes of groundwater contamination can be natural or anthropogenic; they can be of a point source like landfills, waste dumps, septic tanks, underground tanks, etc. However, the majority of the contamination arises from anthropogenic/industrial ones; mining; use of fertilizers, pesticides, and insecticides; and disposal of industrial wastewater and nuclear energy waste.

Misuse of other harmful chemicals, disposal of organic, and inorganic elements. In addition, these contaminations can arise through intense evaporation in shallow aquifers, degradation of water sources in areas located in geothermal/volcanic fields, and rock oxidation.

Some pharmaceutical compounds in landfill sites had contaminated the groundwater that has been reported in the USA, in Croatia, and Denmark. Mining activities cause it to mix with water creating acidic mine water, which later contaminates the groundwater, and heavy metals are a real health hazard that can cause cancers.

2.3.2 Proposed Methods/Recommendations

The wastes responsible for groundwater contamination should be properly discharged in dedicated pipelines, and if possible, floor drains must be eliminated. This plan must have scheduled maintenance and proper use of an on-site septic tank. In addition, the plug and cover dumpster must be provided. If there are any hazardous material, then these must be stored in surface tanks before sent to the municipality. All these storage areas should be at the surface, so that they can be monitored easily if need to be removed then that can be done easily.

The authors also suggested that to prevent any spread of this waste, the drains should be properly covered as rain and floods can spread these by overflow into the aquifers. The resident and businesses must be educated and well informed about their effects on human health and environment; if any business or resident does not comply with the standard limits of contamination rate, then immediate action should be taken against them.

For agriculture, the use of insecticides and pesticides should be minimized, and manure should be used. However, if one is incapable of maintaining the waste that could lead to groundwater contamination, then the government should aid such person or business.

2.3.3 Conclusions

The approaches suggested can be achieved through own effort or through nearby authorities, the channelized discharge pipelines, in situ septic tanks/surface tanks, and these can be maintained by the farmer, or the businesses dealing with those chemicals can maintain the standard limit by their own. The author proposed the proper disposal of these hazardous substances to be in the hands of authorities, if someone requires government assist, then it should be properly given. I accept the methods proposed by the author as the cover aspects of proper maintenance largely.

2.4 Contamination of Groundwater Systems in the US and Canada by Enteric Pathogens, 1990–2013

- PAUL DYLAN HYNDS,
- M. KATE THOMAS,
- KATARINA DOROTHY MILENA PINTAR [2]

2.4.1 Background

The people of North America uses groundwater as the major source of drinking. These systems are highly exposed to the pathogens such as virus and bacteria that becomes a major factor to the contribution of waterborne disease. For the past two decades, waterborne disease has been a major threat to the people of US and CANADA.

2.4.2 Proposed Methods/Recommendations

A peer review along with robust analysis was used to investigate groundwater contamination in Canada and USA from 1990 to 2013. More than fifty-five studies met the eligibility criteria after the review was done. The different factors affecting the groundwater contamination were identified. Some of the factors that affect the groundwater contamination were study location along with study design, sample data rate, and pathogen category. Based on the sample of groundwater collected, about 15% (316/2210) of samples were positive for pathogens, with no difference observed based on system type across USA and CANADA. The research helps us to identify that knowledge gaps exist, in exposure assessment for attributing disease to groundwater supplies along with lack of consistency in risk factor reporting (local hydrogeology, well type, well use, etc.).

2.4.3 Conclusions

This review explains how groundwater study design and location are critical for subsequent data interpretation and use. The existence of awareness gaps on viral, bacterial, and protozoan pathogen occurrence in Canadian and the US groundwater systems, as well as requirement of standardized approaches for reporting study design and results. The fecal indicators are tested as a surrogate for health risk assessments; caution is advised in their widespread use. The analysis is useful during alleged waterborne outbreaks linked with a groundwater supply to identify the likely etiological agent and potential transport pathway.

2.5 Drastic Approach to Controlling Groundwater Pollution

LAWRENCE NG [3]

2.5.1 Background

In the late 1960s and early 1970s, public disgust with the nation's brown skies and befouled water provoked widespread pollution abatement campaigns and prompted the enactment of federal air and water pollution control legislation aimed at alleviating the esthetic and public health costs of pollution. The prevention of groundwater contamination has been the major concern for today's world. The contamination of groundwater will lead to the situation where there will be no groundwater available for drinking and other human activities. A stage will come when people will have to buy water in exchange of money, food, clothes, etc., which is not a desirable one.

2.5.2 Proposed Methods/Recommendations

The paper illustrates about the problem of groundwater pollution when groundwater mixes with different organic and inorganic chemicals, radioactive chemicals, etc. It has been written in the paper about the existing legal framework, the federal framework, and different acts that have been taken so far, and the efforts made by each state toward the prevention of groundwater contamination. The paper gives a brief idea about the EFFLUENT CHARGE SYSTEM which can be taken as the remedy to prevent groundwater pollution.

2.5.3 Conclusions

The methods suggested in the paper are nice and comprehensive approach for prevention of groundwater. It is not possible for the people to remember all the acts that are taken by the government in preventing groundwater contamination and perform accordingly. So, the steps that can be taken by the people to prevent groundwater contamination are:

- Reduce Chemical Use: Use of fewer chemicals in our home and yard along with proper disposal of the chemicals.
- Reduce, Reuse, and Recycle: By reducing and reusing the amount of "stuff" wherever possible. Recycle paper, plastic, cardboard, glass, aluminum, and other materials.
- Natural Alternatives: Use all natural/nontoxic household cleaners whenever possible. Materials such as lemon juice, baking soda, and vinegar make great cleaning products that are inexpensive and environmentally-friendly.

- Go Native: Use of native plants in different areas and landscape. They look great and do not need much water or fertilizer. Manage Waste: Proper disposal of potentially toxic substances like unused chemicals, pharmaceuticals, paint, motor oil, and other substances.

2.6 Possible Methods of Preventing Groundwater Contamination at Landfill Sites; Case Studies from Nepal

SUMAN PANTHEE, CENTRAL DEPARTMENT OF GEOLOGY, TRIBHUVAN UNIVERSITY, KIRTIPUR, KATHMANDU, NEPAL [4]

2.6.1 Background

There has been a significant rise in the municipal solid waste in Nepal which has led to growing of landfill sites in urban areas. Groundwater and soil contamination are the major problems that occurs in a landfill site. The main causes of the mentioned problems are leachate and design parameters. The rise in population in the third world nations has led to the contamination of groundwater and its resources.

2.6.2 Proposed Methods/Recommendations

The paper describes about the leakage and contamination problem in landfill sites that have led to groundwater and soil contamination in landfill sites such as puncture of geo-membrane and clay lining and chemical reaction between leachate and drainage material. The paper describes the possible measures that can be taken by a third world nation to prevent groundwater contamination such as water table, vegetative technique for leachate treatment, and acidity--alkalinity.

2.6.3 Conclusion

The initiatives mentioned in the paper are very basic and crucial steps for preventing groundwater from contamination. Water table is the surface where the water pressure head is equal to the atmospheric pressure (where gauge pressure = 0). It may be visualized as the "surface" of the subsurface materials that are saturated with groundwater in a particular vicinity. The water table of the landfill site should be lowered if the landfill site has shallow water table. Acidity and alkalinity of the water should be checked regularly. If the pH value of water is >8, it means the water is alkaline in nature, whereas if the pH value of water is $\leq$5, it is acidic in nature. This study is necessary as it is determining how much the water is contaminated and possible

measures can be taken to prevent the contamination of water such as by identifying the source of contamination and the chemicals mixed in the groundwater.

3 Conclusion

We have reviewed the major problems those are causing pollution in groundwater. The preventions are also narrated individually with respect to the problem. The major preventive steps should be taken by individual as well as government body.

References

1. Safiuddin, M., Karim, M.M.: Groundwater arsenic contamination in Bangladesh: causes, effects and remediation. In: Proceedings of the 1st IEB International Conference and 7th Annual Paper Meet on Civil Engineering, pp. 2–3 (2001)
2. Hynds PD, Thomas MK, Pintar KDM (2014) Contamination of groundwater systems in the US and Canada by enteric pathogens, 1990–2013: a review and pooled-analysis. PLoS ONE 9(5):e93301
3. Ng L (1989) A DRASTIC approach to controlling groundwater pollution. Yale Law J. 98(4):773–791
4. Panthee S (2008) Possible methods of preventing groundwater contamination at landfill sites; case studies from Nepal. Bull. Depart. Geol. 11:51–60
5. Lal, K.: Ground Water: It's contamination, pollution, and its prevention in India. Assistant Professor, Department of Education Ranchi Women's College, Ranchi, Jharkhand
6. Talabi, A.O., Kayode, T.J.: Groundwater Pollution and Remediation. Department of Geology, Ekiti State University, Ado-Ekiti, Nigeria

Sensitivity Study on the Classical Biofilm Model Using a Simplified Solution Method

Baibaswata Das and Sushovan Sarkar

1 Introduction

Biofilms are widely used in biological treatment of wastewater which is designated as the attached growth process. It has several advantages including easy maintenance, better stability, excellent biomass retention and resistance to toxicity and shock loading. Immobilized biofilms are better alternatives to the traditional suspended growth bioreactor systems due to its consistent and well-acclimated nature. Biofilm process has been modelled by several researchers to depict its performance, but unfortunately all of them have certain limitations towards application. In general, biofilm models correlate three distinct phenomena—substrate diffusion through liquid--biofilm interface, overall substrate removal by the biofilm and substrate utilization kinetics within the biofilm.

Williamson and McCarty [1] applied Runge--Kutta finite difference method in the approximate solution of a biofilm model contains second-order differential equation of substrate utilization. The above biofilm model had a drawback that it had not considered the term specific surface area, hydraulic retention time, etc., which are the crucial parameters in designing a biofilm reactor. Biofilm models were also derived on the basis of substrate balance of active biomass inside the biofilm to determine the total biofilm thickness [2, 3]. However, the effective biofilm thickness could not be determined using these models. It is also observed that all the biofilm models are elaborate and can be solved up to an approximate level. Consequently, the differential equation was eliminated by semi-empirical algebraic biofilm expression with a view

B. Das · S. Sarkar (✉)
Civil Engineering Department, Dr. Sudhir Chandra Sur Institute of Technology and Sports Complex, 540 Dumdum Road, Kolkata 700074, India
e-mail: sushovan.sarkar@dsec.ac.in

B. Das
e-mail: baiba.tanan@dsec.ac.in

S. Kumar et al. (eds.), *Sustainability in Environmental Engineering and Science*, Lecture Notes in Civil Engineering 93,
https://doi.org/10.1007/978-981-15-6887-9_4

to develop a single substrate dimensionless biofilm model [4]. This model was also an approximate one and only the total biofilm thickness could be calculated instead of effective part. Later an approximate solution having an explicit algebraic form was developed using the orthogonal collocation method to predict the effluent substrate concentration from a continuous stirred–tank reactor [4]. The drawback of this model was its inaccuracy in case of deep biofilm, where the substrate partially penetrates the biofilm. Further, biofilm model was developed using normalized loading curves with dimensionless variables [5]. The model was an approximate solution and as before the effective biofilm thickness could not be determined.

Saez et al. [6] proposed a pseudoanalytical solution for steady-state biofilms without considering any substrate balance in attached growth and also the specific surface area, hydraulic retention time, etc. The steady-state biofilm model for the simultaneous utilization of the dual substrates was also developed by Shaoying et al. [7]. Mudliar et al. [8] proposed another steady-state biofilm model for the evaluation of external liquid film diffusion and internal pore diffusion effects in the biofilm under continuous mode of operation. The model took into account substrate diffusion through external liquid film and biofilm. In a study of a new sewer biofilm model, simulation was performed with the pollutant transformation and biofilm variation under aerobic, anoxic and anaerobic conditions.

Past research works on biofilm model revealed that calculations under all the model are tedious, cumbersome and also approximate. Although various pseudo-analytical solutions appeared to be accurate in most cases, the findings of such solutions are not in good agreement with each other. Moreover, effective biofilm thickness cannot be measured explicitly from earlier methods of solution. Therefore, the tentative nature of biodegradation like aerobic, facultative and anaerobic cannot be ascertained from the total biofilm thickness.

Under this circumstance, a simplistic biofilm model has been developed to correlate the substrate concentration in the effluent, at the biofilm--liquid interface and at the attachment surface, substrate flux, biofilm thickness, etc. The analytical solution was mainly done by Runge--Kutta Method and accordingly two model programs were developed using FORTRAN. In order to judge the sensitivity of important variables, a set of simulations were done using those two programs. For this purpose, the relevant parameters were varied within their possible ranges and accordingly the variation profiles were plotted. Thus, the sensitivity of such important process variables is ascertained from the trend of the graphical profiles.

2 Objective

2.1 Materials and Methods

2.1.1 Model Description

The concept diagram of a typical biofilm bioreactor comprising of attached phase biomass is shown in Fig. 1.

In the above system, substrate flows through the biofilm--liquid interface and then through the biofilm as shown in Fig. 2.

Now, from the external mass transport according to Fick's fist law

$$J = \frac{D}{L} * (S_0 - S_s) \tag{1}$$

where

J = substrate flux into the biofilm (mg/cm^2/day),
D = molecular diffusion coefficient in liquid (cm^2/day),
L = thickness of effective diffusion layer (cm),
S_0, S_s = substrate concentrations in the bulk liquid and at the biofilm--liquid interface, respectively (mg/cm^3).

The steady-state substrate balance for the attached growth is

$$S_0 - S_w - aJ\theta = 0 \tag{2}$$

where

a = specific surface area of supporting media (cm^{-1}),

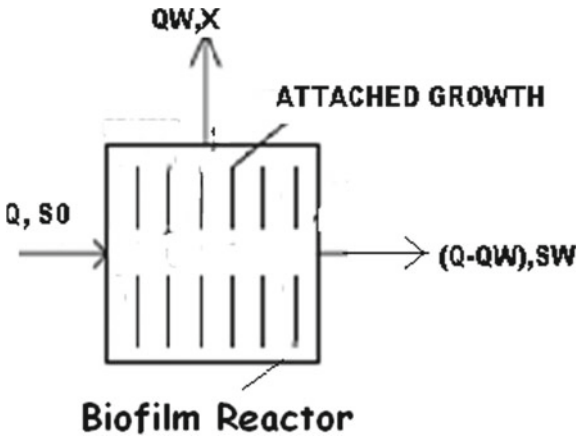

Fig. 1 Schematic diagram of a Fixed Biofilm reactor

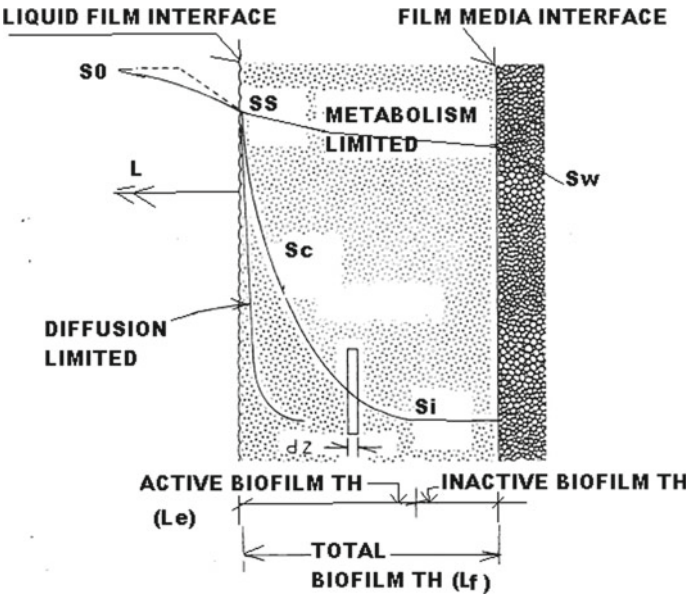

Fig. 2 Profile of substrate concentration in a Fixed Biofilm reactor

θ = empty bed hydraulic detention time (h),
S_w = effluent substrate concentration (mg/cm^3)

From Eqs. (1) and (2), $J = \frac{S_0 - S_w}{a\theta} = \frac{D}{L} * (S_0 - S_s)$

$$\text{i.e.,}\ \ S_s = S_0 - \frac{L}{D} * \left\{ \frac{S_0 - S_w}{a\theta} \right\} \tag{3}$$

Again, from the mass balance equation for substrate in the biofilm,

$$\frac{d^2 S_f}{dz^2} = \frac{k X_f S_f}{D_f \left(K + S_f\right)} \tag{4}$$

where

S_f = substrate concentration at a point in the biofilm (mg/cm^3),
k = maximum specific rate of substrate use (per day),
X_f = active biomass density within the biofilm (mg/cm^3),
D_f = molecular diffusion coefficient of the substrate in the biofilm (cm^2/day),
K = half velocity coefficient (mg/cm^3)

Referring Fig. 2, the boundary conditions for solving above second order: differential equation may be taken as,

(i) At the attachment surface (i.e. at $z = 0$) there will be no flux, i.e. $\frac{ds_{f0}}{dz} = 0$.

(ii) At the biofilm--water interface (i.e. at $z = L_e$) $J = D_f * \frac{dS_f}{dz} = \mathrm{D} * \frac{(S_0 - S_s)}{L}$

2.1.2 Methodology of Solution

Applying Runge--Kutta method, solution of Eq. (4) can be obtained as follows:

$$\frac{d^2S_f}{dz^2} = f\left(z, \frac{dS_f}{dz}\right), \quad \frac{dS_f}{dz}(z_0) = \frac{dS_{f_0}}{dz} = K1 = 0 \quad \left[S_{f0} = S_w \text{ at } z = 0\right]$$

$$L1 = f\left(z_0, \frac{ds_{f0}}{dz}\right) = \frac{d^2s_{f0}}{dz} = \frac{kX_f S_{f0}}{Df\left(K + S_{f0}\right)}$$

$\frac{dS_{f1}}{dz} = \frac{dS_{f0}}{dz} + 0.5 * L1 * h = K2$, where $h =$ step $=$ effective biofilm thickness (cm)

h is the distance between $z = 0$ (at the attachment surface) and $z = L_e$ (at the biofilm--water interface)

$$L2 = h * f\left(z_0 + \frac{h}{2}, \frac{dS_{f1}}{dz}\right) = h * \frac{d^2S_{f1}}{dz^2} = \frac{kX_f\left(S_{f0} + 0.5K1 * h\right)}{D_f\left(K + S_{f0} + 0.5K1 * h\right)}$$

$$\frac{dS_{f2}}{dz} = \frac{dS_{f0}}{dz} + 0.5 * L2 * h = K3$$

$$L3 = h * f\left(z_0 + \frac{h}{2}, \frac{dS_{f2}}{dz}\right) = h * \frac{d^2S_{f2}}{dz^2} = \frac{kX_f\left(S_{f0} + 0.5K2 * h\right)}{D_f\left(K + S_{f0} + 0.5K2 * h\right)}$$

$$\frac{dS_{f3}}{dz} = \frac{dS_{f0}}{dz} + L3 * h = K4$$

$$L4 = h * f\left(z_0 + h, \frac{dS_{f3}}{dz}\right) = h * \frac{d^2S_{f3}}{dz^2} = \frac{kX_f\left(S_{f0} + K3 * h\right)}{D_f\left(K + S_{f0} + K3 * h\right)}$$

$$\Delta Y(1) = \frac{h}{6} * (K1 + 2 * K2 + 2 * K3 + K4) \tag{5}$$

$$\Delta Y(2) = \frac{h}{6} * (L1 + 2 * L2 + 2 * L3 + L4) \tag{6}$$

where $\Delta Y(1)$ stands for increment of substrate concentration and ΔY(2) stands for $\frac{dS_f}{dz}$

The substrate concentration and the respective flux at the liquid--biofilm interface can be denoted as S_s and J, respectively.

Therefore,

$$S_s = S_w + \Delta Y(1) \tag{7}$$

$$J = D_f * \Delta Y(2) \tag{8}$$

Equation (4) can also be solved without considering the effective biofilm thickness to find out 'J' as follows:

$$J = \sqrt{2kXfDf(Ss - Sw) + K \ln\left[(K + Sw)/(K + Ss)\right]} \tag{9}$$

Again, $S_{\min} = K * \frac{b_t}{Y*k-b_t}$, where b_t = an overall specific biofilm loss rate(day^{-1}), Y = bacteria yield coefficient,

$S_{\min}$ = minimum bulk concentration of rate-limiting substrate able to support a steady-state biofilm (mg/cm^3)

Now, from the steady-state mass balance of active microorganisms in a biofilm,

$$L_f = \frac{J * Y}{X_f * b_t}, \quad \text{where } L_f = \text{total biofilm thickness (cm)} \tag{10}$$

The above model equation is useful to determine the total biofilm thickness in a biofilm model reactor system where purely attached growth is considered.

In order to calculate S_s, S_w, L_e and L_f, J using Eqs. (3), (4), (9) and (10), i.e. to solve the biofilm model reactor, two FORTRAN programs are written, for details of which the corresponding author may kindly be referred.

2.1.3 Selection of Variables for Sensitivity Study

In order to study the sensitivity of the biofilm model developed here, a reference set of proper data was chosen as per Rittmann and McCarty [2]. Each relevant input data was varied within its viable range in such a way that the reference value remains intermediate between the boundaries. Those relevant input parameters were taken as initial substrate concentration (S_0), hydraulic retention time (HRT), specific surface area (a) and attached phase biomass density (X_f). As a result, the process output parameters were substrate concentration in the effluent (S_w) and at liquid--biofilm interface (S_s), substrate flux (J), total and effective biofilm thickness (L_f and L_e).

2.1.4 Sensitivity Study with the Biofilm Model

In order to study the sensitivity of the biofilm model using the solution method developed here, the representative parameters like the specific surface area (a) was varied in the range of (0.45–0.90) cm^{-1} @ 0.05 cm^{-1} interval, the hydraulic retention time (HRT) was varied in the range of (0.2–1.0) h at an interval of 0.1 h, the influent substrate concentration (S_0, COD) was varied in the range of (0.4–1.3) mg/cc

@0.1 mg/cc interval, the biomass density (X_f) was also varied in the range of (2.5–25) mg/cc @ 2.5 gm/cc interval. A reference input data set (Ritmann and Mc Carty 1980) was used in the entire sensitivity study as follows,

$S_0 = 0.43$ mg/cc, $\theta = 1$ h, $a = 0.9$ cm^{-1}, $X_f = 25$ mg/cc

In addition, a set of reference kinetic coefficients (Rittmann and McCarty) was also taken into consideration as follows:

K = 10 day^{-1}, k = 0.01 mg/COD/cc, Y = 0.5 mg/mg, b_t = 0.41 day^{-1}, D = 0.75 cm^2/day, D_f = 1.25 cm^2/day.

2.2 Results and Discussion

2.2.1 Sensitivity Analysis

When the influent substrate concentration (S_0, COD) was varied, keeping other input variables constant the relevant output parameters were determined using the above-mentioned computer program and shown in Table 1.

The bold face value of 'S_0', i.e. 0.43 mg/cc is considered as a reference value intermediate between 0.4 and 1.3 mg/cc in the sensitivity study. The sensitivity analysis depicts that a minimum input organic substrate concentration is required for maintaining a desired amount of biomass density, which is 0.4 mg/cc under the present case. It is also observed that the values of substrate concentration both at

Table 1 Sensitivity study by varying initial substrate concentration (S_0)

Run no.	S_0 (mg/cc)	S_s (mg/cc)	S_w (mg/cc)	J (mg/cm^2/day)	L_e (cm)	L_f (cm)	Reference set of input parameters
1	0.4	0.334	0.003	10.58	0.066	0.516	k = 10 day^{-1}, θ = 1 h, Y = 0.5, a = 0.9 cm^{-1}, K = 0.01 mg/cm^3, b_t = 0.41 day^{-1}, D = 1.25 cm^2/day, D_f = 0.75 cm^2/day, L = 0.0078 cm, X_f = 25 mg/cc
2	**0.43**	0.362	0.0215	10.89	0.051	0.531	
3	0.5	0.43	0.0796	11.2	0.048	0.547	
4	0.6	0.529	0.173	11.38	0.047	0.555	
5	0.7	0.628	0.269	11.47	0.047	0.559	
6	0.8	0.728	0.368	11.52	0.047	0.562	
7	0.9	0.828	0.466	11.55	0.047	0.564	
8	1	0.928	0.565	11.58	0.047	0.565	
9	1.1	1.027	0.665	11.6	0.047	0.566	
10	1.2	1.127	0.764	11.61	0.047	0.567	
11	1.3	1.227	0.863	11.63	0.047	0.5673	

Table 2 Sensitivity study by varying specific surface area (a)

Run no.	a cm^{-1}	S_s (mg/cc)	S_w (mg/cc)	J (mg/cm^2/day)	L_e (cm)	L_f (cm)	Reference set of input parameters
1	0.45	0.401	0.344	4.58	0.0187	0.224	S_0 = 0.43 mg/cc, k = 10 day^{-1}, θ = 1 h, Y = 0.5, K = 0.01 mg/cm^3, b_t = 0.41 day^{-1}, D = 1.25 cm^2/day, D_f = 0.75 cm^2/day, L = 0.0078 cm, X_f = 25 mg/cc
2	0.5	0.396	0.318	5.34	0.0219	0.26	
3	0.55	0.392	0.29	6.09	0.025	0.297	
4	0.6	0.387	0.259	6.84	0.028	0.334	
5	0.65	0.383	0.225	7.58	0.031	0.369	
6	0.7	0.378	0.187	8.31	0.034	0.405	
7	0.75	0.374	0.148	9.02	0.0378	0.44	
8	0.8	0.369	0.106	9.72	0.041	0.474	
9	0.85	0.365	0.0628	10.36	0.045	0.506	
10	**0.9**	0.362	0.0215	10.89	0.0515	0.53	

attached surface (i.e. S_w) and at biofilm--liquid interface (i.e. S_s), substrate flux (J) and both the effective and total biofilm thickness increase with the increase in the values of initial substrate concentration S_0. However, all the output parameters except S_w appear to attain their limiting values, when S_0 is increasing.

In case of the specific surface area 'a' (in cm^{-1}) was varied, keeping other input variables constant the relevant output parameters were estimated using the computer program as stated earlier and shown in Table 2.

The bold face value of 'a', i.e. 0.9 cm^{-1} is considered as a reference value lying in the range from 0.45 cm^{-1} to 0.9 cm^{-1} in the sensitivity study. The sensitivity analysis reveals that the values of substrate flux (J), effective biofilm thickness (L_e) and total biofilm thickness (L_f) increase with the increase in the values of specific surface area of the attached growth media. It is also observed that both the substrate concentrations at the attached surface and biofilm--liquid interface decrease as the value of specific surface area (a) increases. Hence, the substrate removal efficiency is better in case of greater specific surface area of the attached growth media for a given set of parameters.

When the hydraulic retention time (θ) was varied, keeping other input variables constant the relevant output parameters were determined using the computer program as stated earlier and shown in Table 3.

The bold face value of 'θ', i.e. 1.0 h is considered as a reference value lying in the range from 0.20 to 1.0 h in the sensitivity study. The sensitivity analysis depicts that a minimum hydraulic retention time is required for maintaining a desired amount of biomass density, which is 0.2 h under the present case. It demonstrates that the values of substrate flux (J), effective biofilm thickness (L_e) and total biofilm thickness (L_f) increase with the increase in the value of hydraulic retention time. It is also

Table 3 Sensitivity study by varying hydraulic retention time (ɵ)

Run no.	θ (h)	S_s (mg/cc)	S_w (mg/cc)	J (mg/cm^2/day)	L_e (cm)	L_f (cm)	Reference set of input parameters
1	0.2	0.427	0.426	0.48	0.001	0.023	$S_0 =$ 0.43 mg/cc, k = 10 day^{-1}, a = 0.9 cm^{-1}, Y = 0.5, K = 0.01 mg/cm^3, b_t = 0.41 day^{-1}, D = 1.25 cm^2/day, D_f = 0.75 cm^2/day, L = 0. 0078 cm, X_f = 25 mg/cc
2	0.3	0.418	0.409	1.85	0.007	0.09	
3	0.4	0.409	0.381	3.22	0.013	0.157	
4	0.5	0.401	0.344	4.58	0.019	0.224	
5	0.6	0.393	0.296	5.94	0.024	0.289	
6	0.7	0.384	0.238	7.28	0.03	0.355	
7	0.8	0.376	0.172	8.6	0.036	0.419	
8	0.9	0.368	0.0973	9.85	0.0419	0.48	
9	**1**	0.362	0.0215	10.89	0.0515	0.531	

evident that both the substrate concentrations at the attached surface and the biofilm--liquid interface decrease with the increase in the value of hydraulic retention time (θ). Therefore, the substrate removal efficiency is better in case of higher hydraulic retention time for a given set of parameters.

In case of the attached biomass concentration (X_f) was varied, keeping other input variables constant the relevant output parameters were calculated using the computer program as stated earlier and shown in Table 4. The bold face value of 'X_f', i.e. 25 mg/cc is considered as a reference value lying in the range from 2.5 to 25 mg/cc in the sensitivity study. The sensitivity analysis shows that a maximum biomass density can be developed for a given influent substrate concentration, hydraulic retention time and other kinetic parameters. Under the present case, this maximum biomass density is obtained as 25 mg/cc.

It is observed that the values of substrate flux (J) and the effective biofilm thickness (L_e) increase with the increase in the value of attached biomass concentration. It is also to note that the total biofilm thickness and both the substrate concentrations at the attached surface and the biofilm--liquid interface decrease with the increase in the value of attached biomass concentration (X_f). Therefore, the substrate removal efficiency enhances in case of higher attached biomass concentration for a given set of parameters.

2.2.2 Development of Sensitivity Profiles

In order to study the sensitivity, the variation profiles of the relevant output parameters due to change in the input parameters within their feasible range are drawn. As a result, five output parameters, viz. S_s, S_w, J, L_e, L_f are plotted with respect to input

Table 4 Sensitivity study by varying attached biomass concentration (X_f)

Trial no.	X_f (mg/cc)	S_s (mg/cc)	S_w (mg/cc)	J (mg/cm^2/day)	L_e (cm)	L_f (cm)	Reference set of input parameters
1	2.5	0.423	0.386	1.16	0.0469	0.567	S_0 = 0.43 mg/cc, k = 10 day^{-1}, a = 0.9 cm^{-1}, Y = 0.5, K = 0.01 mg/cm^3, b_t = 0.41 day^{-1}, D = 1.25 cm^2/day, D_f = 0.75 cm^2/day, L = 0.0078 cm, θ = 1 h
2	5	0.416	0.343	2.3	0.0469	0.562	
3	7.5	0.408	0.301	3.43	0.0469	0.559	
4	10	0.401	0.258	4.56	0.047	0.557	
5	12.5	0.394	0.217	5.69	0.047	0.555	
6	15	0.387	0.175	6.8	0.0472	0.553	
7	17.5	0.38	0.134	7.89	0.0474	0.55	
8	20	0.374	0.094	8.96	0.0477	0.546	
9	22.5	0.367	0.056	9.97	0.0485	0.54	
10	**25**	0.362	0.0215	10.89	0.0515	0.531	

parameters, viz. S_0, 'a', θ and X_f separately. Thus, the variation profiles of S_s, S_w, J, L_e, L_f versus S_0 are shown in Fig. 3a–c. Similarly, the variation profiles of S_s, S_w, J, L_e, L_f versus 'a' are presented in Fig. 4a–c. On the other hand, the variation profiles of S_s, S_w, J, L_e, L_f versus θ are shown in Fig. 5a–c. Lastly, the variation profiles of S_s, S_w, J, L_e, L_f versus X_f are presented in Fig. 6a–c.

2.2.3 Discussion on Sensitivity Profiles

It is obvious from Fig. 3a that both S_s and S_w increase almost linearly with the increase in S_0. However, the rate of increase is higher in case of S_w than that of S_s. The substrate flux (J) sharply increases with the increase in S_0 at the initial stage and thereafter reaches to a limiting condition as shown in Fig. 3b. It implies that there will be no further increase in the substrate flux, in spite of enhancement in S_0. It is quite expected that a given attached biomass concentration can uptake the substrate up to its maximum possible capacity. It is observed from Fig. 3c that the effective biofilm thickness sharply decreases with the increase in S_o at the initial stage and thereafter it verges to steady-state value. This is so, because in case of increase in S_0, the substrate gradient becomes high at the liquid--biofilm interface and thereby the effective biofilm thickness decreases to maintain its uniformity from the biofilm side. However, a steady-state condition is attained after a certain value of S_0 and thereafter no further decrease in effective biofilm thickness is required. A reverse picture is observed for the total biofilm thickness (L_f), which sharply increases up to a certain value of S_0, but thereafter attains a steady-state condition. It corroborates

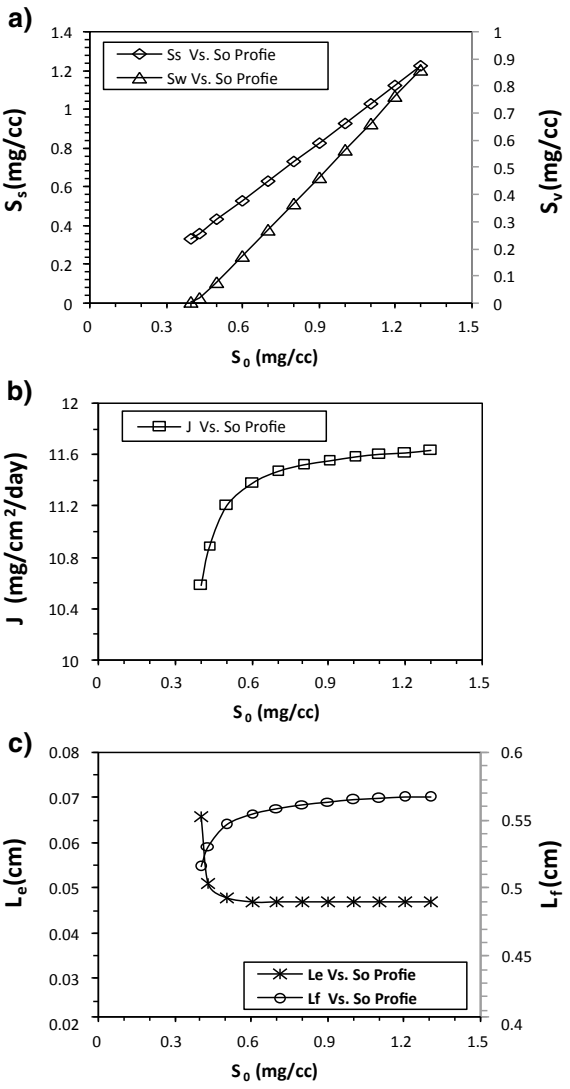

Fig. 3 **a** Sensitivity of S_s and S_w due to variation in S_0 value. **b** Sensitivity of J due to variation in S_0 value. **c** Sensitivity of L_e and L_f due to variation in S_0 value

to the fact that the biofilm growth, in turn the total biofilm thickness should reach to a maximum value, when the substrate utilization tends to a limiting stage.

Figure 4a depicts that both S_s and S_w decrease almost linearly with the increase in specific surface area (a). However, the rate of decrease is greater in case of S_w than that of S_s. The substrate flux (J) also increases almost linearly with the increase in 'a' throughout its variation as shown in Fig. 4b. It implies that the substrate flux is directly proportional to the specific surface area. Figure 4c reveals that the effective biofilm thickness increases almost linearly with the increase in 'a' up to a certain extent and thereafter it tends to increase rapidly. This is obvious, because in case of

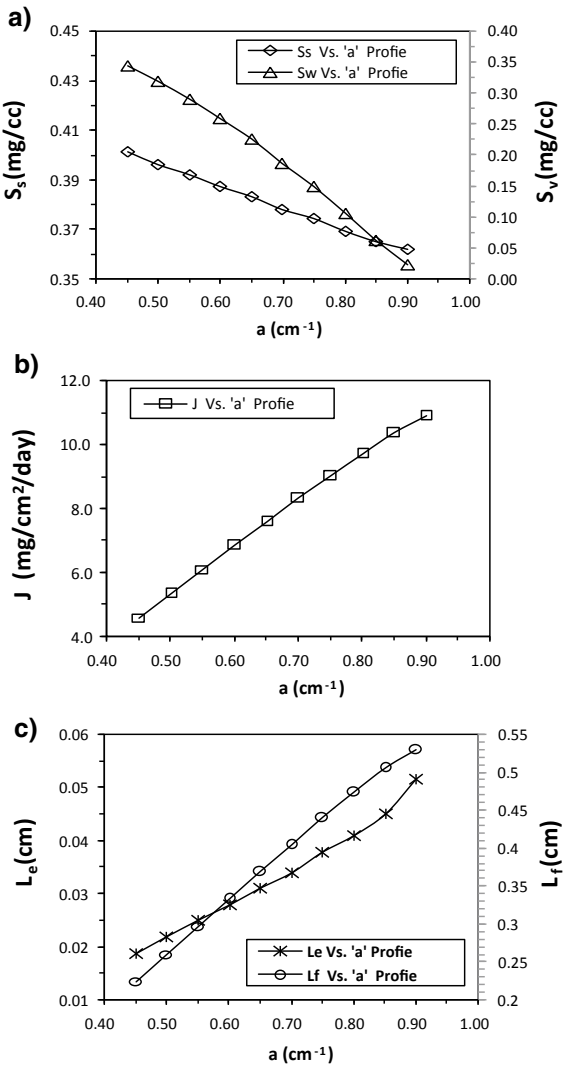

Fig. 4 **a** Sensitivity of S_s and S_w due to variation in 'a' value. **b** Sensitivity of J due to variation in 'a' value. **c** Sensitivity of L_e and L_f due to variation in 'a' value

increase in 'a', total attached biomass content also gets enhanced and thereby the effective biofilm thickness increases. However, a sharp increase in L_e is observed, when L_f also increases rapidly. Almost same profile is envisaged for the total biofilm thickness (L_f) linearly increases up to a certain value of S_0, but thereafter tends to attain a steady-state condition. It tallies with the fact that the biofilm growth, in turn the total biofilm thickness should reach to a maximum value, in spite of continuous increase in the specific surface area.

It is observed from Fig. 5a that S_s decreases almost linearly with the increase in hydraulic retention time (θ). But, the effluent substrate concentration (S_w) decreases

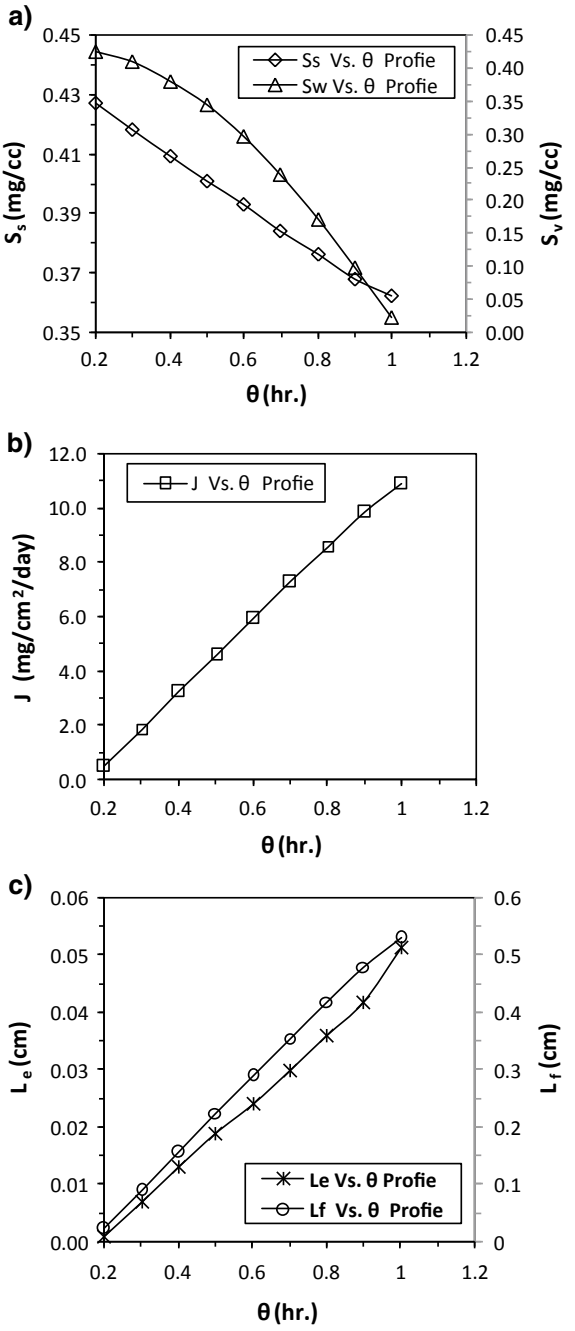

Fig. 5 **a** Sensitivity of S_s and S_w due to variation in θ value. **b** Sensitivity of J due to variation in θ value. **c** Sensitivity of L_e and L_f due to variation in θ value

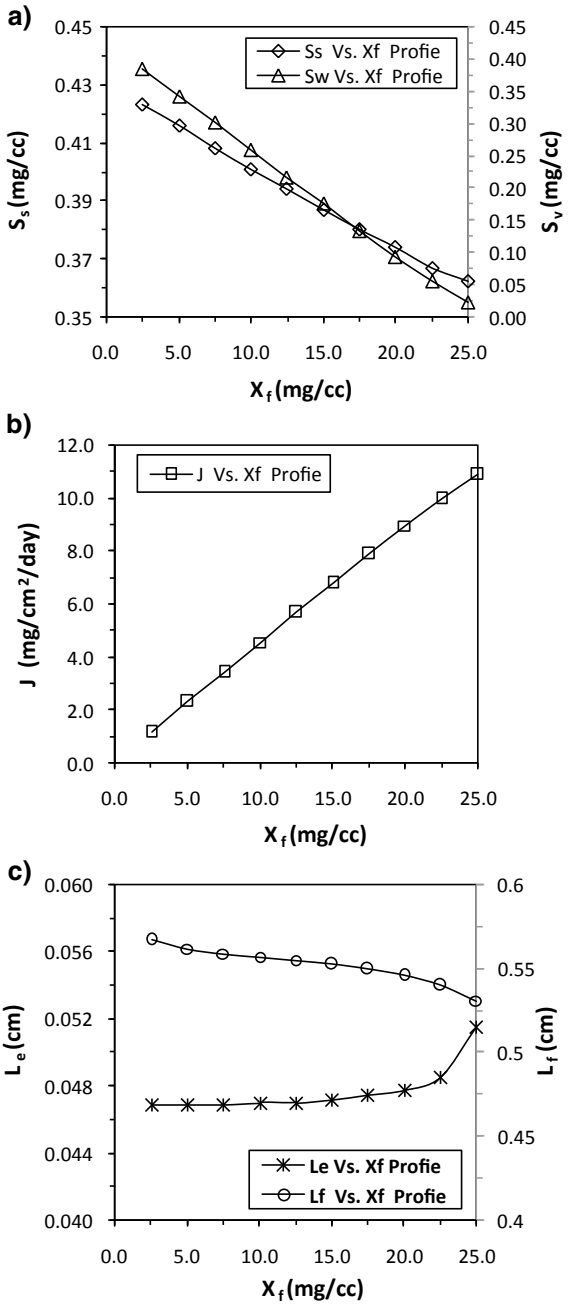

Fig. 6 **a** Sensitivity of S_s and S_w due to variation in X_f value. **b** Sensitivity of J due to variation in X_f value. **c** Sensitivity of L_e and L_f due to variation in X_f value

with a rate faster than S_s and showing a nonlinear profile. It implies that the hydraulic retention time has significant impact on the performance of a biofilm reactor. As observed in the earlier cases, the substrate flux (J) also increases almost linearly with the increase in θ as shown in Fig. 5b. Figure 5c shows that the effective biofilm thickness increases almost linearly with the enhancement in θ up to a certain extent and thereafter it tends to increase rapidly. This is reasonable, because in case of increase in θ, total attached biomass content also increases and thereby the effective biofilm thickness gets enhanced. However, the total biofilm thickness (L_f) linearly increases with the increase in θ, throughout its variation.

Figure 6a shows that both S_s and S_w decrease almost linearly with the increase in attached biomass concentration (X_f). But, the rate of decrease in effluent substrate concentration (S_w) appears to be faster than S_s. It implies that the attached biomass concentration has significant impact on the performance of a biofilm reactor. Like the earlier cases, the substrate flux (J) also increases almost linearly with the increase in X_f as shown in Fig. 6b. It is observed from Fig. 6c that the effective biofilm thickness increases very slowly with the increase in X_f up to a certain extent and thereafter it tends to increase sharply. It implies that X_f has a little impact on the effective biofilm thickness up to a great extent. However, the total biofilm thickness (L_f) decreases slowly with the increase in X_f, showing a nonlinear pattern. It is attributed to the fact that the amount of total biomass loss (due to shear and decay) also gets enhanced, when X_f increases, causing decrease in total biofilm thickness.

3 Conclusions

The present biofilm model provides a simple tool to estimate the substrate concentration at liquid--biofilm interface and in the effluent, substrate flux and effective as well as total biofilm thickness. Alternatively, the same model can be applied for a desired effluent substrate concentration and to find out the necessary values of the relevant variables. The sensitivity study on this simplistic biofilm model established that for a given set of kinetic parameters there should be some minimum and maximum values of crucial input variables for process design of a biofilm reactor. The novelty of the simplistic biofilm model lies in determining the acceptable ranges of input variables like S_0, 'a', θ and X_f for a given set of kinetic coefficients. The accuracy of the model is also proved from the profiles of output parameters on varying relevant input variables.

The substrate concentration at liquid--biofilm interface and in the effluent is almost linearly sensitive to the influent substrate concentration with a positive impact. However, the effluent substrate concentration is more influenced by the influent substrate concentration. The substrate flux also gets affected positively by the influent substrate concentration at the initial stage and thereafter practically no influence is noticed. The effective biofilm thickness is highly sensitive to the influent substrate concentration with a negative impact up to a certain stage, and beyond that there is hardly any effect. The total biofilm thickness is also severely affected with a positive

impact by the influent substrate concentration, but there is no plausible effect beyond a threshold value.

The substrate concentration at liquid--biofilm interface and in the effluent is almost linearly sensitive to the specific surface area having a negative influence. But, the effluent substrate concentration is more influenced by the specific surface area. The substrate flux also gets influenced positively by the specific surface area. The effective biofilm thickness is also linearly sensitive to the specific surface area with a positive impact up to a certain extent, and beyond that it tends to get more influenced. The total biofilm thickness is also greatly influenced having a positive impact by the specific surface area.

The substrate concentration at liquid--biofilm interface is almost linearly sensitive to the hydraulic retention time with a negative influence. But, the effluent substrate concentration is more affected by the hydraulic retention time with a nonlinear profile. The substrate flux also gets influenced positively by the hydraulic retention time. The effective biofilm thickness is also linearly sensitive to the hydraulic retention time with a positive impact up to a certain extent, and beyond that it tends to get more affected. The total biofilm thickness is also linearly sensitive with a positive impact due to hydraulic retention time.

The substrate concentration at liquid--biofilm interface and in the effluent is more or less linearly sensitive to the attached biomass concentration having a negative influence. But, the effluent substrate concentration is more influenced by the attached biomass concentration. The substrate flux is also affected positively by the attached biomass concentration. The effective biofilm thickness is less sensitive to the attached biomass concentration with a positive impact up to a certain extent, and beyond that it tends to get more influenced. The total biofilm thickness is also less sensitive with a negative impact on account of attached biomass concentration.

References

1. Williamson K, McCarty PL (1976) A model of substrate utilization by bacterial films. 48(1):9–23
2. Rittmann BE, McCarty Perry L (1980) Model of steady state biofilm kinetics. Biotechnol Bioeng XXII:2343–2357
3. Huang JS, Jih CG (1997) Deep biofilm kinetics of substrate utilization in anaerobic filters. Water Res 31(9):2309–2317
4. Suidan MT, Wang YT (1985) Unified analysis of biofilm kinetics. ASCE Ill(5):634–646
5. Heath MS, Wirtel SA, Rittmann BE (1990) Simplified design of biofilm processes using normalized loading curves. Water Pollut Control Fed 62:185–191
6. Saez PB, Rittmann BE (1991) Accurate Pseudo analytical solutions for steady state biofilm. Biotechnol Bioeng 39:790–793
7. Shaoying Q, Eberhard M (2005) Modeling steady-state biofilms with dual-substrate limitations. J Environ Eng 131(2):99. https://doi.org/10.1061/(ASCE)0733-9372(2005)131:2(320)
8. Mudliar S, Banerjee S, Vaidya A, Devotta S (2007) Steady state model for evaluation of external and internal mass transfer effects in an immobilized biofilm. Bioresour Technol 99:3468–3474

Risk of Extinction of Species in an Ecological System: Estimation and Analysis

Bapi Saha, Rupak Bhattacharjee, and Debasish Majumder

1 Introduction

Predicting the risk of extinction of species from their demographic history and to find the physical or behavioral features showing such patterns is difficult. Stochastic population is more appropriate compared to deterministic counterpart in modern ecological theory and it is being applied in various interdisciplinary research areas such as population ecology [1], conservation biology [2], epidemiology [3] and many others. When the rates of different possible transitions are available, the Kolmogorov differential equation (Master equation [4]) is used to compute the transition probability distributions. In addition, the equilibrium distribution may be obtained by taking time sufficiently large.

The ecological models governed by deterministic differential or difference equations play a crucial role in quantitative studies of the dynamics of natural populations. The dynamical characteristics of the systems, viz. stability of equilibrium points, stability of limit cycles etc. can be predicted using the deterministic set up. In real life situation applying these models in natural populations, it is more realistic to consider the stochastic model of the system, where the randomness is generated either from variation among individual growth rates or due to environmental fluctuations. In stochastic models the common characteristic of the deterministic models are replaced by the probability statements. For example, in stochastic version of

B. Saha (✉)
Department of Mathematics, Govt. College of Engg. & Textile Technology, Berhampore, Berhampore, India
e-mail: bapi.math@gmail.com

R. Bhattacharjee · D. Majumder
Department of Mathematics, JIS College of Engineering, Kalyani, India
e-mail: rupakb13@yahoo.co.in

D. Majumder
e-mail: debamath@rediffmail.com

S. Kumar et al. (eds.), *Sustainability in Environmental Engineering and Science*, Lecture Notes in Civil Engineering 93,
https://doi.org/10.1007/978-981-15-6887-9_5

the logistic model, the equilibrium point is replaced by the equilibrium distribution, which is represented by the cloud points around the equilibrium point rather than a fixed value [5].

In deterministic modeling, the system approach towards the unique stable equilibrium with certainty which may not be the actual case in reality. The deterministic models some times fail to capture the actual fate of the system in long run. For example, in logistic growth, the carrying capacity is the only stable point, hence the population never reaches zero for positive value of intrinsic growth rate, whereas, in stochastic environment there is always a positive probability associated with the extinction of the population and thus making the stochastic model framework more appropriate in real life scenarios [6, 7]. In addition, stochastic models are used to obtain different extinction related parameters such as probability of extinction, time to extinction and few more. Recently [8] used the stochastic differential equation model including demographic stochasticity and predicted the time to extinction and probability of extinction for the Atlantic Herring populations.

To incorporate the randomness in dynamical system, three types of stochastic models are used and they are discrete time Markov chain (DTMC) model, continuous time Markov chain (CTMC) model and stochastic differential equation (SDE) model. The application of DTMC models in stochastic modelling can be found in many cases [8, 9]. In this paper, we shall use the Discrete time Markov chain model (DTMC) to predict the different extinction measures viz. expected extinction time and the probability of extinction given a starting population size in ecological and epidemiological system. The DTMC model is a popular stochastic modeling technique to answer various questions in ecology, invasion biology, species coexistence of single or multiple species [10]. Here we have used DTMC process in prey-predator dynamical system to obtain the joint probability distribution of prey and predator and mean persistence time of the same.

2 Joint Probability Distribution of Prey-Predator in a Two Dimensional Ecological Model

To begin with we consider a simple two dimensional predator prey system, where the different ecological mechanisms such as predation, death, birth etc. are modeled by general functions. Note that the process can also be applied to general disease models of infectious diseases. The approach will be applicable to populations of the same species or to populations of different species. Populations of the prey or predator species may differ, for example, by geographic location or by interaction status of them. Let us consider the following prey-predator dynamical system,

$$\begin{aligned} \frac{\mathrm{d}x(t)}{\mathrm{d}t} &= b_1(x(t)) - d_1(x(t)) - g(x(t), y(t)) \\ \frac{\mathrm{d}y(t)}{\mathrm{d}t} &= \alpha g(x(t), y(t)) - d_2(y(t)) \end{aligned} \tag{1}$$

Here, $x(t)$, $y(t)$ denote the population densities of the prey and predator at time t respectively; $b_1(x)$ is the birth rate of the prey species; $d_i(\cdot)$ $(i = 1, 2)$ are the death rates (natural) of the prey and predator populations respectively. The initial conditions are, $x(0) \geq 0$, $y(0) \geq 0$. Depending on the biological background of the two interacting species the birth and death rates are density dependent or density independent. The function $g(x, y)$ known as predator's functional response, represents the inter-specific interaction between the prey and predators. α is the conversion rate of ingested prey into new predators and it lies between 0 and 1.

In absence of predators, model (1) reduces to a single species model with birth and death rates $b_1(x)$ and $d_1(x)$ respectively. Various stochastic formulations of the logistic model have been studied in the literature [11–15]. In general, infinitely many choices of functions are possible for birth and death rates for different choices of parameters. The choices of the functions are mainly governed by the collected data on the species under investigation [16].

Model (1) is the deterministic part of analogous stochastic models that account for the variability in births, deaths, transmission and recovery.

In the stochastic formulation we assume $X(t)$ and $Y(t)$ are two discrete random variables which represent the number of prey and predator populations respectively taking values in the state space $\{(x, y)$: $x = 0, 1, \ldots M$; $y = 0, 1, \ldots N\}$. Here M and N are the maximum sustainable population size of prey and predator population respectively. We assume the time step Δt to be sufficiently small so that at most one transition is possible during this time interval, i. e. $\Delta X(t) = X(t + \Delta t) - X(t) \in \{-1, 0, 1\}$ and $\Delta Y(t) = Y(t + \Delta t) - Y(t) \in \{-1, 0, 1\}$. Multiple births, deaths, or transformations in time Δt which have probabilities of order $(\Delta t)^2$ are neglected. The possible transitions in the size of the population and the corresponding probabilities for the model (1) is depicted in Table 1. Note that $(\Delta X(t), \Delta Y(t)) = (1, 0)$ denotes event of the birth of a prey and no change in predator abundance in time Δt, whose probability is equal to the product of the probabilities of one birth of prey $(b_1(x)\Delta t)$ and no death of predator $((1 - d_2(y)\Delta t))$. Similarly probabilities of the other events are defined.

Here the randomness in population growth rate is due to demographic stochasticity which is the variation in the number of individual births and deaths and usually modeled using birth and death process.

3 Derivation of Joint Probability Distribution

In this section we will derive the joint probability distribution of prey and predator using the transition probabilities given in Table 1. The state of the system at time t can be characterized by the probability $p_{xy}(t)$ of having x individuals of prey and y individuals of predator, where (x, y) takes values in $\{0, 1, \ldots, M\} \times \{0, 1, \ldots, N\}$, in notation, $p_{xy}(t) = \mathbb{P}\{X(t) = x, Y(t) = y\}$.

Table 1 Possible changes in the predator-prey densities with the corresponding probabilities

Event	Transition	Transition probability
Prey birth and no birth or death of predator	$(x, y) \longrightarrow (x+1, y)$	$b_1(x)\Delta t(1 - d_2(y)\Delta t)$
One death of prey due to predation	$(x, y) \longrightarrow (x-1, y+1)$	$\alpha g(x, y)\Delta t$
No birth or death of prey and one death of predator	$(x, y) \longrightarrow (x, y-1)$	$d_2(y)\Delta t(1 - b_1(x)\Delta t)$
Death of one prey due to intra-species competition or predation and no birth or death of predator	$(x, y) \longrightarrow (x-1, y)$	$d_1(x)\Delta t + (1-\alpha)g(x, y)\Delta t$
No birth or death of either population	$(x, y) \longrightarrow (x, y)$	$1 - [b_1(x) + \alpha g(x, y) + d_2(y) + d_1(x) + (1 - \alpha)g(x, y)]\Delta t$

$$
\begin{aligned}
p_{xy}(t+\Delta t) = {} & p_{x-1,y}(t)b_1(x-1)\Delta t \\
& + p_{x+1,y-1}(t)\alpha g(x+1, y-1)\Delta t + p_{x+1,y}(t)[d_1(x+1) \\
& + (1-\alpha)g(x+1, y)]\Delta t + p_{x,y+1}(t)d_2(y+1)\Delta t \\
& + [1 - (b_1(x) + g(x, y) + d_1(x) + d_2(y))\,\Delta t]p_{xy}(t)
\end{aligned}
$$

where $0 < x < M, 0 < y < N$.

This system of equations generates the probability distribution of the prey and predator populations at time $t + \Delta t$ which can be obtained using numerical methods. This process can be extended for higher dimension also, although the process will be cumbersome.

3.1 Marginal Distribution of Prey

The mathematical complexity increases with the increase in the dimension of the model. The analysis of extinction related issues like probability of extinction, time to extinction for a particular single species is made easy by considering the marginal distribution of that species. Here we consider the marginal distribution of prey and predator to avoid the complexity involved in the calculation.

Let $p_{x\cdot}(t) = \mathbb{P}\{X(t) = x\}$ and $p_x^{ji} = \mathbb{P}\{X(t+\Delta t) = j | X(t) = i\}$.

$$\begin{aligned} p_x^{i+1,i}(\Delta t) &= \mathbb{P}\{X(t+\Delta t) = i+1 | X(t) = i\} \\ &= \frac{\mathbb{P}\{X(t+\Delta t) = i+1 \cap X(t) = i\}}{\mathbb{P}\{X(t) = i\}} \\ &= \frac{\sum_k p_{ik} b_1(i)\Delta t}{\sum_k p_{ik}} \\ &= b_1(i)\Delta t \end{aligned} \tag{2}$$

$$\begin{aligned} p_x^{i-1,i}(\Delta t) &= \mathbb{P}\{X(t+\Delta t) = i-1 | X(t) = i\} \\ &= \frac{\mathbb{P}\{X(t+\Delta t) = i-1 \cap X(t) = i\}}{\mathbb{P}\{X(t) = i\}} \\ &= \frac{\sum_k p_{ik} \left(g(i,k) + d_1(i)\right) \Delta t}{\sum_k p_{ik}} \\ &= \left[\frac{\sum_k p_{ik} g(i,k)}{\sum_k p_{ik}} + d_1(i)\right] \Delta t \end{aligned} \tag{3}$$

$$\begin{aligned} p_x^{ii}(\Delta t) &= \mathbb{P}\{X(t+\Delta t) = i | X(t) = i\} \\ &= \frac{\mathbb{P}\{X(t+\Delta t) = i \cap X(t) = i\}}{\mathbb{P}\{X(t) = i\}} \\ &= \frac{\sum_k \mathbb{P}\{X(t+\Delta t) = i \cap X(t) = i \cap Y(t) = k\}}{\sum \mathbb{P}\{X(t) = i \cap Y(t) = k\}} \\ &= \frac{\sum_k p_{ik} \left(1 - (b_1(i) + g(i,k) + d_1(i)) \Delta t\right)}{\sum_k p_{ik}} \\ &= \frac{\sum_k p_{ik} \left(1 - (b_1(i) + g(i,k) + d_1(i)) \Delta t\right)}{\sum_k p_{ik}} \\ &= 1 - \left[b_1(i) + d_1(i) + \frac{\sum_k p_{ik} g(i,k)}{\sum_k p_{ik}}\right] \Delta t \end{aligned} \tag{4}$$

Hence we can write that,

$$\begin{aligned} p_x^{ji}(\Delta t) &= \lambda_1(i)\Delta t, \qquad i = j-1,\ j \in \{2, 3, \ldots, M\} \\ &= \lambda_2(i)\Delta t, \qquad i = j+1,\ j \in \{0, 1, \ldots, M-1\} \\ &= 1 - \lambda_3(i)\Delta t,\ \ j = i, \quad j \in \{0, 1, \ldots, M\} \\ &= 0 \qquad\qquad \text{otherwise} \end{aligned} \tag{5}$$

where

$$\begin{aligned}\lambda_1(i) &= b_1(i)\\ \lambda_2(i) &= d_1(i) + \frac{\sum_k p_{ik} g(i,k)}{\sum_k p_{ik}}\\ \lambda_3(i) &= b_1(i) + d_1(i) + \frac{\sum_k p_{ik} g(i,k)}{\sum_k p_{ik}}\end{aligned} \tag{6}$$

Then, $p_{x\cdot}(t+\Delta t)$ satisfies the following difference equations,

$$\begin{aligned}p_{x\cdot}(t+\Delta t) &= \lambda_1(x-1)\Delta t p_{x-1\cdot}(t) + \lambda_2(x+1)\Delta t p_{x+1\cdot}(t)\\ &\quad +(1-\lambda_3(x)\Delta t)p_{x\cdot}(t)\\ p_{0\cdot}(t+\Delta t) &= p_{1\cdot}(t)\lambda_2(1)\Delta t + p_{0\cdot}(t)\\ p_{M\cdot}(t+\Delta t) &= \lambda_1(M-1)\Delta t p_{M-1\cdot}(t) + (1-\lambda_3(M)\Delta t)p_{M\cdot}(t)\end{aligned}$$

where $x = 1, 2, \ldots, M-1$.

The difference equations, can be expressed in matrix form as

$$p_X(t+\Delta t) = P p_X(t), \quad p_{x_0}(0) = 1$$

where $p_X(t) = (p_0.(t), p_1 \cdot (t), \ldots, p_M \cdot (t))^T$ and the matrix P is the one step transition matrix given by

$$P = \begin{pmatrix} 1 & \lambda_2(1)\Delta t & 0 & 0 & \ldots & 0\\ 0 & 1-\lambda_3(1)\Delta t & \lambda_2(2)\Delta t & 0 & \ldots & 0\\ 0 & \lambda_1(1)\Delta t & 1-\lambda_3(2)\Delta t & \lambda_2(3)\Delta t & \ldots & 0\\ 0 & 0 & \lambda_1(2)\Delta t & 1-\lambda_3(3)\Delta t & \ldots & 0\\ \vdots & \vdots & \vdots & \vdots & \vdots & \vdots\\ 0 & 0 & 0 & 0 & \ldots & \lambda_2(M)\Delta t\\ 0 & 0 & 0 & 0 & \ldots & 1-\lambda_3(M)\Delta t \end{pmatrix}$$

To ensure that P is a stochastic matrix (non-negative and column sum to 1) it is assumed that

$$\max_{x\in\{1,2,\ldots,M\}} \lambda_3(x)\Delta t \leq 1.$$

The equilibrium (0, 0) is the absorbing state, since, once the population reaches this state, the process stops. Thus, $p_{00}(\Delta t) = 1$. Eventually population extinction occur with probability 1 i.e $\lim_{t\longrightarrow\infty} p_{0\cdot}(t) = 1$. Now as $\Delta t \longrightarrow 0$ the system of difference equations (7) reduces to

$$\begin{aligned}
\frac{\mathrm{d}p_{0\cdot}(t)}{\mathrm{d}t} &= p_{1\cdot}(t)\lambda_2(1) \\
\frac{\mathrm{d}p_{x\cdot}(t)}{\mathrm{d}t} &= \lambda_1(x-1)p_{x-1\cdot}(t) + \lambda_2(x+1)p_{x+1\cdot}(t) \\
&\quad -\lambda_3(x)p_{x\cdot}(t) \\
\frac{\mathrm{d}p_{M\cdot}(t)}{\mathrm{d}t} &= \lambda_1(M-1)p_{M-1\cdot}(t) - \lambda_3(M)p_{M\cdot}(t)
\end{aligned} \tag{7}$$

Following [23], a convenient notation for the system of equations (7) is given by

$$\frac{\mathrm{d}p}{\mathrm{d}t} = Ap$$

where A is given by

$$\begin{pmatrix}
-\lambda_3(0) & \lambda_2(1) & 0 & \cdots & 0 \\
\lambda_1(0) & -\lambda_3(1) & \lambda_2(2) & \cdots & 0 \\
0 & \lambda_1(1) & -\lambda_3(2) & \cdots & 0 \\
\vdots & \vdots & \vdots & \vdots & \vdots \\
0 & 0 & 0 & \cdots & -\lambda_3(M)
\end{pmatrix}$$

In absence of predators the above system of equations are well studied in the literature. For example, when the birth and death rates are governed by the logistic and power law logistic model, the associated equilibrium probability distributions are found in [11, 12]. In such cases, the analytical solutions of the differential equations can not be obtained, however, for small M, numerical methods can be employed to solve the above systems of equations. [17] obtains a representation of the solution using Laplace transforms and continued fractions approximations. [18] studied the stochastic dynamics of the Allee effect in the context of invasion biology by suitably defining the birth and death process from the deterministic skeleton of the model depicting the Allee effect.

Similar process can be followed to show that the transition probabilities for the predator population are given by

$$\begin{aligned}
p_y^{ji}(\Delta t) &= \nu_1(i)\Delta t, && i = j-1,\ j \in \{1, 2, \ldots, N\} \\
&= \nu_2(i)\Delta t, && i = j+1,\ j \in \{1, 2, \ldots, N\} \\
&= 1 - \nu_3(i)\Delta t, && j \in \{1, 2, \ldots, N\} \\
&= 0 && \text{otherwise}
\end{aligned}$$

where

$$\nu_1(i) = \alpha \frac{\sum_k p_{ki} g(k,i)}{\sum_k p_{ki}}$$
$$\nu_2(i) = d_2(i)$$
$$\nu_3(i) = d_2(i) + \alpha \frac{\sum_k p_{ki} g(k,i)}{\sum_k p_{ki}}$$

Then, $p_{\cdot y}(t + \Delta t)$ satisfies the following difference equations,

$$\begin{aligned} p_{\cdot y}(t + \Delta t) &= \nu_1(y-1)\Delta t p_{\cdot y-1}(t) + \nu_2(y+1)\Delta t p_{\cdot y+1}(t) \\ &\quad + (1 - \nu_3(y)\Delta t) p_{\cdot y}(t) \\ p_{\cdot 0}(t + \Delta t) &= p_{\cdot 1}(t)\nu_2(1)\Delta t + p_{\cdot 0}(t) \\ p_{\cdot N}(t + \Delta t) &= \nu_1(N-1)\Delta t p_{\cdot N-1}(t) + (1 - \nu_3(N)\Delta t) p_{\cdot N}(t) \end{aligned}$$

where $y = 1, 2, \ldots, N-1$.

The difference equations project forward in time and can be expressed in matrix form as

$$p_Y(t + \Delta t) = P p_Y(t),\ p_{y_0}(0) = 1$$

where $p_Y(t) = (p_{\cdot 0}(t), p_{\cdot 1}(t), \ldots, p_{\cdot N}(t))^T$ and the matrix P is the one step transition probability matrix given by

$$P = \begin{pmatrix} 1 & \nu_2(1)\Delta t & 0 & 0 & \ldots & 0 \\ 0 & 1 - \nu_3(1)\Delta t & \nu_2(2)\Delta t & 0 & \ldots & 0 \\ 0 & \nu_1(1)\Delta t & 1 - \nu_3(2)\Delta t & \nu_2(3)\Delta t & \ldots & 0 \\ 0 & 0 & \nu_1(2)\Delta t & 1 - \nu_3(3)\Delta t & \ldots & 0 \\ \vdots & \vdots & \vdots & \vdots & \vdots & \vdots \\ 0 & 0 & 0 & 0 & \ldots & \nu_2(N)\Delta t \\ 0 & 0 & 0 & 0 & \ldots & 1 - \nu_3(N)\Delta t \end{pmatrix}$$

To ensure that P is a stochastic matrix (non-negative and column sum to 1) it is assumed that

$$\max_{y \in \{1,2,\ldots,N\}} \nu_3(y)\Delta t \leq 1.$$

In this case also $(0, 0)$ is the absorbing state and hence $p_{00}(\Delta t) = 1$.

Taking $\Delta t \longrightarrow 0$ the system of difference equations (8) reduces to

$$\begin{aligned}
\frac{\mathrm{d}p_{\cdot 0}(t)}{\mathrm{d}t} &= p_{\cdot 1}(t)\mu_2(1) \\
\frac{\mathrm{d}p_{\cdot y}(t)}{\mathrm{d}t} &= \mu_1(y-1)p_{\cdot y-1}(t) + \mu_2(y+1)p_{\cdot y+1}(t) \\
&\quad -\mu_3(y)p_{\cdot y}(t) \\
\frac{\mathrm{d}p_{\cdot N}(t)}{\mathrm{d}t} &= \mu_1(N-1)p_{\cdot N-1}(t) - \mu_3(N)p_{\cdot N}(t)
\end{aligned} \tag{8}$$

4 Derivation of Difference Equation for Persistence Time of Prey

The persistence time of the prey and predator populations may be defined as either the time when both the population numbers are zero or the time when the prey population size is zero. Let T be the random variable for the time until population extinction. It is to be noted that the distribution of T depends on the initial population size, and hence we shall denote this dependence by T_{x_0}. Let τ_{x_0} denote the expected time until extinction occur when initial population size is x_0 i.e. $\mathbb{E}(T_{x_0}) = \tau_{x_0}$. The mean persistence time for the DTMC model satisfies the following difference equations:

$$\begin{aligned}
\tau_x &= \lambda_1(x)\Delta t(\tau_{x+1} + \Delta t) + \lambda_2(x)\Delta t(\tau_{x-1} + \Delta t) \\
&\quad +(1 - \lambda_3(x)\Delta t)(\tau_x + \Delta t)
\end{aligned}$$

where $x = 1, 2, \ldots M$. This difference equations can be simplified as

$$\lambda_2(x)\tau_{x-1} - \lambda_3(x)\tau_x + \lambda_1(x)\tau_{x+1} = -1 \tag{9}$$

Equation (9) can be written in the matrix form as $D\tau = -\mathbf{1}$, where $\mathbf{1} = (1, \ldots, 1)^T$ and

$$D = \begin{pmatrix}
-\lambda_3(1) & \lambda_1(1) & 0 & \ldots & 0 & 0 \\
\lambda_2(2) & -\lambda_3(2) & \lambda_1(2) & \ldots & 0 & 0 \\
\vdots & \vdots & \vdots & \vdots & \vdots & \vdots \\
0 & 0 & 0 & \ldots & \lambda_2(M) & -\lambda_3(M)
\end{pmatrix}$$

The solution for the mean persistence time is given by $\tau = D^{-1}\mathbf{1}$, where the inverse always exists. The matrix D is irreducibly diagonally dominant, hence nonsingular. The persistence time of predator can also be found using similar technique. The

difference equation to evaluate the persistence time takes the form of a differential equation for continuous processes, where the stochastic growth equations are described by diffusion process [19].

In order to find the time to extinction, the initial distribution is to be known. Here the initial distribution is the probability distribution of prey and predator at a time when we start to observe the dynamical system. Suppose at any time we observe that there are x_0 number of prey and y_0 number of predator. In order to find the expected time to extinction, the following initial distribution should be considered.

$$\begin{aligned} p_{xy}(t) &= 1 \quad \text{if } X = x_0, Y = y_0 \\ &= 0 \quad \text{otherwise} \end{aligned}$$

5 Application to Predator-Prey Models

The primary goal of this paper is to assess the expected time to extinction of a given dynamical system when the system variables are population size of different species belonging to different trophic levels. To justify the theoretical finding we take a two trophic food chain model where the growth process of the prey species follow logistic growth process.

In most of the prey-predator systems the growth process of prey populations are assumed to follow the logistic growth process. The logistic model assumes a linear decline in the per-capita growth rate with abundance (often called $r - n$ curve). The logistic growth process takes the following form:

$$\frac{1}{x(t)}\frac{\mathrm{d}x(t)}{\mathrm{d}t} = r_m\left[1 - \left(\frac{x(t)}{K}\right)\right] \tag{10}$$

For this model we have to identify the birth rate $b_1(x)$ and death rate $d_1(x)$. In case of logistic growth many forms of birth rate and death rates are available [12]. Here we consider the form of $b_1(x)$ and $d_1(x)$ as follows,

$$b_1(x) = a_1x - c_1x \qquad \text{and} \qquad d_1(x) = a_2x + c_2x$$

respectively, called power law logistic model. The a_i are "intrinsic rate" and c_i are the "crowding coefficients".

In most of the cases we consider the idealized linear interactions which is basically a valid first order approximation of more general interaction. Due to unavoidable heterogeneity exact fit is not expected in testing the linear model with biological data [20]. Different versions of the type II functional responses were utilized to study the evidence of group formation in the prey and predator [21]. We consider the following differential equation to describe the interactive predator-prey dynamics.

Table 2 Expected time to extinction of prey population

Initial predator population (y_0)	Expected time to extinction of prey (τ)
1	1.9066
2	3.8949
3	5.9849
4	8.0890
5	10.1094
6	11.9660
7	13.6061
8	15.0042
9	16.1579
10	17.0808
11	17.7970
12	18.3351
13	18.7249
14	18.9944
15	19.1689
16	19.2699
17	19.3152
18	19.3191

$$\begin{aligned}\frac{\mathrm{d}x(t)}{\mathrm{d}t} &= rx(t)\left[1-\left(\frac{x(t)}{K}\right)\right]-\frac{ax(t)y(t)}{1+ahx(t)}\\ \frac{\mathrm{d}y(t)}{\mathrm{d}t} &= \alpha\frac{ax(t)y(t)}{1+ahx(t)}-dy(t)\end{aligned} \tag{11}$$

In comparison of this model with the model 1, the following birth, death and interaction terms are considered [22].

$$b_1(x) = (r+1)x - \frac{r}{2K}x^2 \tag{12}$$

$$d_1(x) = x + \frac{r}{2K}x^2 \tag{13}$$

$$g(x, y) = xy \tag{14}$$

$$d_2(y) = dy \tag{15}$$

The time to extinction for the prey species with different initial predator population, is evaluated (see Table 2) considering the following parameter values. $\alpha = 0.5, r = 1$, $a = 0.5, K = 100, h = 0.5$. Similarly the same can be found for predator population also.

We also observe the effect of initial predator population on the expected time to extinction of prey population. The expected time to extinction (τ) increases with

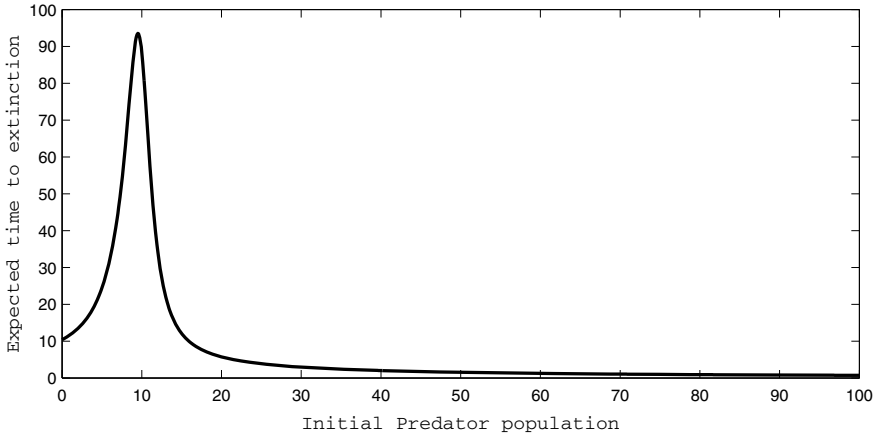

Fig. 1 The parameters are $\alpha = 0.5$, $r = 1$, $a = 0.5$, $K = 100$, $h = 0.5$

increase in the initial predator population (y_0) up to a certain maximum value of τ. The further increase in the initial predator population results in the decrease of τ (Fig. 1). This observation suggests that the presence of moderate amount of predator helps the prey population to sustain long rather than very low abundance of predator (y_0). A similar observation can be found in [22] where the author shows that the presence of moderate amount of predator in the system helps to decrease the chance of extinction of prey species.

6 Result and Discussion

The disappearance of different rare endangered species for the last few decades is affecting the ecological balance. This needs immediate implementation of proper management and conservation policies. To do this the assessment of probability of extinction and time to extinction is important. The idea of finding the probability of extinction can be found in [22]. In this paper we formulate a method to find expected time to extinction of discrete population involving in a given dynamical system. The implementation of the method on a simple prey-predator model reveals the fact that the presence of a certain amount of predator is helpful for prey to sustain longer than the absence of predator. The relationship between the expected time to extinction and other relevant model parameters can also open a new window towards the solution of many ecological problems which may help to frame proper conservation and management policies.

References

1. Keeling MJ (2000) Multiplicative moments and measures of persistence in ecology. J Theor Biol 205:269–281
2. Lande R, Engen S, Sæther B-E (2003) Stochastic population dynamics in ecology and conservation. Oxford University Press, Oxford
3. Krishnarajah I, Cook A, Marion G, Gibson G (2005) Novel moment closure approximations in stochastic epidemics. Bull Math Biol 67:855–873
4. Bailey NTJ (1964) Element of stochastic processes with applications to the natural sciences. Wiley, New York
5. May RM (1973) Stability in randomly fluctuating versus deterministic environments. Am Nat 107:621–650
6. Renshaw E (1991) Modelling biological populations in space and time. Cambridge University Press, Cambridge
7. Renshaw E (2011) Stochastic population processes: analysis, approximations, simulations. Oxford University Press, Oxford
8. Saha B, Bhowmick AR, Chattopadhyay J, Bhattacharya S (2013) On the evidence of an Allee effect in Herring populations and consequences for population survival: a model-based study. Ecol. Model. 250:72–80
9. Allen LJS, Allen EJ (2003) A comparison of three different stochastic population models with regard to persistence time. Theor Popul Biol 64:439–449
10. Allen LJS, Bokil VA (2012) Stochastic models for competing species with a shared pathogen. Math Biosci Eng 9:461–485
11. Matis JH, Kiffe TR (1996) On approximating the moments of the equilibrium distribution of a stochastic logistic model. Biometrics 52:980–991
12. Matis JH, Kiffe TR, Parthasarathy PR (1998) On the cumulants of population size for the stochastic power law logistic model. Theor Popul Biol 53:16–29
13. Matis JH, Kiffe TR (1999) Effects of immigration on some stochastic logistic models: a cumulant truncation analysis. Theor Popul Biol 56:139–161
14. Nåsell I (2001) Extinction and quasi-stationarity in the Verhulst logistic model. J Theor Biol 211:11–27
15. Nåsell I (2003) Moment closure and the stochastic logistic model. Theor Popul Biol 63:159–168
16. Bhowmick AR, Saha B, Roy S, Chattopadhyay J, Bhattacharya S (2015) Cooperation in species: interplay of population regulation and extinction through global population dynamics database. Ecol Model 312:150–165
17. Parthasarathy PR (1996) The effect of super infection on the distribution of infectious period–a continued fraction approximation. J Math Appl Med Biol
18. Ackleh AS, Allen LJS, Carter J (2007) Establishing a beachhead: a stochastic population model with an Allee effect applied to species invasion. Theor Popul Biol 71:290–300
19. Lande R (1993) Risks of population extinction from demographic and environmental stochasticity and random catastrophes. Am Nat 142:911–927
20. Gilpin ME, Ayala FJ (1973) Global models of growth and competition. Proc Natl Acad Sci USA 70:3590–3593
21. Fryxell JM, Mosser A, Sinclair ARE, Packer C (2007) Group formation stabilizes predator-prey dynamics. Nature 449:1041–1043
22. Saha B (2019) Chance of extinction of populations in food chain model under demographic stochasticity. Math Biosci Eng 16:3537–3560
23. Nisbet RM, Gurney WCS (1982) Modelling fluctuating population. The Blackburn Press, Caldwell

An Experimental Study on Integrated Power-Free Shock Electrodialysis for Desalination

Bhaven N. Tandel and Bibin K. Suresh

1 Introduction

Desalination advances have been utilized quickly in recent decades all through the globe to create clean drinking water from groundwater, seawater, and salty water, to improve the nature of previously existing supplies of new water for human utilization, business applications or to treat mechanical and city wastewater before reuse or release [3]. Various desalination technologies are present such as electrodialysis (ED), reverse osmosis (RO), vacuum distillation (VD), and membrane filtration (MF) can produce both freshwater and table salt from salty water with the aids of ion exchange membranes and direct current (DC) [2]. ED is an electrochemical procedure for the partition of particles across charged films or anodes starting with one arrangement then onto the next affected by an electrical potential distinction utilized as driving force. Also, the energy utilization represents practically 50% of the all-out procedure cost, for example, vitality cost, capital speculation, and operational and upkeep cost, and so forth, the sustainable power source is getting significantly more consideration for water desalination. One of the new electrochemical approaches to water purification is shock electrodialysis (SED), which is based on the emerging science of deionization shocks in porous media [1]. The SED process involves flowing feed water through a weakly charged porous slab with micrometer-sized pores that are placed between two ion-selective elements, such as ion-exchange membranes or electrodes.

At the point when current is gone through the device, zones of particle consumption and enhancement are shaped to keep up electroneutrality close to the particle

B. N. Tandel (✉) · B. K. Suresh
Sardar Vallabhbhai National Institute of Technology, Surat, India
e-mail: bnt@ced.svnit.ac.in

B. K. Suresh
e-mail: bibin18021@gmail.com

S. Kumar et al. (eds.), *Sustainability in Environmental Engineering and Science*, Lecture Notes in Civil Engineering 93,
https://doi.org/10.1007/978-981-15-6887-9_6

particular surfaces [4]. When current is passed through the shock ED cell, an ion depleted zone is formed along with an ion-selective element (the cathode). As the applied voltage is expanded, particle concentration close to this component approaches zero, and the framework can arrive at the traditional dispersion restricted current. Seawater contains a critical convergence of broke up salts. The salt concentration shifts as per spots and mainlands. Seawater concentration is communicated in saltiness, practical saltiness units. The preparation synthetic seawater sample is done by using IS 8770. It is impossible to prepare solutions that exactly duplicate the properties of seawater because the ions (salts) in which the elements occur in seawater are not always known, elements that occur in seawater in small amounts are present as contaminants in other compounds in quantities which may far exceed those that should be added and many of the salts which must be added in fairly large amounts are hygroscopic or contain water of crystallization and are difficult to weigh accurately.

2 Objectives

Desalination technologies can alleviate the water shortage problem. However, the production cost of fresh water by desalination is high due to expensive equipment, more energy consumption, and a complicated mechanism. Energy requirements in desalination can be reduced to a certain extent by reusing the rejected brine water as an electrolyte in an electrochemical cell and generate power. Hence, the current research work was taken with the following objectives:

Evaluate the efficiency of the proposed desalination system. Study the trend of electrodialysis treatment in the synthetic seawater at different concentrations and to work out, the power generated from brackish water produced from the desalinator optimization of voltage, time of reaction, and power consumption for the integrated desalination system.

3 Materials and Methodology

3.1 Constituents of Synthetic Seawater

It contains a significant concentration of dissolved salts. The salt concentration varies according to places and continents. The main constituents of synthetic seawater are given in Table 1 as per IS 8770.

It is important to determine the initial characteristics of synthetic seawater that is to be treated. The following physical and chemical parameters were analyzed. Electrical conductivity pH, salinity, solids (total suspended solids, total dissolved solids), turbidity.

Table 1 Composition of synthetic seawater

S. No.	Salt components	g/kg of solution
1	Sodium chloride	23.5
2	Magnesium	5.0
3	Sodium sulfate	3.9
4	Calcium chloride	1.3
5	Potassium chloride	0.66
6	Sodium	0.2
7	Potassium bromide	0.1
8	Boric acid	0.0260

3.2 Desalinator Setup

The reactor consists up of an electrochemical cell. DC power supply and porous medium (Silica gel having a mean diameter of 0.15–2.5 mm). The electrochemical cell is made up of fiber material and its capacity is 1 L. Aluminum plates of 16 × 6 × 0.15 cm are used as electrodes; the total effective area of the electrode is 65 sqm. The minimum amount of potential difference required for the desalination to take place in the case of saltwater is 4.07 V, why because the potential required to convert chloride ions into chlorine is −1.36 V and potential needed to reduce sodium ions into sodium is 2.7 V.

3.3 Power Generator Setup

Power generator consists of electrodes, and the electrolyte used is brine water as waste from the desalination unit. Based on the efficiency of the desalination process, brine water concentration varies. The aluminum electrodes are made up of the soft drink cans and the copper electrodes are purchased. The size of the electrodes is 20 cm × 9 cm; anode and cathode are arranged alternatively as shown in Fig. 1 with

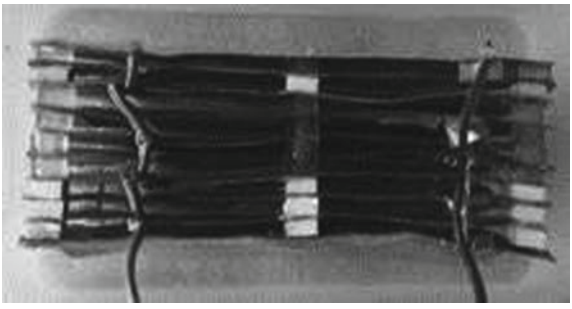

Fig. 1 Arrangement of electrodes

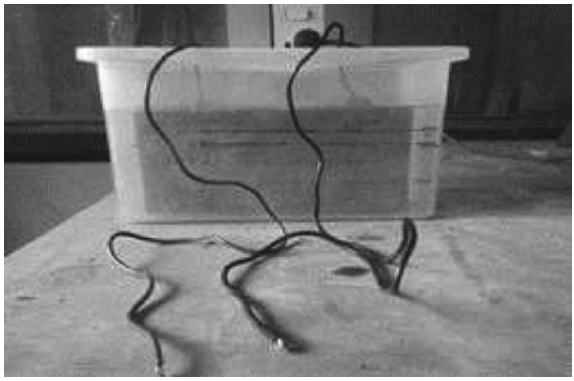

Fig. 2 Power generation cell

a spacing of 5 mm and spacers are made out of rubber. The size of the spacer is 1 cm × 1 cm × 0.5 cm and it is placed at the corner of the electrodes as well as in the middle of the length. The capacity of the reactor is 2.2 L having dimension 22 cm × 10 cm × 10 cm are the alternatively arranged electrodes copper wires are connected as shown in Fig. 2.

3.4 Experimental Procedure

Shock electrodialysis was carried out in synthetic seawater. In this treatment, a batch-wise experiment is carried out with a sample volume of 500 mL. The voltage was adjusted accordingly to experiment. At the end of ED time (0, 5, 10, 15, 20, and 25 min), the treated water was collected and characteristics were analyzed. Before each run, electrodes were washed several times with distilled water to remove impurities and dried. At the end of the run, electrodes were again washed thoroughly to remove solid residues on the surfaces, dried, and reweighed. During the electrolysis, the experimental runs were conducted for a voltage range of 5–25 V.

4 Results and Discussions

Desalination is done in the readied manufactured seawater according to IS 8770 and ASTM D1141 test with various trial conditions by shifting certain parameters, for example, applied voltage, time of response. The principle goal of the work is to think about the pattern of stun electrodialysis in the desalination, the effectiveness of the desalinator at various focuses, and the measure of electric vitality that can be delivered from the saline solution water as a waste item from desalination. After the detailed study of kinds of literature, the treatment has been carried out by keeping the pH in the above-mentioned range and the voltage is kept varied from 5 to 25 V with

an increment of 2.5 V. The treated water is taken for the analysis for the parameters like electrical conductivity, total dissolved solids, and salinity. After the detailed study, came to know that the minimum electrode potential required to separate NaCl is 4.71 V, so the treatment had been carried out by keeping minimum voltage of 5 V and reaction time staring from 0 min with a constant interval of 5 min up to 20 min. The brine water created during the treatment was utilized for power creation in the force age unit. Parameters, for example, current, power generation, and voltage are seen in the trial.

4.1 Effect of Time and Voltage on the Electrodialysis Process

Time of reaction and applied voltage has a great influence in the electrodialysis. When the applied voltage increases, the TDS concentration decreases. This is due to the movement of ions toward the respective electrodes, i.e., anions (Cl^-) will move toward cathode and cations (Na^+) to the anode. The initial application of voltage leads to the immediate separation of ions after that the process decelerates. As the applied voltage increases, the TDS concentration decreases. From Fig. 3, it is clear that there is a rapid reduction in the TDS concentration when reaction time increased from 5 to 20 min. When the voltage increased from 5 to 7.5 V, the reduction of TDS concentration was found to be 27,450–20,679 mg/L. From the above data, it is clear that maximum reduction in the TDS was found when the voltage is increased from 5 to 20 V, i.e., 31,110 to 10,449 mg/L at a reaction time of 5 min.

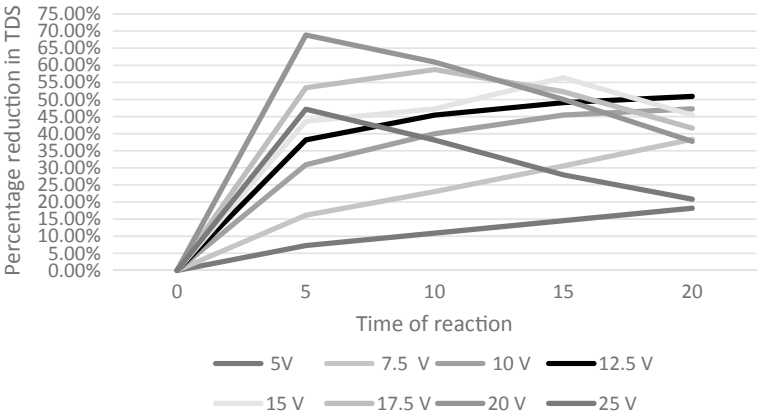

Fig. 3 Percentage reduction in TDS with respect to time of ED at different voltages

4.2 Effect of Voltage on % Removal of TDS

A maximum percentage reduction of TDS has occurred when the voltage reaches 20 V at a reaction time of 5 min. From Fig. 3, a maximum reduction of 68.13% in the TDS has occurred at a reaction time of 5 min at higher voltages 20 and 25 V. Then, the percentage reduction increases as the reaction time increases at lesser voltages, i.e., from 5 to 15 V.

4.3 Effect of Voltage on EC Reduction

From Fig. 4, it is clear that as the applied voltage increases, the electrical conductivity decreases. Reduction in electrical conductivity is because the removal of the ions from the saltwater is due to the attraction of ions toward the electrodes. The separation of ions was caused by the charged silica granules. As the voltage increased from 5 to 25 V, the current also gets increased, which leads to more separation of ions from the sample, thereby a reduction in the electrical conductivity of treated water. Due to the decrement in the EC of the treated water, there was an increment in the concentration of ions in the brine.

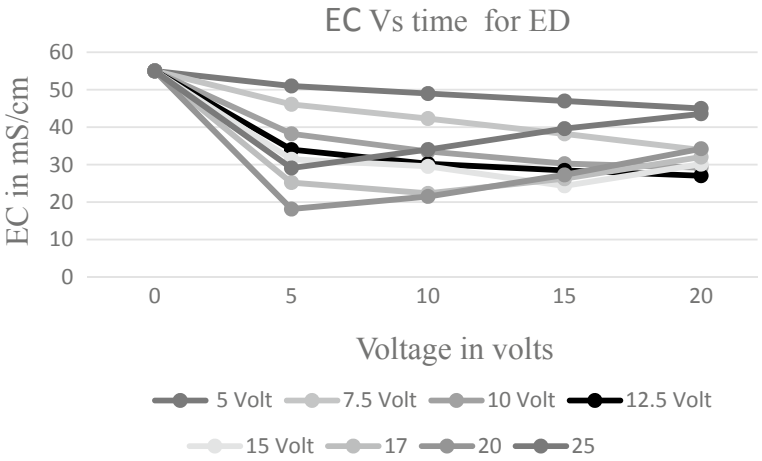

Fig. 4 Variation electrical conductivity concerning time of ED at different voltage

Table 2 Desalination at constant reaction time of 5 min and applied voltage of 20 V

S. No.	Voltage (V)	Initial EC (mS/cm)	Initial TDS (mg/L)	Final EC (mS/cm)	Final TDS (mg/L)	Current (A)	% reduction in TDS	Power consumed (W)
1	0	55	33,550	55.00	33,550	0	0	0
2	5	55	33,550	52.50	32,025	0.44	4.54545	2.2
3	10	55	33,550	38.30	23,363	0.75	30.3636	7.5
4	15	55	33,550	30.50	18,605	1.10	44.5455	16.5
5	20	55	33,550	17.12	10,443.2	1.65	68.8727	33
6	25	55	33,550	21.71	13,243.1	2.44	60.5273	61

4.4 Power Consumption at Different Voltage

The variation in the power consumption at different time intervals follows a trend such that as the time of reaction is increasing, the power consumption is also increasing and but the variation in the power consumption for a specific voltage does not have that much change, but in case of different voltages for the same time of reaction, the power consumption varies abruptly, i.e., for a reaction time of 5 min at 5 V, the power consumed is 2.25 W and it goes to 4.85 W after 10 min of reaction time, then it is increased to 7.8 W after a reaction time of 15 min (Table 2).

4.5 Optimization of Electrodialysis Process Using Response Surface Methodology (RSM)

The procedure factors, for example, voltage/current power and time of electrodialysis, were enhanced by utilizing the response surface system (RSM); central composite design (CCD) method was used for the design of the experiment. Design Expert Version 10 programming was utilized to plot the reaction surfaces. This product is likewise helpful in structuring the investigation, detailing the numerical model, and checking its sufficiency utilizing ANOVA. optimization was done dependent on TDS expulsion productivity, decrease in EC, and force utilization for engineered seawater tests.

4.6 Experimental Procedure for Optimization

The input and output information required for the improvement of numerical models were gotten through a test study led. The whole comprehension of the procedure required countless trials to be directed, which was a lot of tedious. This can be overwhelmed by receiving the trial format plan dependent on the structure of analyses

Table 3 Responses of synthetic water sample

Sample	Goal	Time for electrodialysis (min)	Voltage (V)	Electrical conductivity (mS/cm)	TDS (mg/L)	Power consumption (W)
Synthetic sample	Minimize	9.35	8.37	5.9	21,983	3.10
	In range	13.64	15.40	26.9	16,490	14.90

utilizing various levels characterized for every one of the procedure factors. The present study consists of two parameters such as voltage and time for ED are denoted as 'A' and 'B', respectively, are considered. The model is designed to investigate the effect voltage and time for electrodialysis, by considering TDS removal and power consumption as main responses for the experiment. The considered process parameters were varied up to three levels for each factor as, the upper level of a factor coded as +1, center level as 0, and the lower level as −1. CCD design was adopted to plan the experiments. The maximum and minimum limit of parameter 'A' varies from 0 to 20 min and for parameter 'B', it varies from 5 to 20 V, respectively. Summary of design of the experiment, based on CCD strategy values, is shown in Table 3. RSM is used to develop a second-order regression equation to relate response characteristics with variables. Factors A and B represent the time for electrodialysis and voltage or current density, the range in which the optimization was carried out for time was from 0 to 20 min and for voltage from 5 to 20 V.

4.7 Summary of Responses for Synthetic Seawater Sample

Responses R1, R2, and R3 correspond to electrical conductivity, TDS, and power consumption, respectively. In the central composite design (CCD) method, a total of 13 numbers of experimental results is obtained. For response R1 (EC) minimum limit is 22.5 and maximum limit of 55 mS/cm, and in the case TDS (R2), minimum and maximum limit corresponds to 13,725 and 33,550 mg/L and the model is quadratic for the three responses.

Optimization refers to the process of meeting the optimum values of process variables to get the desired output. In this work voltage, the time of electrodialysis was the process variables that were optimized to produce a maximum removal of TDS on treating the synthetic seawater samples using the electrocoagulation process. The goal on optimizing the process variables was kept to be a minimum to make the process economical for the synthetic wastewater, optimum voltage and time of ED were found to be 13.64 min and 15.40 V, respectively, corresponding brine water conductivity is 73.34 mS/cm and the power consumption is 14.90 mW (Table 3).

Table 4 Electrodialysis on synthetic seawater at different NaCl molar conc. and a reaction time of 5 min

S. No.	NaCl conc. (M)	Initial EC (mS/cm)	Final EC (mS/cm)	Initial TDS (mg/L)	Final TDS (mg/L)	% reduction in TDS	Current (A)	Power consumed (W)
1	0.1	9.9	2.74	5940	1644	72.32	1.03	20.6
2	0.2	18.0	5.42	10,800	3252	69.89	1.17	23.4
3	0.3	29.4	9.27	17,640	5562	68.47	1.31	26.2
4	0.4	40.0	13.4	24,000	8040	66.50	1.44	28.8
5	0.5	48.5	17.1	29,100	10,260	64.74	1.65	33

4.8 Electrodialysis on Synthetic Seawater at Different NaCl Molar Concentration

To understand the performance of the desalination unit, synthetic seawater sample is prepared by varying the molarity of NaCl from 0.1 to 0.5 M. As the concentration of synthetic sample increases, the efficiency of the desalination system also increases (Table 4).

4.9 Results of Power Generation

From Fig. 5, it is clear that variation in the power generation concerning electrical conductivity follows a common trend such that power generated is almost constant up to a time of 20–25 min in the case of samples with different electrical conductivity

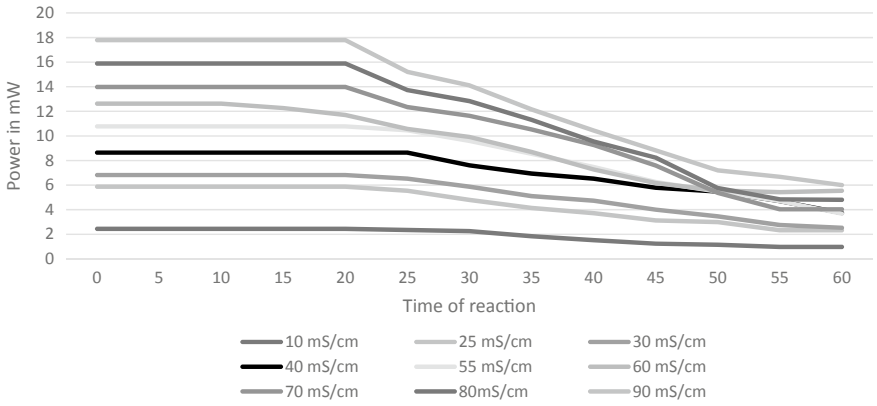

Fig. 5 Variation of power generated at different electrical conductivity of brine water concerning time

varying from 10 to 90 mS/cm. But the voltage of the electrochemical cell or the power generator is almost constant, i.e., 0.48 V and maximum power produced 17.79 mW at EC of 90 mS/cm. In this study, the electrical conductivity restricted to 90 mS/cm because brine water conductivity at maximum TDS removal condition is 79.89 mS/cm.

5 Conclusion

In this study, the SED process has been assessed for desalination of seawater experiments were done on synthetic seawater sample. Shock electrodialysis was observed to be successful in the experiments. SED process factors, for example, voltage/current density, time of electrodialysis were optimized by response surface methodology. Maximum TDS removal (68.13%) and EC reduction (18.13 S/cm from 55 mS/cm) were observed at the voltage of 20 V and a reaction time of 5 min. The power consumed during this reaction time was 48.80 W for treating a 500 mL of sample. And the brine solution rejected at this reaction phase has an EC of 79.58 mS/cm which can generate a power of 15.889 mW from an electrode area of 924 cm^2. By varying the concentration of seawater (NaCl concentration), desalinator shows a trend that as seawater concentration increases, efficiency decreases. Maximum efficiency (73.12%) was observed at a lesser concentration (0.1 M). Optimization was done by varying the applied voltage and time of electrodialysis. Improvement in optimization for synthetic sample was obtained by Response surface method. According to RSM, an optimized voltage was observed to be 13.64 V at a reaction time 15.40 min. Electrical conductivity was decreased to 26.9 mS/cm from 33,550 mg/L, TDS decreased to 16,490 mg/L from 33,550 mg/L and power consumption was 14.90 W. And the rejected brine solution has an electrical conductivity of 73.66 mS/cm produced 14.67 mW of power as per RSM.

References

1. Deng D, Dydek EV, Han J, Schlumpberger S, Mani A, Zaltzman B, Bazant MZ (2013) Overlimiting current and shock electrodialysis in porous media
2. Khawaji AD, Kutubkhanah IK, Wie JM (2008) Advances in seawater desalination technologies. Desalination 221(1–3):47–69
3. Le NL, Nunes SP (2016) Materials and membrane technologies for water and energy sustainability. Sustain Mater Technol 7:1–28
4. Schlumpberger S, Lu NB, Suss ME, Bazant MZ (2015) Scalable and continuous water deionization by shock electrodialysis. Environ Sci Technol Lett 2(12):367–372

Brassica Juncea (L.) Czern. (Indian Mustard): A Potential Candidate for the Phytoremediation of Mercury from Soil

Deep Raj and Subodh Kumar Maiti

1 Introduction

Mercury (Hg) is a global threat due to its high toxicity in nature. It has long-term persistence and high mobility in the air [3]. The soil, air, and water contamination due to the presence of Hg are the serious concern to the human beings [9, 10]. The global average background range of Hg concentrations in various soil types was found to be 0.58–1.8 mg/kg with mean value of 1.1 mg/kg [4]. In recent times, the Hg concentrations in soils have been increased by a factor of 3–10 due to the burning of coal in thermal power plants [14]. Due to the increasing Hg pollution in soil, its remediation has become an urgent task for the welfare of human beings [15].

Several techniques have been proposed for Hg removal from soil. Some of them are immobilization, chemical treatment, adsorption, electro-remediation, physical separation (soil washing), and thermal desorption [9, 10]. Among all the remediation techniques, the phytoremediation has emerged as widely accepted and best approach for the removal of Hg from soil. Phytoremediation is an environmentally friendly and cost-effective techniques for Hg removal from soil. This technique does not require any toxic chemicals, costly equipment, and any heat treatment [12].

Plant species like *Jatropha curcas*, *Pistia stratiotes*, *Azolla pinnata*, and *Cyrtomium macrophyllum* have been reported as the good accumulator of Hg. These plants are known to have the excellent Hg translocation abilities along with the high resistance capacities to Hg stress [6, 7, 15]. *B. juncea* (Indian mustard) is also considered as the promising candidate for the removal of Hg from highly contaminated soil [11]. Xun et al. [15] examined the phytoremediation efficiency of a wild plant species

D. Raj · S. K. Maiti (✉)
Indian Institute of Technology (Indian School of Mines), Dhanbad, India
e-mail: subodh@iitism.ac.in

D. Raj
e-mail: deepraj2587@gmail.com

S. Kumar et al. (eds.), *Sustainability in Environmental Engineering and Science*, Lecture Notes in Civil Engineering 93,
https://doi.org/10.1007/978-981-15-6887-9_7

(*C. macrophyllum*), and found that the plant species could grow better even at high Hg concentration of 500 mg/kg in the soil without any observed toxic symptoms. Similarly, Marrugo-Negrete et al. [6] reported that *J. curcas* grew well on the soil with Hg concentration of 10 mg/kg.

The objective of this study is to analyze the potential of *B. juncea* to remediate Hg from contaminated soil at various contamination levels (10, 50, and 100 mg Hg/kg of soil). The Hg accumulation in the plant's tissue (root, stem and leaf) was examined at 30th, 60th, and 90th day of the exposure. The volatilization of Hg at different exposure from Hg-treated blank soil (without the plantation of the plant) was also determined.

2 Materials and Method

The non-contaminated and pre-analyzed garden soil was collected at depth of 0–30 cm from the garden of department of environmental science and engineering, II(ISM), Dhanbad, India. The collected soil samples were air dried for 48 h. Further, the samples were homogenized and sieved through <2 mm stainless steel sieve. The seeds were collected from matured *B. juncea* plants growing on uncontaminated soils with Hg. The similar sized seeds were selected without any visible blot and submerged in 10% (v/v) solution of sodium hypochlorite for 15 min followed by the rinsing with de-ionized water (Millipore, USA). The experiment was based on pot-scale study, which was established on the basis of randomized block design. The entire set-up was performed in an open garden of department of environmental science and engineering, IIT(ISM), Dhanbad, for the period of 90 days. A total of three treatments of Hg (T10, T50 and T100) were prepared through proper and uniform mixing of mercury chloride ($HgCl_2$) to the garden soil. The three treatments of known Hg concentrations were 10, 50, and 100 mg Hg/kg in the soil. A total of 7 kg of soil was kept in each pot and Hg was mixed as the salt of $HgCl_2$. After the Hg treatment, 20 seeds were sown immediately to each pots. The experiment was carried-out in three-replicates during dry winter season (November–January). Hg-free water was sprinkled in the pots at the regular interval.

After the exposure of 30th, 60th, and 90th day, the plant and soil samples were collected from the pots of every Hg treatments. The soil samples were also collected from the pots containing blank soils in which no seeds of *B. juncea* was sown. Initially, the plant samples were separated into roots, stems, and leaves. Further, the plant's tissues were washed three times with de-ionized water to remove the adhered soil particles. The roots, stems, and leaves tissues were oven dried at 40 °C and powdered in a mortar and pestle. The fine-sized accurately weighed (0.5 g) plant samples were subjected to microwave-assisted digestion (Ethos One, Milestone Srl, Italy) in an acid solution of HNO_3/H_2O_2 (5 + 2 mL) [5]. The oven dried, properly sieved (100 mesh), and accurately weighed (0.5 g) soil samples were also digested in a microwave digester at the temperature of 90 °C by using acid mixture of HNO_3 and HCl (1:3, v/v) [5, 6, 11]. Afterwards, the digested soil and plant samples were

filtered through Whatman#42 filter paper (pore size, 2.5 μm) and diluted with de-ionized water. Hg was analyzed in cold vapor-atomic absorption spectrophotometer (CV-AAS, GBC Avanta, Australia). ANOVA test was applied to the submitted data through which and the difference between the average Hg concentrations in various treatments were determined. The average concentrations were presented in triplicate.

3 Results and Discussion

3.1 Hg Concentration in Plant's Tissues (Root, Stem, and Leaf)

Hg was accumulated by the plant tissues in decreasing order of roots > stems > leaves at the 30th day of exposure, while the order was found as roots > leaves > stems at the 60th and 90th day of exposure in all the treatments (Fig. 1). The concentrations of Hg in roots and the aerial parts (leaves) were generally increased with the increase in Hg treatments and exposure time. The results were consistent with the results of other studies, which have also reported the increased level of Hg in roots than shoots due to the direct exposure of Hg to the roots in soils [2, 5]. The highest amount of Hg was found to be accumulated during the third month of exposure in all the treatments, which showed that the increasing exposure duration support the uptake of Hg to the roots from soils. The presence of high amount of Hg in the root's cell wall prevents the toxic effects in the aerial parts of the plants [13]. Xun et al. [15] also reported the

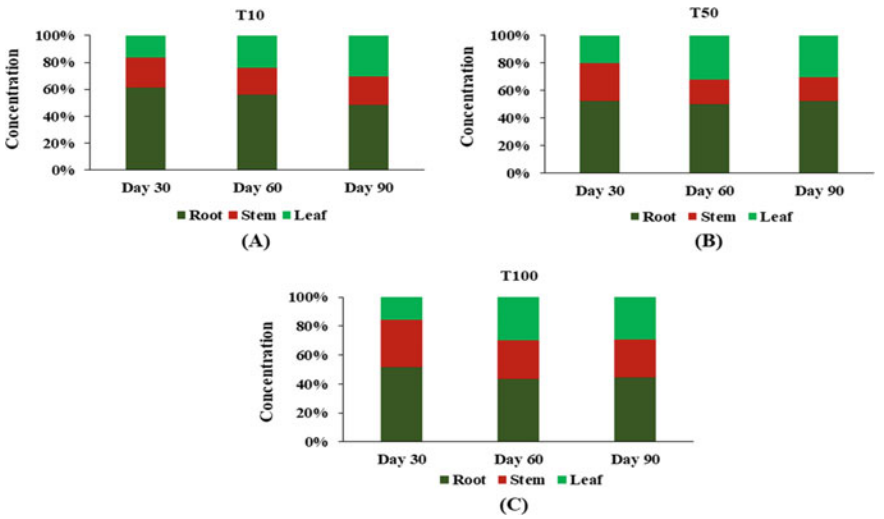

Fig. 1 Hg accumulation in plant's root, stem and leaf at day 30, 60, and 90 in Hg-treated soils **a** T10; **b** T50 and **c** T100

Table 1 Phytoremediation of Hg through various plant species

S. No.	Plant species	Hg concentrations level in the substrate	References
1	*Cyrtomium macrophyllum*	5, 10, 20, 50, 100, 200, 500, and 1000 mg/kg	[15]
2	*Jatropha curcas*	5, 10, 20, 40, and 80 μg Hg/mL	[6]
3	*Jatropha curcas*	1, 5, and 10 μg Hg per g soil	[5]
4	*Pistia stratiotes*	10 μg/L	[7]
5	*Azolla pinnata*	10 μg/L	
6	*Brassica juncea*	100 and 500 mg/kg	[11]
7	*Polypogon monospeliensis*	250, 500, and 1000 mg/kg	
8	*Pteris vittata*	250, 500, and 1000 mg/kg	

high accumulation of Hg in the root parts of a wild plant species of *C. macrophyllum* (Table 1). The Hg concentrations in the plant's leaves growing on the treatment of 10 mg Hg/kg (T10) of soil were 0.24, 1.25, and 2.49 mg/kg at 30th, 60th, and 90th day of exposure, whereas the concentrations were 1.90, 9.28, and 11.99 mg/kg in the treatments of 50 mg Hg/kg (T50) of soil after the first, second, and third months of exposure, respectively. A total of 2.88% Hg was accumulated in the leaf tissue at 30th day of exposure in the treatment of 100 mg Hg/kg of soil (T100), while the percentage Hg accumulations during second and third months of exposure were 16 and 19%, respectively, in the same treatment. According to Moreno et al. [8], the final recipient of Hg in plant is leaf, and contains higher Hg than stems. This is explained by the changes in oxidation state of Hg from Hg^{2+} to Hg^0, since Hg^0 is phytochelated and accumulated into the cell's vacuoles due to the development of toxic resistance mechanism. The lesser Hg accumulation in stems than leaves during the 2nd and 3rd month of exposure in all the three treatments could be related to the primary function of stem. The transport of water, food, and minerals to the aerial parts of the plant are the primary function of stem. So, along with food and minerals, stem also transports metals to the superior part of the plant. Therefore, metals do not get accumulated in the higher amount to the stem tissues of the plant [1].

3.2 Volatilization of Hg from Hg-Treated Blank Soil at 30th, 60th, and 90th Day of Exposure

In this experiment, Hg content was determined in the Hg-treated blank soil (without the plantation of *B. juncea*) to know the remaining Hg concentration after the volatilization of Hg from the soil. At the 30th, 60th, and 90th day, the remaining Hg contents in the blank soil treated with 10 mg Hg/kg, were found to be 9.98, 9.6, and 9.21 mg Hg/kg, respectively. At 30th day, Hg concentrations in 50 and 100 mg/kg

Table 2 Amount of Hg (mg/kg) remaining in Hg-treated blank soil (without plantation of *B. juncea*) after the volatilization of Hg

Treatments/exposure duration	T10	T50	T100	T0
Day 30	$9.98^{a} \pm 0.015$	$49.46^{a} \pm 0.378$	$99.23^{a} \pm 0.886$	Not detected
Day 60	$9.6^{a} \pm 0.108$	$49.18^{a} \pm 0.312$	$98.59^{a} \pm 1.02$	Not detected
Day 90	$9.21^{b} \pm 0.308$	$49.03^{a} \pm 0.37$	$97.70^{b} \pm 0.596$	Not detected

Different alphabets in the same column for the same treatment of Hg represent the significant difference at $p < 0.05$ according to Duncan's multiple tests. One soil samples were collected from each pot (three pots) of the same treatment ($n = 3$)

Hg-treated blank soil, were 49.46 and 99.23 mg/kg, respectively. The result demonstrated that in all the three treatments, the rate of Hg volatilization from the soil was not significantly different at 30th and 60th day of the exposure [1]. The accumulation and deposition of Hg was not observed in the pot (control), in which Hg was not added to the soil (Table 2).

4 Conclusions

The present study demonstrated that the development and growth of *B. juncea* plants occurred in the soil with high Hg concentrations (up to 100 mg/kg). The maximum concentrations of Hg was found in the root tissue of the plant followed by leaf and stem at 60th and 90th day of exposure in all treatments. The maximum removal of Hg from the soil was reported after the third month of exposure in all the treatments. The results of the study have expanded our knowledge on phytoremediation of Hg through *B. juncea* plant growing on the soil of contamination level up to 100 mg Hg/kg.

Acknowledgements The authors are highly indebted to the Ministry of Human Resource Development (Govt. of India) and IIT (ISM), Dhanbad, for providing research fellowship and basic research facilities.

References

1. Alloway BJ (2013) Sources of heavy metals and metalloids in soils. In: Heavy metals in soils. Springer, Dordrecht, pp 11–50
2. Cargnelutti D, Tabaldi LA, Spanevello RM, de Oliveira Jucoski G, Battisti V, Redin M, Linares CEB, Dressler VL, de Moraes Flores EM, Nicoloso FT, Morsch VM (2006) Mercury toxicity induces oxidative stress in growing cucumber seedlings. Chemosphere 65(6):999–1006
3. Du W, Zhang CY, Kong XM, Zhuo YQ, Zhu ZW (2018) Mercury release from fly ashes and hydrated fly ash cement pastes. Atmos Environ 178:11–18
4. Kabata-Pendias A (2010) Trace elements in soils and plants. CRC Press, Boca Raton

5. Marrugo-Negrete J, Durango-Hernández J, Pinedo-Hernández J, Olivero-Verbel J, Díez S (2015) Phytoremediation of mercury-contaminated soils by *Jatropha curcas*. Chemosphere 127:58–63
6. Marrugo-Negrete J, Durango-Hernández J, Pinedo-Hernández J, Enamorado-Montes G, Díez S (2016) Mercury uptake and effects on growth in *Jatropha curcas*. J Environ Sci 48:120–125
7. Mishra VK, Tripathi BD, Kim KH (2009) Removal and accumulation of mercury by aquatic macrophytes from an open cast coal mine effluent. J Hazard Mater 172(2–3):749–754
8. Moreno FN, Anderson CW, Stewart RB, Robinson BH (2008) Phytofiltration of mercury-contaminated water: volatilisation and plant-accumulation aspects. Environ Exp Bot 62(1):78–85
9. Raj D, Maiti SK (2019) Bioaccumulation of potentially toxic elements in tree and vegetable species with associated health and ecological risks: a case study from a thermal power plant, Chandrapura, India. Rendiconti Lincei. Scienze Fisiche e Naturali 30(3):649–665
10. Raj D, Maiti SK (2019) Sources, toxicity, and remediation of mercury: an essence review. Environ Monit Assess 191(9):566
11. Su Y, Han FX, Chen J, Sridhar BM, Monts DL (2008) Phytoextraction and accumulation of mercury in three plant species: Indian mustard (*Brassica juncea*), beard grass (*Polypogon monospeliensis*), and Chinese brake fern (*Pteris vittata*). Int J Phytorem 10(6):547–560
12. Wang J, Feng X, Anderson CW, Xing Y, Shang L (2012) Remediation of mercury contaminated sites—a review. J Hazard Mater 221:1–18
13. Wang Y, Greger M (2004) Clonal differences in mercury tolerance, accumulation, and distribution in willow. J Environ Qual 33(5):1779–1785
14. Xu J, Bravo AG, Lagerkvist A, Bertilsson S, Sjöblom R, Kumpiene J (2015) Sources and remediation techniques for mercury contaminated soil. Environ Int 74:42–53
15. Xun Y, Feng L, Li Y, Dong H (2017) Mercury accumulation plant *Cyrtomium macrophyllum* and its potential for phytoremediation of mercury polluted sites. Chemosphere 189:161–170

Stabilization of Expansive Soil Using Saw Dust

Gargi De, Shamim Raja, and Avishek Mukherjee

1 Introduction

For every country, the budget required by the transportation department is huge for the replacement and maintenance of the pavements. Hence, we need to find some sustainable materials or methods to reduce the cost of maintenance of the pavements as also to increase the life span of the pavements, which will be more economical and can be completed within limited budgets. A great variability in the characteristics of the subgrade of the soil may lead us to the application of conservative estimate which may result in the design of thicker pavement with rise in construction cost and large maintenance cost. To avoid these problems, new methods have to be developed to minimize the variability of subgrade characteristics.

Expansive soil has the property of swelling when moisture is added to it and to shrink when the moisture is removed. These sudden changes of volume in expansive soils cause many problems to the structure which come in contact with them or are constructed above them. In India, the expansive soils have liquid limit value from 40 to 100%, and their plasticity index value ranges between 20 and 65%.

G. De (✉) · S. Raja · A. Mukherjee
Amity University Kolkata, Newtown, Kolkata, India
e-mail: gargi09@hotmail.com

S. Raja
e-mail: shamimraja.1994@gmail.com

A. Mukherjee
e-mail: amukherjee1@kol.amity.edu

S. Kumar et al. (eds.), *Sustainability in Environmental Engineering and Science*, Lecture Notes in Civil Engineering 93,
https://doi.org/10.1007/978-981-15-6887-9_8

Table 1 Degree of expansiveness

Expansiveness	DFS (%)
Low	<20
Moderate	20–35
High	35–50
Very High	>50

2 Objectives of Study

Limited research work is available on the effect of saw dust for different soil properties of expansive soil. The current paper discusses the properties of locally available expansive soil.

Expansive soil and saw dust mixed into it in different proportions. Index properties (plastic limit, liquid limit, plasticity index), compaction properties (OMC and MDD), direct shear test (DST) are considered in this investigation.

Most commonly for the improvement of soil, stabilized additives which improve properties of soil by physical and chemical changes are used. Before modification or stabilization of soil, the behaviour of the fine soils is to be studied well, for achieving the following goals:

1. To evaluate the index property of soil.
2. To study the effect of saw dust on Atterberg's limits of soil.
3. To study the effect of saw dust on soil by CBR test (Table 1).

3 Expansive Soil

Expansive soil is a type of soil that has a tendency for huge volume changes (swelling along with shrinking) which are directly relatable with the change in percentage of water content. In drier seasons of the years, the soils having more quantity of expansive minerals may form deep cracks; these types of soils are generally termed as vertisols. Soils having smectite clay minerals, which include montmorillonite and bentonite, have greater capacity to shrink and swell.

Expansive soil is the type of soil which exhibits moderate to high plasticity, low to moderate strength and shows characteristics of swelling and shrinking. They generally show large volume changes under change of moisture conditions. Such soils are usually found in semi-arid and arid areas of world such as India, Israel, UK, USA, Italy and China. 20% of India's land area have expansive soil which also include almost entire Deccan plateau, western Madhya Pradesh, Maharashtra, parts of Gujarat, Andhra Pradesh, Uttar Pradesh and Karnataka. In our country, the typical example of expansive soils are black cotton soil, mar and kabar. Mainly three factors which play important role in shrinkage and swelling properties of soil are (i) soil properties like compaction, dry density, natural moisture content variation and

plasticity index, (ii) environmental conditions like humidity and temperature and (iii) foundation loading condition and natural overburden pressure (Figs. 1 and 2).

Saw Dust: Saw dust is a by-product that generates from wood cutting factories. At the time of cutting of trees, we generally get about 78% of its weight, and the rest weight around 22% of the total trees is received as saw dust. Saw dust is mainly used as a fuel in brick factories to generate heat in the kiln.

As day by day transportation system is expanding, the desire for more stable foundation for embankments of roads is increasing. The huge earthwork required for such systems is unacceptable due to the long-term settlement and the shear failure

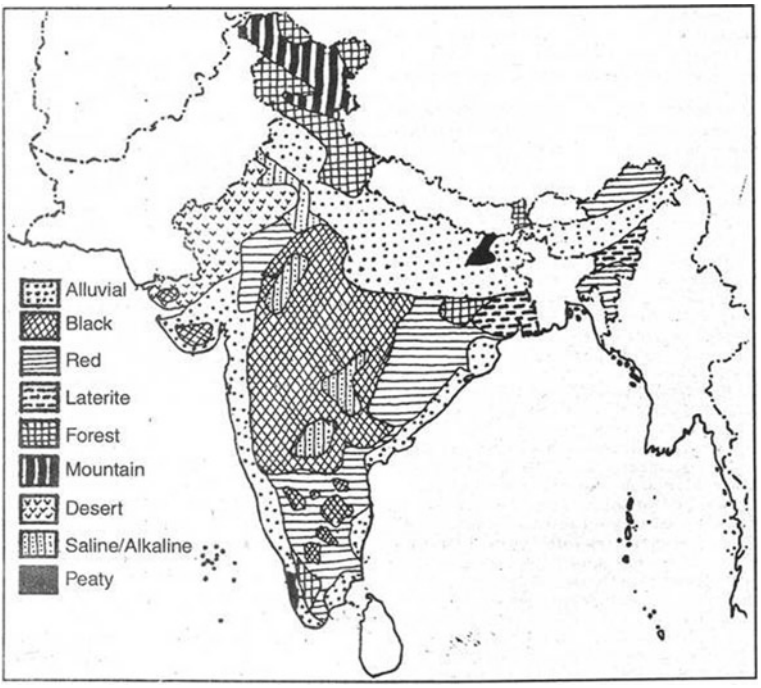

Fig. 1 Major soil types in India

Fig. 2 Saw dust sample

Table 2 Chemical composition of saw dust [3]

Chemical composition	Amount in %
SiO_2	86
Al_2O_3	2.60
Fe_2O_3	1.80
CaO	3.60
MgO	0.27
Loss in ignition	4.20

of the soil deposits. The alternative such as geofoam provides a very lightweight embankment fill, but there are some disadvantages of such material as fire hazards and less economical, whereas using saw dust is known to be economical and also lightweight for soil filling and ground improvement technique (Table 2).

4 Laboratory Studies

The laboratory tests were conducted on the expansive soil sample (expansive soil + saw dust) collected from Haroa bricks field.

4.1 Standard Proctor Compaction Test

Preparation of soil sample for proctor compaction test was done to determine optimum moisture content and max. Dry density of the soil sample as per IS: 2720 part-6 (1974).

Liquid limit: Liquid limit test was performed on expansive soil + saw dust using Casagrande's liquid limit apparatus as per the procedures laid down in IS: 2720 part 4 (1970).

Plastic limit: Plastic limit test was performed on expansive soil + saw dust as per the specifications laid down in IS: 2720 part 4 (1970).

Plasticity Index: This test is also performed on expansive soil + saw dust as per IS: 2720 part 5 (1985).

California bearing ratio Test: The California bearing ratio tests are performed on expansive soil, expansive soil + saw dust mixtures as per IS 2720 part 16 (1979). The test was performed under a constant strain rate of 1.25 mm/min. The proving ring reading is taken for each 50 divisions, and loading was recorded until three (or) more readings are gradually decreasing (or) constant. The test was performed at OMC. The samples were tested in unsoaked condition.

Direct Shear Test: Direct shear test is also conducted on expansive soil + saw dust to determine C and ϕ of the soil sample as per IS: 2720 part 13 (1986).

5 Results and Discussion

5.1 Effect of Saw Dust on Proctor Compaction Tests

Many tests were conducted to get the optimum moisture content and max. Dry density of the mix of different proportions of soil and saw dust using standard proctor compaction machine (Table 3; Figs. 3 and 4).

During the observation, it was observed that maximum dry density is increased and the moisture content is decreased by adding of saw dust from 0 to 15% and also observed that the moisture content is increased and maximum dry density has increased primarily and then decreased by adding of saw dust from 15 to 25%.

Table 3 OMC and MDD values of expansive soil with saw dust

Mix proportion	Water content (%)	Dry density (kN/m^3)
Pure soil	28	13.1
95%soil + 5%SD	24.5	13
90%soil + 10%SD	23.5	13.2
85%soil + 15%SD	22	13.3
80%soil + 20%SD	24.5	13.2
75%soil + 25%SD	25	12.9

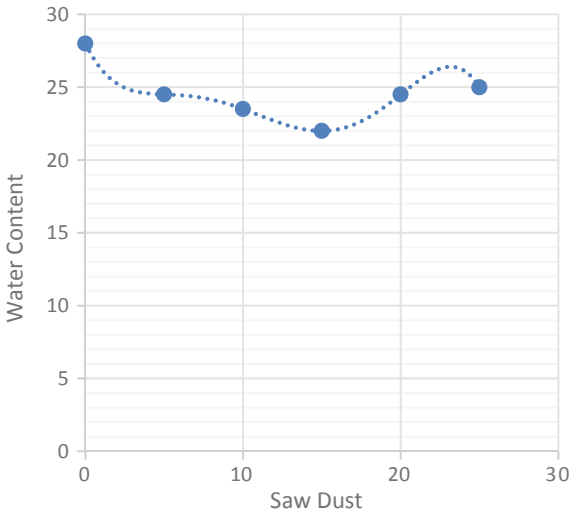

Fig. 3 Saw dust % versus water content

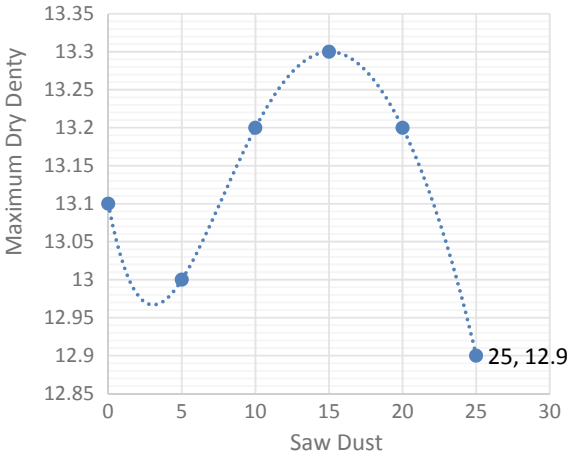

Fig. 4 Saw dust % versus maximum dry density

5.2 *Effect of Saw Dust on Atterberg's Limits of Soil*

With increase in percentage of saw dust, the liquid limit of soil is found to be decreasing from 0 to 15% and increasing from 15 to 25%. From the graph, the optimum liquid limit of the soil is found by adding 14% of saw dust (Tables 4 and 5; Figs. 5 and 6).

Table 4 Effect of saw dust on liquid limits

Saw dust (%)	Liquid limit (%)
0	48
5	45.8
10	45
15	44.4
20	46.5
25	47.8

Table 5 Effect of saw dust on plastic limits

Saw dust (%)	Plastic limit (%)
0	26.19
5	30.159
10	33.868
15	34.921
20	34.343
25	32.28

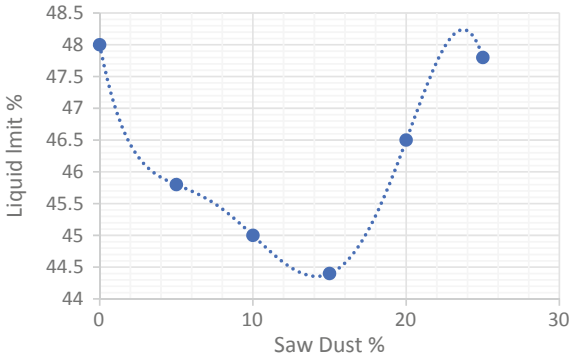

Fig. 5 Saw dust% versus liquid limit %

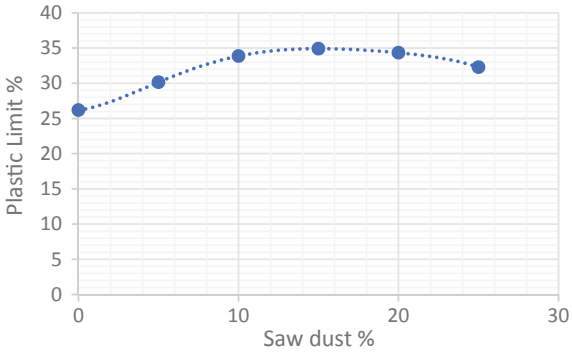

Fig. 6 Saw dust% versus plastic limit%

5.3 Effect of Saw Dust on Plasticity Index

The optimum plasticity index of the soil is found by adding about 14% of saw dust (Table 6; Fig. 7).

Table 6 Effect of saw dust on plasticity index

Saw dust (%)	Plasticity index (%)
0	21.81
5	15.641
10	11.132
15	9.4794
20	12.157
25	15.52

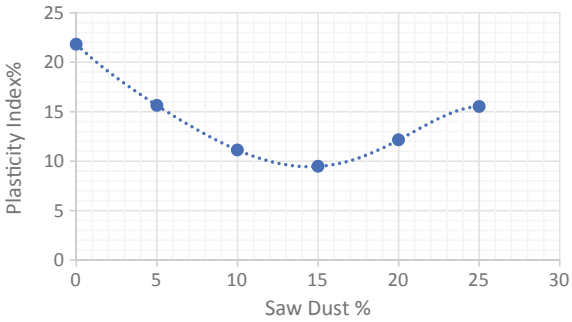

Fig. 7 Saw dust% versus plasticity index%

Table 7 Variation of CBR with saw dust

Mix proportion	Water content (%)	CBR
Pure soil	28	2.9401
95%soil + 5%SD	24.5	3.2378
90%soil + 10%SD	23.5	3.5728
85%soil + 15%SD	22	4.1496
80%soil + 20%SD	24.5	3.9821
75%soil + 25%SD	25	3.0889

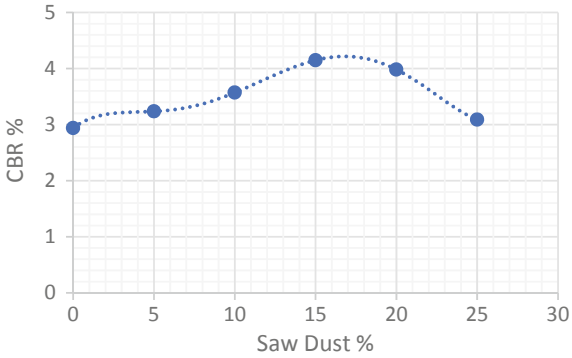

Fig. 8 Variation of CBR % with saw dust

5.4 Effect of Saw Dust on CBR Tests Result

It is seen that the optimum value of saw dust is about 17% (Table 7; Fig. 8).

5.5 Effect of Saw Dust on Direct Shear Test

See Table 8 and Figs. 9 and 10.

Table 8 Effect of saw dust in cohesion and ϕ

Mix proportion	Cohesion (C)	Angle of friction (ϕ)
Pure soil	0.85	8
95%soil + 5%SD	0.77	10
90%soil + 10%SD	0.72	12.6
85%soil + 15%SD	0.65	14.5
80%soil + 20%SD	0.56	17.4
75%soil + 25%SD	0.44	19.8

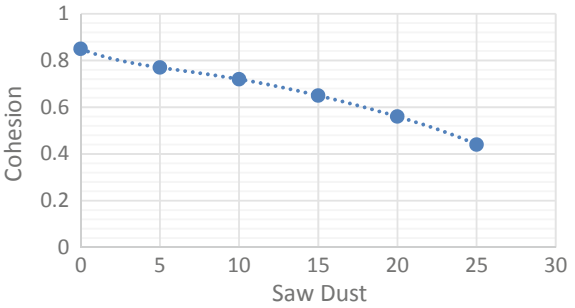

Fig. 9 Variation of cohesion with saw dust%

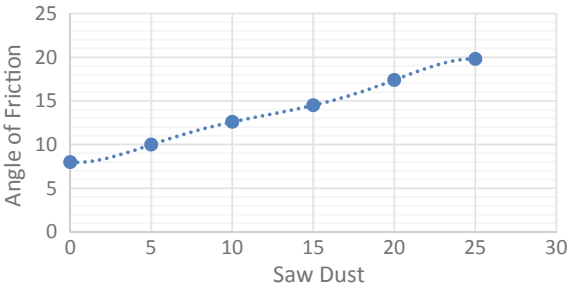

Fig. 10 Variation of angle of friction with saw dust %

6 Conclusion

The liquid limit of the soil has decreased from 48 to 44.3% with the addition of 14% saw dust and has increased with addition of more saw dust.

The plastic limit of the soil has increased from 26.19 to 34.92% with the addition of 15.6% saw dust. Further, it is noticed that the plastic limit of the soil has decreased with addition of more saw dust.

The OMC of the soil has decreased from 28 to 22% with increase of saw dust up to 15%, and further, OMC of the soil has increased with the addition of more saw dust.

It is found from the results that the MDD of the soil has increased from 13.1 to 13.3 kN/m^3 on addition of 15% saw dust. On further addition of saw dust, MDD of the soil decreased.

It is observed from the results that the CBR value of the soil increases as percentage of saw dust increases up to 15% and then decreases on further addition. So, we found that the optimum amount of saw dust for CBR is 15%.

With the addition of saw dust up to 25% to the soil, cohesion of the soil has decreased continuously and vice versa for the angle of internal friction.

References

1. Naranagowda MJ (2015) Effect of saw dust ash and fly ash on stability of expansive soil. Int J Res Eng Technol
2. Butt WA, Gupta K, Jha JN (2016) Strength behavior of clayey soil stabilized with saw dust ash. Int J Geo-Eng
3. Koteswara RD et al (2012) A laboratory study on the stabilization of marine clay using saw dust and lime. Int J Eng Sci Adv Technol 2(4):851–862
4. Prasad ASSV, Ashok NAS (2016) Stabilization of marine clay with saw dust and lime for pavement subgrades. Int J Sci Res Dev 4(07):1033–1037
5. Twinkle S, Sayida MK (2011) Effect of polypropylene fibre and lime admixture on engineering properties of expansive soil, pp 2–5
6. Subramanyam LS, Babu YSGG, Raju GVRP (2015) Evaluation of efficacy of chemical stabilizers on expansive soil. Int J Curr Eng Technol 5(6):3888–3895
7. IS: 2720 part-4 (1975) Grain size analysis
8. IS: 2720 part-6 (1974) Determination of Dry density and Optimum moisture content
9. IS: 2720 part-40 (1977) Determination of Free Swell Index
10. IS: 2720 part-5 (1970) Determination of Liquid limit and Plastic limit
11. IS: 2720 Part-16 (1979) Determination of California bearing ratio
12. IS 2720-16 (1987) Laboratory determination of CBR
13. IS 2720-13: part 13: Direct shear test

Analysing the Influence of Groundwater Exploitation on Its Quality in Kolkata

Bernadette John, Priyanka Roy, and Subhasish Das

1 Introduction

Groundwater is one of the most important sources of freshwater. Around half of the world's population is dependent on groundwater for their daily needs, and more than 40% of the world's water for irrigation is extracted from groundwater. The usage of groundwater entirely depends on its quality and quantity. Over exploitation of the resource might also lead to the deterioration of its quality. There are several factors affecting the groundwater quality like landuse/landcover and soil type [1].

In developing countries, the water usually gets contaminated by anthropogenic influence. The water to be in use needs to meet the national and international standards failing which it will lead to several health ailments [2]. According to The Pollution Control Board under Government of India, there is a large gap between generation, collection and treatment of wastewater. The untreated water pollutes the surface water and also finds an inlet in the groundwater, thus polluting it. Major groundwater problems are caused by contamination, over exploitation or both [3].

Though the groundwater of the city is free from arsenic contamination which is present in many deltaic plains, it suffers from the problem of iron and chloride contamination [4]. Many tube wells in the city have been abandoned since it has been iron infected. Apart from this, the groundwater has high dissolved salts due to which the tube wells need to be abandoned after a certain period of usage. The groundwater quality is also getting affected by the presence of dissolved magnesium and calcium,

B. John (✉) · P. Roy · S. Das
School of Water Resources Engineering, Jadavpur University, Kolkata, India
e-mail: bernadettejohn1@gmail.com

P. Roy
e-mail: roypriyanka2604@gmail.com

S. Das
e-mail: subhasishju@gmail.com

S. Kumar et al. (eds.), *Sustainability in Environmental Engineering and Science*, Lecture Notes in Civil Engineering 93,
https://doi.org/10.1007/978-981-15-6887-9_9

leading to water hardness problems. The city thus suffers both from the problem of groundwater quality and its depletion. The excessive withdrawal of groundwater is due to a shortage of treated water supply.

Groundwater quality gets degraded naturally as well as by human interference. Variation in groundwater quality in an area gets mainly influenced by geology and human activities. The over exploitation of the resource is leading to its degradation. Once the pollutants enter the sub-surface, it remains there for many years and get dispersed. Hence, the management of the resource becomes important [5].

The present research is an attempt to study the relationship between groundwater quality and groundwater level, if any, for the city of Kolkata. The impact of the excessive withdrawal of groundwater on its quality. The effect of lowering of groundwater is witnessed in land subsidence, but its effect on the quality needs to be assessed. The Bureau of Indian Standard [6] has been considered to assess the suitability of groundwater for drinking purposes and for the calculation of WQI [7].

2 Location of the Study Area

The study areas are situated in the Kolkata district of West Bengal, consuming a geographic area of 187.33 km^2. The district lies between 22.5726° North latitude and 88.3639° East longitude. Kolkata is bounded in the north and east by North 24 Parganas district and in the south by South 24 Parganas district along with Howrah district in the west. The area experiences a tropical climate with maximum temperature of around 40 °C and a minimum temperature of around 10 °C, accompanied by an average rainfall of 1647 mm. The entire district is divided into eight stations for monitoring groundwater and its quality by the government of West Bengal.

The stations namely are Behala (22.5016° N, 88.3209° E), Central Kolkata (22.5725° N, 88.3588° E), Cossipore (22.6236° N, 88.3725° E), Dhapa (22.5373° N, 88.4334° E), Garia (22.4660° N, 88.3928° E), Leather Complex (22.4984° N, 88.5172° E), Tangra (22.5563° N, 88.3888° E) and Topsia (22.5400° N, 88.3875° E).

3 Methodology

The emergent problem of groundwater pollution requires an elucidation which can be attained by thorough analysis of groundwater quality and maintaining its parameters within permissible limits. The monitoring locations all over the study area are provided in the map as shown in Fig. 1.

The water quality data for this study have been collected from the West Bengal Pollution Control Board Central Laboratory [8]. The data obtained are represented in graphical arrangements as shown in Fig. 2 for detailed examination.

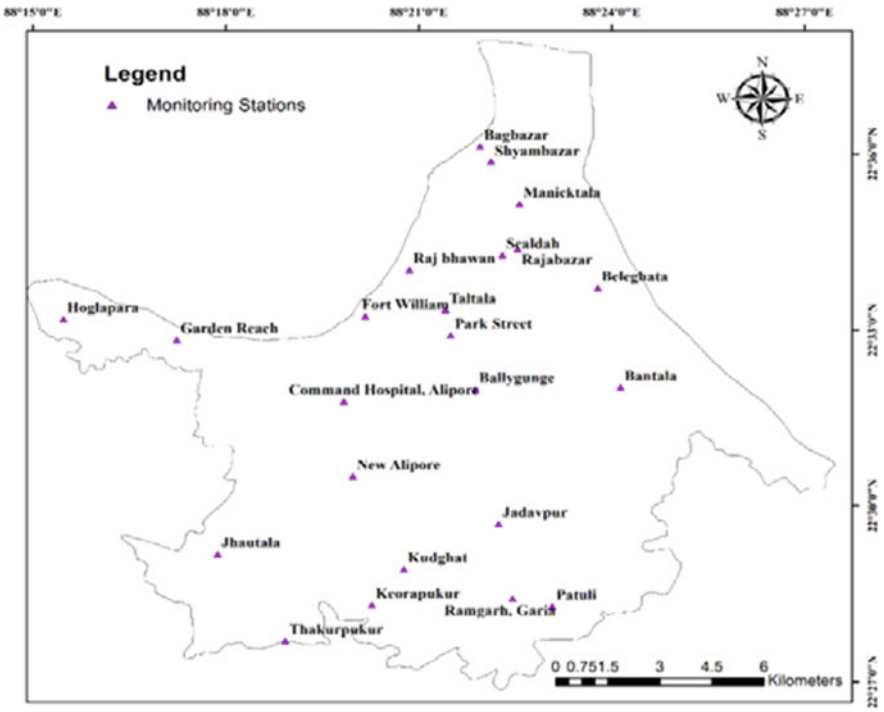

Fig. 1 Location map of the monitoring stations in Kolkata

To analyse the groundwater quality of the city, the data for various groundwater parameters were taken from West Bengal Pollution Control Board. The parameters were then linked to groundwater level (pre monsoon) which was accumulated from Central Ground Water Board, to investigate the relationship between the same. Isoline maps were prepared using geographical information system techniques for a better comparison of the data. The parameters were assessed for the year 2010, 2012, 2014, 2016 and 2018. The following parameters taken into account are electrical conductivity, total hardness, alkalinity, TDS, pH, chloride and nitrate as these were considered important for the study area.

Secondly, a water quality index (WQI) for the considered parameters was calculated to come to a proper understanding of the levels of contamination in water. The water quality index was calculated following the weighted arithmetic index method by the formula given in Eq. 1 [9, 10].

$$\mathrm{WQI} = \sum_{i=1}^{n} Q_i W_i \tag{1}$$

where Q_i = sub-index for ith water quality parameter; W_i = weight associated with ith water quality parameter; and n = number of water quality parameters.

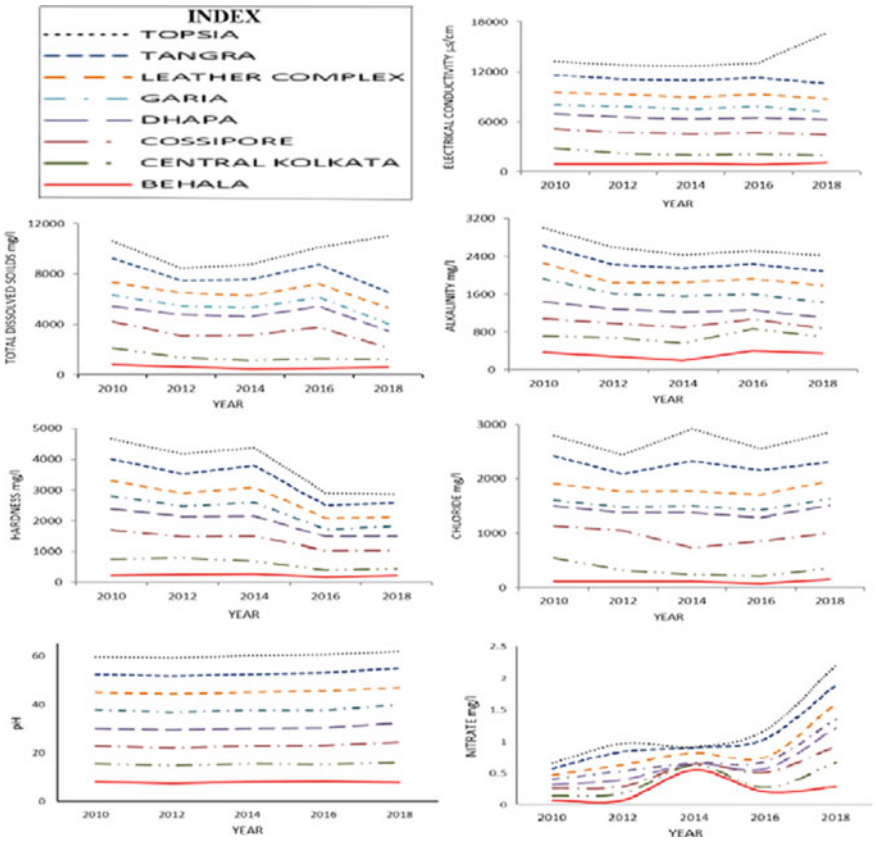

Fig. 2 Graphical representation of collected data of different water quality parameters

4 Results and Discussion

The study area mainly constitutes of eight monitoring stations at different locations in Kolkata district. As already discussed, data from those locations were collected from the West Bengal Pollution Control Board and analysed. It can easily be stated that the average values of electrical conductivity (EC) over the years have increased and is beyond the permissible range provided by BIS 2012. It was noted from the maps in Fig. 3 that lower the groundwater table, higher is the value of EC in Behala, Dhapa, Leather Complex, Tangra and Topsia areas specifically. Thus, there has been intrusion of ions and pollutants into the groundwater during recharging in those areas. Also as the groundwater goes deeper, its temperature increases causing more ions to get dissolved into the groundwater, resulting into electrical conductivity to increase. The total dissolved solids (TDS) refer to the presence of available solids thawed in the water. The average values of TDS over the years at all the eight monitoring stations have been found within the permissible range. The depletion in groundwater table

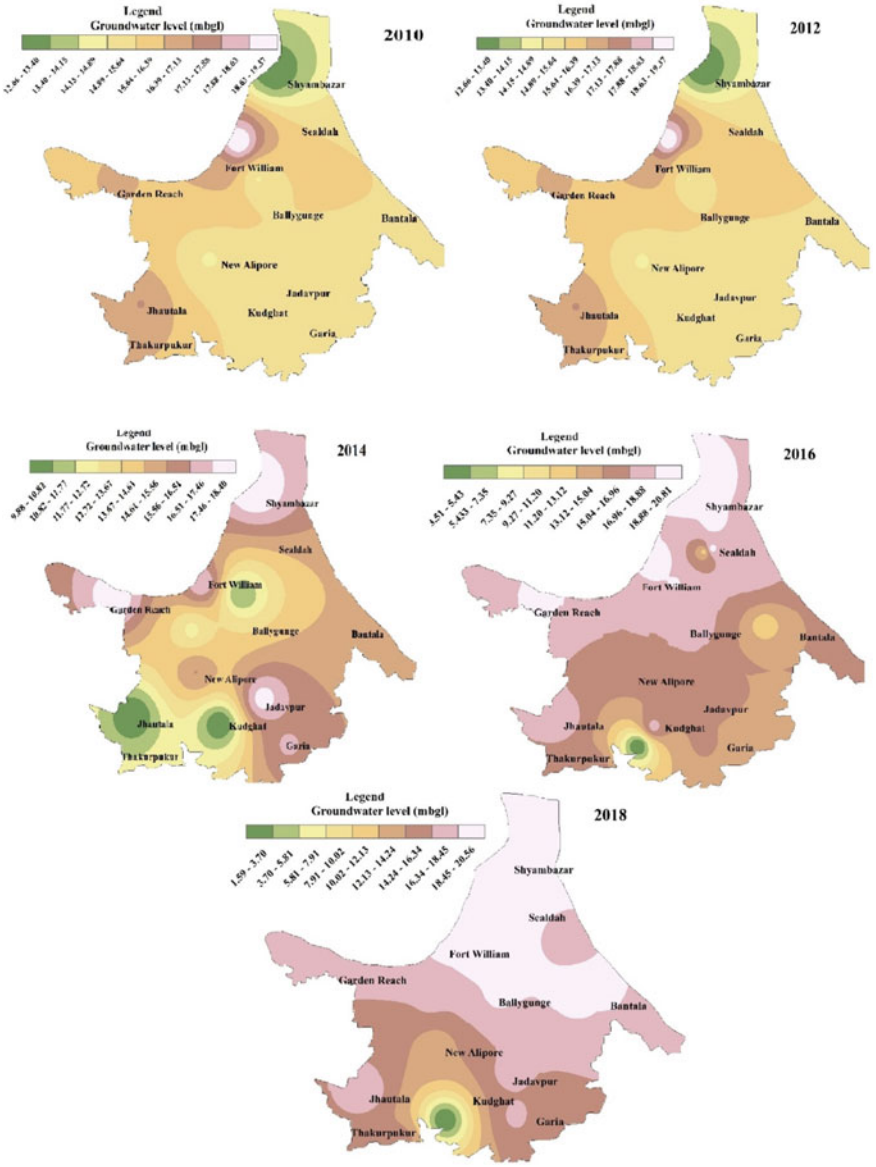

Fig. 3 Year-wise groundwater level maps of Kolkata

has resulted in increase of TDS, which also indicates the presence of calcium and magnesium. Also EC is directly proportional to TDS, and the coefficient varies from 0.6 to 0.8. Total alkalinity indicates the presence of carbonates and bicarbonates in water, and total hardness indicates the presence of calcium and magnesium in water. Analysing the data both the parameters have been found to be within the permissible limits. Similar pattern has been noticed in case of these parameters as well, i.e., with the depletion in groundwater table; the values of the impurities in the groundwater go on increasing. Chloride and nitrate content have been found higher in Dhapa, Tangra and Topsia areas precisely in comparison with other areas. The land in these areas, once used for garbage dumping purposes, has now been indulged in farming. Thus, ions like chloride and nitrate easily get encroached into the groundwater. pH is a parameter used to determine the acidic conditions of a given water sample. The introduction of external detritus matter increases the acidity of the water of an underlying unexposed unconfined aquifer. The pH values ranges between 7.2 and 7.6, indicating a stable and steady array.

The water quality Index for each year at all eight station points have been calculated and the results indicate a singular coefficient for determining an easy appreciative value for the water quality parameter of the underlying aquifer. The outcomes also indicate that the water quality index all through the city lies within medium--good condition, according to water research centre's water quality index parameters. The average value of water quality index, however, conveys a validation that the qualities have been depreciated over years. The graphical illustration in Fig. 4 evidently implies that there has been a gradual decline of quality of water with time. The bottom portion of the graph specifies medium condition, whereas the upper portion indicates good condition with respect to water quality index range.

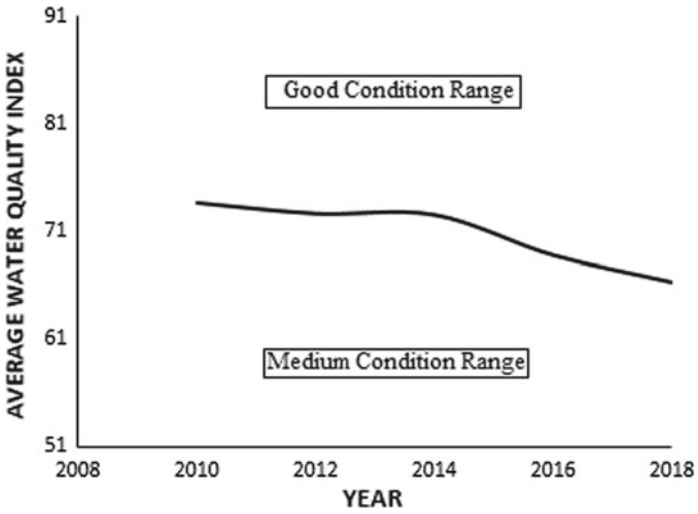

Fig. 4 Graphical representation of the average water quality index in variance with time

5 Conclusions

The data shows rather profound yet unstable conditions in the parameters of the aquifer conditions in the region. The aquifer being confined in its geophysical state is majorly susceptible to external parameters for its fluctuations in the water quality. The data likewise depicts that although the pH is stable and suitable for drinking water purposes, the TDS, EC, chloride and nitrate contents of the aquifer are majorly distressed in the Dhapa, Tangra and Topsia regions. This could be related to the overlaying activities in the region leading to leaching events affecting the aquifer water quality parameters. In inference the manuscript leads the postulation of not only the anomalies in the water quality parameters of the region but also the effect of external human activities fundamentally affecting the underlying groundwater conditions in the region. In major places of the city it has been noted that the water quality index varies from medium--good condition. The comparative analysis of water quality index over the years suggests a coherent deterioration of the water quality. Although at the current water quality, conditions of groundwater in the region could be advocated, but the rapid decline in aquifer level should be taken into consideration.

References

1. Riedel T (2019) Temperature-associated changes in groundwater quality. J Hydrol 572:206–212
2. Banerji S, Mitra D (2019) Geographical information system-based groundwater quality index assessment of northern part of Kolkata, India for drinking Purpose. Geocarto Int 34:943–958
3. Central Pollution Control Board (2007) Ministry of environment and forest
4. Groundwater Information Booklet (2007) Kolkata Municipal Corporation
5. Ramesh K, Elango L (2006) Groundwater quality assessment in Tondair Basin. Indian J Environ Prot 26:497–504
6. Bureau of Indian Standards (2012) Drinking water specification IS 10500, New Delhi
7. Khan R, Jhariya DC (2017) Groundwater quality assessment for drinking purpose in Raipur City, Chhattisgarh using water quality index and geographic information system. J Geol Soc India 90:69–76
8. West Bengal Pollution Control Board (2019). https://cpcb.nic.in/water-pollution/
9. Ramakrishnaiah RC, Sadashivaiah C, Ranganna G (2009) Assessment of water quality index for the groundwater in Tumkur Taluk, Karnataka State, India. E-J Chem 6:523–530
10. Ponsadailakshmia S, Sankarib SG, Prasannac SM, Madhurambald G (2019) Evaluation of water quality suitability for drinking using drinking water quality index in Nagapattinam district, Tamil Nadu in Southern India. Groundwater Sustain Dev 6:43–49

Efficacy Evaluation of Conventional Water Treatment Process and THMs Modeling in Drinking Water of Five Cities in India

Jaydev Kumar Mahato and S. K. Gupta

1 Introduction

The need for safe drinking water is one of the major concerns in developing countries to ensure public health. Chlorine effectively reduces the risk of waterborne disease and most commonly applied disinfectants in water industries due to its residuality, low cost, and simple operation [1, 2]. However, chlorine reacts with natural organic matter (NOM) present in water and results in the formation of trihalomethane (THM), which are reported to be possible carcinogens for humans [2, 3]. THMs include four substances viz. chloroform (CF), bromodichloromethane (BDCM), dibromochloromethane (DBCM) as well as bromoform (BF), and the sum of these refer as total THMs (TTHMs) [4]. The Bureau of Indian standard has formulated the guideline value of CF, BDCM, DBCM, and BF to be 200 μg/L, 60 μg/L, 100 μg/L, and 100 μg/in drinking water, respectively. However, no guideline value was given for total TTHMs. The level of these compounds primarily depends on many factor like concentration and content of NOM [measured as total organic carbon (TOC), dissolved organic carbon (DOC), UV_{254}, and specific ultraviolet absorbance (SUVA)], pH, temperature, bromide, and residual chlorine (RC) [5]. Thus, removal of NOM and control regulation of operational parameters in the treatment system may provide a vital corridor for the obliteration of THMs formation. The conventional water treatment technology like coagulation, sedimentation rapid sand filtration, and chlorination can remove only part of NOM, i.e., up to 30% [6]. Therefore, it is essential to upgrade the existing treatment system with some advanced technology to cope up with this problem. The up-gradation in the system required lots of capital which will again increase the treatment cost. Thus, the quality control procedures may be one of the best alternatives to prevent the formation of the THMs within the

J. K. Mahato (✉) · S. K. Gupta
Department of Environmental Science and Engineering, IIT (ISM), Dhanbad, 826004, India
e-mail: jay_devkumar@rediff.com

S. Kumar et al. (eds.), *Sustainability in Environmental Engineering and Science*, Lecture Notes in Civil Engineering 93,
https://doi.org/10.1007/978-981-15-6887-9_10

existing treatment system. In this context, the development of mathematical models can provide pre-knowledge of their level in the water, which will help the utility manager for its management and control.

Hence, the present study was undertaken with the objective (i) to provide information about the occurrence and concentrations of THMs in treated water, (ii) efficacy evaluation of conventional drinking water treatment system for the removal of THMs precursors, and (iii) development of machine learning mathematical model to predict the THMs, with special reference to drinking water supplies of five cities in India.

2 Material and Methods

2.1 Sample Collection

Water sample used in this study was collected from five water treatment plants (WTP) situated in five different cities of India which are Varanasi (VWTP), Dhanbad (DWTP), Raipur (RWTP), Bhubaneswar (BWTP), and Kolkata (IGWTP). All the WTP follows the conventional water treatment process comprised of coagulation-flocculation, sedimentation, sand filtration, and finally chlorination. Two points from each location were selected to cover river intake (raw water) and after final treatment (treated water). The sample was collected in triplicate in a dry and clean 5 L plastic container from each WTP. On the other hand to analyze the THM, separate samples were taken in 30 mL clean glass vials with polypropylene cap and PTFE-faced rubber septa and sodium sulfite (0.010 g) were added as dechlorination agent to eliminate any further formation of THMs.

2.2 Analytical Methods

The determination of physic–chemical water quality parameters of the collected water sample was conducted by the standard method of APHA-2012, in the laboratory of ESE, IIT(ISM), Dhanbad. However, the variables like pH, temperature, DO and residual chlorine (RC) were measured immediately on the site itself. TOC and DOC were analyzed by TOC analyzer (SHIMADZU TOC-L/CSH/E200) equipped with NDIR detector. UV_{254} was measured with a UV–visible spectrophotometer (Motras Scientific Instrument, India) at 254 mn using quartz cell (1 cm). SUVA is the ratio of UV_{254} and DOC concentration. CHEMITO CERES-800 PLUS gas chromatography with 63Ni EV detector was used for the estimation of THMs. All the experiments were led in triplicates for reproducibility reason.

2.3 Predictive Modeling Approaches of THMs

An artificial-intelligent-based machine learning modeling approach viz. Support vector machine (SVM) was applied for the prediction of THMs in the treated water by using MATLAB 9.5. It is based on statistical learning theory where the input data space was mapped out into a high-dimensional feature space using a suitable kernel function to construct a maximal separating hyperplane (separating plane). Which further minimizes the distance of data over a large number of data sets and reduces the model dimensions and estimated errors. In this modeling, pH, temperature, RC, TOC, and UV_{254} were considered independent variables, whereas THMs was designated as the dependent. Validation of the model was done by analyzing the different sets of independent data from the same source.

3 Result and Discussion

3.1 Water Quality Status and Distribution of THMs Precursors

Raw and treated water quality parameters of all five selected WTPs are reported in Table 1. The value of pH was found well within the prescribed drinking water quality standard (pH: 6.5–8.5) as per the IS 10500 (2012) for both raw and treated water. The temperature of all the WTPs appeared to be slightly higher, as the sampling was done during the months of March and April. The concentration range of RC was observed between 0.3 and 1.4 mg/l exceeded guideline value (0.2 mg/l) of the Bureau of Indian standard (BIS). This may due to the fact that the execution of an inappropriate chlorine dose in the treatment system of WTPs under this study. In terms of dissolved oxygen, the quality of water was found to be good for drinking purposes. TDS, turbidity, alkalinity, and total hardness were also fairly good in raw and treated water. Bromide which is one of the major precursors contributing to brominated THMs [7, 8] were not detected in any of the samples. The possible reason could be the no sea/saltwater intrusion was observed in the intake system of any selected WTPs.

TOC, DOC, UV_{254}, and SUVA have all been suggested as suitable surrogates for THMs precursors in chlorinated drinking water [5]. Figure 1a–d illustrated that the distribution of these THMs precursors was relatively higher in raw water than treated water for all the WTPs. The concentration range of TOC and DOC was appeared to be higher in VWTPs, and lower in BWTPs for both the case raw as well as treated water. In addition, the value of TOC exhibits similar to that of DOC indicated that majority of NOM is in dissolved fraction. Owen et al. [9] also reported that the DOC constitutes approximately 83–98% of TOC in freshwater. The content of these THMs precursors in collected water is fairly good as the concentration of NOM in surface water varied between 2 and 10 mg/L [10]. Beside TOC and DOC, NOM can

Table 1 Average value of water quality parameters at raw and treated water

Parameters	Raw water					Treated water				
	VWTP	DWTP	RWTP	BWTP	IGWTP	VWTP	DWTP	RWTP	BWTP	IGWTP
pH	7.7	7.6	7.9	7.7	7.8	7.5	7.4	7.4	7.4	7.6
Temp. (°C)	32.1	28.8	28.7	30.1	30.4	31.9	28.8	28.6	29.9	30.4
RC (mg/L)	Nil	Nil	Nil	Nil	Nil	1.3	1.4	1.2	0.3	0.4
DO (mg/L)	6.8	6.9	7.1	7.1	6.2	6.8	6.5	7.2	7.0	6.0
TDS (mg/L)	320.0	155.1	135.1	145.3	249.7	305.4	148.3	126.7	144.4	239.6
Turbidity (NTU)	6.5	2.1	4.1	3.7	6.1	1.2	0.9	1.2	0.8	1.2
Alkalinity (mg/L)	119.1	166.0	180.7	210.0	160.7	171.7	163.9	101.7	133.2	176.9
Total hardness (mg/L)	102.0	157.3	174.0	190.0	134.0	159.0	156.3	89.5	132.2	163.6
Bromide ion (mg Br/L)	Nil	Nil	Nil	Nil	Nil	Nil	Nil	Nil	Nil	Nil
TOC (mg/L)	4.3	3.1	3.1	2.7	3.1	2.8	2.4	1.8	1.8	2.1
DOC (mg/L)	4.1	2.9	2.8	2.5	3.0	2.6	2.4	1.8	1.7	2.0
UV_{254} (cm^{-1})	0.09	0.07	0.07	0.08	0.06	0.04	0.04	0.03	0.03	0.03
SUVA (L mg^{-1} m^{-1})	2.2	2.5	2.6	3.3	2.0	1.7	1.7	1.6	1.7	1.6
CF (μg/L)	Nil	Nil	Nil	Nil	Nil	380.9	360.2	324.3	319.7	353.1
BDCM (μg/L)	Nil	Nil	Nil	Nil	Nil	18.3	16.9	21.7	20.3	18.8
DBCM (μg/L)	Nil	Nil	Nil	Nil	Nil	15.5	12.3	14.2	8.5	12.1
BF (μg/L)	Nil	Nil	Nil	Nil	Nil	0.0	0.0	0.0	0.0	0.0
TTHMs (μg/L)	Nil	Nil	Nil	Nil	Nil	414.6	389.4	360.2	348.6	384.1

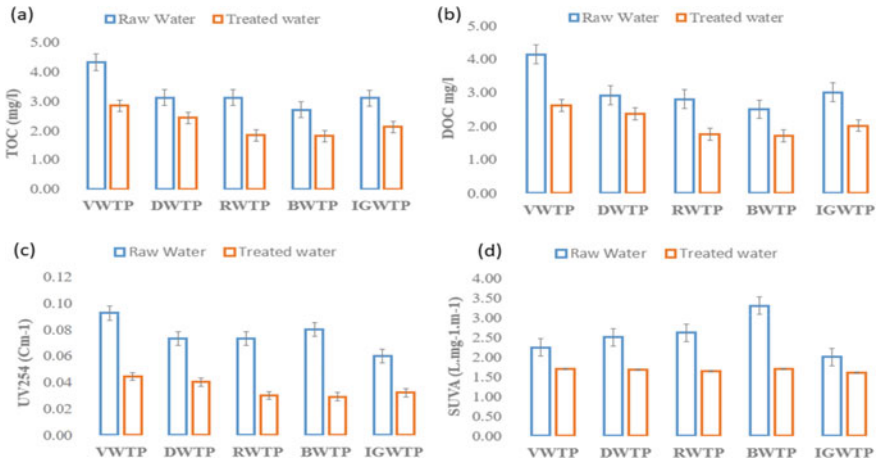

Fig. 1 Distribution of THMs precursors **a** TOC, **b** DOC, **c** UV_{254}, **d** SUVA in various WTPs

also be directly measured through its surrogate or ultraviolet absorbance at 254 nm (UV254). The value of UV_{254} seems to be slightly higher in raw water than the treated water, due to the presence of high TOC. The nature of NOM in water can be determined by SUVA, if value value > 4 L mg^{-1} m^{-1} indicate the humic nature (hydrophobicity) with high molecular weight and value < 2 L mg^{-1} m^{-1} indicate non humic nature (hydrophilic) with low molecular weight whereas range value between 2 and 4 L mg^{-1} m^{-1} indicate mixture of hydrophobic and hydrophilic of NOM fraction [9]. In the present study, the SUVA value range between 1.9 and 3.3 L mg^{-1} m^{-1} illustrated the mixed nature of NOM.

During the period under study, the concentration of THMs was ranged between 348 and 414 µg/L, exceeded the prescribed limits of Bureau of Indian Standard (IS 10500: 2012) (200 µg/l) and USEPA (80 µg/l) and WHO (300 µg/l) in all five WTPs.The maximum concentration was found in the treated water of VWTP whereas the minimum in BWTP. The possible reason could be the similar trend concentration of TOC and DOC found in these WTPs. According to a study by Zhang et al. [11] higher the concentration of TOC, greater the formation of THMs in water. The similar concentration range of THMs was also reported by Kumari et al. [12], in Indian drinking water supplies. The data listed in Table 2 also confirmed that the CF tends to be present in the greatest concentration to that of other three THMs compounds, which is well support with the finding of Zhang et al. [11].

Table 2 Model summary of THMs formation

R^2	0.981
Adjusted R^2	0.977
Error degree of freedom (DF)	24
RMSE	3.74
Statistical coefficient	
a	−202.16
b	78.343
c	−5.1045
d	−4.7726
e	80.193
f	−630.01

3.2 *Efficacy Evaluation of Existing Treatment System for Removal of THMs Precursors*

The purpose of this study is to evaluate the efficiency of existing treatment technology of selected WTPs with respect to percentage removal of turbidity and THMs precursors. All the WTPs for this study have various capacity and specification, follows traditional treatment processes comprised of aeration followed by coagulation (alum, PACl, and lime), flocculation, sand filtration and finally chlorination (bleaching powder or chlorine gas). Efficacy of WTPs was evaluated by using the following formula:

$$\text{Efficacy}(\%) = (\text{Raw water quality} - \text{Treated Water quality})/\text{Treated water quality} \times 100$$

Figure 2 depicted the percentage efficiency of the conventional treatment process for the removal of turbidity and THMs precursors. Efficacy of existing technology in these WTP seems very good for turbidity (up to 82%,) whereas in terms of THMs precursors it showed marginal efficiency SUVA (up to 48%) followed by UV254 (up to 47%), DOC (up to 37%), and TOC (up to 34%). Literature survey also revealed that the conventional treatment system like coagulation, sedimentation, and rapid sand filtration can remove only part of NOM, i.e., up to 30% from the drinking water [6]. According to the USEPA Stage I (1999), the implementation of enhanced coagulation or softening is necessary when the concentration TOC is higher than 2 mg/L in raw water. Hence, conventional treatment is not enough for the eradication of THMs precursors, as the Indian raw drinking water supplies content NOM higher than 2 mg/L.

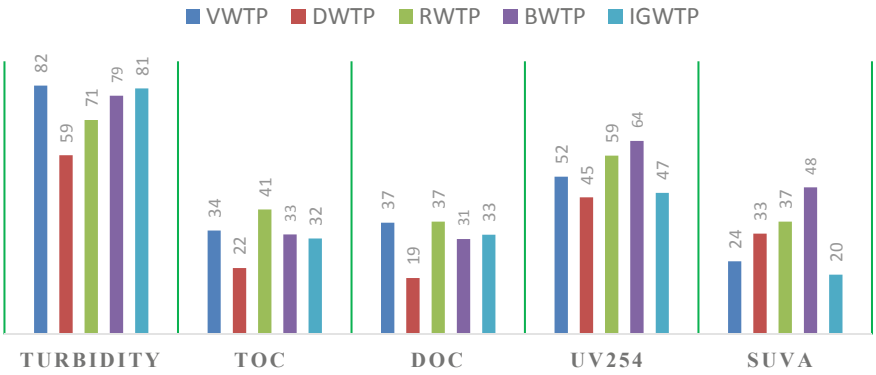

Fig. 2 Efficiency of various WTPs for % removal of THMs precursors and Turbidity

3.3 Modeling of THMs Formation Using SVM

In order to develop the SVM model, the data of all the five WTPs were selected and organized in the ratio of 60:40. Then, the various combination of this 60% data was tested using the MATLAB 9.5 software to find the suitable model and the remaining 40% of data set were used for testing purpose. In this approach, parameters like pH, temperature, RC, TOC, and UV_{254} were designated as the independent variable and THM as the dependent variable. The best suitable linear regression model models proposed by SVM for predicting THMs are shown in Eq. (1).

$$\text{THM} = -a + b(\text{pH}) - c(\text{temp.}) - d(\text{RC}) + e(\text{TOC}) - f(\text{UV}_{254}) \quad (1)$$

where the temp. is in °C, RC, and TOC expressed in mg/L. UV_{254} is the ultraviolet absorbance expressed in cm^{-1}, and a, b, c, d, e, and f are the estimated model values of statistical coefficients.

Table 2 illustrated the SVM model summary. Fairly high and closely comparable values of the coefficient of determination (R^2) to the adjusted R^2 confirm the adequacy of SVM modeling approach for the prediction of THM in treated water. Additionally, a relatively lower value of root means square error (RMSE) of training data also emphasize good generalization and predictive abilities of SVM model.

3.4 Validation of SVM Model

The purpose of validation is to evaluate the applicability of the model to the real data, and also to determine how well the model fits the experimental data. As discussed earlier, all the data was organized in the ratio of 60:40, of which the 40% remaining data were used for the validation. A very high correlation coefficient ($R^2 - 0.9554$)

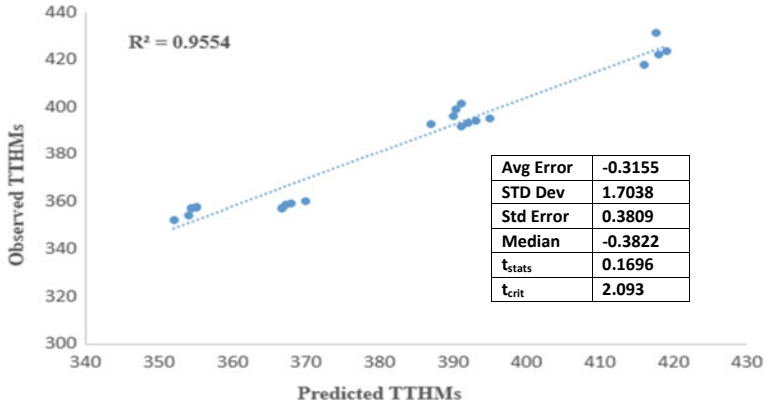

Fig. 3 Validation of SVM model plot

was observed between predicted and observed THMs that signify the adequacy of the model to field scale (Fig. 3). The other validation statistics of the model also confirmed that the model can successfully be applied for the prediction of THMs with least error of precision ($-0.3155\% \pm 1.7038$). Additionally, the assessment of t test specified that the biasness of the model was insignificant as the value of t_{stats} (0.1696) was comparatively lower than t_{critical} (2.093). Overall modeling assessment suggesting that SVM modeling approach can provide immense help to WTP manager for the pre-knowledge of THMs in the water for its better management and control.

4 Conclusion

An elevated concentration range of TTHMs (348 and 414 μg/L) was observed in the water distribution network of all five selected WTP across India, which is approx. 2 times higher than the prescribed guideline value of Bureau of Indian Standard. The distribution of THMs precursor was found was relatively higher in raw water than treated water. The efficacy of existing treatment technology adopted in these WTP seems to marginal for removal of THMs precursors (TOC 34% and DOC 37%). Modeling result indicated that the prediction precision of SVM models is good, which can provide immense help to WTP manager for the pre-knowledge of THMs in the water for its better management and control.

Acknowledgements The author acknowledges the financial grant from the Ministry of Drinking Water and Sanitation (GOI), New Delhi (Project# MDWS/2015-16/453/ESE).

References

1. Ding S, Deng Y, Bond T, Fang C, Cao Z, Chu W (2019) Disinfection byproduct formation during drinking water treatment and distribution: a review of unintended effects of engineering agents and materials. Water Res 160:313–329
2. Hasan A, Thacker NP, Bassin J (2010) Trihalomethane formation potential in treated water supplies in urban metro city. Environ Monit Assess 168(1–4):489–497
3. Hassani AH, Jafari MA, Torabifar B (2010) Trihalomethanes concentration in different components of water treatment plant and water distribution system in the North of Iran. Int J Environ Res 4(4):887–892
4. Wei J, Ye B, Wang W, Yang L, Tao J, Hang Z (2010) Spatial and temporal evaluations of disinfection by-products in drinking water distribution systems in Beijing, China. Sci Total Environ 408(20):4600–4606
5. Toroz I, Uyak V (2005) Seasonal variations of trihalomethanes (THMs) in water distribution networks of Istanbul City. Desalination 176(1–3):127–141
6. Randtke SJ (1988) Organic contaminant removal by coagulation and related process combinations. J Am Water Works Assoc 80(5):40–56
7. Ates N, Kitis M, Yetis Ulku (2007) Formation of chlorination by-products in waters with low SUVA—correlations with SUVA and differential UV spectroscopy. Water Res 41:4139–4148
8. Golfinopoulos SK, Nikolaou AD (2005) Survey of disinfection by-products in drinking water in Athens, Greece. Desalination 176(1–3):13–24
9. Owen DM, Amy GL, Chowdhury ZK (1993) Characterization of natural organic matter and its relationship to treatability. AWWA Research Foundation and the American Water Works Association, Denver CO
10. Bolto B, Dixon D, Eldridge R, King S (2002) Removal of THM precursors by coagulation or ion exchange. Water Res 36(20):5066–5073
11. Zhang J, Yu J, An W, Liu J, Wang Y, Chen Y, Tai J, Yang M (2011) Characterization of disinfection byproduct formation potential in 13 source waters in fa. J Environ Sci 23(2):183–188
12. Kumari M, Gupta SK (2015) Modeling of trihalomethanes (THMs) in drinking water supplies: a case study of eastern part of India. Environ Sci Pollut Res 22(16):12615–12623

Study of Water Quality Index to Ascertain the Suitability of Surface Water for Domestic Purposes

Joyoti Biswas and Rinku Supakar

Nomenclature

S-1	Site-1 where sampling was done
S-2	Site-2 where sampling was done
S-3	Site-3 where sampling was done
WQI	Water quality index
TDS	Total dissolved solids in mg/L
DO	Dissolved oxygen in mg/L

1 Introduction

Sustainability of life on earth greatly depends on the availability of water which is an essential natural resource. Water is an indispensable component for human beings as the entire fluid balance of our body depends on adequate supply of water in our body [1]. Water quality depends on several physico-chemical factors and any abnormality shown may cause hazards to the entire biotic community [2]. Rapid industrialization and subsequent urbanizations of great concern to the environment as it has given rise to various types of pollution. The health of the future generation is at stake due to environmental pollution. Untreated domestic wastes are discharged into the receiving water bodies through sewage, outfalls, drains, etc.

J. Biswas (✉)
Department of Chemistry, DSCSDEC, Kolkata, India
e-mail: jaysagnik@yahoo.com

R. Supakar
Department of Computer Science, DSCSDEC, Kolkata, India
e-mail: rsupakar@gmail.com

S. Kumar et al. (eds.), *Sustainability in Environmental Engineering and Science*, Lecture Notes in Civil Engineering 93,
https://doi.org/10.1007/978-981-15-6887-9_11

The surface and the ground water pollution can be effectively determined by measurement of WQI which can be further used efficiently for the up gradation of water quality management programs [3]. WQI gives a numerical digit representation that expresses overall quality based on the different parameters. The physico-chemical characteristics like pH, dissolved oxygen, total alkalinity, total hardness, chloride content, etc., in one way are representative parameters to determine the quality of water. Besides, the entire aqua world are seriously affected due to the drastic change in water quality as reported by [4]. Several aquatic organisms are getting extinct day by day due to drastic alterations in the physico-chemical characteristics of water caused by natural as well as anthropogenic activities.

2 Materials and Methods

A. Chemicals and reagents

All chemicals and reagents used to study surface water of the chosen area were of analytical grade.

B. Study area

North 24-Parganas of West Bengal (India) was chosen as the study area. Three sampling sites, namely S-1, S-2, and S-3 were chosen which were mainly urban water bodies near river Ganges. These water bodies practically received domestic wastes and drainage water from the residential area throughout the year

C. Sample Collection and Preparation

The water samples were collected at two weeks interval for a period of two months in three different seasons, namely summer, monsoon, and winter. Samples were collected in 2l plastic bottles cleaned properly to avoid contamination. The containers were then sealed with tight fitting corks and stoppers after collection, in order to avoid air bubbles. The samples were then immediately refrigerated at (4 °C) prior to analysis. The water samples from the water body were collected at an interval of 30 days and analyzed for six physico-chemical parameters, namely pH, alkalinity, total hardness, TDS, chlorides, DO according to the standard procedures outlined by APHA 1995 [5].

Determination of water quality index is defined as a rating reflecting the cumulative influence of different water quality parameters on the overall quality of water. In this study, calculation of WQI was based on six important physico-chemical parameters. The WQI calculated using the different standards of drinking water quality recommended by WHO, BIS, and ICMR. WQI was calculated by weighted arithmetic index method given by [4].

Table 1 Categorization of WQI based on permissibility for human consumption [6]

WQI level	Water quality status
0–25	Excellent water quality
26–50	Good water quality
51–75	Poor water quality
76–100	Very poor water quality
>100	Unsuitable for drinking

3 Theoretical Analysis

$$\text{WQI} = \sum_{n=1}^{n} q_n w_n / \sum_{n=1}^{n} w_n$$

where $q_n = 100[(v_n - v_i)/(s_n - v_i)]$

q_n = quality rating for the nth water quality parameter.

v_n = estimated value of the given parameter at a given sampling station. s_n = Standard permissible value of the nth parameter. v_i = ideal value of the nth parameter in pure water. w_n = unit weight of the nth parameter.

In this study, the WQI level was categorized based on permissibility for human consumption as shown in Table 1.

4 Results and Discussion

WQI of three sampling stations, namely S-1, S-2, and S-3 was calculated for three seasons. WQI rating presented a very poor quality of water as evident from (Tables 2, 3, and 4) in all the sampling stations throughout the year but the poorest quality of water unsuitable for drinking was found in sampling site S-3. This may be due to high immense man made and direct discharge of various industrial effluent.

The eutrophic nature of water as reflected from the above-mentioned data is alarming and raises a question on the portability of water. It also reflects the fact that water pollution is particularly high in summer when compared to winter and rainy seasons.

Among all the physico-chemical parameters selected for water quality calculation, pH is an important parameter which determines the extent to which the water is corrosive. The pH in all the sampling sites varied between 6.6 and 7.9 which showed that the water bodies were slightly alkaline in nature.

The slight variation can be due to exposure of water bodies to the various physical, chemical, and biological changes occurring in the water bodies [7]. Dissolved oxygen can be generally attributed to the various aerobic and anaerobic activities taking place in water [8]. The oxygen balance is maintained in water by the atmospheric oxygen as well as by various photosynthetic activities. The DO level in the present study

Table 2 WQI calculated in various seasons at site (S-1)

Parameter	Standard values (s_n)	Measured values in summer season (v_n)	Measured values in rainy season (v_n)	Measured values in winter season (v_n)	Water quality index (WQI)
pH	6.5–8.5	7.66	6.8	7.20	89.48 in summer season
Alkalinity in mg/L	120	175	160	171	
Total hardness in mg/L	300	211.50	175.2	185.70	78.92 in rainy season
Total dissolved solids (TDS) in mg/Ll	500	489	475.3	386.70	
Chloride in mg/L	250	42	38	36	94.07 in winter season
Dissolved oxygen (DO) in mg/L	5.0	3.5	4.89	4.2	

Table 3 WQI calculated in various seasons at site (S-2)

Parameter	Standard values (s_n)	Measured values in summer season (v_n)	Measured values in rainy season (v_n)	Measured values in winte season (v_n)	Water quality index (WQI)
pH	6.5–8.5	7.85	6.65	6.89	WQI in summer season—104.66
Alkalinity in mg/L	120	185	167	175	
Total hardness in mg/L	300	299.5	215.60	255.60	WQI in rainy season—106.85
Total dissolved solids (TDS) in mg/L	500	650	627.60	580.56	
Chloride in mg/L	250	50	46	40	WQI in winter season—97.59
Dissolved oxygen (DO) in mg/L	5.0	1.89	2.18	1.22	

varied between 1.22 and 4.89 mg/L. The reduction in dissolved oxygen level was due to degradation of various organic and inorganic wastes, respiratory activities of the various flora and fauna inside water, etc. [9].

Total dissolved solids (TDS) analysis has great implications in the control of biological and physical waste water treatment process. The TDS is generally seen

Table 4 WQI calculated in various seasons at site (S-3)

Parameter	Standard values (*sn*)	Measured values in summer season (v_n)	Measured values in rainy season (v_n)	Measured values in winter season (v_n)	Water quality index (WQI)
pH	6.5–8.5	7.51	6.77	7.31	109.70 in summer season
Alkalinity in mg/L	120	325	294	304	
Total hardness in mg/L	300	247	158	220	101.82 in rainy season
Total dissolved solids (TDS) in mg/L	500	200	156.7	186.50	
Chloride in mg/L	250	35	20	29	97.55 in winter season
Dissolved oxygen (DO) in mg/L	5.0	1.39	1.92	1.25	

to be higher in all the sampling sites during the summer season. The total pollution load of water is reflected by the values depicted as TDS [10].

Alkalinity is influenced by carbonates, bicarbonates, and other ions [11]. Srivastava and Patil in 2002 suggested that activity of phytoplankton in converting bicarbonates into carbonates and carbon-dioxide has largely contributed to the increased alkalinity in water. Carbon-dioxide which is released facilitates the process of photosynthesis. In the present study, alkalinity is ranged from 165 to 325 mg/L. The alkalinity values are under the reasonable limit of 600 mg/L according to the World Health Organization.

Surface waters collected from all the three sampling sites showed low hardness (158–299.5 mg/L) and low chloride content (20–50 mg/L).

5 Conclusion

The present study indicated very poor water quality as evident from the values of WQI which varied from 89.48 to 109.70 in different seasons and found unsuitable for drinking purposes. From the detailed discussion presented, it can be concluded all the surface water sources under observation in the present study shows the onset of eutrophication in various water bodies. Hence, there is a need for regular monitoring of water quality in order to detect changes in the physico-chemical parameters examined at the sites under our study followed by implementation of the remedial measures with proper public awareness.

Acknowledgements Authors highly acknowledge the financial support rendered by Dr. Sudhir Chandra Sur Degree Engineering College, Dum Dum, kolkata, for rendering the Infrastructural facilities for the present research work. Authors also acknowledge the help given by Mr. Arup Kanti Hazra in carrying out various technical work in the laboratory.

References

1. Sinha DK, Saxena S, Saxena R (1955) Water quality index for Ramganga. Pollut Res 23:527–531
2. Pitchard M, Mkandawire T, O'Neill GJ (2008) Assessment of ground water quality in shallow wells within the southern districts of Malawi Water. Phys Chem Earth 33:812–823
3. Rossiter HMA, Owusu PA, Awuah E, MacDonald AM, Schaffer AI (2010) Chemical drinking water scope for advanced treatment. Sci Total Environ 408:2378–2386
4. Brown RM, Mcleiland NJ, Deininger RA, O' Connor MF (1972) Water quality index. In: Jenkis SH (ed) Proceedings of international conference on water pollution research, Jerusalem, vol 6, pp 787–797
5. APHA, AWWA RA, WPCF (1998) Standard methods for examination of water, 20th Edn
6. Gangwar RK, Singh J, Singh AP, O' Singh DP (2013) Assessment of water quality index: a case study of river Ramganga at Bareilly U.P. India. Int J Sci Int Res 4:2325–2329
7. Bahadur Y, Chandra R (1996) Monitoring the quality of river Ramganawaters at Bareilly. Pollut Res 15:31–33
8. Gangwar RK, Khare P, Singh J, Singh AP (2012) Assessment of physico-chemical properties of water: River Ramganga at Bareilly. J Chem Pharm Res 4:4231–4234
9. Saxena DN, Garg RK, Rao RJ (2008) Water quality and pollution status of Chambal river in National Chambal sanctuary, Madhya Pradesh. J Environ Biol 29:701–710
10. Parmar K, Parmar V (2010) Evaluation of water quality index for drinking water purposes of river Subarnarekha in Sighbhum. Int J Environ Sci 1:77–81
11. Srivastava VS, Patil PR (2002) Tapti river water pollution by industrial wastes: a statistical approach. Nat Environ Pollut Technol 1:279–283

Evaluation of Anthropogenic-Driven Water Pollution Effects in an Urban Freshwater Resource Using Integration Pollution Index Method

Avinash Pratap Gupta, Joystu Dutta, Manish Kumar Shriwas, Rajesh Yadav, Tirthankar Sen, and Madhur Mohan Ranga

1 Introduction

Water is one of the most valuable resources on the planet. No lifeform, be it animals, plants, insects or microorganisms, can survive without water. Water also plays a central role in human growth, development, and socio-economic progression. Water plays a big role in the field of agriculture. Water also serves a variety of domestic uses like laundry, bathing, cooking, etc. Industries like fertilizers, chemicals, cement, paper, etc., are also heavily dependent on water for a variety of purposes such as cleaning, cooling, power generation, and fire protection. Recreational activities such as swimming, boating, and fishing are also possible because of water.

The increase in human activities occurring as a result of rapid urbanization significantly impacts the ecological balance. This, in turn, affects the lives, aquatic livelihoods and agriculture of the humans who reside in those areas. For example, surface water pollution has been found to have a significant effect on the rate of infant mortality in China [1]. The challenge for any country is to undertake sustainable development without causing damage to nature. Issues leading to the deterioration of water quality at the water supply intake points need to be avoided at all costs. Many studies have found untreated sewage effluent to be the most critical issue with respect to water contamination. Given the fact that globally 2 billion people still do not have access to basic sanitation facilities, this is not surprising [14]. Activities that change land use and land cover patterns such as high-scale agricultural activities and

A. P. Gupta (✉) · J. Dutta · M. K. Shriwas · R. Yadav · M. M. Ranga
Department of Environment Science, Sant Gahira Guru University, Sarguja, Ambikapur, Chhattisgarh, India
e-mail: avi.gupta005@gmail.com

T. Sen
Department of Biotechnology, Techno India University, Kolkata, West Bengal, India

S. Kumar et al. (eds.), *Sustainability in Environmental Engineering and Science*, Lecture Notes in Civil Engineering 93,
https://doi.org/10.1007/978-981-15-6887-9_12

unplanned infrastructure developments result in the regional degradation of water quality and water balance.

According to Roberts and Prince [2], urbanization "involves the conversion of croplands, forests, grasslands, pastures, wetlands and other cover types to residential, transportation, commercial and industrial uses, thereby increasing the areas of impervious surfaces [3]." Human activities such as urbanization, especially improperly planned and uncontrolled urbanization [4], may alter the chemical composition of the local aquatic resources [5]. Bu et al. [6] conducted a study on the Jinshui River in China, where it was observed that the population density had a significant impact on the measured water quality parameters. An earlier study analyzing the physicochemical properties of water samples in the Surguja District observed that the pH and electrical conductivity ranged between 7.47 and 8.50 and 200 μs/cm–1230 μs/cm respectively. In the same study, the Total Dissolved Solids (TDS) was found to range between 104 mg/L and 390 mg/L [7].

WQI is a numeric expression which allows us to transform a set of physicochemical parameters into a single number [8]. It is generally used to represent the quality of surface water w.r.t its fitness for human consumption. The Pollution Integration Index, on the other hand, was found to be rarely used in the academic literature to determine the natural as well as anthropogenic impacts of point and non-point sources on water pollution levels. Thus, the aim of our study was to use the Integration Pollution Index to obtain actionable insights about the anthropogenic influences community water bodies such as the *Joda Talab* are subjected to. These insights, once available in the public domain, can be used to explore potential remediation and bioremediation routes. We also aimed to understand whether some water quality parameters are better indicators of anthropogenic pollution than others by calculating how the individual parameters are correlated with population density. Answering this question would allow us to better segregate between surface freshwater bodies unfit for human use and hence design efficient remediation strategies.

2 Study Area

The present investigation was carried out to evaluate the status of surface water quality of *Joda Talab* in Ambikapur, a prolific city of the Sarguja district in Chhattisgarh, India. As par Census 2011 reports, the population of Chhattisgarh is around 25.5 million, which ranks it as the 16th most-populated state in the country.

Ambikapur (23°12′ N 83°2′ E) is the divisional headquarters of Surguja Division that consists of the five districts: Surguja, Koriya, Balrampur, Surajpur, and Jashpur. Ambikapur has an average elevation of 623 m (2078 feet). The climate of the district is characterized by hot summers and well-distributed precipitation throughout the monsoon season. With its general monsoonal character, the district falls within the Tropical Thermal belt, as par Thornthwaite's classification (Fig. 1).

Fig. 1 Map of the study area. *Source* Google Maps, 2019. Joda Talab, Ambikapur, Chhattisgarh [Accessed 30 November, 2019]

3 Materials and Methods

Water samples were collected from three roughly equidistant points of *Joda Talab.*

The water samples were collected from the three sites during the pre-monsoon, monsoon, and post-monsoon seasons of 2018–2019. Ten different parameters characterizing the water quality were measured and the Integration Pollution Index (IPI) for the parameters were evaluated. The parameters measured were the turbidity (N.T.U), color (Pt/Co scale), pH, electrical conductivity (μS/cm), total alkalinity (mg/L), chloride concentration (mg/L), nitrate concentration (mg/L), magnesium concentration (mg/L), TDS (mg/L) and sulfate concentration (mg/L).

The sampling and analysis of the ten aforementioned physico-chemical attributes were done following the protocols detailed in APHA [9]. The obtained experimental results for each parameter were compared to their respective permissible limits for drinking and irrigation quality water, as laid out by the following standards: BIS [10], WHO [15].

For each parameter, the values obtained from the three sampling sites were used to calculate the Integration Pollution Index using the formula given below where,

IPI is the Integration Pollution Index, **Cb** is the actual water quality parameter value for each sample, **Co** is the value of the corresponding water quality standard, and **m** is the number of parameters being monitored.

$$\mathrm{IPI} = \frac{1}{m}\sum_{b=0}^{m}\frac{\mathrm{Cb}}{\mathrm{Co}}(b = 1, 2, \ldots, m)$$

The Integration Pollution Index was then used to evaluate the water quality. The basis of evaluating the water quality was human pressure, i.e., the effect of the local population as well as the rampant urbanization of the surrounding region, on the water quality of *Joda Talab.*

4 Results and Discussions

Our study throws light on the anthropogenic stress caused as a result of point and non-point sources of pollution. The findings of our study are in agreement with that of past studies where urbanization related activities were found to result in the increase of nitrogen, phosphorus, alkalinity, and TDS of the surface waters [11–13]. The Pollution Integration Index represents the ratio of the experimentally measured value for each parameter to the corresponding standard value of that parameter. The mean values of all the ten parameters considered in the study were well above the standard values. The Pollution Integration Index of each sample developed on the basis of each of their water quality parameters and their corresponding standard values is discussed in Table 1. From the Pearson correlation matrix represented in Table 2, it can be concluded that the total alkalinity (0.96) of pond water is highly correlated

Table 1 Observed values at the different sites with their IPI values

Parameter	Mean values at different sites			Standard values	Pollution integration index		
	Site I	Site II	Site III		Site I	Site II	Site III
Turbidity (N.T.U)	3.72	5.04	4.08	1	4.092	5.544	4.48
Color (Pt/Co Scale)	5	5	5	5	1.1	1.1	1.1
pH	8.5	8.1	7.86	7.5	1.246	1.188	1.152
Electrical conductivity (μs/cm)	662	832	568	1000	0.72	0.91	0.62
Total alkalinity (mg/L)	216	226	229	200	1.188	1.24	1.259
Chlorides (mg/L)	145	165	157	200	0.797	0.907	0.863
Nitrates (mg/L)	45	5	23	15	3.3	0.366	1.686
Magnesium (mg/L)	23.81	40.33	29.51	30	0.873	1.478	1.082
Total dissolved solids (mg/L)	424	533	469	500	0.932	1.172	1.031
Sulfates (mg/L)	210	136	186	200	1.155	0.748	1.023

Table 2 Pearson correlation matrix for the parameters

Variables	T	C	pH	EC	TA	Cl^-	NO^{3-}	Mg^{+2}	TDS	$SO_4{}^{2-}$	P
Turbidity (T)	1	–	−0.38	0.82	0.50	0.93	−0.94	0.99	0.98	−0.99	0.25
Color (C)	–	–	–	–	–	–	–	–	–	–	–
pH	−0.38	–	1	0.21	−0.99	−0.69	0.65	−0.46	−0.52	0.44	−0.99
Electrical conductivity (EC)	0.82	–	0.21	1	−0.08	0.55	−0.60	0.76	0.71	−0.78	−0.33
Total alkalinity (TA)	0.50	–	−0.99	−0.08	1	0.78	−0.74	0.57	0.63	−0.55	**0.96**
Chlorides (Cl^-)	0.93	–	−0.69	0.55	0.78	1	−0.99	0.95	0.97	−0.95	**0.59**
Nitrates (NO^{3-})	−0.94	–	0.65	−0.60	−0.74	−0.99	1	−0.97	−0.98	0.96	−0.54
Magnesium (Mg^{+2})	0.99	–	−0.46	0.76	0.57	0.95	−0.97	1	0.99	−1.00	0.34
Total dissolved solids (TDS)	0.98	–	−0.52	0.71	0.63	0.97	−0.98	0.99	1	−0.99	**0.41**
Sulfates ($SO_4{}^{2-}$)	−0.99	–	0.44	−0.78	−0.55	−0.95	0.96	−1.00	−0.99	1	−0.31
Population (P)	0.25	–	−0.99	−0.33	0.96	0.59	−0.54	0.34	0.41	−0.31	1

Significance level (alpha) = 0.05

with anthropogenic activities generated due to increasing population stress. Chlorides (0.59) and TDS (0.41) also appear to be moderately influenced by human activities. The size of the local population around each of the three different sites are as follows: site I—558, site II—600, and site III—642.

5 Conclusion

Pond ecosystems (like the *Joda Talab*) are highly susceptible to anthropogenic interference from point and non-point sources as they are lentic ecosystems. Therefore, it is imperative that we aim for the sustainable conservation of locked freshwater ecosystems in a time when surface freshwater is a globally critical resource.

This is a prototype project demonstrating a potential strategy which the governing authorities can use to lay out an action plan to control and remediate water pollution. Surface freshwater ecosystems need stringent monitoring to ensure the supply of

potable water in water compromised areas. Community sensitization is necessary to ensure zero contamination of freshwater from point and non-point sources. We must ensure the stabilization of freshwater ecosystems through buffering of aquatic and ambient media using a bouquet of practices. In this regard, the plugging of point and non-point sources is needed with immediate effect.

Our research suggests that decision makers and the local administration should be more aware of the recent increase in pollution of the surface water bodies and frame protocols and policies to protect them from further environmental degradation.

References

1. Dhanaji Kanase G, Sheikh Shagufta A, Jagdale Pramod N (2016) Physico-chemical analysis of drinking water samples of different place in Kadegaon Tehsil. Maharashtra. Adv Appl Sci Res 7(6):41–44
2. Roberts AD, Prince SD (2010) Effects of urban and non-urban land cover on nitrogen and phosphorus runoff to Chesapeake Bay. Ecol Ind 10(2):459–474
3. Tsegaye T, Sheppard D, Islam KR, Tadesse W, Atalay A, Marzen L (2006) Development of chemical index as a measure of in-stream water quality in response to land-use and land cover changes. Water Air Soil Pollut 174(1–4):161–179
4. Pompeu PS, Alves CBM, Callisto M ARCOS (2005) The effects of urbanization on biodiversity and water quality in the Rio das Velhas basin, Brazil. In: American fisheries society symposium, vol 47, pp 11–22
5. Groppo JD, De Moraes JM, Beduschi CE, Genovez AM, Martinelli LA (2008) Trend analysis of water quality in some rivers with different degrees of development within the São Paulo State, Brazil. River Res Appl 24(8):1056–1067
6. Bu H, Liu W, Song X, Zhang Q (2016) Quantitative impacts of population on river water quality in the Jinshui River basin of the South Qinling Mts., China. Environ Earth Sci 75(4):292
7. Kumari K, Upadhay M (2013) Assessment of drinking water quality of Sarguja district. Chhattisgarh. Int J Adv Res 1(12):1–6
8. Sánchez E, Colmenarejo MF, Vicente J, Rubio A, García MG, Travieso L, Borja R (2007) Use of the water quality index and dissolved oxygen deficit as simple indicators of watersheds pollution. Ecol Ind 7(2):315–328
9. APHA (1998) Standard methods for the examination of water and waste water, 20th edn. American Public Health Association, pp 10–161
10. BIS (as per IS 2296) Indian standard drinking water specification
11. Johnson L, Richards C, Host G, Arthur J (1997) Landscape influences on water chemistry in Midwestern stream ecosystems. Freshw Biol 37(1):193–208
12. Boyer EW, Goodale CL, Jaworski NA, Howarth RW (2002) Anthropogenic nitrogen sources and relationships to riverine nitrogen export in the northeastern USA. Biogeochemistry 57(1):137–169
13. Gergel SE (2005) Spatial and non-spatial factors: when do they affect landscape indicators of watershed loading? Landscape Ecol 20(2):177–189
14. WHO Fact sheets. https://www.who.int/en/news-room/fact-sheets/detail/sanitation
15. World Health Organization (2017) Guidelines for drinking-water quality: first addendum to the fourth edition

Improved Sequential Approach for Hybrid Bioleaching of Metals from E-Waste

Kavita Kanaujia and Subrata Hait

1 Introduction

Continuous, accelerating number of discarded electrical and electronic equipment (EEE), often termed as waste electrical and electronic equipment (WEEE) or electronic waste (e-waste), is one of the significant challenges these days from the waste management and environmental protection points of view. As per the Global E-waste Monitor Report 2017, around 44.7 Mt (million metric ton) of e-waste was generated worldwide in 2016 and is projected to be around 52.2 Mt by 2021 [1]. The depletion of natural resources makes e-waste recycling a critical aspect not only from the point of waste treatment but also economic development as well as a secondary resource. The printed circuit board (PCB) (around 3–6% of EEE) is the mainstay of any EEE and containing a considerable amount of base, toxic, and precious metals [2]. That is why they are considered as a secondary metal reserve. Environment-friendly methods are high in demand to recover metals from the waste PCBs. Being an emerging technique, biometallurgy or bioleaching involves employing acidophilic microorganisms for metal extraction from waste PCBs. *Acidithiobacillus ferrooxidans* are chemolithoautotrophs, acid-loving, mesophiles, commonly found in acid mine drainage, have the potential to leach metal in solution from solid matrices [2, 3]. The major impediment associated with the bioleaching technique for metal extraction is time consuming despite higher efficiency. A hybrid process comprising of both chemical and biological leaching involving combination of safer, non-toxic ligands, and bioleaching microbes has shown enhanced metal extraction from waste

K. Kanaujia · S. Hait (✉)
Department of Civil and Environmental Engineering, Indian Institute of Technology Patna, Bihta, Patna, India
e-mail: shait@iitp.ac.in

K. Kanaujia
e-mail: kavita8960@gmail.com

S. Kumar et al. (eds.), *Sustainability in Environmental Engineering and Science*, Lecture Notes in Civil Engineering 93,
https://doi.org/10.1007/978-981-15-6887-9_13

PCBs albeit time consuming [2]. In this context, a sequential strategy consisting of maximum biological production of ferric iron (Fe^{3+}) by *A. ferrooxidans* in the first step followed by hybrid bioleaching of metals from high-grade PCB of obsolete desktop using commercial citric acid as a safer ligand has been devised in the present study to overcome the impediment of higher time requirement. E-waste in the form of comminuted PCB was added in the second step when the system achieved maximum oxidation-reduction potential (ORP) and Fe^{3+} concentration.

2 Materials and Methods

2.1 E-Waste Collection and Processing

E-waste in the form of PCBs of discarded desktops was collected from local scrap dealers and electronic repairing shops at Bihta, Patna, Bihar, India, for further processing. The attached electrical components, i.e., capacitors, resistors, and semiconductor chips, were removed from the PCBs by using tools such as hammer, screwdriver, and pliers. The PCBs were then cut into pieces of dimensions approximately 2 cm × 2 cm for subsequent processing. The homogeneous mixture of PCB in the size range of 0.038–1 mm was obtained by first crushing the cut pieces in a cutting mill (SM200, Retsch, Germany) for size reduction followed by screening in a sieve shaker (AS200, Retsch, Germany). A sub-set of the homogeneous mixture of pulverized PCB intended to be used for the study was chemically characterized for the content of target base metals, i.e., Cu, Zn, and Ni.

2.2 Bacteria and Culture Conditions

A pure culture of *A. ferrooxidans* (NCIM 5371; ATCC 19859) was obtained from the National Collection of Industrial Microorganism (NCIM), Pune, India. Optimized 4.5 K medium, composed of mineral salts [$(NH_4)_2SO_4$: 2.0 g/L, K_2HPO_4: 0.25 g/L, $MgSO_4.7H_2O$: 0.25 g/L, KCl: 0.1 g/L, $Ca(NO_3)_2$: 0.01 g/L] and 22.2 g/L of $FeSO_4.7H_2O$, was used for culturing purpose in the study [4]. The bacteria were cultured in freshly prepared and autoclaved optimized 4.5 K media. Initially, the pH of the culturing media was adjusted to 2 using 1N H_2SO_4. The biomass growth was measured using an improved Neubauer chamber under a microscope (Ti-2, Nikon, Japan). As the biomass concentration reached about 10^7 cells/mL, the above fresh culture was used as inoculum for further study.

2.3 Biological Oxidation of Ferrous Iron

The acidophiles, i.e., *A. ferrooxidans*, were allowed to grow in the optimized 4.5 K media in 250 mL shake flasks containing 100 mL media with the addition of 1 mL of inoculum in each flask, whereas control flasks were not inoculated. The experiment was conducted in a shaker incubator (SIF-5000R, Jeiotech, Korea) at 30 °C and 170 rpm. Flask contents were monitored for pH, ORP, and ferrous (Fe^{2+}) and ferric (Fe^{3+}) iron concentrations during the experiment. The maximization of ferric iron was achieved via biological oxidation of ferrous to ferric during the growth of bacteria in the shake flasks. Since no bacterium was there in the control flasks, the oxidation was only due to the presence of oxygen inside the flasks.

2.4 Hybrid Bioleaching

Hybrid bioleaching was subsequently carried out in the same flasks once the maximization of Fe^{3+} was achieved. Pulverized PCB in the size range of 0.038–1 mm was added in each flask including the control ones at an e-waste pulp density of 10 g/L. To imitate the hybrid condition, 1 mL of 0.2 M commercial citric acid was added to each flask at the time of PCB addition. The pH, ORP, and ferrous (Fe^{2+}) and ferric (Fe^{3+}) iron concentrations of the bioleaching medium were monitored during the hybrid bioleaching. Additionally, the leachates from the hybrid reactors along with respective control reactors were withdrawn periodically and analyzed for target base metals, i.e., Cu, Zn, and Ni, to assess the hybrid bioleaching efficiency. In order to assess the change in surface morphology, the raw pulverized PCB as well as PCB residues upon hybrid bioleaching was observed using scanning electron microscopy (SEM) (EVO 18, Carl Zeiss, Germany).

2.5 Analytical Procedure

Microscopic features of pulverized and homogenized raw PCB as well as the PCB residue upon hybrid bioleaching were scanned using a scanning electron microscope (SEM) (EVO 18, Carl Zeiss, Germany) at the magnification of 2000× operated at 5 keV. The chemical analysis of PCB for the content of selected metal, viz Cu, Zn, and Ni, was performed using inductively coupled plasma mass spectrometry (ICP-MS) (7800, Agilent, USA) following microwave-assisted sample preparation using a microwave digester (Ethos Easy, Milestone, Italy) as per the USEPA 3052 acid digestion method [5]. The bioleachate obtained from hybrid bioleaching was analyzed for selected metal, viz Cu, Zn, and Ni, using ICP-MS (7800, Agilent, USA). The pH was measured using pH meter (F71, Horiba, Japan), and ORP was measured using ORP meter (A214, Orion star, Thermo Scientific USA). Total iron and ferrous

iron concentrations were measured colorimetrically using the phenanthroline method employing UV-Vis Spectrophotometer (Evolution 220, Thermo Scientific, USA) at 510 nm [6]. All the analyses were performed in triplicate, and average values were reported.

3 Results and Discussion

3.1 Metallic Content and Surface Morphology of Comminuted PCB Before and After Hybrid Bioleaching

Microwave-assisted metal digestion of raw pulverized PCB was carried out as per the procedure outlined in USEPA 3052 [5]. The content of selected metal, viz Cu, Zn, and Ni, in the comminuted PCB was determined by analyzing pre-filtered digestate through 0.22 μm in ICP-MS. The pulverized PCB of obsolete desktop was found to contain the selected base metals, viz 21.01% Cu, 2.65% Zn, and 0.08% Ni. The PCBs of obsolete desktop can be regarded as a high-grade secondary metal reserve considering the abundance of base metals in them. In order to assess the change in surface morphology, the micrographs of the raw pulverized PCB as well as PCB residues upon hybrid bioleaching as obtained from scanning electron microscopy (SEM) are presented in Fig. 1. It is evident from Fig. 1 that pulverized raw PCB particles exhibiting rods and wire-like structures with smooth metallic surfaces. Further, the broken and distorted ends of the rods signify the various shearing, tensile, and composite forces under which the PCBs are subjected during the pulverization operation in a cutting mill. However, the rough and scratched surface of PCB residues with potholes upon hybrid bioleaching indicates that the abundant metals were leached out of the PCB particle surface by the joint actions of acidophiles and citric acid.

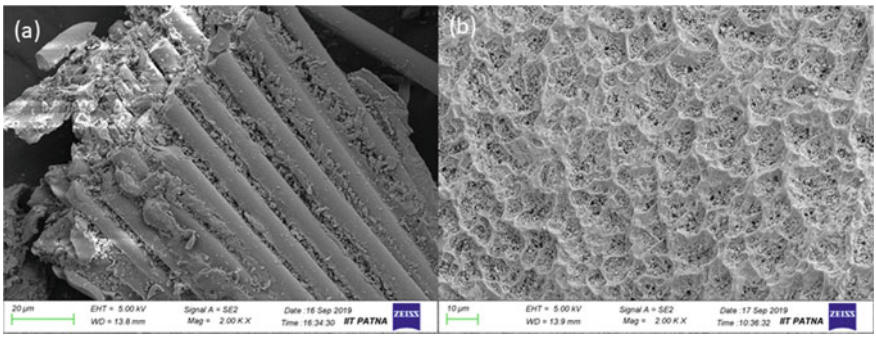

Fig. 1 SEM micrographs showing **(a)** comminuted raw PCB before bioleaching, and **(b)** PCB residue after bioleaching

3.2 Variation in Fe^{2+} and Fe^{3+} Concentrations, pH, and ORP Before and After PCB Addition

The sequential strategy for improved hybrid bioleaching adopted in the present study is targeted at the maximization of biological oxidation of ferrous iron (Fe^{2+}) present in the media by *A. ferrooxidans* in the first step followed by hybrid bioleaching of metals from the pulverized PCB. Variation in ferrous (Fe^{2+}) and ferric (Fe^{3+}) iron concentrations before and after PCB addition following sequential approach for hybrid bioleaching is depicted in Fig. 2. It is clear from Fig. 2 that the complete bio-oxidation of ferrous (Fe^{2+}) to ferric (Fe^{3+}) iron was observed in 60 h of biomass growth, following which pulverized PCB was added to the system. Complete bio-oxidation of ferrous iron in 60 h of biomass growth in the system indicated that the acidophiles were at the late log growth phase. Maximum ferric (Fe^{3+}) iron concentration of 0.6 g Fe^{3+}/L was attained in the system with an initial ferrous (Fe^{2+}) iron concentration of 4 g Fe^{2+}/L in the media (Fig. 2). The bio-oxidation of ferrous (Fe^{2+}) to ferric (Fe^{3+}) iron and subsequently ferric (Fe^{3+}) iron as a strong oxidant facilitates the knocking metals (M) out of the PCB matrix by elevating their oxidation state leading to metal solubilization and thereby reduces to ferrous (Fe^{2+}) iron. Bacteria-catalyzed continuous Fe^{2+}–Fe^{3+} redox cycle facilitating metal solubilization takes place in the system as per the following reactions:

$$4Fe^{2+} + 4H^{+} + O_2 \xrightarrow{\text{Bacteria}} 4Fe^{3+} + 2H_2O \quad (1)$$

$$Fe^{3+} + M^{0} \rightarrow Fe^{2+} + M^{2+} \quad (2)$$

The complete biological oxidation of Fe^{2+} in the system can be corroborated from the maximum oxidation-reduction potential (ORP). It has been reported that the ORP as a parameter is indicative of Fe^{3+}/Fe^{2+} ratio in a system where higher concentration

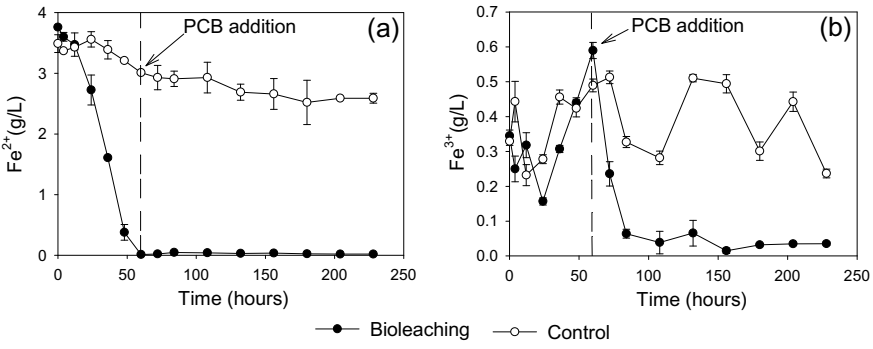

Fig. 2 Variation in ferrous (Fe^{2+}) and ferric (Fe^{3+}) iron concentrations before and after PCB addition following sequential approach for hybrid bioleaching

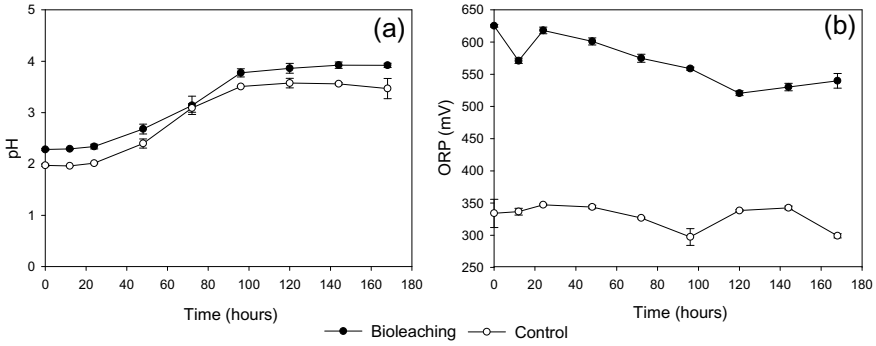

Fig. 3 Variation in **(a)** pH and **(b)** ORP after PCB addition during hybrid bioleaching

of Fe^{2+} is present [7]. Prior to the PCB addition, the maximum ORP of 625 mV was recorded in 60 h of bacterial growth from an initial value of 315 mV. Following the hybrid bioleaching of metals upon addition of PCB in the system, the reduction of Fe^{3+} back to Fe^{2+} and subsequent bio-generation of Fe^{3+} in the process as a part of the continuous Fe^{2+}–Fe^{3+} redox cycle caused a gradual drop of ORP with bioleaching time as presented in Fig. 3.

During the biomass growth in the first step, pH of the media was observed to increase from 2 to 2.3 in 60 h, i.e., at the time of PCB addition. Further, a gradual increase in pH from 2.3 to 2.6 in bioleaching duration of 96 h of PCB addition was observed as shown in Fig. 3. The increase in pH with the bioleaching duration can be attributed to the consumption of H^+ ions during the bio-oxidation of ferrous (Fe^{2+}) to ferric (Fe^{3+}) iron following the reaction (1). Further, the increase in pH can also be linked to the alkaline nature of the PCB.

3.3 Metal Extraction Following Sequential Approach for Hybrid Bioleaching

Metal extraction following sequential approach for hybrid bioleaching in terms of selected base metals, i.e., Cu, Zn, and Ni, from waste PCBs of desktop at an e-waste pulp density of 10 g/L is presented in Fig. 4. It is evident from Fig. 4 that the metal extraction was observed to happen rapidly and subsequently stabilized following an asymptotic trend. In the present study, maximum metal leaching efficiency was achieved to be 85% Cu, 71% Zn, and 54% Ni at an excellent duration of 96 h of PCB addition (Fig. 4). This faster rate of metal extraction in the present study can be ascribed to the complete bio-oxidation of ferrous (Fe^{2+}) iron present in the media by *A. ferrooxidans* in the first step and abundant availability of ferric (Fe^{3+}) iron in the system at the onset of hybrid bioleaching. Further, the combined effect of bacterial action in metal solubilization and the chelating action in metal complexation due to

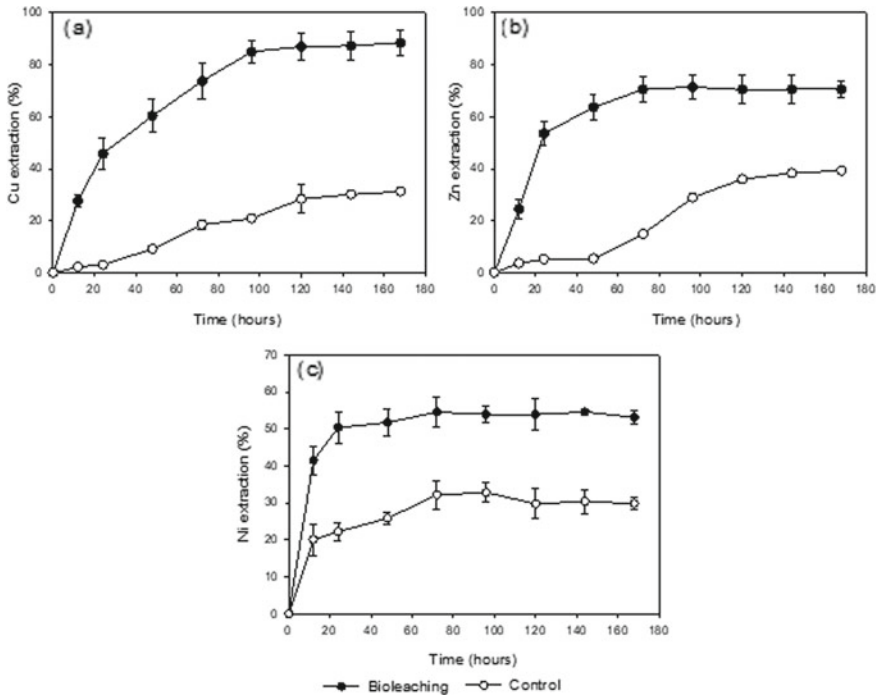

Fig. 4 Metal extraction efficiency for **(a)** Cu, **(b)** Zn, and **(c)** Ni following sequential approach for hybrid bioleaching

the addition of citric acid as a safer ligand during hybrid bioleaching can be attributed to higher metal extraction at faster rate [2].

4 Conclusions

A sequential approach comprising of maximum biological oxidation of ferrous to ferric iron by *A. ferrooxidans* in the first step followed by hybrid bioleaching of metals from waste PCBs of obsolete desktop using commercial citric acid as a safer ligand has been devised in the present study to overcome the limitation of higher time requirement. Maximum biological oxidation of Fe^{2+} was achieved at 60 h using initial concentration of 4 g Fe^{2+}/L prior to the addition of comminuted PCB. At an e-waste pulp density of 10 g/L, a maximum of 85% Cu, 71% Zn, and 54% Ni extraction was attained in the second step at an impressive time duration of 96 h of PCB addition. Hybrid bioleaching using citric acid as a safer ligand following the sequential approach of maximization of biological production of ferric iron can be developed as an eco-friendly technique for faster and efficient metal extraction from e-waste for resource recovery.

References

1. Baldé CP, Forti V, Gray V, Kuehr R, Stegmann P (2017) The global e-waste monitor 2017: quantities, flows and resources. United Nations University, International Telecommunication Union, and International Solid Waste Association
2. Priya A, Hait S (2018) Extraction of metals from high grade waste printed circuit board by conventional and hybrid bioleaching using *Acidithiobacillus ferrooxidans.* Hydrometallurgy 177:132–139
3. Mahmoud KK, Leduc LG, Ferroni GD (2005) Detection of *Acidithiobacillus ferrooxidans* in acid mine drainage environments using fluorescent in situ hybridization (FISH). J Microbiol Methods 61(1):33–45
4. Yang Y, Chen S, Li S, Chen M, Chen H, Liu B (2014) Bioleaching waste printed circuit boards by *Acidithiobacillus ferrooxidans* and its kinetics aspect. Journal of Biotechnol 173:24–30
5. USEPA (1995) Microwave assisted acid digestion of siliceous and organically based matrices. USEPA Method 3052, 3 edn. United States Environmental Protection Agency, Washington, DC
6. APHA (2012) Standard methods for the examination of water and wastewater. In: American Public Health Association, American Water Works Association. Water Environment Federation. American Public Health Association (APHA), Washington, DC
7. Christel S, Herold M, Bellenberg A, Buetti-Dinh M, El Hajjami M, Pivkin IV, Dopson M (2018) Weak iron oxidation by *Sulfobacillus thermosulfidooxidans* maintains a favorable redox potential for chalcopyrite bioleaching. Frontiers Microbiol 9:3059

Green Energy Based Low Cost Smart Indoor Air Quality Monitoring and Purifying System

Madhurima Chattopadhyay, Neha Surbhi, Jaynee Rawal, Shahla Khursheed, Sakshi Agarwal, and Shimona Francis

1 Introduction

At present in India, air quality has been degrading day by day due to presence of harmful chemicals and other materials. It has been observed that the indoor air quality can be up to 10 times worse than outdoor air pollution [1]. This is because confined areas facilitate impending pollutants to develop more than open spaces [2].

In domestic applications like cooking and heating with solid fuels such as dung, wood, and coal, it is likely to be the largest source of indoor air pollution around the whole world [3]. It has been reported that almost three billion people rely on biomass (wood, charcoal, crop residues, and dung) and coal as their primary source of domestic energy globally. As a result, the global mortality due to interior air pollution from solid fuels attributed to 1.5 million and 2 million deaths by 2010 [4]. Moreover, in last few decades, the condition of indoor air quality (IAQ) has reached to an alarming stage, so got intense attention from the international scientific community, political institutions, and environmental governances for minimizing the health hazards, uncomforting, and health risk of building occupants.

According to the report of the Global Burden of Disease, southeast Asia ranked third among risk factors from household air pollution created by solid fuel still 2010 [5]. But still today, air pollution has mainly focused on quantifying the health effects of outdoor air, and much improvement has been made toward monitoring and control of outdoor air quality and trying to regulate sources of outdoor air pollution (European Commission, 2008), whereas such efforts are taken for indoor air pollution (IAP) only in the workplace and enclosed public places. There is no such regulation provided for maintaining indoor air quality in domestic purposes [6].

M. Chattopadhyay (✉) · N. Surbhi · J. Rawal · S. Khursheed · S. Agarwal · S. Francis
Department of AEIE, Heritage Institute of Technology, Kolkata, West Bengal 700107, India
e-mail: madhurima.chattopadhyay@heritageit.edu

S. Kumar et al. (eds.), *Sustainability in Environmental Engineering and Science*, Lecture Notes in Civil Engineering 93,
https://doi.org/10.1007/978-981-15-6887-9_14

2 Literature Review

2.1 Existing Works

2.1.1 Blueair Classic 280*i*

Meant for room sizes of 280 sq. ft, the unique feature in the 'I' models is the presence of an air quality sensor that speeds up the fans automatically whenever it detects a drop in the air quality of the room. It costs for around Rs. 34,000 [7].

2.1.2 Dyson Pure Cool

Packed with IoT features, voice commands, diffused air flow mode, and more, the device is recommended for those who want a good-looking, feature-rich air purifier that performs well when the IAQ is in moderate to a slightly higher range. It costs for around Rs. 44,900 [8].

2.1.3 Honeywell Air Touch S8

The Air Touch S8 is capable of covering an area of 450 sq. ft. Although it supports app control, the buggy implementation of the app is a letdown. It is most suitable for office and manual operation. It costs for around Rs. 26,490 [9].

2.1.4 Experimental Setup

The project is built on Arduino Uno, and MQ gas sensors are used to monitor ambient air quality levels as shown in Fig. 1. The Arduino sketch prompts the system to collect samples, determine a threshold level, and activate a buzzer and an LED when air quality degrades beyond a certain threshold, and the relay circuit activates the air purifier unit whenever pollution level exceeds the limit. The Arduino code is written on Arduino IDE and burnt to the board using AVR Dude. In closed spaces (like living rooms, cars and offices), the level of CO_2 is increasing due to human activities. Thus, the current project is developed to detect the level of air pollution and control the pollution level in a restricted area by activating an air purifier system. In addition, developed low cost system can be installed in houses, offices, or cars. The sensors attached to the developed system first take multiple samples of air and determine a threshold level. If the level of CO_2 is more than the threshold level (1000 ppm), the air purifier is activated through a relay circuit.

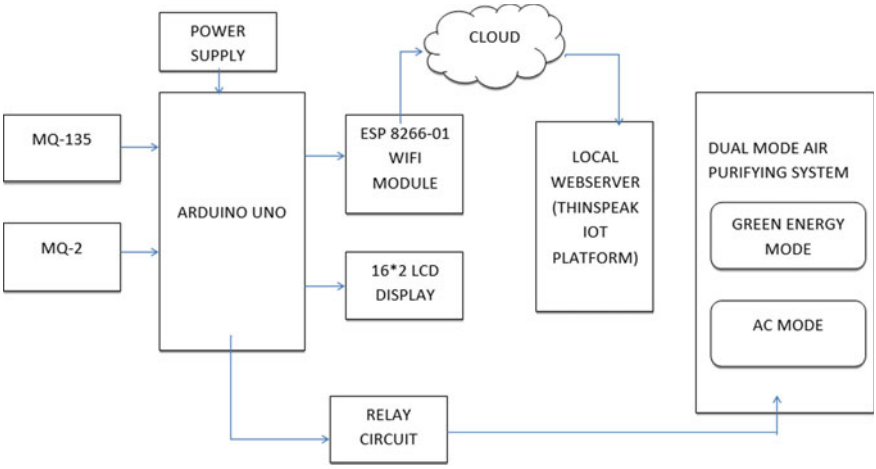

Fig. 1 Block diagram of the system

3 Principle of Working

3.1 Monitoring Unit

As shown in Fig. 2, by activating the Arduino board, it loads the required libraries and starts sampling data from the MQ-2 and MQ-135 gas sensors. From the collected samples, the Arduino code determines the mean CO_2 level of air and sets it as the threshold level for comparison. The Arduino keeps reading the air quality level from the gas sensors, and if the current air quality level increases beyond the threshold level, it activates the buzzer and an alert LED and sends a HIGH logic to relay connecting pin, automatically switching the air purifier ON. The reverse condition means when the air CO_2 is under threshold, it switches OFF the air purifier by sending a LOW logic at the relay connecting pin. Thus, there is a active feedback loop to monitor the air quality continuously which further compared with determined limit and finally operate relay circuit switching as required (Fig. 1).

3.2 Control Unit

The control unit along with the purifying system is shown in Fig. 3. This part is the heart of our project and is of paramount importance as it is IoT enabled, so one can monitor/control from a far end. The whole IoT is implemented using ESP8266 and thingspeak.com platform. For monitoring air quality levels, a Wi-Fi connection is established and real-time data are obtained every 15 s and are shown in Fig. 4.

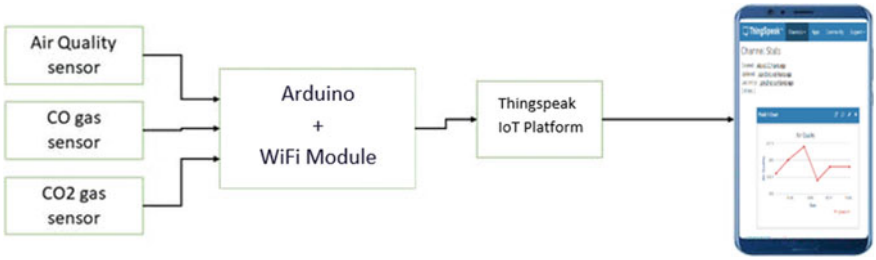

Fig. 2 Block diagram of air quality monitoring unit

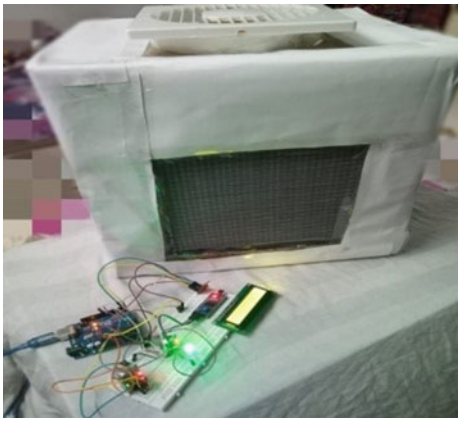

Fig. 3 Control unit with purifying filters

This part becomes disparate in nature because it includes the implementation of green energy and hence becomes cost effective and power efficient. The whole setup has been devised inside a cardboard box of 40 cm * 30 cm * 24 cm; two fans are used for the setup, one of which runs on household A.C supply (220 V), and the other one works on D.C supply (12 V) using green energy.

The control unit is a dual mode air purifier, i.e., it operates on either green energy mode (using solar energy) or AC mode to purify the air. Therefore, simple ON--OFF control logic is implemented there to start and stop the purifying circuit automatically. The developed purifier helps to remove harmful PM 2.5 and PM 10 air pollutants and keeps air free from bad odor and suspended dust. It further removes pollen, allergens, and airborne bacteria/virus/fungi (Fig. 3).

4 Results and Discussions

We used our device to monitor air quality indoors. The sensors MQ2 and MQ135 take readings from the environment and determine the air quality of the place in parts

per million (PPM). We have taken readings in two conditions: (i) readings of the air quality before the air purifier was turned on and (ii) readings of the air quality after the air purifier was switched on. We got satisfactory results as the air quality after the air purifier was switched on improved significantly as compared to air quality before.

Condition (i): Before the air purifier was turned on

When we tested the setup in the living room and kitchen, respectively, and have found satisfactory results. The quality of air before purification has been discussed further.

Condition (ii): After the air purifier was turned on

There is a drastically drop in ppm values of different sensor outputs as shown in Fig. 4 after uploaded in cloud on thingspeak platform. In the said figure, the left hand parts show the sensor results before the purifier is ON while the right one represents the results after switching ON the filtering circuit. The figures show the time, date, and the change in their graph whuch is recorded at an interval of every five minutes in thingspeak.

5 Conclusion

In this present work, the IoT based indoor air quality monitoring device is developed to display and aggregate real-time values of LPG, smoke, CO, and air quality in general. The use of IoT makes the system more viable, so at a time, a person can also monitor his household air quality even if he is away from home. Here, HEPA filter is used to drop the bigger particles while activated carbon sheet for smaller particles. A filter box is created with AC (220 V) fan for creating faster circulation. In order to make the device energy efficient, a 12 V–10 W solar panel with 12 V BLDC fan is incorporated. Thus, it can also be used without AC power and henceforth finds applications in cars as well as in rural areas also.

The developed system is a proof of concept, and we will introduce CCS811 sensor and NDIR CO_2 sensor instead of MQ series for better selectivity in future. At the same time to increase the portability of the device, we must incorporate optimization of filter size along with other components to give the system a compact and marketable look. The main outcome of this work is that the development and maintenance cost of the system is much less compared to the commercially available devices.

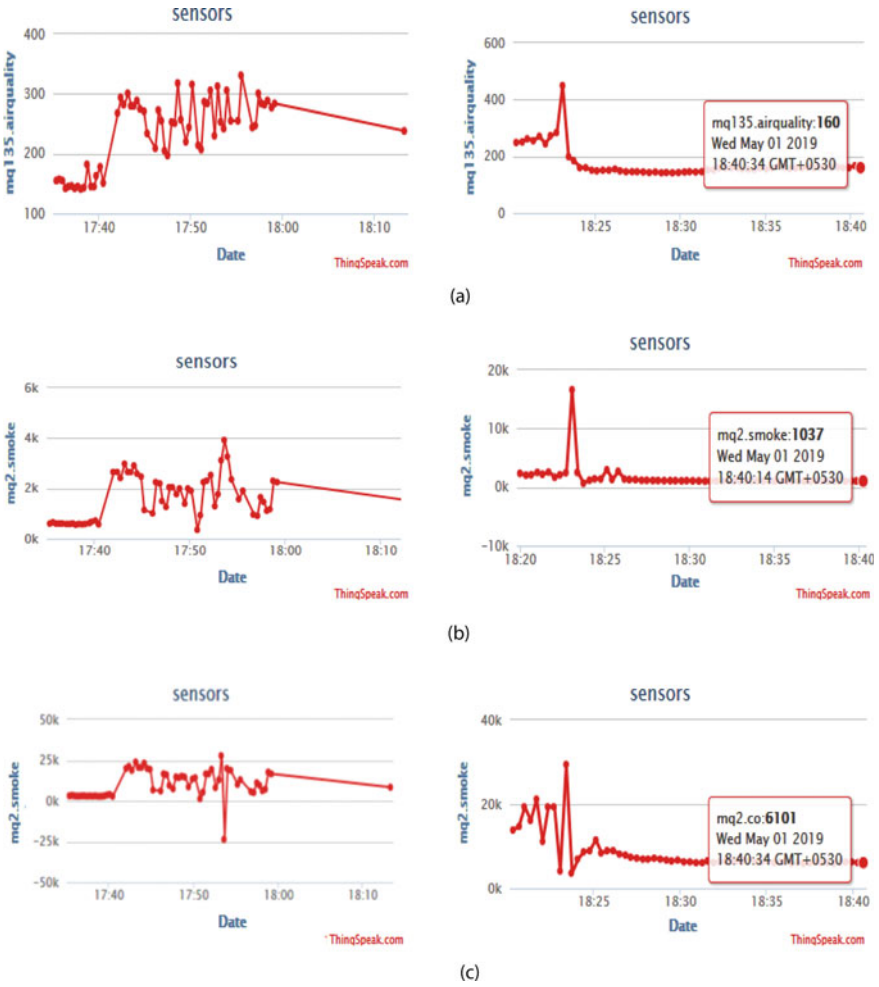

Fig. 4 **a–c** Depict the levels of air quality, smoke, and CO before and after the filter was turned on, respectively, on thingspeak

References

1. Cincinelli A, Martellini T (2017) On indoor air quality and health. Int J Environ Res Public Health [Online]. 14(11):1286. Available https://www.ncbi.nlm.nih.gov/pmc/articles/PMC5707925/
2. Kankaria A, Nongkynrih B, Gupta SK (2014) Indoor air pollution in India: implications on health and its control. Indian J Commun Med 39:203–207
3. Murray C, Lopez A (2002) The world health report 2002: reducing risks, promoting healthy life. [Online] Available https://www.who.int/whr/2002/en/whr02_en.pdf?ua=1
4. Ezzati M, Kammen DM The health impacts of exposure to indoor air pollution from solid fuels in developing countries: knowledge, gaps, and data needs. [Online] Available https://www.rff.org/documents/903/RFF-DP-02-24.pdf

5. Lim SS, Vos T, Flaxman AD, Danaei G, Shibuya K, Adair-Rohani H et al (2012) A comparative risk assessment of burden of disease and injury attributable to 67 risk factors and risk factor clusters in 21 regions, 1990–2010: A systematic analysis for the Global Burden of Disease Study 2010. Lancet 380:2224–2260
6. Coggins MA, Semple S, Hurley F, Shafrir A, Galea KS, Cowie H, Sanchez-Jimenez A, Garden C, Whelan P, Ayres JS Indoor Air Pollution and Health (IAPAH), Environmental Protection Agency Johnstown Castle, Co Wexford, Ireland, STRIVE Report (2008-EH-MS-8-S3), 2007–2013
7. https://www2.blueair.com/in/air-purifiers
8. https://patents.justia.com/assignee/dyson-technology-limited
9. https://patents.google.com/patent/USD737946S1/en

Degradation of Phenol Using Batch-Fluidization Process by Transition Metal Impregnated Red Mud as Modified Catalyst in Heterogeneous Fenton Process

Manisha and Prabir Ghosh

1 Introduction

With the rapidly growing population and industrialization, a large amount of waste is either discharged in water bodies as effluents or dumped in landfills leading to water pollution, groundwater and soil contamination. Red mud (RM) is one such industrial waste produced during aluminium extraction using Bayer's process [1, 2]. RM is usually disposed of either in stack as red mud ponds in the location close to the plant or discharged directly into the sea through a pipeline hence occupies a large area for storage, leads to dust pollution which caused severe health issues in the nearby areas and increases its cost disposal [3]. One such accident was witnessed by Ajka alumina plant in Hungary in which the dam of RM reservoir collapsed and resulted in contamination of lakes and rivers. These reasons accentuate us to find other alternatives that are economical as well as eco-friendly. Various methods have been investigated for utilization of RM in the most economical and environment-friendly ways and these are as follows: adsorbents, catalyst, recovery of Fe, Al, Ti and other trace metals [4].

Major sources of phenol effluents are petroleum, petrochemical, conversion process of coal and steel plants [5]. So, we should opt for other alternatives for degradation of phenols such as advanced oxidation processes (AOPs) [6, 7]. There are various practical disadvantages of heterogeneous iron-based Fenton process. Therefore, many researches shown that elements such as transition elements having multiple oxidation states can efficiently decompose H_2O_2 [8]. Various studies have been investigated in batch and column studies (fixed and fluidized bed) [9]. Among

Manisha · P. Ghosh (✉)
Department of Chemical Engineering, NIT, Raipur 492010, India
e-mail: prabirg.che@nitrr.ac.in

Manisha
e-mail: manisha.mtech2018.che@nitrr.ac.in

S. Kumar et al. (eds.), *Sustainability in Environmental Engineering and Science*, Lecture Notes in Civil Engineering 93,
https://doi.org/10.1007/978-981-15-6887-9_15

all the contacting patterns, fluidized bed was found to be highly effective and economical due to numerous advantages such as better heat transfer, mass transfer, excellent contact between the solid and the fluid (gas or liquid), and regeneration of catalyst is possible without shutting down the process [10, 11].

2 Materials and Methods

Bauxite residue or red mud used in this study was collected from red mud pond of NALCO, Damanjodi, Orissa, India. The RM lumps were grounded to a fine powder, sieved in a 75 μm mesh and stored. Phenol crystals are of analytical grade obtained from Molychem. Cobalt (II) nitrate hexahydrate and H_2O_2 are also of analytical grade purchased from Lobe Chemie PVT.LTD. 1000 ppm stock solution was prepared using Millipore and was stored in below 4 °C.

3 Preparation of N-RM and RM-Co Catalyst

Raw RM was added in Millipore water and mixed properly on a magnetic stirrer. All glassware and chemicals were washed and prepared with Millipore water. The raw RM has strongly alkaline character (pH 12–13). Therefore, it was neutralized by using acid and base for activating the catalyst and removing impurities to pH 7–7.5 [12, 13]. Then, the catalyst was placed in an autoclave for 4 h at 121 °C for precipitation. The catalyst was filtered and washed with Millipore water. RM (50 g) was taken separately to prepare cobalt impregnated catalyst for which 6.15 gm of cobalt (II) nitrate hexahydrate was dissolved in Millipore water and mixed properly [14, 15]. Now this solution was added to N-RM with 200 ml of Millipore water. Continuous stirring with heating (80 °C) was carried out for both N-RM and RM-Co. The catalyst was oven-dried at 120 °C in a hot air oven and then calcined at 500 °C for 4 h in a muffle furnace. Then, a desiccator was used to remove moisture from the catalyst. The preparation of the N-RM and RM-Co is shown in Fig. 1.

4 Experimental Set-up

In this study, the fluidized bed of length 0.22 m, ID of 0.028 m and a thickness of 0.003 m was used. An air pump was used to fluidize the bed of catalyst. In this batch fluidization or aggregate fluidization, a batch liquid and catalyst along with inert particles (silica beads) are fluidized by air (gas) [10]. For the determination of phenol concentration in the samples using UV-Vis spectrophotometry at 500 nm, a colorimetric method was employed. The 4-aminoantipyrine method was applied to analyse the samples [16].

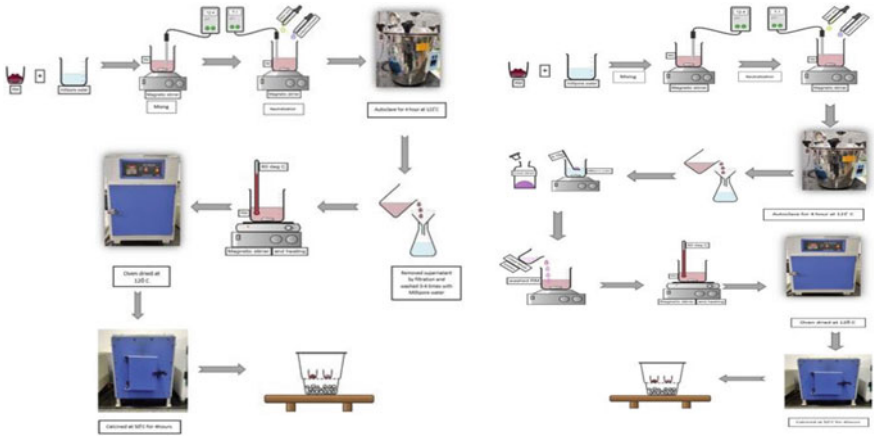

Fig. 1 Preparation of N-RM and RM-Co catalyst, respectively

5 Results and Discussion

5.1 N-RM and RM-Co Characterization

The surface morphology and elemental composition of the samples were studied using SEM and EDX, respectively. The SEM images of RM samples are shown in Fig. 2. It was observed that the particles are relatively loose and particles are poorly crystalline. The tendency to form agglomerates was also observed. For RM-Co, most of the particles present are irregular. The elemental analysis of RM sample provided by EDX showed the presence of Fe, Si, Al, Ti and Na. the EDX spectrum is shown in Fig. 3.

The XRD patterns were analysed using PANalytical X-ray diffractometer (CuK α radiation source) in 2θ range of 10°–70°. From the High Score Plus software, it is evident that the major phases are haematite, gibbsite, rutile, calcite, sodium

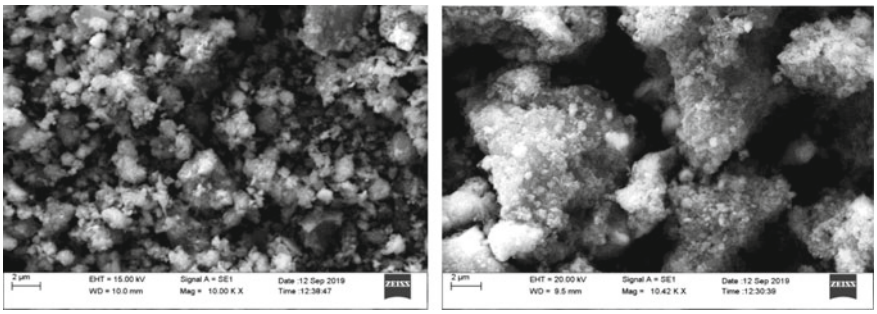

Fig. 2 SEM images of N-RM and RM-Co

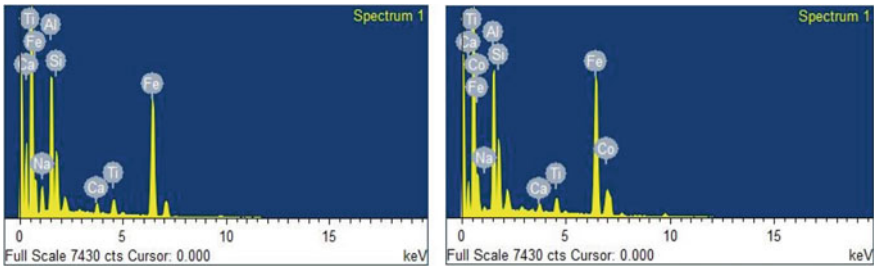

Fig. 3 EDX analysis of N-RM and RM-Co

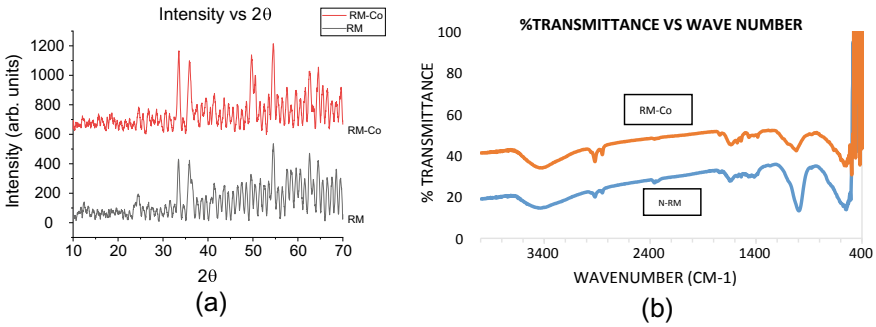

Fig. 4 **a** XRD and **b** FT-IR spectrum

aluminium silicate, dicalcium silicate and quartz [9, 17]. XRD results show the presence of certain compounds which are confirmed by the EDX and FT-IR. The profile of RM-Co was found to be different profile from N-RM after the incipient wetness impregnation. Characterization shows the presence of Cobalt oxide (Co_3O_4) on RM was highly dispersed in the form of fine particles. Hence, this shows that there are the more active sites for H_2O_2 activation. XRD pattern is shown in Fig. 4a.

FT-IR of the samples by KBr method was analysed using Bruker, Alpha Model in the wave number range of 400 cm^{-1} and 4000 cm^{-1}. Group characterization is shown in Table 1 and FT-IR spectrum is shown in Fig. 4b.

6 Degradation Study

Degradation study was carried out for phenol for both N-RM and (RM-Co) at different pH, catalyst dosage, H_2O_2 in a batch liquid gas fluidization process as shown in Table 2 [20]. The degradation of phenol was observed using UV-Vis Spectrophotometer. Phenol was measured with a colorimetric method (4-aminoantipyrine method).

Table 1 FT-IR group characterization

Group characterization	Wave number (cm^{-1}) (N-RM)	Wave number (cm^{-1}) (RM-Co)	Reference
O–H, H–O–H	2919.866	2919.866	Nath and Sahoo [18], Liang et al. [19]
C=O	1651.17	1635.73	Nath and Sahoo [18],
Si–O	995.4	1019.87	Nath and Sahoo [18], Liang et al. [19]
O–Si–O	547.72	1019.87	Nath and Sahoo [18], Liang et al. [19]
Fe–O	437.57	438.37	Nath and Sahoo [18]

Table 2 Degradation study

Pollutant	Catalyst	Catalyst dose (g)	pH	H_2O_2 mM	Initial pollutant concentration (ppm)	Degradation %
Phenol	N-RM	20	4	20	50	86.37
Phenol	N-RM	50	2.5	20	100	78.98
Phenol	N-RM	10	3.5	10	1000	88
Phenol	RM-Co	10	3	10	50	60.8
Phenol	RM-Co	1	3	10	100	86.12
Phenol	RM-Co	10	3	10	1000	87.32

7 Conclusions

The red mud can be utilized for other application such as a Fenton catalyst, and the process is simple, eco-friendly and low cost. It has a potential to degrade number of pollutants such as phenol and dyes. From the degradation study, it was observed that RM-Co showed higher degradation than N-RM. Also, for same degradation, the chemical consumption used for RM-Co was less compared to N-RM. Hence, it is evident that the transition elements supported on red mud can be used in substitution of iron for heterogeneous Fenton catalyst.

References

1. Li W, Hu G, Fei L, Tong Y, Honghu T, Han H, Yang Y, Liu R, Sun W (2019) Application of red mud in wastewater treatment. Minerals 9(5):281
2. Sahu MK, Patel RK (2016) Methods for utilization of red mud and its management. Int Environ Mater Waste 485–524
3. Sutar H, Mishra SC, Sahoo SK, Maharana HS (2014) Progress of red mud utilization: an overview. Int J Chem Sci 255–279

4. Ali T, Cengeloglu Y, Ersoz M (2009) Increasing the phenol adsorption capacity of neutralized red mud by application of acid activation procedure. Desalination 242(1–3):19–28
5. Bello MM, Raman AAA, Purushothaman M (2017) Applications of fluidized bed reactors in wastewater treatment—a review of the major design and operational parameters. J Clean Prod 141:1492–1514
6. Garcia-Segura S, Bellotindos LM, Huang Y-H, Brillas E, Lu M-C (2016) Fluidized-bed Fenton process as alternative wastewater treatment technology—a review. J Taiwan Inst Chem E 67:211–225
7. Lacson CFZ, de Luna MDG, Dong C, Garcia-Segura S, Lu M-C (2018) Fluidized-bed Fenton treatment of imidacloprid: optimization and degradation pathway. Sustain Environ Res 28(6):309–314
8. Matavos-Aramyan S, Moussavi M (2017) Advances in Fenton and Fenton based oxidation processes for industrial effluent contaminants control—a review. Int Environ Nat Resour J 2(4):1–18
9. Gupta VK, Ali I (2006) Removal of 2, 4-dinitrophenol from wastewater by adsorption technology: a batch and column study. Int J Environ Pollut 27(1–3):104–120
10. Pare A (2013) Hydrodynamics of three phase fluidized bed using low density particles. Ph.D. dissertation
11. Tisa F, Raman AAA, Daud WMAW (2014) Basic design of a fluidized bed reactor for wastewater treatment using fenton oxidation. Int J Innov Manag Technol 5(2):93
12. Bokare AD, Choi W (2014) Review of iron-free Fenton-like systems for activating H_2O_2 in advanced oxidation processes. J Hazard Mater 275:121–135
13. Genç H, Tjell JC, McConchie D, Schuiling O (2003) Adsorption of arsenate from water using neutralized red mud. J Colloid Interface Sci 264(2):327–334
14. Muhammad S, Saputra E, Sun H, Ang H-M, Tadé MO, Wang S (2012) Heterogeneous catalytic oxidation of aqueous phenol on red mud-supported cobalt catalysts. Ind Eng Chem Res 51(47):15351–15359
15. Hu P, Long M (2016) Cobalt-catalyzed sulfate radical-based advanced oxidation: a review on heterogeneous catalysts and applications. Appl Catal B Environ 181:103–117
16. Tor A, Cengeloglu Y, Aydin ME, Ersoz M (2006) Removal of phenol from aqueous phase by using neutralized red mud. J Colloid Interface Sci 300(2):498–503
17. Saputra E, Muhammad S, Sun H, Ang HM, Tadé MO, Wang S (2012) Red mud and fly ash supported co catalysts for phenol oxidation. Catal Today 190(1):68–72
18. Nath H, Sahoo A (2018) Red mud and its applicability in fluoride abatement. Mater Today Proc 5(1):2207–2215
19. Liang W, Couperthwaite SJ, Kaur G, Yan C, Johnstone DW, Millar GJ (2014) Effect of strong acids on red mud structural and fluoride adsorption properties. J Colloid Interface Sci 423:158–165
20. Farshchi ME, Aghdasinia H, Khataee A (2019) Heterogeneous Fenton reaction for elimination of Acid Yellow 36 in both fluidized-bed and stirred-tank reactors: computational fluid dynamics versus experiments. Water Res 151:203–214

Application of Low-Cost Air Quality Monitoring Sensor to Assess the Exposure of Ambient Air Pollution Due to $PM_{2.5}$ and PM_{10}

Md. Noman Munshi, S. M. Nihab Ahsan, Md. Shafinur Rahman, and M. Tauhid Ur Rahman

1 Introduction

Air pollution is a global-scale environmental problem with an adverse effect on rural and urban areas. It is declared as one of the major root causes of cancer by the World Health Organization (WHO) [11]. Pollutants that are suspended in the air in the form of dust, droplets, biological material, and solids are termed as PM. Aerodynamically PM is classified as coarse PM or PM_{10} (10–2.5 μm) and fine PM or $PM_{2.5}$ (2.5–1 μm). All of these have a significant adverse effect on human health which increases with the decrease in their diameter [8]. Air pollution alone can harm human respiratory, cardiovascular, cardiopulmonary, and reproductive systems [11]. Urban air pollution is posing serious health threats including 3.2 million death cases which have made it the first environmental health risk factor. However, low-income countries are subjected to worsened air quality standards [6]. Association between short-term exposure to $PM_{2.5}$ and increased death rate, increased numbers of hospital admissions, and increased risks of cardiovascular diseases (CVD) have also been proved [5]. PM is found to be comprised of mainly organic and inorganic carbon and sulfates from both natural and artificial sources. Nitrate, inorganic elements, and pollens also contribute as PM. Generally, PM is sourced from industry, vehicles, nucleation, and aerosol [8]. Dhaka, being the capital of Bangladesh, is experiencing major urbanization and development project. Air pollution in Bangladesh has been supplemented by the inherent problem of industrialization, vehicle emissions, generators, and rotary kilns [3].

Md. Noman Munshi (✉) · S. M. Nihab Ahsan · Md. Shafinur Rahman · M. Tauhid Ur Rahman
Department of Civil Engineering, Military Institute of Science and Technology, Dhaka 1216, Bangladesh
e-mail: noman.munshi@gmail.com

M. Tauhid Ur Rahman
e-mail: tauhid@ce.mist.ac.bd

S. Kumar et al. (eds.), *Sustainability in Environmental Engineering and Science*, Lecture Notes in Civil Engineering 93,
https://doi.org/10.1007/978-981-15-6887-9_16

It is a fact that human exposure to ambient air pollution has a significant relationship with health risks. Land-use regression and dispersion models or a combination of both are applied using PM concentrations from the nearest AQM station for human exposure assessment. A study showed that PM concentrations vary spatially due to the neighborhood of source locations significantly. This variation has made it challenging to assess human exposure more accurately without establishing a compact AQM network [13]. PM monitoring is necessary for reaching important decisions on diurnal variation, long-term trends, etc. [1]. For the developing and low-income countries, one of the major challenges to counter PM associated air pollution is the lack of air quality data. Monitoring air quality is a costly business and in this regard, easily operated and maintained low-cost equipment is a solution [6]. Despite its worries of being accurate, operating low-cost monitors on several locations for a longer period of time has been identified as a data gap in monitoring $PM_{2.5}$ [1]. The USA and Europe have already investigated the low-cost monitoring system; it is high time for us to research for the relevancy of this particular topic [6]. Air pollution is not homogeneous and for that case to relate the spatial and time variation small sensors with light scattering and condensation particle counting techniques should be used to monitor PM. Equipment using light scattering technology has become a popular tool for its compatibility with field campaigns and epidemiological studies [8]. In this research, AirVisual (AV) pro was used which is a laser scattering particle counter with GPS. This 294$ equipment also provides temperature, humidity data in addition to the air quality data like $PM_{2.5}$, PM_{10}, $CO_{2,}$, etc. (IQAir AirVisual). A low-cost monitoring sensor for air pollution was used on a number of occasions. It is explored in a few of the studies that this technique uses Dylos 1700 [6, 11]. This sensor uses light scattering technology but measures the particle number concentrations (PNC) only which are converted to $PM_{2.5}$ based on equations. There is also an issue of non-availability of data of several covariates like temperature, humidity, and wind speed [2, 11]. The novelty of this study is the use of AV pro which gives direct data of $PM_{2.5}$ and PM_{10} with other two covariates information, temperature, and humidity with GPS locations. AV pro feeds readymade data of $PM_{2.5}$ and PM_{10} which can be easily conceived.

There is a requirement of shifting to an intensive low-cost monitoring system from a small number of high-cost equipment. As per Steinle et al. [11], FSM data are not a handy tool to observe the spatial pattern of personal exposure but it can be overcome by using low-cost monitoring systems in large numbers at frequent intervals of locations. Another drawback of mobile monitoring is, it does not stand as a strong means to measure the exposure of mass people as the duration of exposure in one location will vary for each mobile equipment.

The ultimate goal of this study was to determine human exposure to the PM concentrations by a low-cost AQM sensor. The first goal was to validate the low-cost sensors in comparison to standard equivalent equipment. The second goal was to analyze the primary data to find out the variation of PM concentrations spatially, diurnally, and temporally. The terminal objective was to determine the most polluted zone.

2 Materials and Methods

The study was carried out on the basis of quantitative and qualitative primary data and information. The PM concentration level at the ambient environment is measured by low-cost AQM equipment and fixed-site monitoring (FSM) station data. The data were collected and recorded systematically through field study, interviews with relevant expert personnel, online survey, and extensive statistical analysis.

2.1 The Design of the Study and Sites

Four sites were selected to monitor air quality. Figure 1 shows the location of the FSM sites. Brief description of the sites is projected in Table 1. Bangladesh National Standard (BNS) set by the Government of Bangladesh (GoB), US Environmental Protection Agency (USEPA), European Union (EU), and World Health Organization (WHO) is projected in Table 2. The national ambient air quality standard of Bangladesh is lenient in comparison to other standards.

2.2 Low-Cost Monitoring Solution

A validation experiment was conducted to compare the measurements between BAM-1020 and AV sensor. The AV pro has an internal lithium-ion battery with 1900 mAH capacity. It can run for about 4 h on a single charge. The charger is 5 V, 1 A minimum (IQAir AirVisual). Additionally, a 20,000 mAH power bank was used to supply power to the device. To protect the device from excessive sunlight and rainfall, a frame was installed. The frame was designed to facilitate continuous airflow. The device was kept at a height of 5ft from the ground to get the concentration at the human nose level (Fig. 2).

2.3 Data Collection, Extraction, and Processing

A duration of 91 days of data was collected. AV pro data were retrieved from the device wirelessly downloading them as comma-delimited text. Data were measured in two different sites named site-1 and site-2, by AV sensor. US Embassy's (site-3) data were collected from the Web site of the US Embassy. From there only, $PM_{2.5}$ data were extracted due to the unavailability of the data of PM_{10}. Site-4 data were extracted from the case project Web site as PM_{10} and $PM_{2.5}$ in $\mu g/m^3$. To compare the AV sensor data with other FSM stations, AV sensor data were averaged into hourly averages. Temperature and RH data were collected from the AV sensor. Rainfall and

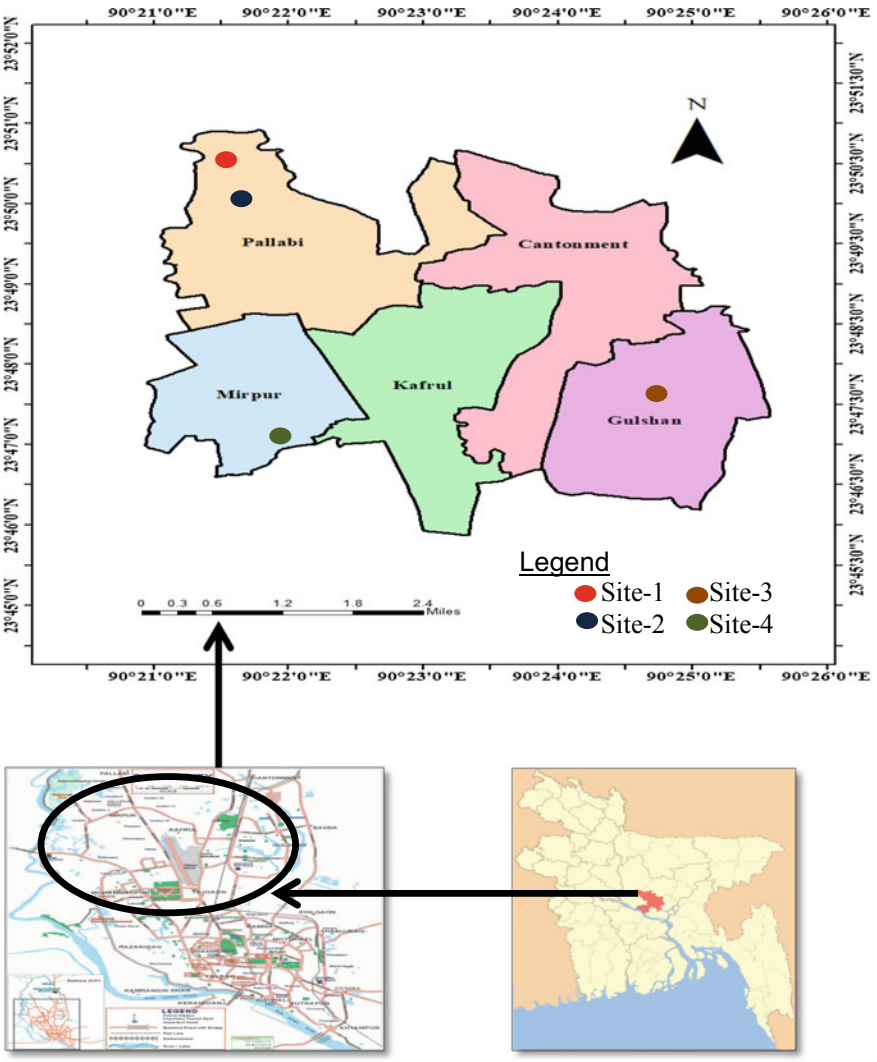

Fig. 1 Location of four FSM in Dhaka city

Table 1 Description of sites

Location	Site	Status of the site
Mirpur Cantonment	Site–1	Educational and residential sites with limited traffic and construction work
Mirpur–12	Site–2	Commercial area with heavy traffic and construction work
US Embassy	Site–3	Commercial area with heavy traffic
Darus Salam	Site–4	Commercial area with medium traffic and construction work

Table 2 Various AQ standards

Component	Averaging time	Standard/guideline values ($\mu g/m^3$)			
		BNS	USEPA	EU	WHO
PM 2.5	24 h	65	35	–	25
	Annual	15	12	25	10
PM 10	24 h	150	150	50	50
	Annual	50	–	40	20

Fig. 2 AV pro with expedient frame during data collection and validation experiment with HIM 6000

wind speed data were collected from the Bangladesh Meteorological Department (BMD). An online survey of 110 respondents was carried out. In this survey, the respondents were asked to submit their response with regards to various air pollution perspectives like overall air quality, source of pollution, and various health effects.

The obtained PM concentration data set was processed for mapping the variation of air quality among the four sites in Arc GIS.

3 Results

This part of the paper provides a comprehensive statistical analysis of the collected data from four different heterogeneous environments of Dhaka city. MS Excel and SPSS were used to analyze the data.

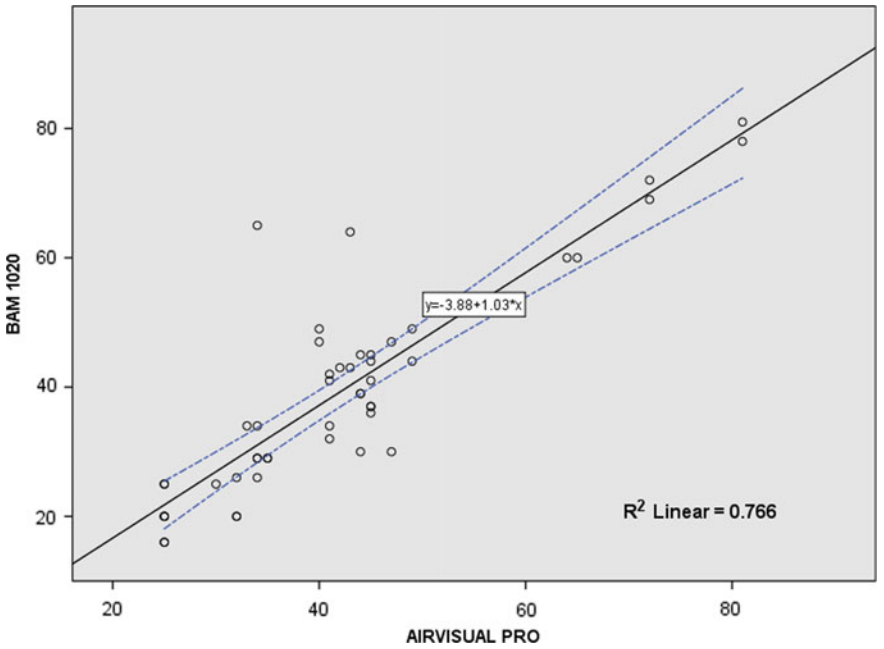

Fig. 3 Validation experiment of AV pro and BAM1020

3.1 Validation Experiment

Figures 3 and 4 display the scatter plots for the standard major axis regression of AV pro vs BAM-1020 and AV pro vs HIM 6000. The correlations between the AV pro with BAM-1020 ($R^2 = 0.77$) and HIM-6000 ($R^2 = 0.91$) were obtained.

The BAM-1020 instrument at the US Embassy provides output data as hourly averages, therefore AV pro data were processed to calculate hourly averages from the data collected at 10-second resolution. HIM 6000 provides data as a one-minute interval. In this case, HIM-6000 data were averaged into hourly averages.

3.2 Spatial Variation

The box and whisker plots in Figs. 5 and 6 illustrate the variation of measured $PM_{2.5}$ and PM_{10} concentrations between the individual sites. Mean concentrations of $PM_{2.5}$ for each site vary between 9 [3] and 210 $\mu g/m^3$. For PM_{10}, mean concentration in each site ranges between 38.4 [3] and 266 $\mu g/m^3$. The variation between sites is also reflected in the summary statistics of $PM_{2.5}$ and PM_{10} collected across four sites reported in Table 3. Mean and standard deviation (Sd) highlight not only the differences between sites but also the range of data within each site.

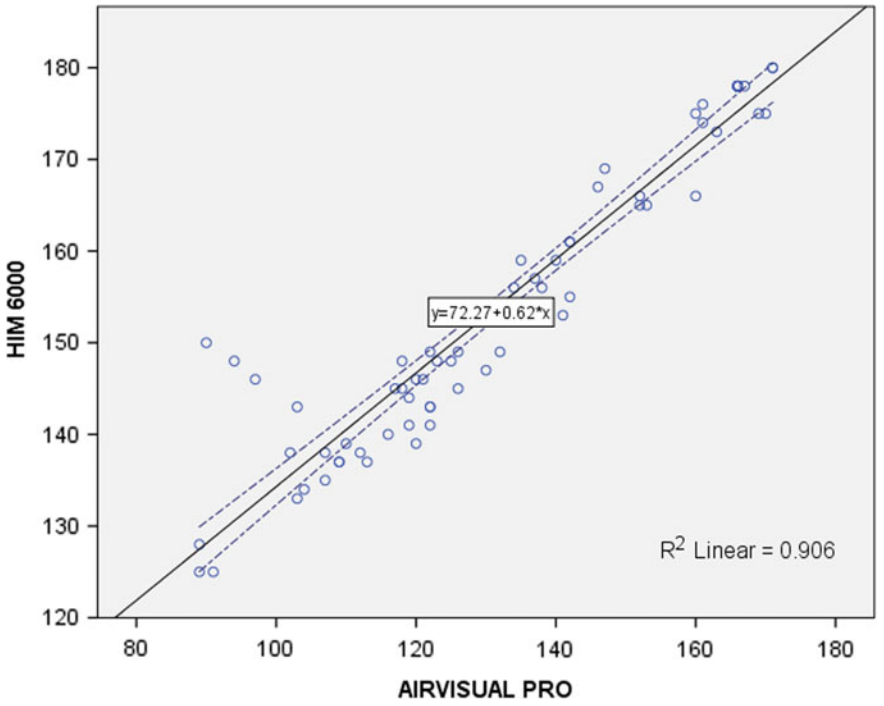

Fig. 4 Validation experiment of AV pro and HIM 6000

Fig. 5 Calculated $PM_{2.5}$ derived for each site

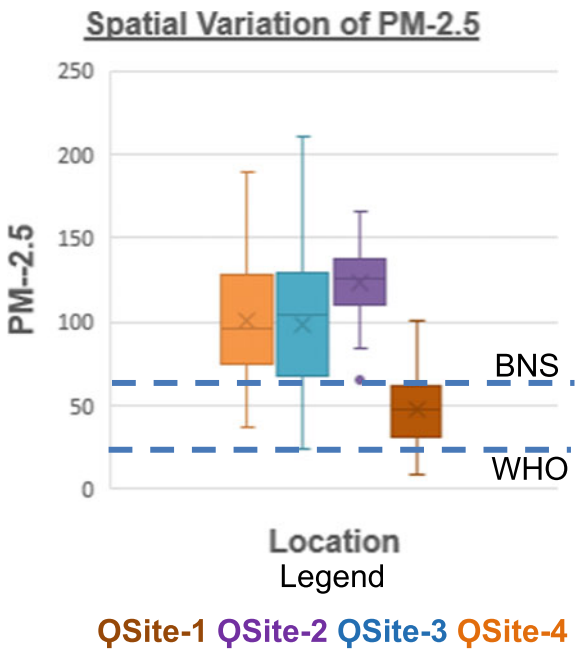

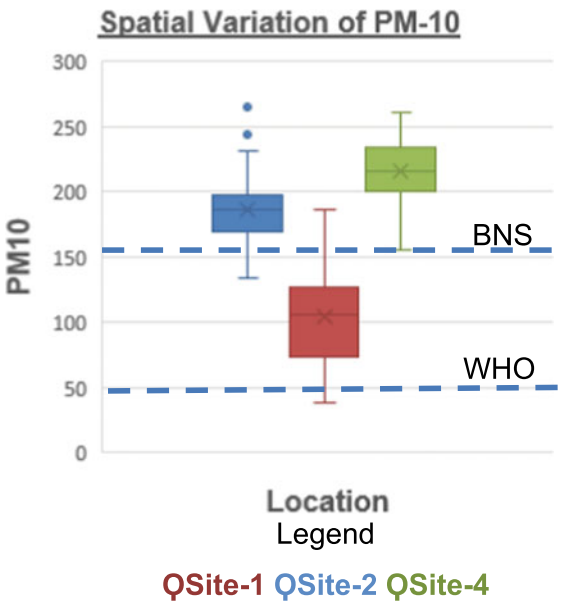

Fig. 6 Calculated PM_{10} derived for each site

Table 3 Variation of PM concentration in four sites

Sites	*n*	$PM_{2.5}$		PM_{10}	
		Mean	Sd	Mean	Sd
US Embassy	90	100.88	33.01	–	–
Darus Salam	91	98.44	38.91	216.44	22.04
Mirpur-12	91	122.63	19.50	186.24	24.87
MIST	91	47.89	20.70	104.46	35.44

A one-way ANOVA was conducted between sites to compare the mean $PM_{2.5}$ concentrations of different sites. There was a significant difference in the mean between sites [$F(3359)$, $p < 0.05$]. Post-hoc comparisons using the Tukey test indicated that the mean concentration of the US Embassy and Darus Salam was significantly different from the mean concentration of MIST and Mirpur-12. However, no significant difference was found in the mean concentration of the US Embassy and Darus Salam. For PM_{10} concentration, it was found that the mean concentrations of three sites are significantly different from each other [F (2270), $p < 0.05$].

3.3 *Diurnal Variation*

Diurnal variations shown in Figs. 7 and 8 were plotted and it was found that for $PM_{2.5}$ in all four sites and for PM_{10} in all three sites followed the same pattern. The observed peak of PM concentrations was found between 0700–0900 h and 1600–1800 h. In the online survey, 77.3% of the respondents think that motor vehicle is the

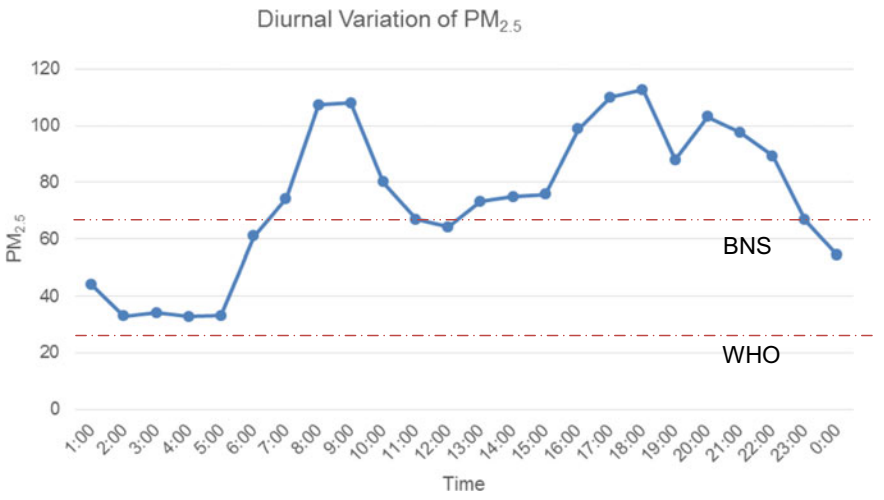

Fig. 7 Diurnal variation of $PM_{2.5}$

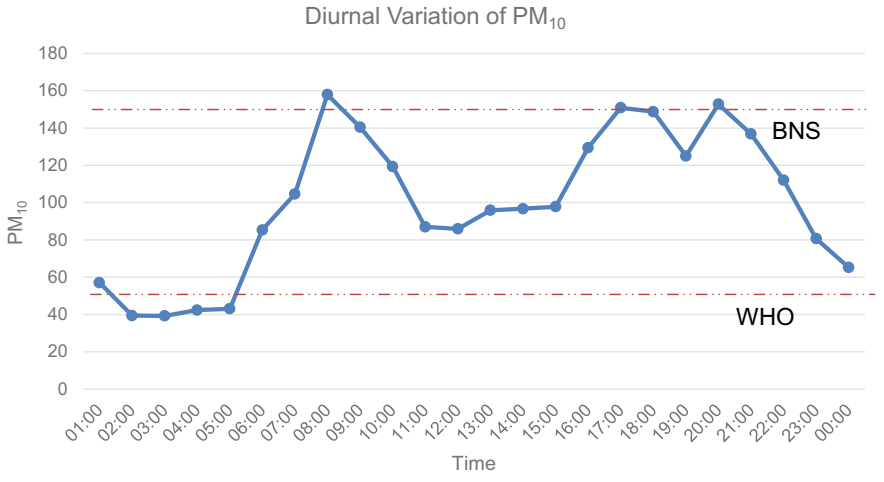

Fig. 8 Diurnal variation of PM_{10}

main reason responsible for air pollution. Traffic density is perceived to be at highest during the time mentioned above.

3.4 Temporal Variation

The $PM_{2.5}$ and PM_{10} concentrations show a decreasing trend with the change in season from pre-monsoon to monsoon. But no significant relationships were found ($p > 0$ .025). The changes in the covariates are given in Table 4. There is a significant difference in PM concentration from pre-monsoon to monsoon season given in Table 5. We observed that the meteorological factors also show a significant variation in both the seasons.

3.5 Most Exposed Zone

The obtained PM concentration data set are being processed for mapping by Arc GIS software. Figure 9 shows the level of PM concentration in the study locations.

4 Discussion

This study formulates a new technique of measuring PM concentrations in a heterogeneous ambient environment statically. This is a unique effort since the study applied portable, readily operated and low-cost equipment instead of costly, labor-intensive, and complicated FSM equipment to assess PM concentration spatially, temporally, and diurnally. Moreover, the limitations of FSM mentioned in the previous studies can be overcome by assessing the exposure in closer proximity increasing the number of sensors [9]. All the relevant data are used to assess the exposure of PM concentrations. Assessment of personal exposure through low-cost equipment has the benefit of measuring a person's daily exposure to PM. But for a developing country, it is difficult to provide equipment to everyone so that everyone can assess their individual exposure level. Again, the effect of covariant in PM concentration is also missing. The method applied in this study has been examined with respect to its feasibility for monitoring and shows the relevant issues with practical applications.

The AV pro is not particularly designed for ambient air quality monitoring. To protect it from rainfall and precipitation, a frame was developed. The entire data were collected at the nose level (5′ from the ground surface). We did not conduct any standard major axis regression between AV pro and Darus Salam FSM equipment since the same equipment is being used as of US Embassy.

To our knowledge, for the first time, this study validated the performance of AV pro against standard air quality monitoring equipment in the ambient environment.

Table 4 Change in covariates

	Rainfall		Temperature		Relative humidity		Wind	
	Pre-monsoon	Monsoon	Pre-monsoon	Monsoon	Pre-monsoon	Monsoon	Pre-monsoon	Monsoon
Mean	3.48	5.25	30.22	29.36	76.71	84.68	19.96	17.13
Sd	5.02	4.8	1.51	1.2	9.32	6.13	4.89	2.99

Table 5 Change in PM concentration

	$PM_{2.5}$		PM_{10}	
	Pre-monsoon	Monsoon	Pre-monsoon	Monsoon
Mean	49.96	45.87	114.91	70.04
Sd	12.71	12.71	29.50	26.67

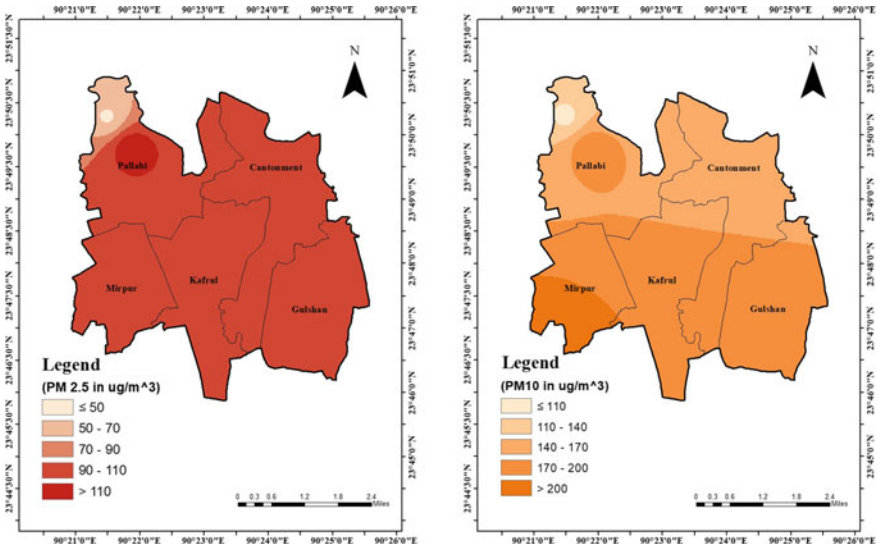

Fig. 9 Variation in $PM_{2.5}$ and PM_{10} concentration in different sites

Steinle et al. [11] found regression coefficient (R) ranging from 0.7 to 0.9 at hourly averaged $PM_{2.5}$ and [7] found regression coefficient between 0.81 and 0.99 at 24 h averaged $PM_{2.5}$ concentrations. In comparison to these two studies, the obtained $R^2 = 0.778$ and $R^2 = 0.96$ are well corrected.

The correlation coefficient for AV pro versus BAM-1020 was obtained $R^2 = 0.77$. This is due to the variation in detection methods between the two instruments. The response time of AV and BAM is different. The distance between the instruments was 50 m. This study showed that spatial and temporal variations of PM concentrations change significantly from one location to another location.

To assess the exposure, the findings provide a better understanding. We considered elevation and local atmosphere inversion as important factors. Though elevation is a significant covariate for the pre-monsoon season [12], we measured the air quality keeping the AV pro at nose level (5′ from the surface).

The average concentration of $PM_{2.5}$ and PM_{10} of site-1, site-2, site-3, and site-4 exceeded the BNS and WHO (Figs. 5 and 6). A study found that PM concentrations in Dhaka city crossed the BNS during the dry season and during the wet season it

remained within BNS [10]. But we found that during the monsoon PM concentration level crossed the BNS. From the diurnal variation, we found that the trends of pollution greatly vary within a day. The maximum PM concentration was observed between 0700–0900 h and 1600–1800 h when the traffic is higher during the day.

We analyzed the PM concentration data diurnally, temporally, and spatially. Combining these data set we produced an Arc GIS map through the color gradient. This map pointed out Mirpur-12 as the most polluted zone among the four sites.

5 Conclusion

The study was designed to assess the PM concentrations in heterogeneous environments via low-cost air quality monitoring sensors. The purpose is to provide adequate air quality data to improve public health conditions and the implementation of environmental policies. In order to do that, we validated the low-cost air quality sensor AV pro against the standard equivalent instrument. We analyzed the collected data extensively for the validation of statistical results.

This feasibility study is a distinctive step in the air quality arena. It shows that the application of low-cost equipment in combination with other monitoring systems provides a more reliable and easier approach in health impact assessment. It is to be mentioned that low-cost equipment does not claim to provide the most accurate data as standard equivalent equipment. It is an effective option for the least developed or developing country to assess the PM concentrations. This study is highly potential. Inclusion of direct meteorological data sets, population density can increase the scope and strength of the study. A further epidemiological and clinical study is needed in the effective application of the device to directly assess the health impact and to create an Internet-based platform to control issues due to air pollution.

References

1. Dhammapala R (2019) Analysis of fine particle pollution data measured at 29 US diplomatic posts worldwide. Atmos Environ 213:367–376. https://doi.org/10.1016/j.atmosenv.2019.05.070
2. Han I, Symanski E, Stock TH (2016) Feasibility of using low-cost portable particle monitors for measurement of fine and coarse particulate matter in urban ambient air. J Air Waste Manag Assoc 67(3):330–340. https://doi.org/10.1080/10962247.2016.1241195
3. Hasan MR, Hossain MA, Sarjana U, Hasan MR (2016) Status of air quality and survey of particle matter pollution in Pabna city, Bangladesh. Am J Eng Res 5(11):1
4. IQAir Air visual. (n.d.). Retrieved November 6, 2019, from https://www.airvisual.com/air-quality-monitor
5. Khan R, Konishi S, Ng CFS, Umezaki M, Kabir AF, Tasmin S, Watanabe C (2019) Association between short-term exposure to fine particulate matter and daily emergency room visits at a cardiovascular hospital in Dhaka, Bangladesh. Sci Total Environ 646:1030–1036. https://doi.org/10.1016/j.scitotenv.2018.07.288

6. Ngo NS, Asseko SVJ, Ebanega MO, Alloo SMA, Hystad P (2019) The relationship among PM2.5, traffic emissions, and socioeconomic status: Evidence from Gabon using low-cost, portable air quality monitors. Transp Res Part D Transp Environ 68:1–2. https://doi.org/10.1016/j.trd.2018.01.029
7. Northcross AL, Edwards RJ, Johnson MA, Wang Z-M, Zhu K, Allen T, Smith K R. (2013) A low-cost particle counter as a realtime fine-particle mass monitor. Environ Sci Processes Impacts 15(2):433–439. https://doi.org/10.1039/c2em30568b
8. Occhipinti L, Oluwasanya P (2017) Particulate matter monitoring: past, present and future. Int J Earth Environ Sci 2(2). https://doi.org/10.15344/2456-351x/2017/144
9. Rai AC, Kumar P (2017) Summary of air quality sensors and recommendations for application. Summary of air quality sensors and recommendations for application. iSCAPE, pp 1–10
10. Rana MM, Sulaiman N, Sivertsen B, Khan MF, Nasreen S (2016) Trends in atmospheric particulate matter in Dhaka, Bangladesh, and the vicinity. Environ Sci Pollut Res 23(17):17393–17403. https://doi.org/10.1007/s11356-016-6950-4
11. Steinle S, Reis S, Sabel CE, Semple S, Twigg MM, Braban CF, Leeson, S.R., Heal MR, Harrison D, Lin C, Wu H (2014) Personal exposure monitoring of PM2.5 in indoor and outdoor microenvironments. Sci Total Environ 1–2. https://doi.org/10.1016/j_scitotenv.2014.12.003
12. Tunno BJ, Shields KN, Lioy P, Chu N, Kadane JB, Parmanto B, Zora J, Davidson C, Holguin F, Clougherty JE (2012) Understanding intra-neighborhood patterns in PM2.5 and PM10 using mobile monitoring in Braddock, PA. Environ Health 11(1):1–3. https://doi.org/10.1186/1476-069x-11-76
13. Xu G, Jiao L, Zhao S, Cheng J (2016) Spatial and temporal variability of PM2.5 concentration in China. Wuhan Univ J Natural Sci 21(4):358–368. https://doi.org/10.1007/s11859-016-1182-5

Estimation of Greenhouse Gases in the Ambient Air

Papiya Mandal, Naveen Kumar, and Ajey Kumar Patel

1 Introduction

Rapid urbanization and initialization and increasing trend of vehicular registrations enhanced emission of large amount of greenhouse gases (GHGs) in the ambient air. The combustion of fossil fuel is directly or indirectly responsible for the global climate change. Major GHGs are CO_2 (carbon di oxide), CH_4 (methane), N_2O (nitrous oxide), O_3 (ozone) and water vapor. The reactive trace gases like nitrogen species (NO_x), carbon monoxide (CO), and volatile organic compounds (VOCs) are having the oxidizing capacity and form ozone in the troposphere. These pollutants are the indirect GHGs and they influence not only O_3, but also on the lifetime of CH_4 and other GHGs. The emissions of NO_x, CO and VOC emissions are dominated by combustion of fossil fuels (coal, natural gas, and oil) and human activities. The main sources for emission of GHGs are combustion of fossil fuels, deforestation, agriculture, waste to energy plant etc. but the emission of GHGs from other sectors like water/waste water treatment plant, constructed waste land, drain are not negligible. Intergovernmental Panel on Climate Change [1] reported that the percentage contribution of GHGs has the adverse effect on earth. The radiative forces are developed on earth due to frequent changes of the atmospheric composition, alteration of surface reflectance due to changes of land use pattern and variation of the sun's position. Radiative forces absorption and their heating and cooling effects on earth is shown in Fig. 1a. GHGs (CO_2, CH_4, N_2O and Halocarbons) have the maximum warming effects as compared to other compounds like aerosols, aviation-induced and solar. The scientific understanding level of each compound varies considerably. GHGs like

P. Mandal (✉) · N. Kumar
National Environmental Engineering Research Institute (NEERI), Delhi, India
e-mail: p_mandal@neeri.res.in; papiya.mandal1942@gmail.com

N. Kumar · A. K. Patel
National Institute of Technology, Warangal (NITW), Warangal, Telangana 506004, India

S. Kumar et al. (eds.), *Sustainability in Environmental Engineering and Science*, Lecture Notes in Civil Engineering 93,
https://doi.org/10.1007/978-981-15-6887-9_17

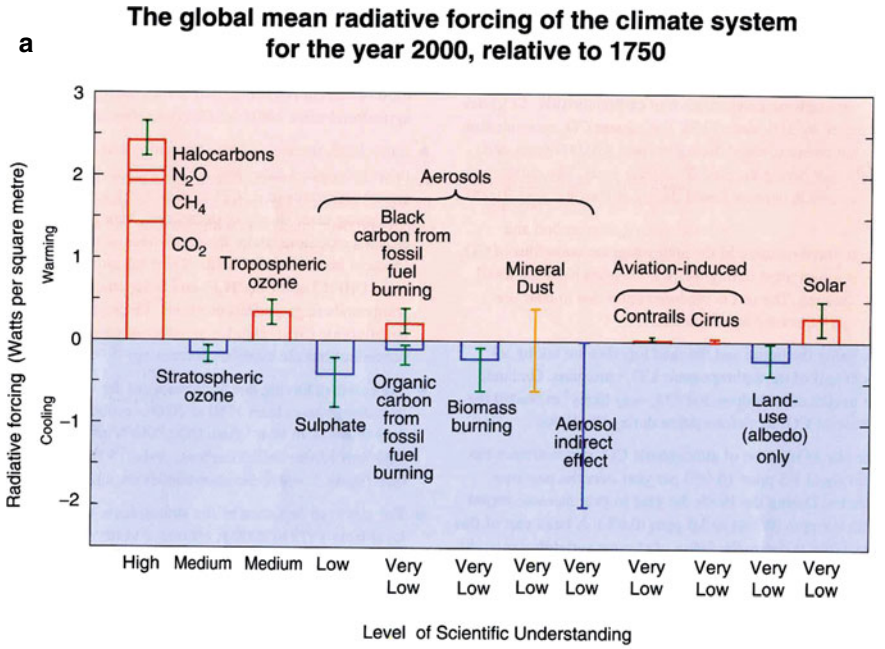

(Source IPCC, 2001)

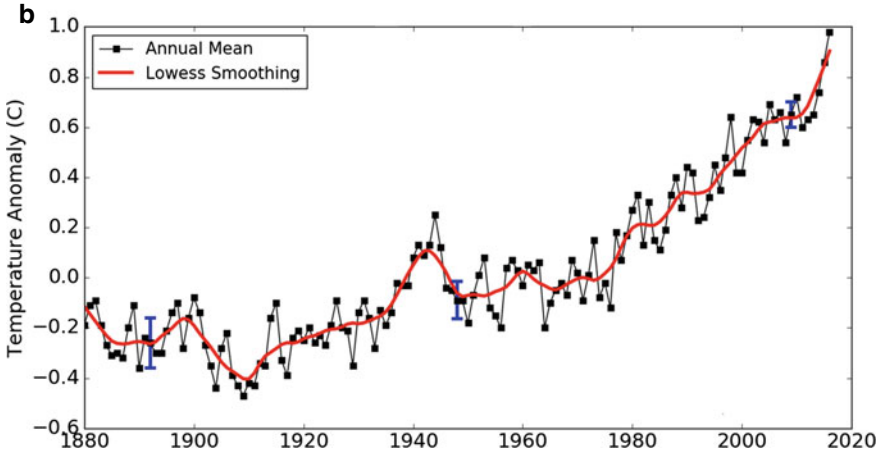

(Source NASA Goddard Institute for Space Studies and IPCC, 2014)

Fig. 1 **a** Radiative forces absorption and heating and cooling effects on earth. **b** Land and ocean temperature index 1880–2016

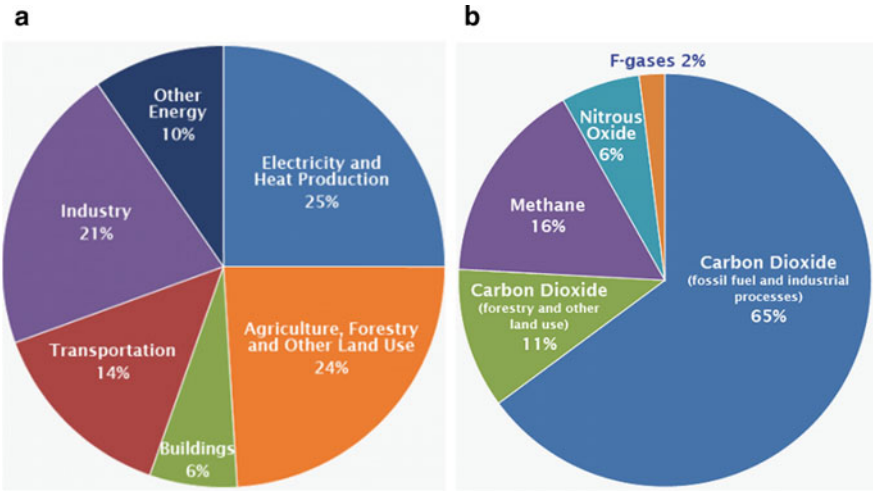

Fig. 2 **a** Global GHGs Emission by Economic Sectors. **b** Percentage contribution of global GHGs Emission

CO_2 responsible for perturbing the global heat balance. People are now facing the adverse effect of climate change on environment. The occurrence of thunder storms, flooding and droughts, are common these days. The changes of weather pattern not only ruin crops production but also spreading water, air and insect-borne diseases and having significant threat to public health. Land and Ocean Temperature Index 1880–2016 is shown in Fig. 1**b**. The average increasing trend of global temperature started after industrial revolution in the year 1940. The average global temperature has increased up to the year 2016 was about 0.8 °C since 1880. It has till now increasing trend and scientists are expecting that the average global temperature will rise an additional 0.3–0.7 °C upto 2035 [2].

IPCC report of 2014 has also reported the emission of GHGs from various economic sectors and percentage contribution of global GHGs emission. Figure 2a show Global GHGs Emission by Economic Sectors [3] and Fig. 2b show Percentage contribution of global GHGs Emission [3].

The major source of GHGs are electricity and heat production sector (25%), followed by agriculture and other land use (24%), industry (21%), transportation (14%), other energy (10%) and building (6%). The emission of CO_2 gas in global scale is about to be 76% (fossil and industrial processes 65% and forestry and other land use 11%) followed by methane (16%), nitrous oxide (6%) and other F gases (Chlorofluorocarbons (CFCs) and Hydrochlorofluorcarbons (HCFCs), Hydrofluorocarbons (HFCs), Perfluorocarbons (PFCs) and Sulfur hexafluoride (SF6)) are 2%. The objective of the study is to evaluate the contribution of GHGs from other small sector like waste water treatment plant (WWTP), constructed wetlands (CWs) and irrigated rice fields (IRF) in India and compared with other countries like Australia,

Europe and China. In the present scenario the emission of GHGs and other gases from drains can not be negligible. The emissions of GHGS from the above mentioned sources are described below.

1.1 Emission from Wastewater Treatment Plant (WWTP)

WWTP emits GHGs like CO_2, CH_4 and N_2O from unit processes and operations, but emissions of CH_4 and N_2O are reported in terms of CO_2 equivalence (CO_2e) because of its biogenic nature. In general GHG emits from both anaerobic and aerobic processes. In the anaerobic process, sludge digestion chamber release CH_4 and CO_2 whereas in the aerobic process GHG produced from primary clarifier and activated sludge process (ASP). CH_4 production depends on aerobic or anaerobic condition, quality of generated sludge and temperature. CH_4 production is directly proportional to temperature. Emission of N_2O in the ambient air occurs due to disintegration of nitrogen compound in the wastewater (i.e. urea, nutrient etc.).

1.2 Emission from Irrigated Rice Fields (IRF)

Cultivation or farming of rice has both natural and anthropogenic impact on environment. Irrigated rice field (IRF) contributes GHGs emission like CH_4 and N_2O. Entire, South Asian region dominates globally for rice production and total 90% of cultivated land is paddy fields in Asia. Since last two decades, Asian region emphasized the cultivation technique from conventional to modern. The emission of CH_4 production is increasingly drastically due to flooding, soil degradation and application of excess use of fertilizer.

1.3 Emission from Constructed Wetlands (CWs)

Constructed Wetlands (CWs) are the largest well-known natural source of CH_4 in the world. It is directly linked with anthropogenic activities. The rate of emission of CH_4 is higher due to development of anaerobic or septic condition. Presently global CH_4 budget estimated is about 115 Tg CH_4/y which released from all worlds wetland sites [4]. The emission of N_2O is the major component of GHG produces from contaminated soil. Nitrous oxide emits from nitrification and de-nitrification process and has increment rate of 0.3%. The emission of N_2O and CH_4 production increased due to incremental growth of organic matter and nutrients input in the ecosystem.

2 Methodology

2.1 Wastewater Treatment Plant (WWTP)

The methods to calculate emission of GHG for waste water treatment plant (WWTP) vary in developing and developed countries. Most of the cases, calculation and estimation of GHG are purely based on population, per capita waste, capacity of treatment plant, characteristics of inlet water parameters like biochemical oxygen demand (BOD), chemical oxygen demand (COD), total organic carbon (TOC), total nitrogen (TN), volatile organic compounds (VOCs) etc. It is understood that the generation and emission of GHG depends on spatial, temporal, biochemical or physical environmental condition. The methodology to estimate emission of GHG depends on technical guidelines of Department of Climate Change and Energy Efficiency [5]. The formula is given below.

$$Y_i = Q_i \times (\mathrm{EF}_i/1000)$$

where, Y_i = Total indirect GHG emission in year (CO_2e)

Q_i = Quantity of electricity purchased by the desalination plant from the electricity grid in year (KW-h) EF_i = Emission factor for electricity consumed in year.

2.2 Irrigated Rice Fields (IRF)

De-nitrification and Decomposition (DNDC) model is generally used to estimate or simulate the emission of CH_4, N_2O and CO_2 emission. This model consists of sub models like decomposition, plant growth, fermentation, soil climate, nitrification and de-nitrification [6–8]. This model is used for agricultural ecosystem and which help to simulate carbon and nitrogen cycle in the ecosystem at day to day basis. DNDC model has been validated by several countries like USA, China, Thailand and Japan and widely accepted by other countries also. The output of the DNDC model helps to understand the fluxes of GHGs, calculate the potential of climate change and to adopt the agricultural management practices.

2.3 Constructed Wetlands (CWs)

A constructed wetland (CW) is an artificial wetland for treatment of municipal/industrial wastewater, grey water or storm water runoff. It is constructed for land reclamation after mining which helps in reduces nutrient content in water bodies and prevent from eutrophication. In India, studies were conducted to Chennai at

the bank of Adyar river and Adyar estuary. These CWs treats industrial effluent, sullage water, laundries effluent etc. Only emission of CH_4 flux has been estimated on monthly, seasonally and annual basis by gas chromatography (GC) method. In Europe, ten locations in different countries (Estonia, Finland, Poland, and Norway) have been carried out emissions of GHGs in the ambient air. GHG flux was measured with static chamber method. This chamber made up of PVC and it is painted white to avoid heating and sealed with water filled ring at the surface of soil. The gas samples were collected periodically and measured by GC method.

3 Result and Discussion

In the present study, the emissions of GHGs (CH_4, CO_2 and N_2O) from wastewater treatment system (WWTP) irrigated rice fields (IRF) and constructed wetlands (CWs) in India and other countries like Australia, Europe and China were reviewed. Emission of GHGs from WWTP and IRF in India Australia and China is shown in Table 1. The emission of CH_4, CO_2 and N_2O from WWTP in Australian condition varied in an average from 0 to 111, 0 to 769 and 0 to 3 ton/year respectively whereas in Indian condition CH_4 and N_2O fluxes varied in an average from 0 to 6, and 0 to 0.01 ton/year. The higher concentrations of CH_4 and N_2O in the ambient air of country like Australia might be due to higher capacity of WWTP and advance biological treatment plant as compared to country like India. In Indian and China climatic condition more or less same. In India, the emission of CH_4, CO_2 and N_2O

Table 1 The comparative evaluation for emission of GHGs from WWTP and IRF in India Australia and China

C	AT	CH_4 ton/year	N_2O ton/year	CO_2 ton/year	min–max {ton/year}		
					CH_4	N_2O	CO_2
From waste water treatment plant (WWTP)							
A	U	111	3	769	0–111	0–3	0–769
I	U/R	6	0.01	–	0–6	0–0.01	–
For irrigated rice fields (IRF): −1. (Continuous flooding)							
I	–	1183000[a]	31265[a]	–	(107–110) × 10^4	(4–5) × 10^4	(2116–6096) × 10^4
C	–	–	–	–	(644–1202) × 10^4	(29–41) × 10^4	(205–1208) × 10^4
For irrigated rice fields: −2. (Mid–season drainage)							
I	–	–	–	–	(12–13) × 10^4	(5–6) × 10^4	(1666–4880) × 10^4
C	–	–	–	–	(171–785) × 10^4	(42–61) × 10^4	(349–1223) × 10^4

A approx, *C* Country, *I* India, *A* Australia, *C* China, *AT* area type, *U* Urban, *R* Rural
Source [6, 9–11]

from IRF varied from (107–110) $\times 10^4$, (2116–6096) $\times 10^4$ and (4–5) $\times 10^4$ ton/year respectively. In China, the emission of CH_4, CO_2 and N_2O from IRF varied from (644–1202) $\times 10^4$, (205–1208) $\times 10^4$ and (29–41) $\times 10^4$ ton/year respectively. In China, the emission of CO_2 is less as compared to India might be utilization of more renewable energy as compared to fossil and biofuels.

China is prone for flooding, so rice fields might be always in overburden pressure for production of rice as compared to India. The application of excess nitrogen in the IRF fertilizers causes high concentration of GHGs as compared to India. GHGs emissions were estimated from constructed Wetlands (CWS) located in ten locations in different countries (Estonia, Finland, Poland, and Norway) in Europe. In India, GHGs emission were estimated from two nos of CWs located in Chennai, South India. The emissions of CH_4 vary from season to season. It was observed that during summer season the emission of GHGs are more as compared to winter season. The comparative evaluation for emission of GHGs from CWs in India and Europe is shown in Table 2.

The average emission of CH_4, N_2O and CO_2 in India and Europe varied from 46 to 1103 and negative to 38000 mg/m^2/day respectively. The emission of GHGs were generally low in winter season as compared to summer season due to temperature slowdown the process of nitrification and de-nitrification in winter season.

3.1 Action Plan

Action plan is required for reduction of emissions of GHGs.

Plantation of trees, conservation of energy, and application of 3R (Reduce, Reuse and Recycle of waste) will minimize the emission of GHGs in the ambient air. Action plan has various steps which has to be followed strictly. Steps are base year inventory, future scenario analysis, target setting, implementation and tracking performance. The legal action plan for reduction of emission of GHGs is shown in Fig. 3a. It is also required the sector wise action plan for reduction of GHGs in the ambient air. The major sectors are waste management, agriculture, industry, forestry, building and transportation. The sector wise requirement of action plan is shown in Fig. 3b.

4 Conclusion

Reduction of increasing trend of Green House Gases (GHGs) is the most critical responses to the climate change. People have already facing the adverse effect of climate change. Till date in India the emissions of GHGs are less as compared to other countries. Implementation of sector wise action plan in India will further reduce the emission of GHGs in the ambient air.

Table 2 The comparative evaluation for emission of GHGs from CW in India and Europe

C	AT	Avg. CH_4 mg/m^2/day		Avg. N_2O mg/m^2/day		Avg. CO_2 mg/m^2/day		Range (min–max) (mg/m^2/day)		
		S	W	S	W	S	W	CH_4	N_2O	CO_2
E*	–	290	63	91	4.6	4500	1200	32–38 x 10^3	2.1 – 1 x 10^3	840 – 93 x 10^3
I	AR (857 km^2)	211	–	–	–	–	–	46–934	–	–
	AE (70 km^2)	374	–	–	–	–	–	53–1103	–	–

4 countries of Europe (Estonia, Finland, Poland, and Norway) represents as E
S summer, *W* winter, *E* Europe, *I* India, *AR* Adyar River, *AE* Adyar Estuary
Source [4, 12]

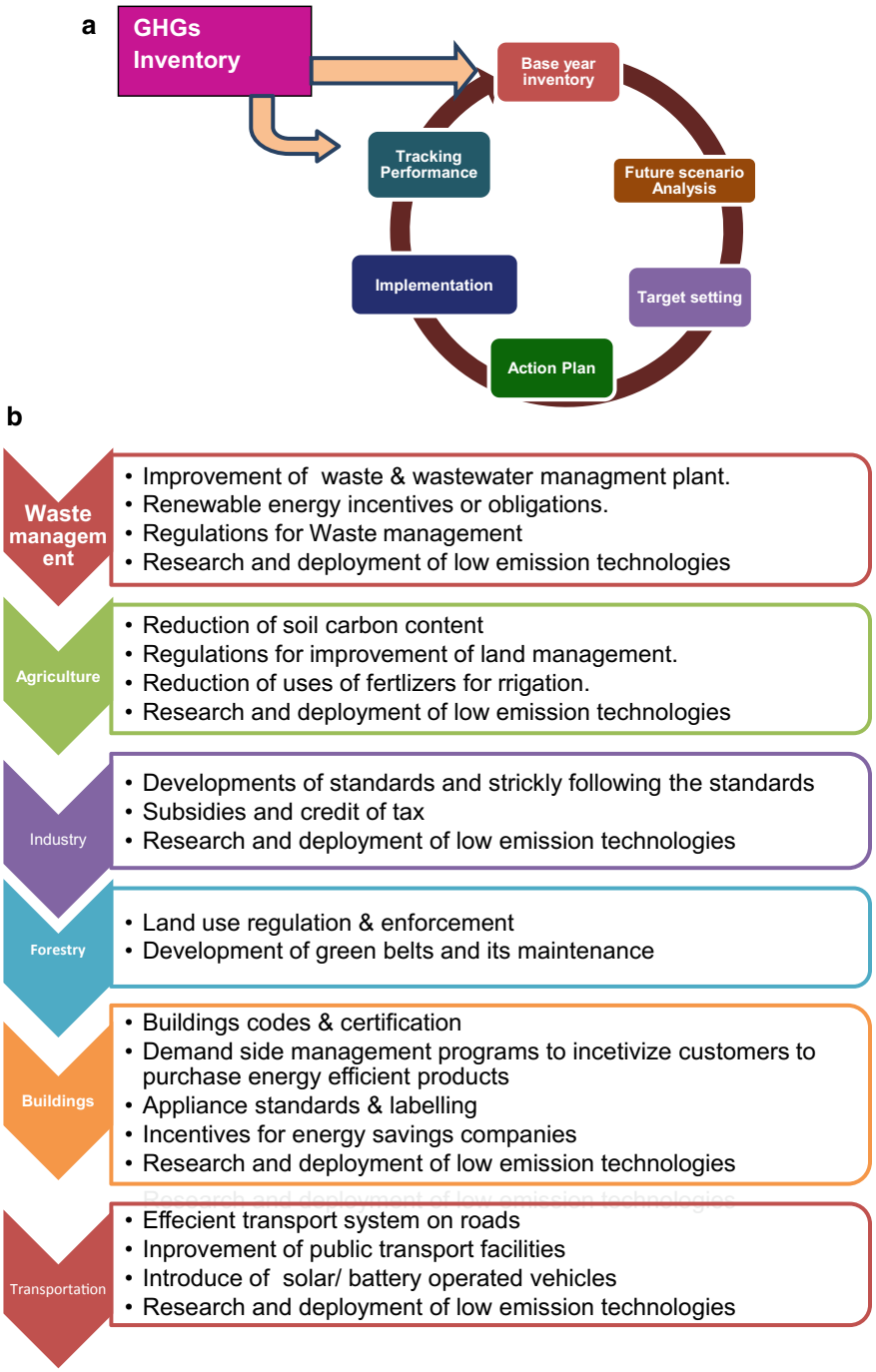

Fig. 3 **b** Sector wise requirement of action plan

References

1. Eggleston HS, Miwa K, Srivastava N, Tanabe K (2006) Intergovernmental panel on climate change (IPCC): guidelines for national greenhouse gas inventories programme. https://www.ipcc-nggip.iges.or.jp/support/Primer_2006GLs.pdf
2. Pachauri RK, Allen MR, Edenhofer O, Barros VR, Broome J et.al (2014) Intergovernmental panel on climate change (IPCC): mitigation of climate change. https://www.ipcc.ch/site/assets/uploads/2018/05/SYR_AR5_FINAL_full_wcover.pdf
3. US EPA (2010) Environmental protection agency, US Greenhouse gas Inventory Report: Inventory of US Greenhouse Gas Emissions and Sinks. https://www.epa.gov/ghgemissions/global-greenhouse-gas-emissions-data
4. Ramesh R, Purvaja GR, Parashar DC, Gupta PK, Mitra AP (2014) Anthropogenic forcing on methane efflux from polluted wetlands (Adyar River) of Madras City, India. Ambio 369–374
5. DCCEE (2010) Department of climate change and energy efficiency: technical guidelines for the estimation of greenhouse gas emissions by facilities in Australia
6. Pathak H, Li C, Wassmann R (2005) Greenhouse gas emissions from Indian rice fields: calibration and upscaling using the DNDC model. Biogeosciences 2(2):113–123
7. Li CS (2000) Modeling trace gas emissions from agricultural ecosystems. In: Methane emissions from major rice ecosystems in Asia. Springer, Dordrecht, pp 259–276
8. Pathak H, Bhatia A, Prasad S, Singh S, Kumar S, Jain MC, Kumar U (2002) Emission of nitrous oxide from rice-wheat systems of Indo-Gangetic plains of India. Environ Monit Assess *77*(2):163–178
9. Gupta D, Singh SK (2012) Greenhouse gas emissions from wastewater treatment plants: a case study of Noida. J Water Sustain 2(2):131–139
10. Listowski A, Ngo HH, Guo WS, Vigneswaran S, Shin HS, Moon H (2011) Greenhouse gas (GHG) emissions from urban wastewater system: future assessment framework and methodology. J Water Sustain 1(1):113–125
11. Li C, Mosier A, Wassmann R, Cai Z, Zheng X, Huang Y, Tsuruta H, Boonjawat J, Lantin, R (2004) Modeling greenhouse gas emissions from rice-based production systems: sensitivity and upscaling. Global Biogeochem Cycles 18(1):GB1043
12. Sovik AK, Augustin J, Heikkinen K, Huttunen JT, Necki JM, Karjalainen SM, Klove B, Liikanen A, Mander U, Puustinen M, Teiter S, Wachniew P (2006) Emission of the greenhouse gases nitrous oxide and methane from constructed wetlands in Europe. J Environ Qual 35(6):2360–2373

Indoor Air Pollution at Restaurant Kitchen in Delhi NCR

Poonam Kumari and Papiya Mandal

1 Introduction

Indoor Air Pollution (IAP) is a grave problem in both rural and urban environment. The major governing factor for IAP is the type of fuels used for cooking purposes. In urban areas coal based tandoor and liquefied petroleum gas (LPG) for cooking purposes whereas in rural areas bio-fuels like wood, straw are used for cooking purposes. The fuels are the contributor for particulate and gaseous pollutants in the indoor environment. Particulate matters having smaller size than 2.5 μm are more harmful than the larger size particulate matter like 10 or bigger. They directly penetrate into the breathing passage of human's alveolus [1] and [2] and cause adverse effect on public health. Gaseous pollutants such as CO and CO_2 also having adverse health effects in urban areas of developed countries [3]. Indoor smoke in poorly ventilated kitchen exceeds the acceptable concentration of total suspended particulate matter by more than 100 times the standard value [4]. In the urban area the uses of coal based tandoor and usages of liquefied petroleum gas (LPG) are the main contributor of IAP. Though IAP is also influenced by the parameters like tobacco smoking, dust, smoke, paints, furniture's, but still usage of fuels is the major contributor of IAP. Burning of cooking fuels such as kerosene, animal dung, wood, coal, LPG, agricultural residues etc. are the major cause for indoor air pollution in rural areas [5]. Most of the people spend 90% of time in indoor environment and exposed to both particulate matter and gaseous pollutants [6]. In world different cooking methods used in kitchens that leads to the emissions of different chemical and physical type particle size and has its ill impacts. The concentrations of PM_{10} and $PM_{2.5}$ are generally low in the steaming method, moderate in boiling and high in the frying based

P. Kumari · P. Mandal (✉)
National Environmental Engineering Research Institute (NEERI), Delhi Zonal Centre Council of Scientific and Industrial Research (CSIR), CSIR R&D Centre, A-93-94, Phase I, Naraina Industrial Area, Delhi, New Delhi 110028, India
e-mail: p_mandal@neeri.res.in; papiya.mandal1942@gmail.com

S. Kumar et al. (eds.), *Sustainability in Environmental Engineering and Science*, Lecture Notes in Civil Engineering 93,
https://doi.org/10.1007/978-981-15-6887-9_18

cooking in different types of restaurant [7]. A study conducted in the rural households in Nepal shows that the concentration of CO and $PM_{2.5}$ in improved cooking stoves and traditional cooking stoves for 24 h sampling was found 27.11 mg/L, 825.4 $\mu g/m^3$, 36.03 mg/L and 1336 $\mu g/m^3$ respectively [8]. Though several studies has been carried out at indoor environment but no study till date has been carried out regarding the pollution emission due to the usage of various types of fuel like coal based tandoor as well as LPG. In the urban areas the contribution of outdoor air pollutants along with meteorological parameter like wind speed, wind direction and relative humidity also play the major role in the indoor environment of the restaurant kitchen/cafeteria. The main objective of the study to evaluate the contribution of size segregated particulate matter like PM_{10} and $PM_{2.5}$ and major gaseous pollutant like CO and CO_2 emission in the kitchen environment due to the usage of various type of cooking fuel like coal based tandoor and LPG.

2 Methodology

Delhi, the capital of India and its NCR is considered to be one of the most polluted in the world. The entire design of Delhi and its NCR has severe environmental impacts with a population of 16,753,235 [9] due to industrial expansion and large number of vehicular registration. The climate of the Delhi NCR falls under the category of arid and semi-arid zone. The wind directions in general predominant in the direction of West, North-West and North-North-West. A few studies has been carried out regarding the IAP in Delhi and its NCR region especially in the restaurant kitchen. A short term study has been carried out in the restaurant kitchen during the month July 2019, which falls in Delhi NCR, one of the hotspot location (Fig. 1). The schematic layout of google map is shown in Fig. 1.

The area of the restaurant is approximately 100 square meters. The preparation of food takes place in two floors. The coal based Tandoor activity takes place in the

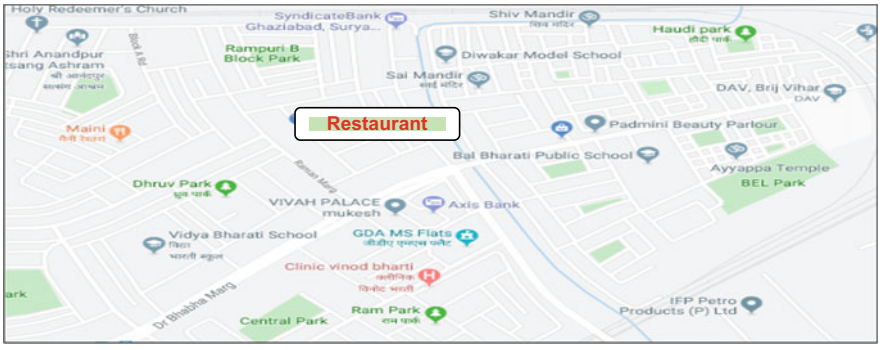

Fig. 1 Schematic layout for Google map

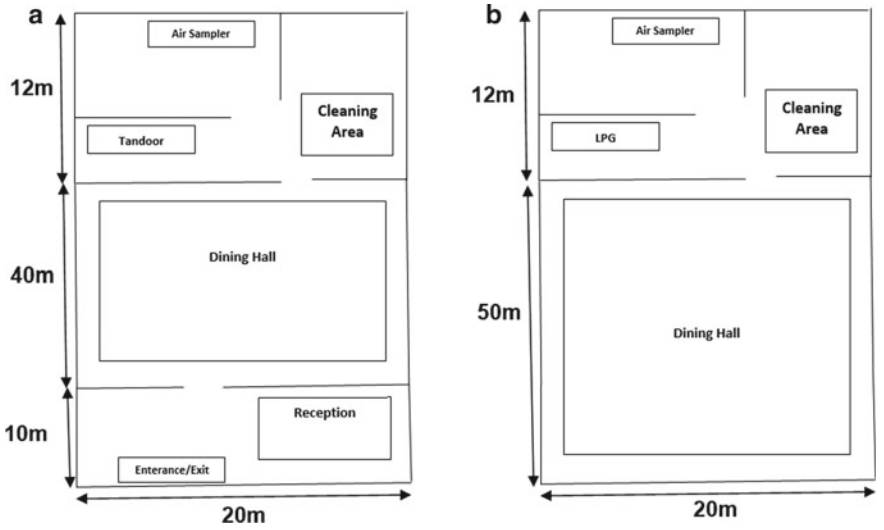

Fig. 2 **a** Placement of tandoor at GF. **b** Placement of LPG at FF

Ground Floor (GF) whereas the preparation of other food by using LPG as fuel takes place in the First Floor (FF). The instrument was placed at a distance of 2–3 m away from the source in kitchen. The placement of the instrument to monitor particulate and gaseous pollutant is shown in Fig. 2a, b.

The sampler was kept with precautionary measures so that it didn't affected by the outdoor environment. A pre-calibrated Mini Vol portable air sampler was used to collect the particulate matter (PM_{10} and $PM_{2.5}$) sample. The air sampler collects the sample at a constant flow rate of 5 lpm [10] and equipped with a programmable timer [11]. The sampling was done on 8 h basis at 5 lpm. Whatman glass fibre filter papers were used for collection of size segregated particulate matter (PM_{10} and $PM_{2.5}$). After collection, samples were kept for desiccation for 24 h. Filter papers were weighed on Mettler Toledo AG balance (Greifensee, Switzerland Europe) with a resolution of ±0.01 mg after the conditioning [12]. The gaseous pollutant (CO_2) and meteorological parameter (Temperature and Relative Humidity) were carried out using Extech $CO_2$50 sampler. The instrument resolution for CO_2, temperature and relative humidity is 1 mg/m^3, 0.1 °C and 0.1%. CO samples were collected by using tedlar bags. The concentrations of CO were measured by using the instrument CO analyser (Environment S. A). Gravimetric method was used to measure the concentration of particulate matter (PM_{10} and $PM_{2.5}$) and NDIR method was used for measurement of gaseous pollutants like CO and CO_2.

3 Result and Discussion

Short time monitoring was carried out in the restaurant's kitchen (RK) over the period of one month July 2019. The parameters selected were particulate matter (PM_{10} and $PM_{2.5}$) and gaseous pollutant (CO and CO_2). The concentration of size segregated particulate matter PM_{10} and $PM_{2.5}$ at Tandoor of the RK is shown in Fig. 3.

The sampling at the Tandoor at RK was carried out for 9 days from 5th July to 13th July 2019. The average concentrations of PM_{10} and $PM_{2.5}$ during the study period varied from 314 to 1130, 206 to 621 $\mu g/m^3$ respectively with an average concentration of 803 ± 256 and 412 ± 126 $\mu g/m^3$.

The concentration of size segregated particulate matter PM_{10} and $PM_{2.5}$ at LPG of the RK is shown in Fig. 4.

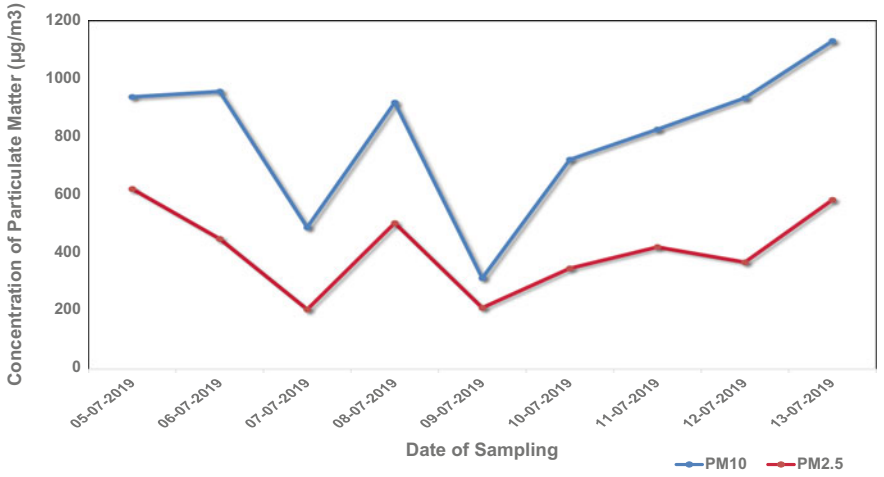

Fig. 3 Concentrations of PM_{10} and $PM_{2.5}$ at tandoor in RK

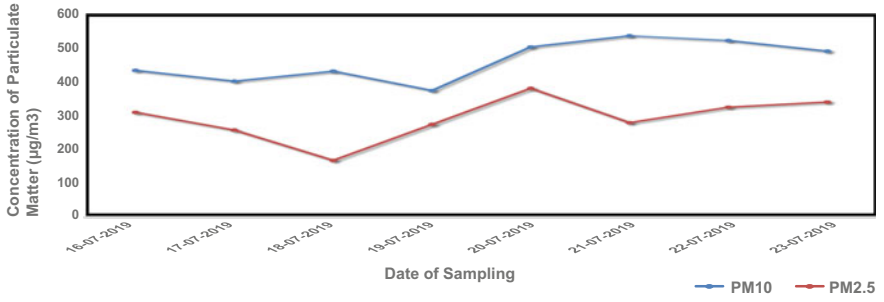

Fig. 4 Concentrations of PM_{10} and $PM_{2.5}$ at LPG in RK

The sampling at the LPG of the RK was carried out for 8 days from 16th July to 23th July 2019. The concentrations of PM_{10} and $PM_{2.5}$ during the study period varied 373–535 and 166–379 $\mu g/m^3$ with an average concentration of 460 ± 60 and 290 ± 64 $\mu g/m^3$.

The concentrations of CO and CO_2 were also measured along with particulate matter at Tandoor and LPG both in the RK. The CO and CO_2 were measured in the Tandoor environment from 5th July to 13th July 2019. The CO and CO_2 were measured in the LPG environment from 16th July to 23th July 2019 The concentration of CO and CO_2 during the study period at Tandoor and LPG is shown in Fig. 5 and Fig. 6.

The average concentration of CO and CO_2 in tandoor were 5 ± 2 and 1636 ± 113 mg/m^3.

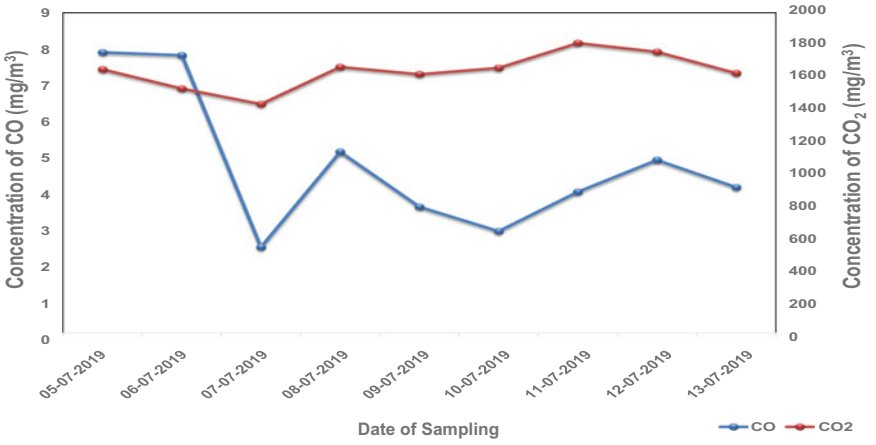

Fig. 5 Concentrations of CO and CO_2 at tandoor in RK

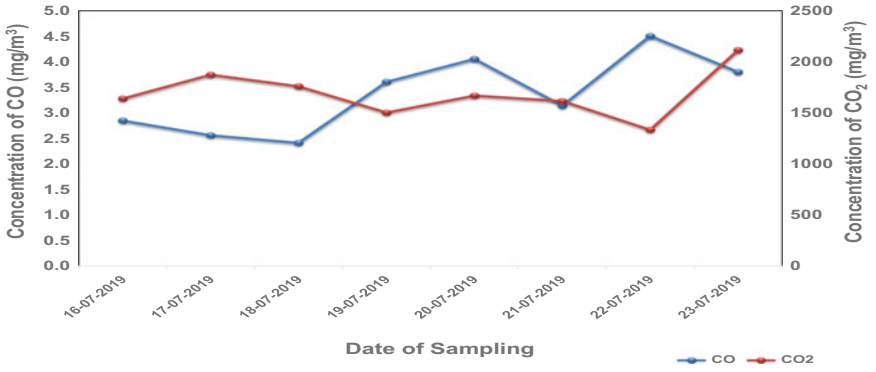

Fig. 6 Concentrations of CO and CO_2 at LPG in RK

Table 1 The variation of temperature and relative humidity at both tandoor and LPG in RK

Statistical parameter	Temperature (°C)		Relative humidity (%)	
	Tandoor	LPG	Tandoor	LPG
Minimum	33	32	49	72
Maximum	38	35	70	90
Average	36	32	59	77
Standard deviation	2	1	7	6

The average concentrations of CO and CO_2 in LPG were 3 ± 1 and 1688 ± 236 mg/m^3. The concentrations of CO were above the permissible standard of National Ambient Air Quality Standards (NAAQS) of Central Pollution Control Board (CPCB 2009). CO_2 is colorless and odorless gas which is exchanged by human exhale and plants inhale. In general CO_2 is not considered as pollutants however increasing trend of ambient CO_2 concentration is responsible for climate change. Till date in India no standard has been formulated for indoor air pollutants. This study will help to formulate the indoor air quality standards in the Indian climatic condition.

The meteorological parameter like temperature and relative humidity were also collected during the monitoring period. The statistical analysis of temperature and relative humidity is shown in Table 1. The average temperature and relative humidity in tandoor section were 36 ± 2 °C and 59 ± 7%, whereas in the LPG the temperature and relative humidity were 32 ± 1 °C and 77 ± 6%.

It was observed that rising of the temperature and lowering of the relative humidity took place in the Tandoor Kitchen environment. It is understood after the study that kitchen environment in the Tandoor location was more contaminated as compared to the LPG location.

4 Conclusion

The concentrations of size segregated particulate matter (PM_{10} and $PM_{2.5}$) and gaseous pollutant (CO and CO_2) in the restaurant kitchen during the monsoon season (July 2019) also were in bad shape. The short time monitoring and assessment in the restaurant kitchen indoor air quality suggested that there is a need for proper planning and management in the kitchen activities. Tandoor food is generally preferred by the public, but Tandoor section was more contaminated as compared to the food prepared in the LPG section. Though exhaust as well as chimney fan were installed in the restaurant kitchen in both Tandoor and LPG but there is a need for assessment of design, capacity of exhaust and chimney according to the size of the kitchen and type of food prepared. Accordingly the requirement of number of chimneys or exhausts can be evaluated. This study will help to take the action or prepare the regulatory frame work to keep the healthy environment inside the restaurant kitchen.

Acknowledgements The authors are very much thankful to Director, CSIR-NEERI for completion of the short term study on Indoor Air Pollution.

References

1. Massey D, Kushrestha J, Mahima, A. Taneja (2009) Indoor/Outdoor relationships of fine particulate less than 2.5 μm ($PM_{2.5}$) in residential homes located in central Indian region. Build Environ 44, 2037–2045
2. Stasangi PG, Kulshrestha A, Taneja A, Rao P.S.P (2011) Measurement of PM10 and PM2.5 aerosols in Agra, a semi arid region of India. Indian J Radio Space Phys 40:203–210
3. Parikh J, Balakrishnan V, Laxmi, Biswas H (2001) Exposure from cooking with biofuels: pollution monitoring and analysis for rural Tami Nadu, India. Energy 26:949–962
4. Dhakkal S (2008) Climate change and cities: the making of a climate friendly future. Chapter 7. http://dx.doi.org/10.1016/B978–0-08-045341-5.00007-4
5. World Bank; India, (2002) Household energy, Indoor air pollution, and health, pp 148–160
6. See SW, Balasubramanian R (2006) Risk assessment of exposure to the indoor aerosols associated with Chinese cooking. Environ Res 102:197–204
7. Lee SC, Li WM, L.Y. Chan, (2001) Indoor air quality at restaurants with different styles of cooking in metropolitan Hong Kong. Sci Total Environ 279:181–193
8. Parajuli I, Lee H, Shrestha KR (2016) Indoor air quality and ventilation assessment of rural mountainous households of Nepal. Int J Sustain Built Environ 5, 301–311
9. http://censusindia.gov.in/2011-prov-results/data_files/delhi/3_PDFC-Paper-1-tables_60_81.pdf
10. See SW, Balasubramanian R (2008) Chemical characteristics of fine particles emitted from different gas cooking methods. Atmos Environ 42:8852–8862
11. Lane DD, Baldauf RW, Marotz GA (2001) Performance characterization of the portable miniVOL particulate matter sampler. Trans Ecol Environ 47:1743–3541
12. Mandal P, Sarkar R, Mandal A, Patel P, Kamal N (2016) Study on airborne heavy metals in industrialized urban area of Delhi, India. Bull Environ Contam Ecotoxicol

Determination of SCS Runoff Curve Number and Landuse Characteristics of Khowai River Catchment, Tripura, India

Prasun Mukherjee, Anubhab Das, and Rajib Das

1 Introduction

Khowai river is a major river in the state of Tripura, India. The hydrological conditions of the river Khowai largely influence the ecological and social conditions in the state. Khowai river originates in eastern Atharamura Hills of Tripura state in India. The river flows further north-north-west at Khowai to enter at Balla in the Habiganj district of Bangladesh. Catchment area of Khowairiver is 1370 km^2. It occupies 13.13% of Tripura state. The river has a length of 70 km within the Tripura state. The catchment lies between 23°58′32″ N to 23°45′18″ N and 91°30′24″ E to 91°43′35″ E. There has been extensive research carried out on various topics as in the channel migration, temporal change of bank line, bank erosion risk, and the impact on landuse/landcover. Debnath et al. [1] has verified and provided a comprehensive assessment of spatio-temporal variation in river channel processes and the adjustment of landuse-Landcover of Khowai river catchment area. They specified that river Khowai had changed from extremely meandering (SI = 2.30) to sinuous (SI = 1.41) which altered the land use and land cover significantly.

However, the paucity of information on the runoff potential of the river catchment made it necessary for this study. Curve Number (CN) determination in the Soil Conservation Service Curve Number method [2] which is established by USDA is crucial to estimate runoff potential. Curve Number might be derived from the

P. Mukherjee (✉) · R. Das
School of Water Resources Engineering, Jadavpur University, Kolkata, India
e-mail: mukherjeeprasun3@gmail.com

R. Das
e-mail: rajibdas79@gmail.com

A. Das
Swami Vivekananda Institute of Science and Technology, Kolkata, India
e-mail: sobujanubhab@gmail.com

S. Kumar et al. (eds.), *Sustainability in Environmental Engineering and Science*, Lecture Notes in Civil Engineering 93,
https://doi.org/10.1007/978-981-15-6887-9_19

SCS CN tables that are based on the hydrological soil groups, landuselandcover, the land management practices, hydrological conditions and Antecedent Moisture Conditions (AMC) of the catchment area. In this manuscript the Curve Number of Khowai Catchment was determined using the SCS CN method and LULC method, so as to complement and verify the calculated Curve Number of the area [3]. The theoretical discharge which was calculated from the Curve Number was verified with recorded field data of the Khowai River collected from Meghna Division, Central Water Commission, Silchar.

2 Methods

The geographical position of the river Khowai was determined by geo-registering the scanned topographical maps −79 M/9 and 78P/12. Initially a shape file was created in ERDAS Imagine v2010 and then the co-ordinate system of the shape file was determined. For contours polyline shape files were used. Digital-Elevation-Model (DEM) was prepared so as to understand the contour characteristics of the terrain. Now, the catchment area was delineated from the Landuse Landcover (50 k): 2011–12 map, by means of watershed delineation tool in ERDAS Imagine v2010 (Fig. 1).

Consecutively, the Hydrological Soil Group was determined from the Soil map—Geomorphology (50 k): 2005–06 at level detail 2, of Bhuvan (ISRO/NRSC) and the specific percentages of corresponding soil groups were distinguished with the help of ERDAS IMAGINE v2010 software. Landuse-Landcover maps obtained from

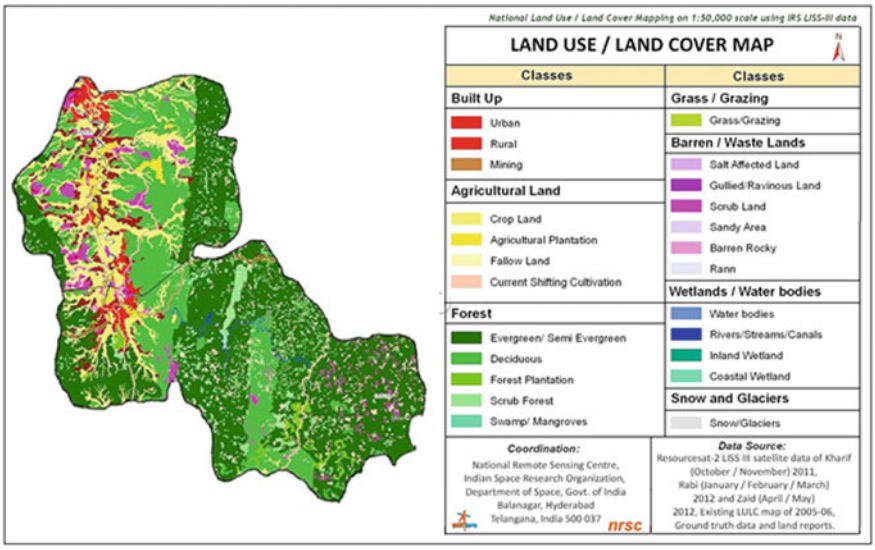

Fig. 1 Landuselandcover map of Khowai river catchment

Table 1 Geomorphological distribution of the catchment area

Geomorphology	Soil group	Color	Percentage (%)
structural origin valleys and dissected hills	B	Orange	80.53
Pediment pediplain complex of denudational origin	C	Pink	9.08
Fluvial origin younger alluvial plain	D	Green	10.39

Bhuvan (ISRO/NRSC), were further delineated in the software ERDAS IMAGINE v2010, so as to obtain the different percentage specifics of the soil groups (Table 1 and Fig. 2).

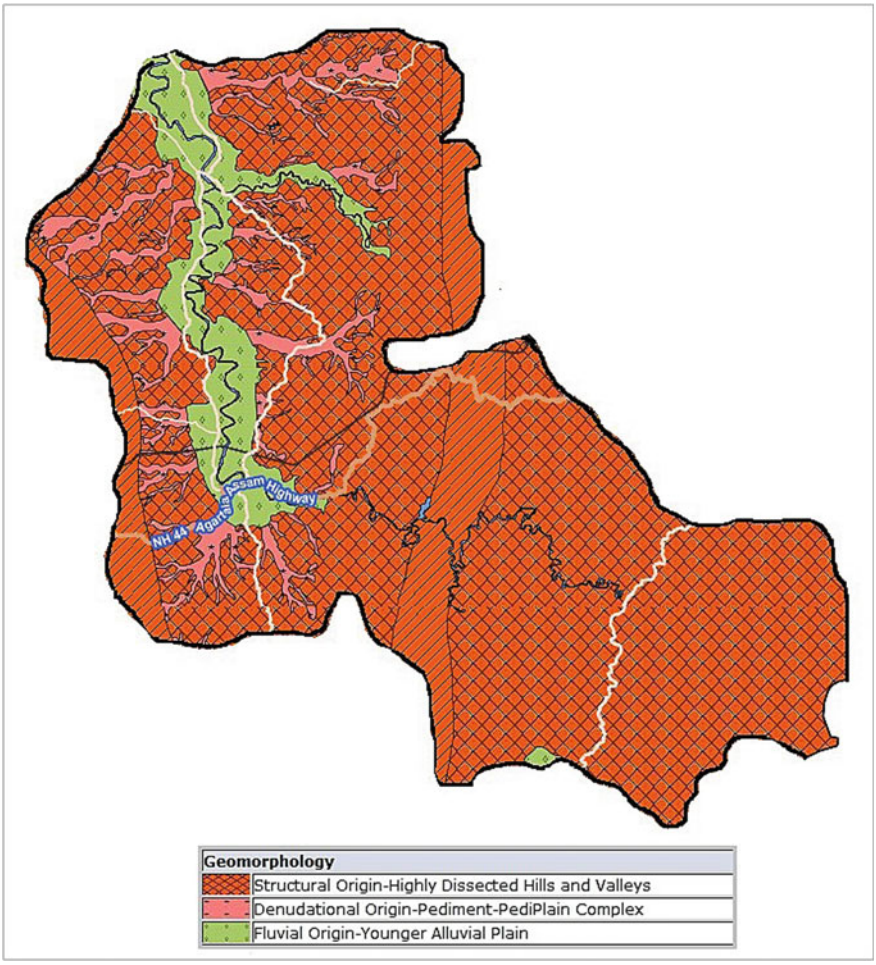

Fig. 2 Hydrological soil groups classification

Rain gauge stations were selected on the basis of proximity to the actual catchment and identified in the catchment map. The specific rainfall data of the different stations were collected for the years 2012–17, from the Department of Agriculture Agartala, Government of Tripura. The average rainfall over the Khowai catchment was calculated by Thiessen Polygon (also known as Voronoi polygon) method [4] by creating raster data model in ArcGIS Pro v2.2.1. software.

AMC denotes the moisture content existing in soil i.e. dry condition (AMC-I), average condition (AMC-II) and wet condition (AMC-III), at the beginning of the rainfall event under consideration. To infer CN for an un-gauged watershed, SCS (1956) provided tables for different soil types, land cover, hydrological conditions, and AMC. Similarly, exact scientific articulations are likewise accessible for CN variations from AMC. Different types of AMCs were determined by detailed analysis of average rainfall data from the tables over the Khowai river catchment. Firstly, the CN for AMC-II condition was determined from the tables provided by SCS (1956). From the value of CN for AMC-II, CN values for other two conditions were determined based on the Hydrologic soil cover complexes. CN1 and CN3 for AMC-I and AMC-III situations were calculated based on the formulas:

$$\text{For AMC-I} : \text{CN}_1 = \frac{\text{CN}_2}{2.281 - 0.01281\text{CN}_2} \tag{1}$$

$$\text{For AMC-III:} \text{CN}_3 = \frac{\text{CN}_2}{0.427 - 0.00573\text{CN}_2} \tag{2}$$

The potential maximum retention after runoff or storage water (S) of the catchment area for the three different AMC conditions was calculated from the Curve Number values, to determine the runoff of the stream.

$$S = \frac{25{,}400}{\text{CN}} - 254 \tag{3}$$

The direct runoff (R) of the catchment was determined from the Storage (S) value by the formula.

$$R = \frac{(P - 0.2S)^2}{(0.8S + P)} \tag{4}$$

The aforementioned equation is valid for $P > 0.2S$. Where P is rainfall (mm) and S is storage (mm).

Daily Actual Discharge data of the Khowai River (2012–2017) were collected from Meghna Division, CWC, Silchar. Baseflow (B) data of the Khowairiver were distinguished from the available discharge pattern. The discharge was calculated by adding direct runoff (R) of the catchment to the baseflow (B) of the Khowai River. Twenty rainfall events over a period of 2012–17 were randomly selected to compare the calculated discharge data with the actual field recorded data to determine the precision and accuracy of the calculated Curve Number of the Khowai Catchment.

3 Results and Discussion

By detailed analysis of the geomorphological map in ERDAS Imagine v2010 software it was found that there are three types of soils in Khowai catchment area.

1. **Group B**—Structural origin valleys and dissected Hills (high infiltration rates with low runoff potential)
2. **Group C**—Pediment pediplain complex of denudational origin(low infiltration rates with moderately high runoff potential)
3. **Group D**—Fluvial origin younger alluvial plain (very low infiltration rates with high runoff potential).

Further delineation of the catchment area from the Landuse Lancover (50 k): 2011–12 map, by means of watershed delineation tool in ERDAS Imagine v2010 helped in detailed analysis and determination of the different patterns in the catchment area. The map distinctly showed the different land cover patterns within the aforementioned catchment area along with the data, ranging for the different land use patterns within the Khowai river catchment. The respective percentages for the associated land cover percentages to the soil groups were calculated and noted (Table 2).

Five rain gauge stations were selected over the Khowai catchment area to determine the average rainfall by Thiessen Polygon method. The stations are

1. Dharmanagar (24° 2242.7″ N 92° 10′41.9″ E),
2. Kamalpur (24.2° N 91.83° E),
3. Khowai (24° 3201354″ N 91° 36′18′ E),
4. Amarpur (23.53° N 91.64° E),
5. Udaipur (23.53°N 91.48°E).

The weighted area of the rain gauge stations was calculated to be (Table 3):

Table 2 Landcover percentage according to soil group

Soil group	Landcover percentage							
	Forest			Agricultural		Pasture (%)	Wasteland (%)	Hard surface (%)
	Dense (%)	Light (%)	Scrub (%)	Bunded (%)	Paddy (%)			
B	21	6	2	0	6	8	4	1
C	7	11	1	5	0	3	0	1
D	1	5	1	7	1	1	1	7

Table 3 Weighted area and total area within the Khowai catchment

Weighted area(km^2)					Total area(km^2)
Dharmanagar	Kamalpur	Khowai	Udaipur	Amarpur	Khowai catchment
69.2	585	77	53.8	585	1370

To determine the Curve Numbers of the Khowai Catchment for different AMC conditions at first CN for AMC-II was determined from the tables provided by SCS (1956) [5] and the CN for AMC-II condition was found to be 58.42. CN values for AMC-I (Dry) and AMC-III (Wet) were determined from CN_2 using Eqs. 1 and 2. The storage (S) of the catchment area was determined using Eq. 3.

1. For AMC-I condition: $S = 412.3169$ mm
2. For AMC-II condition: $S = 180.7826$ mm
3. For AMC-III condition: $S = 77.2035$ mm

The discharge (Q) for different AMC conditions were calculated for different storm events at different AMC conditions. Twenty storm events were randomly selected and the calculated discharge was compared with the actual field data and the difference was noted. The results showed that the fluctuations from the calculated discharge to the actual discharge were negligible. This proved that the calculated Curve Number were correct for the Khowai river catchment area.

4 Conclusion

The Curve Number values for the Khowai River catchment were found to be CN1–38.12, CN2–58.42, CN3–76.69. The storage(S) of the catchment area was determined as 412.32 mm, 180.78 mm, and 77.20 mm for AMC conditions I, II and III respectively. Twenty storm events were selected randomly and The comparison between actual field discharge data and calculated discharge performed for twenty randomly selected storm events showed negligible difference in the two values henceforth proving that the curve number values are correct and usable for practical field estimations. These findings provide extensive insights for further research on precipitation, runoff and discharge estimations and simulations on the Khowai River catchment area. The curve number calculated for the different antecedent moisture conditions would majorly aid in the storm water management profiling and design of flood management procedures for the area but new changes and patterns in the landuse, landcover of the catchment needs to be monitored and updated to acquire the accurate runoff estimations for the region.

References

1. Debnath J, Pan ND, Ahmed I, Bhowmik M (2017) Channel migration and its impact on land use/land cover using RS and GIS: A study on Khowai River of Tripura, North-East India. Egyptian J Remote Sens Space Sci 20(2)
2. Al-Jabari S (2009) Estimation of runoff for agricultural watershed using SCS curve number and GIS. In: Thirteenth international water technology conference, IWTC 13 2009. Hurghada, Egypt

3. Choudhari K (2014) Simulation of rainfall-runoff process using HEC-HMS model for Balijore-Nala watershed, Odisha, India. Int J Geomat Geosci 5(2)
4. Chow VT, Maidment, DK, Mays, LW (2002) Applied hydrology. McGraw-Hill, New York, USA
5. Mishra SK, Kansal AK (2014) Procedure for determination of design runoff curve number for a watershed. J Indian Water Res Soc 34(3)

Degradation of Plastics Causing Pollution Using Bacteria for Improvement of Freshwater Fish Cultivation

Priyadarshini Mallick and Jaydev Misra

1 Introduction

Matter is subjected to creation and destruction, but if this rule is violated, it can be fatal to the existence of life. Such a product is plastic. Plastics are basically inert and mostly resistant to microbial attacks, and thus, they are capable of existing in nature without any deformation for a significant period of time. As per Greek vocabulary, "plastikos" means, "able to be molded into different shapes" [1]. Plastics are made out of inorganic and organic raw products consisting of carbon, silicon, nitrogen, oxygen, chloride, and hydrogen. The basic material used for making plastic is normally extracted from natural sources like coal, oil, and natural gas. Plastics are polymers which become active when they come in contact to heat and thus are capable of being casted into molds. They are organically nonmetallic, moldable compounds, and the materials obtained from them, can be made into any shape, and they are capable of maintaining that particular shape [2]. Plastics are used in packaging, disposable diaper rolling, fishing nets, etc. They are composed of polymers like polyethylene, polypropylene, polystyrene, polyvinylchloride, polyurethane. The plastic sheets resist water and air to penetrate into earth which results in soil infertility, thereby preventing major degradation of commonly occurring substances, causes depletion of underground water source, and becomes a cause of potential danger to animal life too [3]. In oceans, plastics are entirely responsible for entangling marine existence. According to reports from various municipal administrators, plastic bags are a major cause for blockage in sewage systems, and thus, municipal wastes cannot

P. Mallick
Asutosh College, Kolkata, West Bengal, India
e-mail: priyadm1@yahoo.com

J. Misra (✉)
Dhruba Chand Halder College, South 24 Parganas, West Bengal, India
e-mail: jaydevmisra@gmail.com

S. Kumar et al. (eds.), *Sustainability in Environmental Engineering and Science*, Lecture Notes in Civil Engineering 93,
https://doi.org/10.1007/978-981-15-6887-9_20

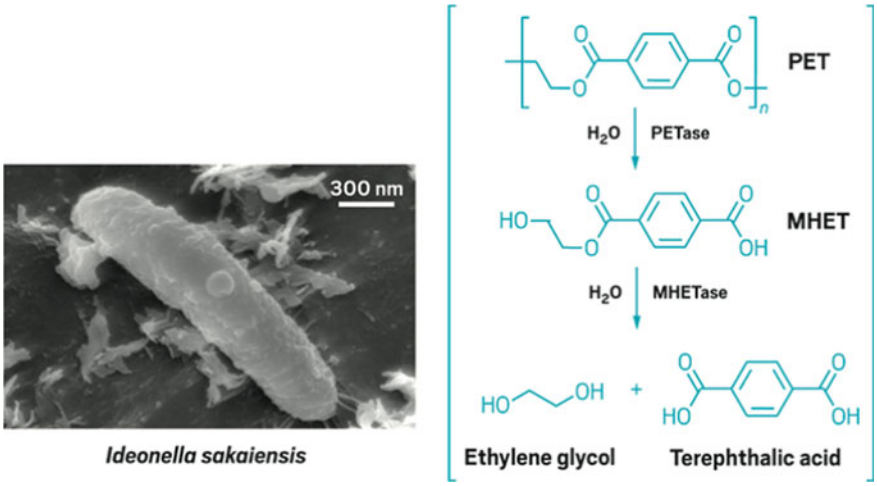

Fig. 1 Microscopic view of Ideonella sakaiensis (left); biogradation pathway followed by Ideonella sakaiensis to degrade plastics (right)

be incinerated most of the time leading to accumulated garbage, sludge compilation, junk accumulation, etc. It can be concluded that plastic is one of the raging parasites that can devour and pollute the existence of life in this planet (Fig. 1).

Early 1980s had witnessed the initiation of research of plastic degradation. Few plastics have been shown the property of biodegradability, and their degradation property has progressively become better with upcoming researches. Various types of plastics which are capable of degradation, such as polylactides, (3-hydroxybutyrate-3-hydroxy valerate), ethylene-carbon monoxide polymers, vinyl ketone copolymers (Guillet process), and starch-filled polyethylene (Griffin process), have gradually developed [4, 5]. These plastics vary in their degradation rate, applications, and cost effectiveness. Three types of degradation of polyethylene are chemical, photo-sensitive, and biological degradation. Chemical degradation takes place when the pro-oxidants are responsible for catalyzing the formation of free radicals in polyethylene molecules, which then reacts with the molecular oxygen in order to attack the entire polyethylene matrix. External factors like heat and oxygen are responsible for accelerating this chain [10]. Photo-sensitive degradation also happens inside the polyethylene matrix where UV radiation catalyzes the auto-oxidation and generates free radicals [6]. While biological degradation of polyethylene films has been repeatedly reported in pure culture studies with microorganisms like *Streptomyces sp.*, *Aspergillus, Aureobasidium, Poecilomyces* after the initiation of chemical degradation with their corresponding extracellular enzymes [7–9]. A significant observation was shown by the usage of a relatively less known species called *Ideonella sakaiensis.*

2 Materials and Methods

Certain methods have been implemented to reach the aim and objective of the study. They are:

1. **Soil burial treatment**: Identical pieces of cellulose which are blended as PVC films (dimensions: 5 × 2.5 cm each) were buried in the soil for a stretch of three months and inoculated in the presence of collected sewage sludge for the isolation of those microbial strains having the ability to adhere and degrade the polymeric film. Figure 2 shows the demonstrative view of the abovementioned process.
2. **Shake flask experiment**: The cellulose-blended PVC films were further incubated with the isolated microbes obtained from the soil burial experiment in shaking condition. The desired mineral salt media (MSM) used per 1000 mL contained in distilled water were as per the following measurements Table 1.

The well-blended cellulose with PVC film (3 pieces) in MSM (90 mL) was inoculated exactly with 10 mL of the collected spore suspension (10 ± 2.1 × 106 spores mL^{-1}) and incubated at 30 °C for a period of 3 months. At an interval of every 4 weeks, those polymer samples were observed and evaluated both manually and visually with the help of an infrared spectroscopy measured on Bio-Rad Merlin FTIR (Instrument specification: Excaliber Series FTS 3000 MX, USA). From Fig. 3, we get a vivid interior view of the shaking incubator performing the experiment.

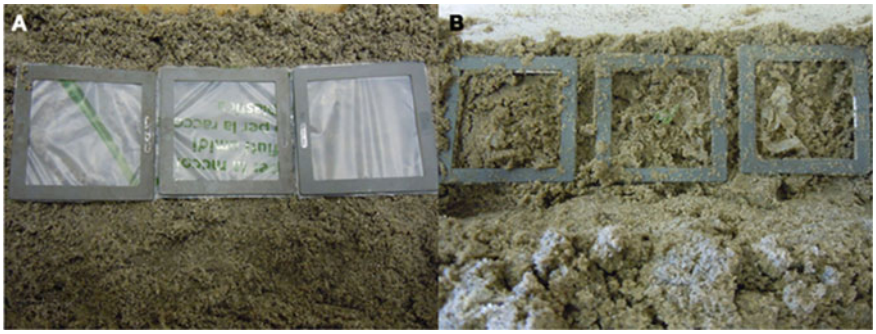

Fig. 2 Picture showing soil burial treatment in a domestic garden

Table 1 Amount of chemicals involved in the shake flask experiment

Ingredients	Amount	Ingredients	Amount	Ingredients	Amount
K_2HPO_4	1 g	KH_2PO_4	0.2 g	Boric acid	0.005 mg
NaCl	1 g	$CaCl_2.2H_2O$	0.2 g	$(NH_4)_2SO$	1 g
$MgSO_4.7H_2O$	0.5 g	$MnSO_4.H_2O$	0.001 g	$ZnSO_4.7H_2O$	0.001 g
$CuSO_4.5H_2O$	0.001 g	$FeSO_4.7H_2O$	0.01 g		

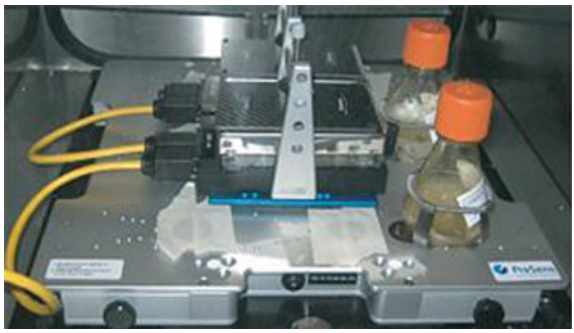

Fig. 3 Interior view of the shaking incubator

3. **Sturm test biodegradation**: CO_2 evolved from the cellulose-blended PVC biodegradation was obtained and further determined by a process called the sturm test. In order to perform this process, the pieces of those polymers were added to the existing culture bottles containing MSM (amounting to 285 mL) without providing them with any proper carbon source. The spore suspensions obtained from the specific strain of *Ideonella sakaiensis* (2.9 × 106 spores mL-1) were used as inoculums of 5% (v/v) in performing the sturm test, and control bottles (without plastic) were employed. Perfectly maintained sterilized air was supplied to maintain aerobic conditions, and the reaction bottles were stirred continuously on a magnetic stirrer. Exactly after a month, gravimetric analysis of CO_2 production was performed by collecting the obtained gas in adsorption bottle already containing a solution of KOH (1 M). The precipitates were obtained after this titration using barium chloride solution (1 M), and then the control was filtered, weighed, and calculated to estimate the CO_2 production per liter (Fig. 4).

Fig. 4 Pictorial view of sturm test biodegradation being performed in laboratory

Emmanuel et al. performed a study where they highlighted the ability of a complex enzyme (LIQ 1) for degrading polymers like sesbania gum and guar gum. The study was based on certain assumptions, one of which was that the polymeric compounds dissolved in water would increase the viscosity of the solution and would be able to connect to an artificial rock sample (made out of pulverized coal) placed in a pressure chamber. This study also took help of the second assumption which states that complex (LIQ1) would gradually degrade the polymeric compounds present, thereby reducing the viscosity of the solution, and hence, it is capable of unplugging that artificial rock. The polymeric compounds obtained were not exactly auto-degradable at room temperature though they showed a considerable decreasing viscosity after an hour.

UV radiation evaluates the photosensitivity of every film of a plastic bag that has been provided as sample [10]. Plastic strips (approximately 2.54 cm by 15.24 cm) were evenly cut in machine and placed inside a UV box (dimensions: 17.78 cm by 40.64 cm) at a significant distance of 17.78 cm from the source lamp for 8 weeks [7]. The plastic strips were then turned upside down, twice a week, in order to ensure that all sides are evenly exposed to the light source. Samples were removed after 1, 2, 3, 4, and 8 weeks, respectively. The mechanical properties, characterizations, and molecular weight distributions were accordingly determined and recorded.

4. **Fungal treatment**: Finally, this method was done where very few fungal strains were obtained from the species *Basidiomycetes.* These fungal cultures were then prescreened with the use enrichment media containing petridishes. Surface-sterilized (3% H_2O_2, 2 min) polyester filaments were gently added on agar-medium surfaces, and inoculation with those fungal strains was done simultaneously. Other degradation tests were also performed using liquid media, where selected fungal strains were obtained in a 250 ml Erlenmeyer flask contains 15 ml of the desired culture media in which pieces of polyester or co-polyester films are immersed for a considerable period of time. Before inserting the content into the nutrient medium, polymer pieces were surface sterilized (3% H_2O_2, 2 min) and stored in sterile conditions. There are two different culture media, namely nitrogen-limited medium and nutrient-rich glucose malt extract medium [11].

3 Summary and Conclusion

Plastics are a major threat to the environment, and specifically, it is posing threat to aqua–marine life. The entire globe is inclined to sort out a convenient process to degrade the polymer and come up with a healthier alternative that is "a biodegradable plastic." Most plastics resist degradation, while very few show properties of degradation to certain extent. Some of them exist for an enormous period of time as a persistent organic pollutant (POP). The objective is to find the best suitable degradation procedure of various kinds of plastics involving biological means as well as other sources of natural means too. The plastics which were taken into consideration are

polyethylenes, polyvinyl chloride, polyesters, polyhydroxyalkanoates, polylcaprolactone, polylactic acid, polyurethane, polyvinyl alcohol, nylon and polyethylene, polyester-polyurethane, etc. Bacterial and fungal species were also widely employed in these degradation processes. Several strains of *Ideonella sakaiensis* were used in developing the desired process. Finally, it was concluded that the organisms which degrade the hydrocarbon present in plastics and use them as proper sources of carbon can be employed. The results are confirmed by the changes in weight, tensile strength, and decrease in the viscous properties in most cases, while in few cases, molecular weight distribution and fragility were also noticed. Thus, it can be also concluded that HDPE plastics are showing more resistance to soil conditions than LDPE plastics. It was observed that the enzymatic degradation of gum was also an effective procedure. The pure culture biodegradation assay shows the ability to identify that which particular portion of the degradation is due to chemical degradation and what can contribute directly to the biological degradation process. Through these studies, degradation of plastic can be made more cost effective, less time consuming, and needless to say that once these methods are incorporated to treat the challenges and threats imposed by plastics, the acute problem of water pollution and disproportion to aquatic life would majorly get solved. Needless to say that neither any of these abovementioned methods nor *Ideonella sakaiensis* as a species poses any threat to the growth and cultivation of fishes. Thus, in near future, plastics causing pollution can be treated using this special variety of bacteria for improvement of freshwater fish cultivation.

References

1. Joel FR (1995) Polymer science and technology, introduction to polymer science, vol 3, pp 4–9
2. Seymour RB (1989) Polymer science before and after 1899: notable developments during the life time of Mautis Dekker. J Macromol Sci chem. 26:1023–1032
3. Shimao M (2001) Biodegradation of plastics. Curr Opin Biotechnol 12:242–247
4. Scott G (1990) Photo-biodegradable plastics: their role in the protection of the environment. Polym. Degrad. Stability 29:135–154
5. Griffin GJL (1973) Biodegradable fillers in thermoplastics. Am Chem Soc Div Org Coat Plast Chem 33:88–92
6. David C, Trojan M, Daro A (1992) Photodegradation of polyethylene: comparison of various photoinitiators in natural weathering conditions. Polym Degrad Stability 37:233–245
7. Lee BAL, Pometto HI, Fratzke A, Bailey TB (1991) Biodegradation of degradable plastic polyethylene by phanerochaete and streptomyces species. Appl Environ Microbiol 57:678–685
8. Ibrahim IN, Maraqa A, Hameed KM, Saadoun IM, Maswadeh HM (2011) Assessment of potential plastic-degrading fungi in Jordanian habitats. Turk J Biol 35
9. Borghei M, Karbassi A, Khoramnejadian S, Oromiehie A, Javid AH (2010) Microbial biodegradable potato starch based low density polyethylene. Afric J Biotech 9(26):4075–4080
10. Kenneth EJ, Anthony L, Pometto, I, Zivko LN (1993) Degradation of degradable starch-polyethylene plastics in a compost environment. App Environ Microbiol 1155–1161
11. Tien M, Lignin KTK (1988) Peroxidase of phanerochaete chrysosporium. Meth Enzymol 161:238–249

Assessment and MLR Modeling of Traffic Noise at Major Urban Roads of Residential and Commercial Areas of Surat City

Ramesh B. Ranpise, B. N. Tandel, and Chandanmal Darjee

1 Introduction

The main source of external noise in the world comes mainly from the transportation system [1] and specifically urban road traffic which is increasing with time [2]. There are many unfavorable effects on human health and well-being in urban areas and large cities due to noise pollution, such as speech communication, sleep disturbance, reading, and concentration of mental work, severe physiological and psychological damages [3]. In urban areas, traffic noise could be a keystone for the awareness of imminent conflicts by endanger urban road users [4]. The noise generated from the interaction of vehicular tires and the road surface is a significant contributor to the overall road noise. The main purpose of this study is to assess and model road traffic noise at major urban roads of residential and commercial areas of Surat city. The most widely recognized application is for assessment where a decision is to be made with respect to some future changes to an environmental noise field. In any case, given the reasonable and specialized difficulties in noise measurement strategies, there is an expanding number of circumstances in which predictions complement or substitute for measurement-based noise assessment techniques. Therefore, traffic noise prediction models are required as aids in the design of roads and the assessment of existing, or envisaged changes in traffic noise conditions.

R. B. Ranpise (✉) · B. N. Tandel · C. Darjee
Civil Engineering Department, Sardar Vallabhbhai National Institute of Technology, Ichchhanath, Surat 395007, Gujarat, India
e-mail: ranpiseramesh6588@gmail.com

S. Kumar et al. (eds.), *Sustainability in Environmental Engineering and Science*, Lecture Notes in Civil Engineering 93,
https://doi.org/10.1007/978-981-15-6887-9_21

Table 1 Geometrical/Geographical features of all roads

S. No.	Road	Geometrical features			Land use
		Width	Lane	Service road	
1.	Big Bazaar-Vesu road	14 m (without divider)	2 lane (two way)	Not available	Mixed (residential/commercial)
2.	Swami Vivekananda Marg	14 m (including divider)	2 lane (two way)	Not available	Residential
3.	Bhatar road	14 m (including divider)	2 lane (two way)	Not available	Mixed (residential/commercial)

2 Materials and Methodology

Surat is a city in the Indian state of Gujarat. It used to be a large seaport and is now a center for diamond cutting and polishing. It is the eighth largest city and ninth largest urban agglomeration in India [5]. Also, the city is very well connected by road, rail, and air transport.

Three roads of the same width (14 m) were selected based on a pilot survey carried out on six streets namely Bhatar road (flexible pavement), Swami Vivekananda Road (flexible pavement), and Big Bazaar-Vesu road (rigid pavement) (Table 1).

Noise level readings were collected for continuous day time 16 h (6.00 am–10.00 pm) with noise level meter held at about 1.5 m over the ground close to the edge of the street. Handycam was utilized for vehicular spot speed recordings. Furthermore, after that, the traffic was checked by playing the recordings on the workstation. There were 4–5 individuals associated with the review for different information gathering: (a) Two individuals were there for noise levels data collection. (b) Two individuals collected the traffic speed estimations by utilizing the radar gun. (c) One individual was there with Handycam. After collecting the information, a model has been created utilizing multiple linear regression in MATLAB programming.

3 Data Analysis and Results

After the appropriate execution of a pilot survey of six streets, three streets were chosen, in which two are flexible pavements and one is rigid pavement. Detailed monitoring has been performed for 16 h on every street. Traffic noise readings have been collected continuously for 16 h beginning from 6:00 am morning to night at 10:00 pm.

Traffic composition and graphical representation of traffic noise level and traffic volume count

3.1 Bhatar Road (Flexible Pavement)

See Figs. 1 and 2; Table 2.

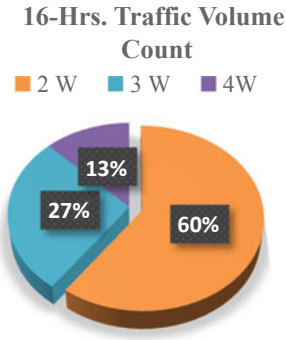

Fig. 1 Traffic compositions at the Bhatar road

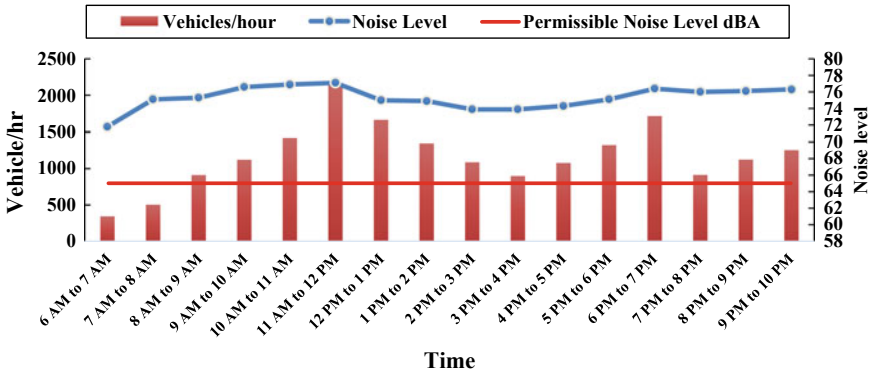

Fig. 2 Graphical representation of traffic noise level and traffic volume count at Bhatar road

Table 2 Traffic composition at Bhatar road

Bhatar road		
Type of vehicles	Volume count	
	Numbers of vehicles	Percentage (%)
2 W	11,170	60.10
3 W	5096	27.42
4 W	2321	12.48
Total	18,587	100.00

3.2 *Swami Vivekananda Marg (Flexible Pavement)*

See Figs. 3 and 4; Table 3.

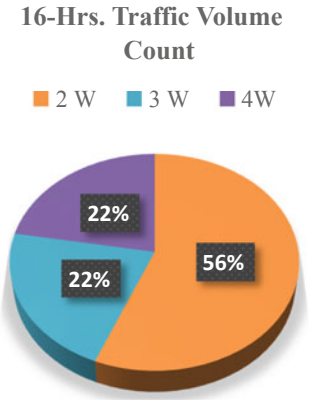

Fig. 3 Traffic compositions at Swami Vivekananda Marg

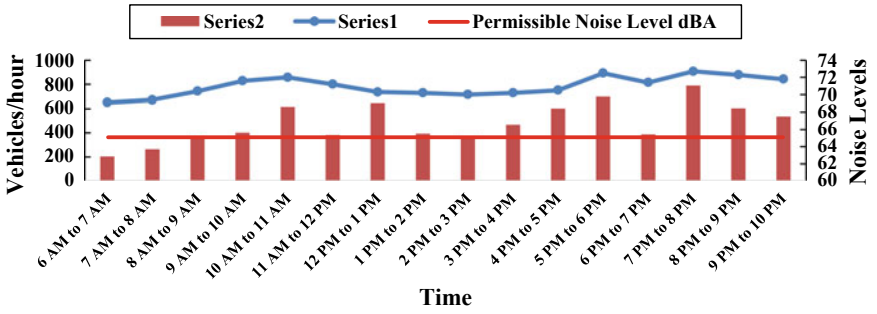

Fig. 4 Graphical representation of traffic noise level and traffic volume at Swami Vivekananda Marg

Table 3 Traffic composition at Swami Vivekananda Marg

Swami Vivekananda Marg		
Type of vehicles	Volume count	
	Numbers of vehicles	Percentage (%)
2 W	4413	56.15
3 W	1699	21.62
4 W	1748	22.24
Total	7860	100.00

3.3 Big Bazaar-Vesu Road (Rigid Pavement)

The maximum noise level (Leq) measured across all three roads is 77.1 dB(A). It is during morning peak hours (11 am–12 pm) and the road is a flexible pavement (Bhatar road). On this road, the minimum noise level is 73.9 dB(A) during the off-peak hour (2 pm–4 pm) which is still far exceeding the permissible noise level 65 dB(A). There is a significant difference of 3.2 dB(A) in between the maximum and minimum noise levels during the morning peak and off-peak hour. The maximum noise level (L_{max}) measured across all three roads is 107.3 dB(A). It is during evening peak hours (7 pm–8 pm) and the road is a flexible pavement (Swami Vivekananda Marg) (Figs. 5, 6 and Tables 4, 5).

The maximum number of vehicles/hour occurred at Bhatar road during morning peak hour (11 am–12 pm) is 2158 vehicles/hour and the corresponding noise level (Leq) is 77.1 dB(A) which is also maximum. On this road, the minimum number of vehicles/hour occurred during the off-peak hour (3 pm–4 pm) is 897 vehicles/hour and the corresponding noise level (Leq) is 73.9 dB(A) which is also minimum.

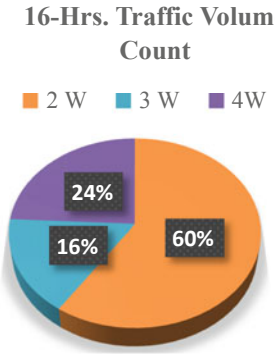

Fig. 5 Traffic compositions at Big Bazaar-Vesu road

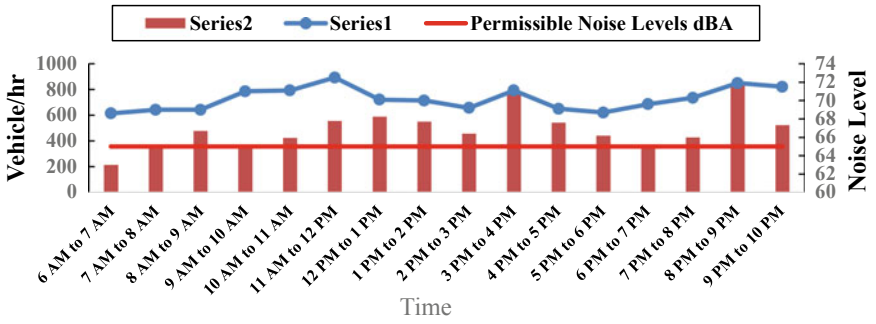

Fig. 6 Graphical representation of traffic noise level and traffic volume count at Big Bazaar-Vesu road

Table 4 Traffic composition at Big Bazaar-Vesu road

Big Bazaar-Vesu road		
Type of vehicles	Volume count	
	Numbers of vehicles	Percentage (%)
2 W	4622	59.42%
3 W	1274	16.38%
4 W	1883	24.21%
Total	7779	100.00%

Table 5 Traffic noise level (Leq) at each location

Location	Noise levels dB(A)		
	Peak (9 am–1 pm) or (5 pm–9 pm)	Off-peak (1 pm–5 pm)	Difference (Leq)
Bhatar road	77.1	73.9	3.2
Swami Vivekananda Marg	72.7	70.0	2.7
Big Bazaar-Vesu road	72.5	68.7	3.8

Among all three roads, Bhatar road has the highest aspect ratio (H/W), i.e., 2.5. The corresponding noise level (Leq) is 75.5 dB(A) which is maximum among all three roads and the aspect ratio for Big Bazaar-Vesu road is 1.64 and the corresponding noise level is 70.3 dB(A) which is minimum among all three roads. Based on this variation of equivalent traffic noise level concerning the aspect ratio, it is clear that when the aspect ratio is increasing for a particular road then the equivalent traffic noise level is also increasing due to the reverberation effect of noise (Table 6).

The maximum and minimum noise level among all rigid pavement under detailed study is 72.5 dB(A) and 68.6 dB(A), respectively. For flexible pavement, the maximum and minimum noise level is 77.1 and 69.1 dB(A). The significant finding here is that minimum noise levels are almost the same for both types of pavement, viz. rigid and flexible. But the maximum noise is more in a flexible type of pavement, by 4.6 dB(A).

Also, it is seen that the 2 W is contributing the maximum (55–60%) in the generation of equivalent traffic noise levels for all three roads.

Table 6 Variation of traffic noise level concerning aspect ratio (H/W)

Location	Noise level dB(A)	Aspect ratio (H/W)
Bhatar road (A)	75.5	2.5
Swami Vivekananda Marg (B)	72.0	2.14
Big Bazaar-Vesu road (C)	70.3	1.64

4 Model Developments

In this research, SPSS STATISTICS 22 programming is utilized for the generation of a multiple linear regression equation which can be represented as below:

$$Y = A + B_1X_1 + B_2X_2 + B_3X_3 + \ldots + B_nX_n \quad (1)$$

where

Y = Dependent variable
Leq = 16 h day time equivalent noise level
X_1, X_2, X_3, and so on = Independent variables (2-W, 3-W, 4-W count)
A = Intercept
B_1, B_2, B_3, and so on = Coefficients of independent variables (Table 7).

From all the above results of the MLR model, we can say that when the number of three-wheeler is increasing for a road then the equivalent noise level is also increasing for that particular road. For Bhatar road, when the number of four wheelers is increasing the equivalent noise level (Leq) is decreasing, and for Big Bazaar-Vesu road, when the number of two wheelers is increasing the equivalent noise level is decreasing.

4.1 For All Three Roads

Developed multiple linear regression model for all three roads is as follows:

$$Y = 30.212 - 2.132\,X_1 + 2.156\,X_2 + 1.6\,X_3 + 25.671\,X_4 \quad (2)$$

where X_4 = Average Height of buildings.

From Eq. (2), it is seen that equivalent traffic noise level (Leq) is increasing with the numbers of the three-wheeler, four-wheeler, and average building heights, and it

Table 7 Multiple linear regression equation for three roads

Location	MLR equation	R^2	Avg. percentage % error
Bhatar road	$Y = 64.562 + 3.573\,X_1 + 1.184\,X_2 + 1.567\,X_3$	0.086	1.804
Big Bazaar-Vesu road	$Y = 61.129 - 3.05\,X_1 + 3.101\,X_2 + 2.315\,X_3$	0.253	2.065
Swami Vivekananda Marg	$Y = 63.840 + 3.379\,X_1 + 0.181\,X_2 + 2.143\,X_3$	0.172	2.272
All roads (combined)	$Y = 30.212 - 2.132\,X_1 + 2.156\,X_2 + 1.6\,X_3 + 25.671\,X_4$	0.511	2.273

is decreasing with the increment of numbers of the two-wheeler. In the MLR model for all three roads, the coefficient for average building height is also obtained because the average building height for all three roads is not constant.

5 Results and Discussion

As per Fig. 7, it is observed that the estimation of the coefficient of determination (R^2) is 0.086 which is less noteworthy. The mean percentage error as indicated by Fig. 8, it is observed that the estimation of the coefficient of determination (R^2) is 0.253 which is additionally less, yet more prominent than the R^2 for Bhatar street, the greatest and least supreme blunder is 5.23 and 0.01% individually. The normal outright blunder is 2.06%. Swami Vivekananda Marg: As indicated by Fig. 9, it is observed that the estimation of the coefficient of determination (R^2) is 0.172 which is likewise exceptionally less yet more noteworthy than the R^2 for Bhatar Street, the most extreme and least total mistake is 9.35 and 0.07% individually. The mean percentage error is 2.27%.

For all three roads according to Fig. 10, it is seen that the value of the coefficient of determination (R^2) is 0.511 which is higher than all the three roads. The maximum and minimum absolute errors are 12.86% and 0.0%, respectively. The mean percentage error is 2.27%.

After the interpretation of the outputs from MLR, it was found that the value of mean square error is higher and the value of the coefficient of determination (R^2) is low. It is a clear indication that the model obtained from the MLR is weak and not adequate. Among the prediction in three urban roads, the predicted output result from

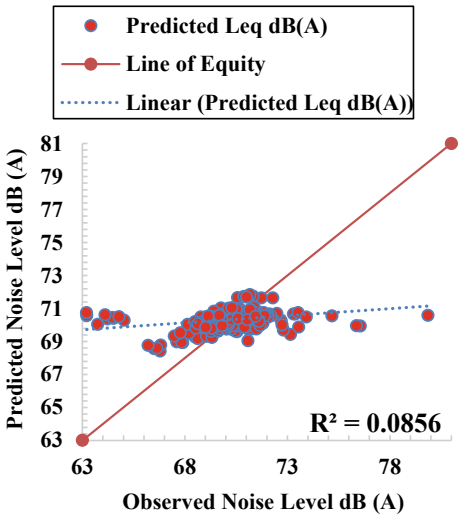

Fig. 7 Observed versus predicted traffic noise level (Leq) for Bhatar road

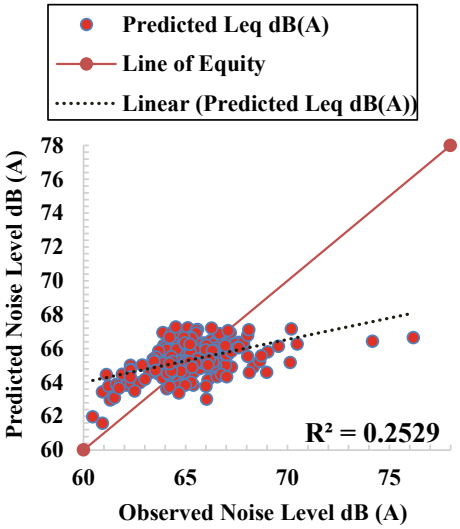

Fig. 8 Observed versus predicted traffic noise level (Leq) for Big Bazaar-Vesu road

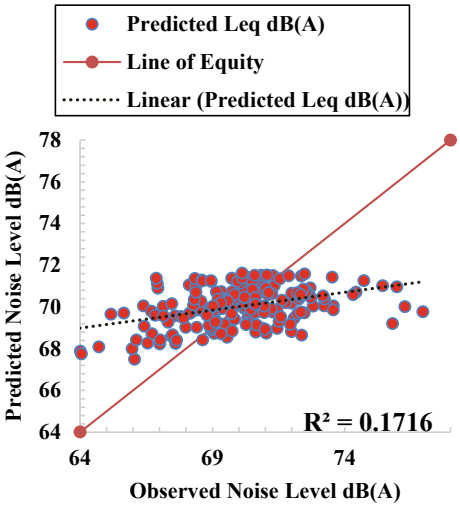

Fig. 9 Observed versus predicted traffic noise level (Leq) for Swami Vivekananda Marg

the MLR model showed not much correlation with a mean percentage error of 2.065 and an R^2 value of 0.25. But with the combined road, there is a significant change in average absolute % error 2.27, with R^2 value 0.51. The factors not considered in this study, but contributing to the generation or absorption of noise are speed of the vehicles, vegetation along the roadside, and the number of heavy vehicles passed through the road from 1:00 pm to 5:00 pm.

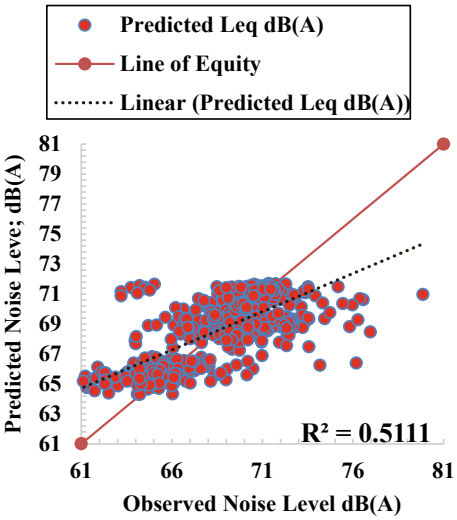

Fig. 10 Observed versus predicted traffic noise level (Leq) for all three roads

6 Conclusion and Recommendations

In this study, noise and traffic information has been collected for continuous 16 h the span at three distinct streets of Surat city. Two streets have flexible pavement surface, and one street has rigid pavement. Multiple regression model has been created by utilizing information gathered during the itemized study in MATLAB R2013b and SPSS Statistics 22 programming. Among all three roads understudy, the noise level during day time and night time is above the permissible limit of Noise Pollution (Regulation and Control) Rules, 2000. It was also found that the maximum noise level obtained on the flexible pavement road surface during the morning peak hours which is 4.6 dB(A) higher than the maximum noise level (Leq) obtained on the rigid pavement road surface during the morning peak hours. Hence, among all the three individual prediction model results, it is found that the Bhatar road and Big Bazaar-Vesu road have approximately the same value of the coefficient of determination and average absolute percentage error. The model developed for these two roads is better than the Swami Vivekananda Marg.

As the equivalent noise level is not linearly dependent upon independent variables traffic count and average building height, the MLR models developed are weak and not reliable. To overcome this problem, road traffic noise prediction models may be developed using evolutionary computing tools like genetic algorithm, neural networks, etc. Also, only two independent variables, viz. vehicular count and building height have been taken into consideration, but generation or reduction of noise also depends largely upon vegetation along roads, types of pavement, speed of the vehicle, etc.

References

1. Gil-Lopez T, Medina-Molina M, Verdu-Vazquez A, Martel-Rodriguez B (2017) Acoustic and economic analysis of the use of palm tree pruning waste in noise barriers to mitigate the environmental impact of motorways. Sci Total Environ 584–585:1066–1076
2. Vivek K, Prapoorna BK (2018) Evolution of tire/road noise research in India: investigations using the statistical pass-by method and noise trailer. Int J Pavement Res Technol 11:253–264
3. Rahmani S, Mousavi SM, Kamali MJ (2011) Modelling of road traffic noise with the use of genetic algorithm. Appl Soft Comput 11:1008–1013
4. Mendonça C, Freitas E, Ferreira JP, Raimundo ID, Santos JA (2013) Noise abatement and traffic safety: the trade-off of quieter engines and pavements on vehicle detection. Accid Anal Prev 51:11–17
5. Surat–News, Newspapers, Books, Scholar, JSTOR (2018, July)
6. Singh VA, Tandel BN (2014) Development of traffic noise prediction model for major arterial roads of Surat city using artificial neural network. PG Section in Environmental Engineering, Department of Civil Engineering, Sardar Vallabhbhai National Institute of Technology, Surat, 395007, Gujarat, India

A Review on the Advanced Techniques Used for the Capturing and Storage of CO_2 from Fossil Fuel Power Plants

Ria Shaw, Sumanta Naskar, Tanmay Das, and Anirban Chowdhury

1 Introduction

The greenhouse gas (GHG) is the main cause for global climate changes happening all over the world. The most significant GHG is CO_2. The CO_2 gas capture and storage is receiving considerable attention as a potential greenhouse gas (GHG) mitigation option that could allow a smoother and less costly transition to a sustainable [1]. According to the International Energy Agency [2] the electricity production from fossil fuels will increase by about 30% by 2035, which will ineludible lead to more CO_2.

The emission of CO_2 from fossil fuel power plants can be reduced by [3]:

i. increasing the efficiency of the plants (1% increase in efficiency reduces CO_2 by 2–3%);
ii. switching, partially or totally, to low-carbon content fuels or to "carbon neutral" fuels;
iii. capturing CO_2 and storing it [4].

R. Shaw · S. Naskar · T. Das (✉) · A. Chowdhury
Department of Electrical Engineering, Dr. Sudhir Chandra Sur Degree Engineering College, Kolkata, India
e-mail: tanmaydas159@gmail.com

R. Shaw
e-mail: ria2000shaw@gmail.com

S. Naskar
e-mail: sumantanaskar18@gmail.com

A. Chowdhury
e-mail: anirbanee2015@gmail.com

S. Kumar et al. (eds.), *Sustainability in Environmental Engineering and Science*, Lecture Notes in Civil Engineering 93,
https://doi.org/10.1007/978-981-15-6887-9_22

There are three different technologies to capture CO_2 from fossil fuel power plants, [4] namely

i. Post-combustion
ii. Oxy-fuel combustion
iii. Pre-combustion.

The actual useful things of post-combustion capture is that it can be degenerated into prevailing power plants without changing the combustion technologies. As we can see, for a amine-based absorption or desorption post-combustion systems, large amounts of low pressure steam would be required to be pull out from the turbine. As a result, it reduces the output of electricity generation by 20–30%. According to UN Framework Convention [5] about the changes of climate was developed, the countries accepted to decrease their emission of six different greenhouse gases to 5.2% over the period 2008–2012. By this statement, it was cleared that greater diminishment will be most required in future. This phenomenon will require action by all countries. To limit the CO_2 concentration to 550 ppm, it is required by all the countries to reduce more than 60% in 2100. These steps are urgently required by major coal-used countries.

This paper briefly reviews the performances of power plant with CO_2 capture and presents current research and development and demonstration projects on CO_2 emission control in power plants.

2 Emissions of CO_2 from Fossil Fuel Power Plant

The amount of CO_2 emissions from fossil fuel, power plants will basically vary on which type of fuel is used and the various types of power generation technologies, the area of the plant and the efficiency.

The quantities of CO_2 emitted, captured, and avoided are shown in Table 1 [6]. The baseline plant should be type of the plant that would be displaced by a plant with CO_2 capture. In Table 1, it shows the amount of emission avoided for three baselines which are

i. The same type of power generation technology,
ii. A pulverized coal (PC) plant
iii. An NGCC plant. In some conditions, the power plants with CO_2 capture may be displaced old inactive power plants in which case the amount of CO_2 emissions avoided would be possibly higher than those shown in Table 1.

As can be seen in Fig. 1 [4], the efficiency of PC and NGCC plant based on post-combustion CO_2 storage is near about 10% points and 8% points independently.

The efficiency decreases for PC plants with sodium-based and potassium-based storage systems in 9–9.5% points, with ammonia-based systems in the range of 8–16% points, but in case of calcium, the efficiency decreases by 6–9% points. For PC

Table 1 Quantities of CO_2 emitted, captured and avoided

CO_2 emissions								
Fuel	Power generation technology	CO_3 capture technology	CO_2 emissions (g/kWh)	CO_2 captured (g/kWh)	CO_2 captured (%)	CO_2 avoided (g/kWh)		
						Same technology baseline	PF baseline	NGCC
Coal	PF	None	743	–	–	–	–	–
		Flour	117	822	87.5	626	626	262
		MHI	92	832	90	651	651	287
		Oxy	84	831	90.8	659	659	295
	IGCC	None	763	–	–	–	–	–
	(Shell)	Selexol	142	809	85	621	601	237
	IGCC	None	833	–	–	–	–	–
	(GE)	Selexol	152	851	85	681	591	227
Gas	IGCC	None	379	–	–	–	–	–
		Flour	66	378	85	313	677	313
		MHI	63	362	85	316	680	316
		Oxy	12	403	97.2	367	731	367

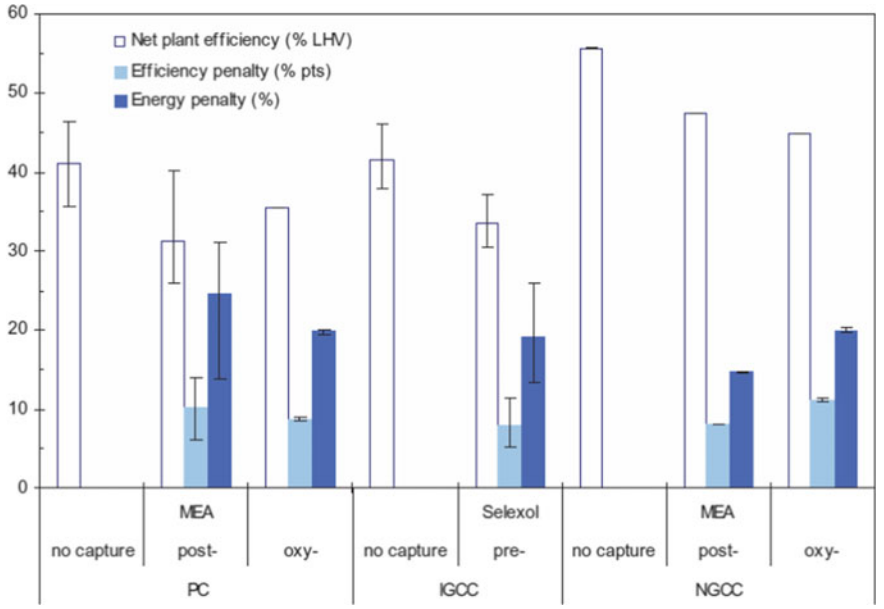

Fig. 1 Efficiency of power plants with and without CO_2

and NGCC power plant with oxy-combustion, the efficiency decreases near about 10% points. To reduce the energy penalty along with O_2, more effective technologies should be used.

3 Cost and Efficiency

The cost of these technologies for capturing and storing CO_2 has been considered in few steps. The pulverized coal is restraining renewable energy sources. Pulverized fuel-based electricity generation is very costly. The fuel generation cost is near about Rs. 100,784/kW, and for post-combustion, the capital cost is Rs. 1,441,656.82–146,237.94/kw. For oxy-fuel combustion, the cost is near about Rs. 157,833.9/kW. The net power output in power generation technology for pulverized fuel is 758 MW. For post-combustion, it varies from 666 to 676 MW, and for oxy-fuel combustion, it has reached up to 532 MW. A pulverized coal plant without the capture of CO_2 was designated as the baseline coal-fired plant. It gives low price of electricity, and hence, it is the technology that would be preferred by making practical and effective use in the unavailability of the required to capture, transmission, and storing CO_2. For coal-fired power plant, the cost of without CO_2 emission is Rs. 1932.66–2791.62 per ton. For gas-fired power plant, the cost of CO_2 is more expensive than the coal-fired power plant, and it is near about Rs. 3435.84–7301.16 per ton [7–10]. The transport

and storage cost of CO_2 is Rs. 715.8/ton-CO_2 which would become strengthening in amount of without CO_2 by about Rs. 930.54/ton-CO_2 for the gas-fired power plant. The cost per ton of CO_2 avoided is more expensive than the cost per ton of CO_2 stored [6].

4 Conclusion

This paper encapsulated the results of current studies of CO_2 capture and storage cost for fossil fuel power plants and also presented the renovated juxtapositions of pulverized coal (PC), NGCC systems. For the recent studies, NGCC plants are found to be more expensive than the coal-fired-based power plants with and without carbon dioxide capture and storage (CCS). According to the recent studies, the cost of gas is Rs. 286.5/GJ or less.

This study also accentuated and identified the immensity of CO_2, capture and storage energy requirements, and their smacks on plant-level resources needs and environmental emissions. Advanced power generation and CCS technology providing better efficiency and less amount of energy, which are necessary for diminishing these impacts and few numbers of possibilities, are in impoverishment.

References

1. Rubin ES, Chen C, Rao AB (2007) Cost and performance of fossil fuel power plants with CO_2 capture and storage. Energ Policy 35(9):4444–4454
2. IEA (2003) CO_2 emissions from fuel combustion 1997–2001. IEA/OECD, Paris, France
3. Cebrucean D, Cebrucean V, Ionel I (2012) Post-combustion CO_2 capture technologies for coal-fired power plants. In: Proceedings of the 2nd international conference "Ecology of Urban areas 2012"
4. Cebrucean D, Cebrucean V, Ionel I (2014) CO_2 capture and storage from fossil fuel power plants. Energ Procediam 63:18–26
5. Freund P (2003) Making deep reductions in CO_2 emissions from coal-fired power plant using capture and storage of CO_2. Proc Inst Mech Eng Part A J Power Energ 217(1):1–7
6. Davison J (2001) Performance and costs of power plants with capture and storage of CO_2. Energy 32(7):1163–1176
7. MIT (2007) The future of coal. MIT
8. IEA (2010) Cost and performance of carbon dioxide capture from power generation. OECD/IEA
9. NETL (2010) Cost and performance baseline for fossil energy plants. Volume 1: bituminous coal and natural gas to electricity. DOE/NETL-2010/1397, Revision 2a, September 2013
10. Rubin ES, Chen C, Rao AB (2007) Cost and performance of fossil fuel power plants with CO_2 capture and storage. Energ Policy 35:4444–4454

Assessment and Characterization of Air Pollution Due to Vehicular Emission Considering the AQI and LOS of Various Roadways in Kolkata

Rupam Sam

1 Introduction

Urbanization is a global phenomenon. There has been rapid urbanization in the cities of India which has led to an increase in demand for mobility. It has resulted in a tremendous increase in the number of motor vehicles. Vehicles are now becoming the major source of air pollution. The growth rate of vehicles is the backbone of economic development as well as the Indian automotive industry. In 2011, India reported 141.8 million registered motorized vehicles. A motorization rate in India is almost 26 vehicles per 1000 population transportation serves as channel for economic development of a country. Besides, the traffic facility in the highway should also be upgraded in order to provide the best quality of service (known as level of service) to the road users.

The most common manual named Highway Capacity Manual (HCM) has developed the capacities standard and Level of Service (LOS) measure for various transportation facilities. More recently, LOS was defined in HCM 2000, as "a quality measure describing operational conditions within a traffic stream, generally in terms of such service measures as speed and travel time, freedom to maneuver, traffic interruptions, and comfort and convenience as perceived by the road users." The latest version of HCM has proposed six levels of services, which range from A to F where A denotes the best quality of service and F denotes the worst quality level of service. As per the current practice, the LOS solely depends on delay and the volume-to-capacity ratio (HCM 2010) [1]. LOS is widely used in transport planning and traffic engineering in order to evaluate problems and potential solutions. Normally, LOS C (LOS D in large urban areas) is used as lowest acceptable level of service.

R. Sam (✉)
Department of Civil Engineering, Heritage Institute of Technology, Kolkata, India
e-mail: rupam.sam1993@gmail.com

S. Kumar et al. (eds.), *Sustainability in Environmental Engineering and Science*, Lecture Notes in Civil Engineering 93,
https://doi.org/10.1007/978-981-15-6887-9_23

In recent years, there has been a growing concern in cities about the rapidly deteriorating environment in the urban areas of this country in terms of air pollution specifically due to automobile considering the total tonnage of pollutants in urban areas. Air pollution generated by road traffic is a great concern in today's society as pollution has an impact on environment and also in human health. Also, many vehicles in Kolkata are backdated, older and made by outmoded technology. This is also another cause of vehicular emission. Vehicular emission includes various types of pollutants. These pollutants are suspected particulate matters, respiratory particulate matters, NO_2, SO_2, CO, and lead, etc. The Clean Air Act of 1970 authorized the federal government in order to promulgate air quality standards and to require states to adopt implementation plans in meeting these standards. Motorized transportation is closely associated with the problem of urban air pollution which can be considered as a major part of the strategies for the improvement of air quality is related to this source of pollution. A great effort has been made to reduce pollution emitted by the automobile by using new automobiles to be fitted with air pollution control devices. A significant part of air pollution control strategy can be achieved through effective traffic engineering measures. It is important that a traffic engineering decision be made not only on the basis of cost savings, increased safety, and improved traffic performance, but also on such aspects as reduced energy requirements and improved quality of environment. In this paper, a brief discussion is presented on the overall considerations of air pollution relating with the traffic level of service.

The Ministry of Environment and Forests launched a National Air Quality Index (AQI) which will put out real-time data about level of pollutants in the air. Generally, an AQI system is devised based on air quality monitoring procedures and protocols, Indian National Air Quality Standards (INAQS), and dose-response relationships of pollutants. Generally, there are eight parameters such as PM10, PM2.5, NO_2, SO_2, CO, O_3, NH_3, and Pb (having short-term standards) which have been considered for near real-time dissemination of AQI. The proposed air quality index has six categories, as shown below: Good (AQI: 0–50), satisfactory (AQI: 51–100), moderately polluted (AQI: 101–200), poor (AQI: 201–300), very poor (AQI: 301–400), and severe (AQI: > 401). Levels of service may be based on such as travel times (or speeds), total delay, probability of delay, comfort, safety, and so forth. By enhancing the level of service (LOS) of the traffic, it will also impact on the environment air quality. For example, higher LOS indicates low traffic congestion which causes low air pollution due to vehicular emission. Therefore, modeling LOS relating with the air pollution actually helps to enhance the quality of air in the environment.

The objectives of our study are following:

- To understand the nature and causes of vehicular emission in various urban areas near major roadways by using factor analysis considering qualitative data.
- To analyze the Air Quality Index based on Level of Service analysis of various roadways using ordered logit model.

2 Literature Review

The LOS at signalized intersection was by Sutaria and Haynes [2] in which a questionnaire survey was carried out and the users were requested to rate the factors before and after viewing the video films. Mitra et al. [3] described a model on traffic congestion considering the Level of service of the road. Kita [4] proposed a driver-utility-based level of service classification, in which utility was defined as the degree of driver's satisfaction of the driving conditions on a road section. Pecheux [5] presents a conceptual model of perceived LOS and describes how this model was used to develop the experimental design and procedure. Data needs for meeting the research objectives were identified as: individual vehicle delays, delay estimates, perceptions and detailed subject, and intersection information. Several alternative methods were considered for obtaining subjects' delay estimates and LOS perceptions. Zhang [6] described how road users perceive LOS at intersection conducting a web-based survey. Based on more than 1300 responses, it was revealed that left turn safety was important besides signal efficiency.

Chiaburu et al. [7] described the impact of highway expansion project on air quality using GIS. Amin et al. [8] described a similar type of case study for understanding from induced traffic during and after construction of a new highway in Montreal by considering 25 roads in analysis. Briggs and Hoogh [9] described a regression-based method for mapping traffic-related air pollution. Singh and Haque [10] described urban air quality in most megacities has been found to be critical in metropolitan city like Kolkata, and an analysis of ambient air quality in Kolkata was done by applying the Exceedance Factor (EF) method, where the presence of listed pollutants' (RPM, SPM, NO_2, and SO_2) annual average concentration is classified into four different categories; namely critical, high, moderate, and low pollution. Sarath et al. [11] explained the nature of air pollution, emission sources, and management in the Indian cities. The global burden of disease study estimated 695,000 premature deaths in 2010 due to continued exposure to outdoor particulate matter and ozone pollution for India. Shrivastava et al. [12] presented a review on assessment of air pollution due to transportation system in India. Diaz et al. [13] presented an intelligent transportation system model based on complex event processing technology and colored Petri nets (CPNs) which takes into consideration the levels of environmental pollution and road traffic, according to the air quality levels accepted by the international recommendations and the handbook emission factors for road transport methodology.

- **Study area**:

Study area	Number of the road segments
Kolkata	10

2.1 Data Collection

There are several factors which affect the satisfaction level of road users' on urban streets. To include both all probable road and traffic variables, this study has used both quantitative (traffic and geometric) and qualitative data (perception and demographic) for the LOS analysis.

2.1.1 Traffic and Geometric Data

Several traffic data such as speed, volume (V) and geometric data such as roadway width (W) are measured using radar gun, video camera, tape, etc., during the peak hour.

2.1.2 Perception Data

Road users were randomly selected while being stopped at a segment and taken a short interview on the basis of a brief questionnaire. They were asked to assess the road and traffic conditions on a segment just after having actually driven along this segment, in a scale from 1 to 6 where 6 being the highest grade and 1 being the lowest as described in table

Rating (6 point scale)	Representation	LOS category
6	Extremely satisfied	A
5	Very satisfied	B
4	Somewhat satisfied	C
3	Somewhat dissatisfied	D
2	Very dissatisfied	E
1	Extremely dissatisfied	F

The survey response rate was quite satisfactory, as very few drivers refused to participate. Moreover, 540 complete perception data sheets were gathered from the study area.

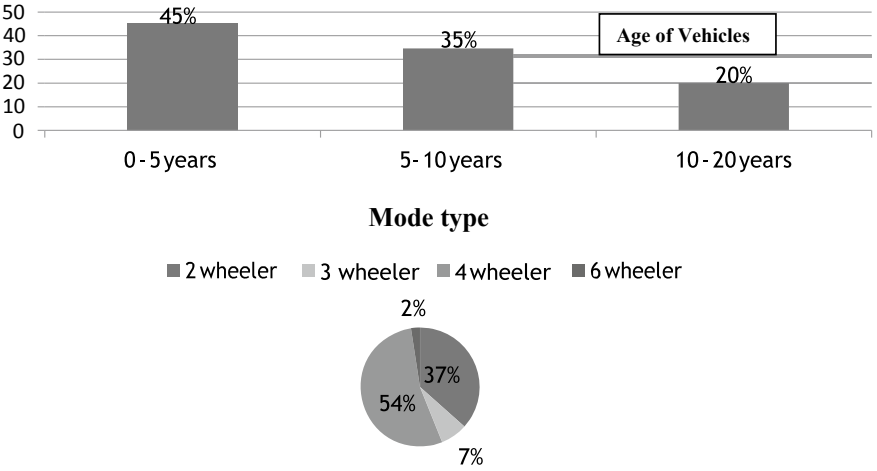

Fig. 1 Demographic data

2.1.3 Demographics

The collected demographic data sets and few their relative bar charts are shown Table and Fig. 1.

Determination of Input Data and Output Data Ratio of volume to road width, speed of the vehicles, number of vehicles encountering (Enc), fuel type (F), pavement condition index (PCI), and age of vehicles (AV) are determined after the required data collection. In order to extract the collected data, SPSS software was used. Based on this, factor analysis and mathematical model are developed using ordered logistic regression methodology.

2.2 Factor Analysis

2.2.1 Pearson's R and KMO Test

Pearson's *r* for the correlation between the road surface and safety variables in our example is 0.717. The KMO and Pearson's *r* value shows the significance of the collected dataset.

KMO and Bartlett's test	
Kaiser–Meyer–Olkin measure sampling adequacy	0.881

2.3 Principle Component Analysis

From the rotated component matrix, the perceptive data can be categorized into three components, i.e., safety convenience, road surface, and traffic operation. The components and the corresponding perceptive variables are shown in the following Table 1.

These above three major components are responsible controlling the LOS of various roadways. The AQI actually depends upon these three variables; therefore, these principle components should be enhanced and developed in order to avoid the congestion and vehicular pollution. Therefore, by analyzing these factors, the overall LOS of the roadways can be considered. Besides, the AQI parameter can be improved by developing the LOS in the prevailing road traffic system.

Table 1 Principle component analysis

S. No.	Components	Variables
1	Safety convenience	• Safety while driving • Chance of accident • Signal coordination
		• Traffic management
		• Average delay
		• Traffic sign
2	Road condition	• Pavement surface condition
		• Cleanliness • Street light
		• Drainage
		• Potholes
3	Traffic operation	• Congestion while driving
		• Frequent stops of transit • Driving in desired speed • U-turn or right turn
		• Entering into main stream during peak hour
		• Parking obstruction
		• Commercial activity
		• Presence of pedestrian and NMV

2.4 Model Development Using Ordered Logit Model

Parameter estimates data:								
		Estimate	Std. Error	Wald	Df	Sig.	95% confidence interval	
							Lower bound	Upper bound
Threshold	[OS = 1]	−5.331	0.411	168.526	1	0.000	−6.136	−4.526
	[OS = 2]	−1.398	0.369	14.363	1	0.000	−2.121	−0.675
	[OS = 3]	2.408	0.364	43.741	1	0.000	1.695	3.122
	[OS = 4]	6.546	0.393	277.234	1	0.000	5.776	7.317
	[OS = 5]	10.391	0.425	597.001	1	0.000	9.557	11.224
	[OS = 6]	12.004	0.475	611.05	1	0.000	11.008	12.432
Location	Vrw	−0.014	0.000	790.669	1	0.000	−0.015	−0.013
	Spd	0.123	0.006	421.695	1	0.000	0.111	0.135
	PCI	1.899	0.067	808.189	1	0.000	1.768	2.030
	LU	−6.193	0.390	251.987	1	0.000	−6.958	−5.429
	AQI	−3.542	0.452	61.494	1	0.000	−4.427	−2.657
	Enc	−3.208	0.208	238.344	1	0.000	−3.616	−2.801

2.5 Case Study: (Amherst Street)

For segment 1 (Amherst Street) the values of six variables are, *V/W* ratio = 232.59, *Spd*= 23.69, *PCI* = 4, *F*= 0.27, *AV* = 0.3 and *Enc*= 0.3.

The equation developed to find the function "*z*" using table:

$$Z_i = K_j - 0.014\left(\frac{V}{W}\right) + 0.123(\text{speed}) + 1.899(\text{PCI}) - 3.542(\text{AV}) + 6.193(F) - 3.208(\text{Enc.})$$

$$Z_1 = -5.331 - 0.014 * 232.59 + 0.123 * 23.69 + 1.899 * 4 - 3.542 * 0.3 + 6.193 * 0.27 - 3.208 * 0.3$$

$$Z_2 = -1.398 - 0.014 * 232.59 + 0.123 * 23.69 + 1.899 * 4 - 3.542 * 0.3 + 6.193 * 0.27 - 3.208 * 0.3$$

$$Z_3 = 2.408 - 0.014 * 232.59 + 0.123 * 23.69 + 1.899 * 4 - 3.542 * 0.3 + 6.193 * 0.27 - 3.208 * 0.3$$

$$Z_4 = 6.545 - 0.014 * 232.59 + 0.123 * 23.69$$

$$+ 1.899 * 4 - 3.542 * 0.3 + 6.193 * 0.27 - 3.208 * 0.3$$

$$Z_5 = 10.391 - 0.014 * 232.59 + 0.123 * 23.69$$
$$+ 1.899 * 4 - 3.542 * 0.3 + 6.193 * 0.27 - 3.208 * 0.3$$

$$Z_6 = 12.004 - 0.014 * 232.59 + 0.123 * 23.69$$
$$+ 1.899 * 4 - 3.542 * 0.3 + 6.193 * 0.27 - 3.208 * 0.3$$

The following formulae are applied to determine the probability of LOS:

$$P(Y_i = j) = \frac{1}{e^{(Z_i - K_j)} + 1} \text{for } j = 1$$

$$\text{P } (Y_i = j) = \frac{1}{e^{(Z_i - K_j)} + 1} - \frac{1}{e^{(Z_i - K_{j-1})} + 1} (\text{for } j = 2, 3, 4 \text{ and } 5)$$

$$P(Y_i = j)) = 1 - \{P(1) + P(2) + \ldots + P(5)\} \quad \text{for } j = 6$$

In this study,

- $P(Y_i = j)$: Probability of scoring ($j = 1, 2, 3, 4, 5, 6$) of segment no. i (in this study, $i = 1, 2, 3, \ldots, 102$).
- Z_i = Location value, i.e., quantitative data estimate value. In order to determine Z_i value, proper model is developed.
- K_j = Threshold value, i.e., overall satisfaction estimate value.
- The LOS of the road segment can be calculated based on the probability scoring 1 to 6.

Now, in Amherst Street,

$$P(Y = 1) = 0.0001,\ P(Y = 2) = 0.0069,\ P(Y = 3) = 0.234,$$
$$P(Y = 4) = 0.712,\ P(Y = 5) = 0.047,\ P(Y = 6) = 0.001$$

$$\text{LOS} = 1 * P(Y = 1) + 2 * P(Y = 2) + 3 * P(Y = 3)$$
$$+ 4 * P(Y = 4) + 5 * P(Y = 5) + 6 * P(Y = 6)$$
$$= 1 * 0.0001 + 2 * 0.0069 + 3 * 0.234$$
$$+ 4 * 0.712 + 5 * 0.047 + 6 * 0.001 = 3.80 \text{ (Signifies LOS D);}$$

AQI value of the adjacent area is 193. (Based on 25.11.19), which also somewhat signifies the categorization similarity with LOS of the roadway.

Model Validation

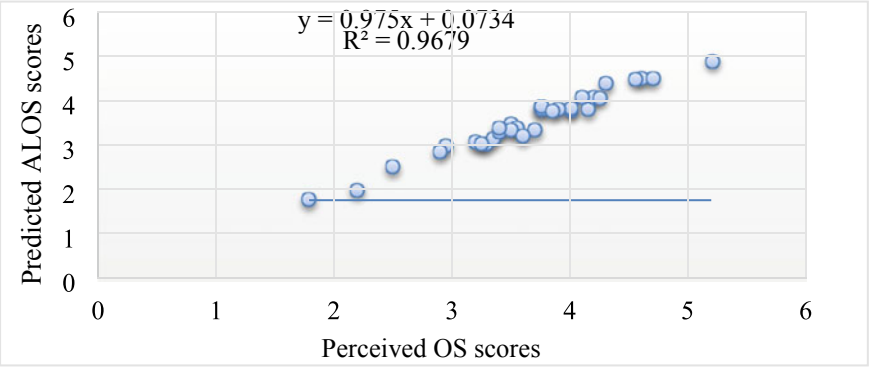

Result Table

S. No.	Segment name Kolkata	LOS(Model)
1	Amherst Street	3.90114 (D)
2	Vivekananda Rd	3.809428 (C)
3	APC Rd	4.062968 (C)
4	VIP Rd	5.113839 (B)
5	Saltlake AB-AC	3.184268 (D)
6	Bhupendra Bose Av	4.211839 (C)
7	CR Avenue	4.38308 (B)
8	Arabinda Sarani	3.493849 (C)
9	SN Banerjee Rd	2.473501 (E)
10	Sealdah	2.959969 (C)

3 Conclusion

The coefficient of determination suggests that the developed model establishes significant relationship between perceived and predicted LOS, also expresses the similarity in the categorization between LOS and AQI. Based on the above analysis, it becomes obvious that by developing the LOS of various roadways, the AQI value can be reduced. Therefore, by factor analysis, major components are categorized to obtain the LOS. Obviously, in the peak hour of traffic volume, the air pollution level also reaches higher. The major components can be developed by the implantation of various strategies over roadways, and it also helps to reduce the pollutants due to vehicular emission.

Limitations

As the factors affecting the AQI parameter is not taken into consideration, thus it can be more accurately analyzed based on such factors affecting the AQI parameter. Therefore, the relationship between AQI and LOS can also established more accurately.

References

1. Highway Capacity Manual (HCM 2000, HCM 2010).
2. Sutaria, Haynes J (1977) Level of service at signalized intersection
3. Mitra B, Sikdar PK, Dhingra SL (1999) Modeling congestion on urban roads and assessing level of service
4. Kita H (2011) Level-of-service measure of road traffic based on the driver's perceptio
5. Pecheux KK (2000) User perception of level of service at signalized intersections: methodological issues
6. Zhang L (2004) Signalized intersection level of service that accounts for user perception
7. Chiaburu M, Diene MS, Dulgheru M, Kendrick B (2010) Assessing the impact of the highway 25 expansion project on air quality in montreal using GIS
8. Amin M, Reza S, Tamima U, Amador Jimenez L (2017) Understanding air pollution from induced traffic during and after the construction of a new highway: case study of highway 25 in Montreal. J Adv Transp 1–14
9. Briggs DJ, de Hoogh K (2000) A regression-based method for mapping traffic-related air pollution: application and testing in four contrasting urban environments
10. Singh RB, Haque MS (2017) Air pollution and human health in Kolkata, India: a case study
11. Guttikunda SK, Goel R, Pant P (2014) Nature of air pollution, emission sources, and management in the Indian cities. Atmos Environ 95:501–510
12. Shrivastava RK, Neeta S, Geeta G (2013) Air pollution due to road transportation in india: a review of assessment and reduction strategies
13. Díaz G, Macià H, Valero V, Boubeta-Puig J, Cuartero F (2018) An intelligent transportation system to control air pollution and road traffic in cities integrating CEP and colored Petri nets

Advent of Graphene Oxide and Carbon Nanotubes in Removal of Heavy Metals from Water: A Review

Satyajit Chaudhuri and Spandan Ghosh

1 Introduction

Water is undoubtedly one of the most basic necessities of all life forms. Rapid urbanization and industrialization have lead to an increasing demand for water, and water scarcity has become a constraint for economic and social advancement. Many natural and artificial factors result in dissolution of heavy metals in water. Heavy metals like arsenic, lead, cadmium, copper, mercury, etc., are known to be toxic and cause multiple medical complicacies in humans in certain concentrations as these metals have a long half life and hence a tendency to bio-accumulate in food chains [1]. Nervous system damages, renal kidney disease, mental retardation, cancer and anemia are few of the diseases that can be caused by heavy metals [2]. Hence, the removal of these heavy metals from the water systems becomes indispensable in making the water potable and palatable. Various methods have been used to separate these heavy meals from water which include co-precipitation, chemical precipitation [3], chemical oxidation or reduction, ion exchange [4], electrochemical treatment, membrane filtration [5], reverse osmosis, extraction [6, 7] and adsorption [8]. Among the techniques available, adsorption has been used extensively owing to its lower cost and higher efficiency (Fig. 1).

Based on the above background, this work reviews the latest development of carbon-based nanomaterials graphene oxide and carbon nanotubes which are used to remove heavy metals from wastewater. Many of the available reviews were all focused on a single kind of nanomaterial, some of which were also outdated and missed the

S. Chaudhuri (✉) · S. Ghosh
Department of Civil Engineering, Indian Institute of Engineering Science and Technology, Shibpur, Howrah, India
e-mail: csatyajit1996@gmail.com

S. Ghosh
e-mail: sgcoolspandan@gmail.com

S. Kumar et al. (eds.), *Sustainability in Environmental Engineering and Science*, Lecture Notes in Civil Engineering 93,
https://doi.org/10.1007/978-981-15-6887-9_24

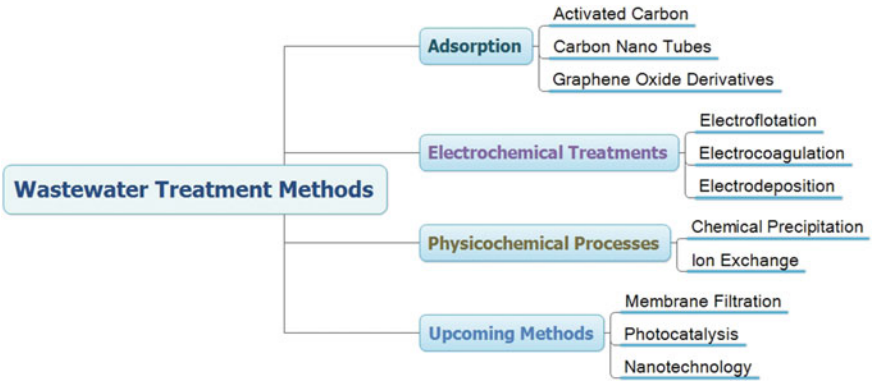

Fig. 1 Wastewater treatment methods

latest developments of nanomaterials for heavy metal treatment. The metals often found dissolved in water and their permissible limits are given in Table 1.

The process of removal of heavy metals by GO and CNTs is adsorption. The heavy metals, i.e., the adsorbates, are adsorbed on the surfaces of these nanomaterials, and hence, this nanomaterials are called as adsorbents. The process of adsorption is studied by knowing the reaction kinetics of the adsorption reaction and the isotherm it follows. Adsorption process is done in one step or in amalgamation of steps, for

Table 1 Various heavy metals dissolved in water and their permissible limits

Parameter (1)	BIS Indian Standards (IS 10500:1991)		World Health Organization guidelines
	Desirable limit (mg/L) (2)	Permissible limit (mg/L) (3)	Maximum allowable (mg/L) concentration (4)
Zinc (as Zn)	5.0	15.0	5.0
Iron (as Fe)	0.3	1.0	0.3
Manganese (asMn)	0.1	0.3	0./1
Copper (as Cu)	0.05	1.5	1.0
Arsenic (as As)	0.05	No relaxation	0.05
Cyanide (as CN)	0.05	No relaxation	0.1
Lead (as Pb)	0.05	No relaxation	0.05
Chromium (as Cr^{6+})	0.05	No relaxation	0.05
Aluminium (as Al)	0.03	0.2	0.2
Cadmium (as Cd)	0.01	No relaxation	0.005
Selenium (as Se)	0.01	No relaxation	0.01
Mercury (as Hg)	0.001	No relaxation	0.001

example pore diffusion, external diffusion, surface diffusion. It was also noted that the adsorption of arsenite and arsenate on the surface of adsorbent continues in three steps: (a) migration (b) dissociation of complexed aqueous [As(III)] and [As(V)], and (c) surface complexation. The process of removal of heavy metals by GO and CNTs is adsorption. The heavy metals, i.e., the adsorbates, are adsorbed on the surfaces of these nanomaterials, and hence, this nanomaterials are called as adsorbents. The process of adsorption is studied by knowing the reaction kinetics of the adsorption reaction and the isotherm it follows (Fig. 2).

2 Carbon Nanotubes

Since their discovery in 1991 by Iijima, carbon nanotubes (CNTs) have been a hot topic of discussion among researchers involved with nanomaterials [9]. The first observed CNTs consisted of up to several tens of graphitic shells with adjacent shell separation of 0.34 nm, diameters of 1 nm and large length/diameter ratio and were called multiwalled carbon nanotubes (MWCNTs) [10]. They can be considered as elongated fullerene [11]. In 1993, smaller diameter, single-walled carbon nanotubes (SWCNTs) were independently discovered by Iijima and Ichihashi [12] and Bethune et al. [13] using arc-discharge method and metal (iron and cobalt) as catalysts. They have received much attention due to their unique properties such as functional, mechanical, thermal, electrical and optoeletronic properties which depend on atomic arrangement, their diameter and length of the tubes along with their morphology and nanostructure [14, 15].

The three mainstream methods of synthesis of CNTs include arc-discharge, laser ablation and chemical vapour deposition (CVD) [16]. Arc-discharge and laser ablation lead to near-perfect nanotube structure with large amount of by-products being formed and are achieved by employing solid state precursors. CVD on the other hand uses hydrocarbon gases as the source of carbon atoms, and to nucleate the growth of the CNT, catalyst particles are used as seeds. Organized patterns of nanotube structures comprising of both SWCNTs and MWCNTs can be produced on surfaces by positioning catalysts seeds in arrayed fashion [17,18]. CNT walls are not reactive, but their fullerene-like tips are known to be more reactive, so end functionalization of CNTs is used relatively often to generate functional group like –COOH, −OH, etc (Fig. 3).

The adsorption properties of CNTs depend on a number of factors, among which the most important being contribution of individual adsorption sites [19]. There are four possible sites in CNT bundles for the adsorption of different groups of pollutants [20, 21], (i) ‘internal sites’—the hollow interior of individual nanotubes (can be accessed only if the caps are removed and the open ends are unblocked); (ii) ‘interstitial channels (ICs)’—the interstitial channels between individual nanotubes in the bundles; (iii) ‘grooves’—here two adjacent parallel tubes meet; (iv) ‘outside surface’—the curved surface of individual nanotubes on the outside of the nanotube bundles.

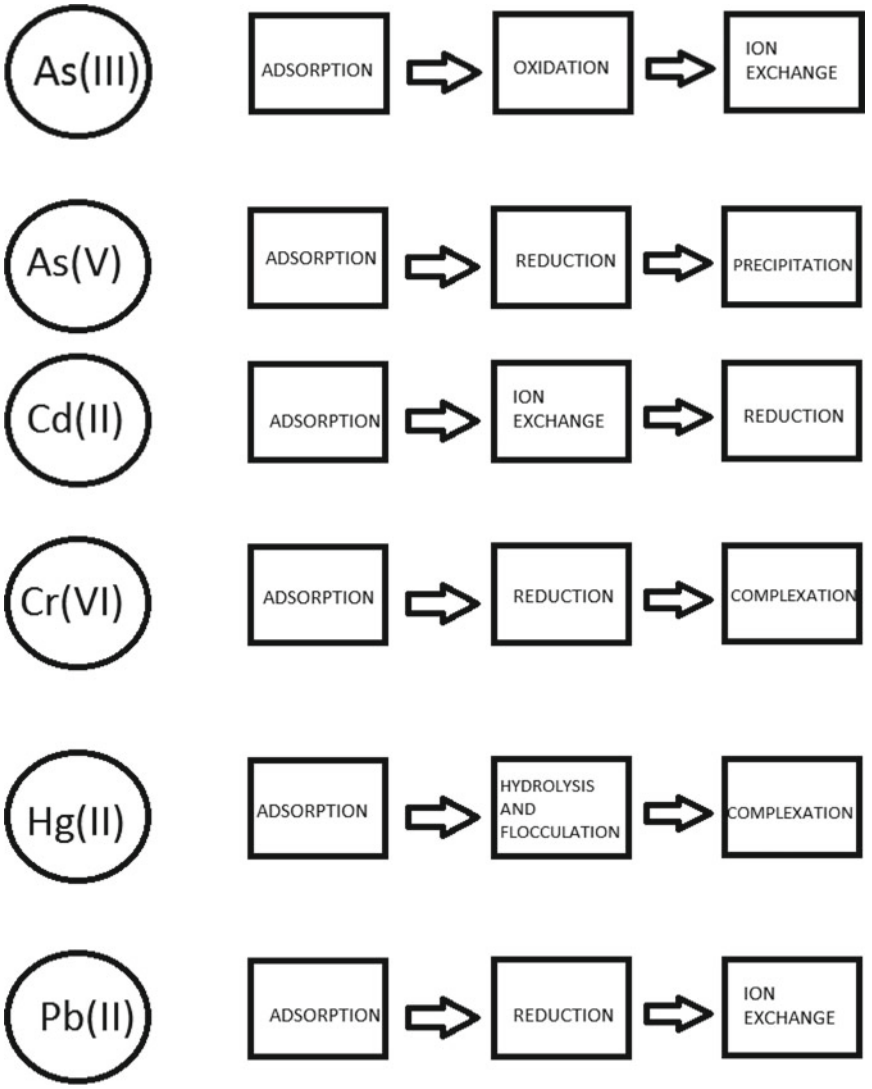

Fig. 2 Removal processes for various heavy metals

The various ambient conditions like temperature and pH. Temperature is a very common parameter affecting physicochemical reactions and has significant impacts on the adsorption of heavy metals. The reaction rate increases with increasing temperature for endothermic reactions and decreases with increasing temperature for exothermic reactions. The pH of the solution affects the ionic forms of heavy metal ions and functionalized nanomaterials, and hence, it is an important parameter

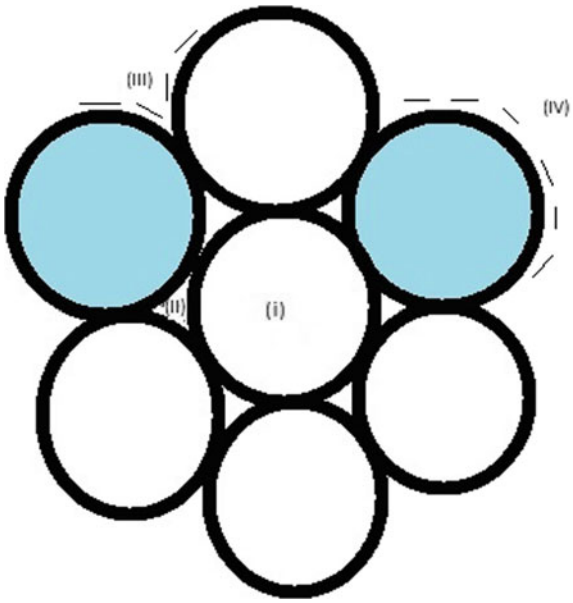

Fig. 3 Different adsorption sites on homogenous bundle of partially open-ended SWCNTs: (i) internal, (ii) interstitial channel, (iii) external groove site and (iv) external surface

for aqueous heavy metal removal. The ionization of the surface acidic groups and charges are also effected by pH values.

The various CNTs that have been synthesised by researchers for removal of heavy metals have been discussed below along with their adsorption capacity of these nanomaterials (Table 2).

3 Graphene Oxide

Graphene has been considered as a promising material for a variety of applications due to its flexibility, large surface area [57], high electrical conductivity, thermal properties [58, 59] and optical and sensory properties [60]. It is two-dimensional carbon nanomaterial comprising a mono-layer of sp2-bonded carbon atoms. Graphene oxide (GO) is formed by oxidation of graphene and contains different oxygen-containing functional groups such as epoxy, hydroxyl and carboxyl [61–63]. It possesses interesting properties including large surface area(), machinability, chemical inertness and hydrophilicity [64–66]. The common method of producing GO involves excessive oxidation of graphite to prepare graphite oxide followed by exfoliation of the product obtained from GO [67]. The presence of the oxygen-containing groups on GO leads to loss of conductivity, but they provide the unique capacity for modification and impregnation of GO [68], and hence, the functionalities of GO sheets can be better utilized [69].

Table 2 Various CNTs and their respective adsorption capacities against target heavy metals

S. No.	Adsorbent	Adsorbate	Maximum adsorption capacity (mg/g)	References
1	CNTs/PAMAM	As(III)	432.00	[22]
2	Iron oxide-MWCNTs	As(III)	1.8	[23]
3	Fe-MWCNTs	As(III) As(V)	210.0 220.0	[24]
4	MIO-MWCNT	As(III) As(V)	17.2 36.3	[25]
5	CNTs	Cd(II)	9.30	[26]
6	As grown CNTs	Cd(II)	1.1–3.5	[27]
7	Oxidized MWCNTs	Cd(II)	10.86	[28]
8	Oxidized CNTs	Cd(II)	75.84	[29]
9	Ethylenediamine functionalized MWCNTs (e-MWCNT)	Cd(II)	101.24	[30]
10	CNTs/PAMAM	Co(II)	494.00	[22]
11	Oxidized CNTs	Co(II)	69.63	[29]
12	AC coated with CNTs	Cr(VI)	9.0	[31]
13	IL-oxi-MWCNTs	Cr(VI)	2.6	[32]
14	CNTs-CeO_2	Cr(VI)	30.2	[33]
15	DBSA-PANI/MWCNTs	Cr(VI)	49.5	[34]
16	AC-CNTs	Cr(VI)	9.0	[31]
17	AA-CNTs	Cr(VI)	142.8	[35]
18	Amino-functionalized Fe_3O_4/MWCNTs	Cu(II)	30.49	[36]
19	CNTs	Cu(II)	27.03	[26]
20	As-produced CNTs	Cu(II)	8.25	[37]
21	Oxidized MWCNTs	Cu(II)	28.49	[27]
22	Oxidized CNTs	Cu(II)	50.37	[29]
23	NaOCl modified CNTs	Cu(II)	47.39	[37]
24	Purified MWCNTs	Cu(II)	37.5	[38]
25	Sulfonated MWCNTs	Cu(II)	59.6	[38]
26	OH-MWCNTs	Cu(II)	7.0	[39]
27	COOH-MWCNTs	Cu(II)	5.5	[39]
28	DESs-CNTs	Hg(II)	186.97	[40]
29	MWCNTs-COOH	Hg(II)	81.6	[41]
30	MWCNTs-OH	Hg(II)	89.4	[41]
31	SWCNTs-SH	Hg(II)	74.2	[42]
32	MWCNTs-iodide	Hg(II)	100.0	[43]

(continued)

Table 2 (continued)

S. No.	Adsorbent	Adsorbate	Maximum adsorption capacity (mg/g)	References
33	MWCNTs-s	Hg(II)	100.0	[43]
34	CNTs-MnO_2	Hg(II)	14.3	[44]
35	$KMnO_4$-DES-CNTs	Hg(II)	187.0	[40]
36	CS-MWCNTs-COOH	Hg(II)	183.2	[45]
37	CS-MWCNTs	Hg(II)	167.5	[45]
38	MWCNTs-Fe_3O_4-SH	Hg(II)	63.7	[46]
39	MWCNTs	Ni(II)	2.9	[47]
40	As-produced CNTs	Ni(II)	18.083	[48]
41	MWCNTs/iron oxides	Ni(II)	9.18	[49]
42	Oxidized CNTs	Ni(II) (aq)	49.261	[48]
43	MWCNTs	Pb(II)	4	[50]
44	CNTs	Pb(II)	62.50	[26]
45	Oxidized MWCNTs	Pb(II)	97.08	[28]
46	Oxidized CNTs	Pb(II)	101.05	[29]
47	Acidified MWCNTs	Pb(II)	85.0	[51]
48	MWCNTs-TiO_2	Pb(II)	4.6	[52]
49	CNTs/Fe_3O_4-NH_2	Pb(II)	37.6	[53]
50	CNTs/Fe_3O_4 -MPTS	Pb(II)	42.1	[46]
51	CNTs/PAMAM	Zn(II)	470.00	[22]
52	SWCNTs	Zn(II)	43.66	[54]
53	Oxidized MWCNTs	Zn(II)	2.0	[55]
54	Oxidized CNTs	Zn(II)	58.00	[29]
55	Purified SWCNTs	Zn(II)	15.4	[56]

The most popular methods for preparation of graphene oxide include Brodie's, Staudenmaier's and Hummer's methods, and all of them include chemical oxidation and subsequent exfoliation of pristine graphite at some stages. Brodie first found that only graphitizable carbons containing regions of graphitic structure could be oxidized to generate graphite oxide (GrO) by using potassium perchlorate and concentrated nitric acid mixture in 1859 [70]. In 1898, Staudenmaier heated a mixture of graphite, sulphuric acid, nitric acid and potassium perchlorate to prepare GrO [71]. Hummers and Offeman prepared GrO by using concentrated sulphuric acid, sodium nitrate and potassium permanganate in 1958, and his method is quite convenient [72]. All these three methods involve chemical oxidation of graphite to various levels and the interlayer distance in GrO increased from 0.34 nm to 0.8–1.0 nm due to intercalation of oxygenous functional groups. This is beneficial for exfoliation of GrO to GO via ultrasonic method or mechanical stirring [73]. The concentration of exfoliated GO in

organic solvents could be up to 1 mg/L while that in water could reach up to 7 mg/L due to hydrophilic oxygenous functional groups on the surface [74] (Table 3).

4 Conclusion

The advancement in the field of nanomaterials has enabled the engineers and the researchers to incorporate a number of functional groups, metals and non-metals in the nanomaterial structures and functionalize them to carry out certain functions. The research works highlighted in this literature review verify this statement. A number of nanomaterials have been synthesized using grapene oxide and carbon nanotube skeletons and have been used to absorb toxic and/or unwanted heavy metals from water. These materials absorb the heavy metals by mono-layer absorption in most cases and have been found to be reusable. The adsorption by graphene oxide follows pseudo-second-order reaction kinetics and Langmuir isotherm. The maximum arsenic removal was seen for GO-$MnFe_2O_4$ with an absorption capacity of 196.0 mg/g among GO derivatives and CNTs/PAMAM with a capacity of 432 mg/g among CNTs. Cadmium ethylenediamine-functionalized MWCNTs shows an adsorption capacity of 101.24 mg/g among CNTs and CNTs/PAMAM (494 mg/g) for cobalt and zinc. For chromium, AA-CNTs (142.8 mg/g adsorption capacity) gives lesser removal efficiency than PPy/α-cyclodextin/GO (666.67 mg/g capacity). L-TRP/GO (capacity 588 mg/g) is quite efficient than its contemporary best performing CNT, namely sulfonated MWCNTs (capacity 59.6 mg/g). For mercury, $KMnO_4$-DES-CNTs (capacity 186.97 mg/g) can be used for effective removal and oxidized CNTs (capacity 49.261 mg/g) for nickel. For lead, oxidized CNTs has 101.05 mg/g adsorption capacity against 1850 mg/g capacity of FGO1. The adsorption capacities are highly dependent on reaction parameters, and hence, the nanomaterials with comparatively lower adsorption capacities can be effective for many heavy metal removal scenarios. A clear line between GO and CNTs cannot be drawn so as to ascertain dominance of one over the other, and hence, selection of the nanomaterial depends on the requirement of the user, and these literature reviews will assist the user to come to a conclusion on which group of nanomaterials to look forward to.

Table 3 Various graphene oxide nanocomposites and their respective adsorption capacities against target heavy metals

S. No.	Adsorbent	Adsorbate	Maximum adsorption capacity (mg/g)	References
1	GO-$MnFe_2O_4$	As(III)	196.0	[75]
2	Fe_3O_4-RGO	As(III)	148	[76]
3	GO-$MnFe_2O_4$	As(V)	196.0	[75]
4	Fe_3O_4-RGO	As(V)	148.0	[76]
5	Mg–Al LDHs/GO	As(V)	35.4	[77]
6	PPy/α-cyclodextin/GO	Cr(VI)	666.67	[78]
7	4PEI/GO	Cr(VI)	539.53	[59]
8	PPy/GO	Cr(VI)	497.10	[79]
9	Chitosan/GO	Cr(VI)	310.40	[80]
10	Fe_3O_4/GO	Cr(VI)	258.6	[81]
11	TOA/EGO	Cr(VI)	232.55	[82]
12	Chitosan/TETA/GO	Cr(VI)	219.50	[83]
13	MCGO-IL	Cr(VI)	145.35	[84]
14	Fe_3O_4 /mTiO_2/GO	Cr(VI)	117.94	[85]
15	MCGN	Cr(VI)	120.19	[86]
16	DCTA/en/MGO	Cr(VI)	80.00	[87]
17	CCGO	Cr(VI)	67.66	[88]
18	Porous Fe_3O_4 hollow microspheres/GO	Cr(VI)	32.33	[89]
19	Chitosan/GO	Cu(II)	423.80	[80]
20	L-TRP/GO	Cu(II)	588.00	[90]
21	Chitosan/GO-SH	Cu(II)	425.00	[91]
22	PAH/GO	Cu(II)	349.03	[92]
23	EDTA/MGO	Cu(II)	301.20	[93]
24	GO1	Cu(II)	294.00	[67]
25	Cross-linked chitosan/GO	Cu(II)	202.50	[68]
26	PVA/CS/GO hydrogel beads	Cu(II)	162.00	[94]
27	PEI/Fe_3O_4/GO	Cu(II)	157.48	[95]
28	GO/CdS(en)	Cu(II)	137.17	[2]
29	GO2	Cu(II)	117.50	[96]
30	GO/PAMAMs	Cu(II)	68.68	[97]
31	SMGO	Cu(II)	62.73	[98]

(continued)

Table 3 (continued)

S. No.	Adsorbent	Adsorbate	Maximum adsorption capacity (mg/g)	References
32	Alginate/GO	Cu(II)	60.24	[99]
33	CSGO	Cu(II)	53.69	[100]
34	GO-SH	Cu(II)	42.30	[101]
35	Amino-SiO_2/GO	Cu(II)	6.00	[102]
36	B-FeOOH/GO	Cu(II)	N/A	[103]
37	Chitosan/GO	Pb(II)	461.30	[104]
38	FGO1	Pb(II)	1850.00	[105]
39	GO	Pb(II)	1119.00	[67]
40	FGO2	Pb(II)	758.00	[106]
41	$MnFe_2O_4$/GO	Pb(II)	673.00	[75]
42	Iron Oxide/GO	Pb(II)	588.24	[107]
43	EDTA/GO	Pb(II)	479.00	[108]
44	Chitosan/GO-SH	Pb(II)	447.00	[91]
45	HPEI/GO	Pb(II)	438.60	[109]
46	MMSP/GO	Pb(II)	333.00	[104]
47	Ag/GO	Pb(II)	312.57	[110]
48	PAS/GO	Pb(II)	312.50	[111]
49	M-CHAP/GO	Pb(II)	277.70	[112]
50	PS/GO	Pb(II)	256.41	[113]
51	L-Trp/GO	Pb(II)	222.00	[90]
52	LS/PANI/GO	Pb(II)	216.40	[114]
53	APTES/GO	Pb(II)	119.05	[111]
54	Chitosan/FeOOH/GO	Pb(II)	111.11	[115]
55	GO-SH	Pb(II)	108.30	[101]
56	Porous Chitosan/GO	Pb(II)	99.00	[116]
57	GO-NH_2	Pb(II)	98.5	[117]
58	MHCGO	Pb(II)	79.30	[118]
59	MCGO	Pb(II)	76.94	[119]
60	Amino-SiO_2/GO	Pb(II)	13.72	[102]
61	EDTA-RGO	Pb(II)	730.0	[108]
62	Ag-$CoFe_2O_4$-GO	Pb(II)	212.7	[120]

References

1. Cheraghi M, Lorestani B, Yousefi N (2009) Effect of waste water on heavy metal accumulation in Hamedan province vegetables. J Bot 5:190–193

2. Jiang T, Yan L, Zhang L (2015) Fabrication of a novel graphene oxide/b-FeOOH composite and its adsorption behavior for copper ions from aqueous solution. J Dalt Trans 44:10448–10456
3. González-Muñoz MJ, Rodríguez MA, Luque S, Álvarez JR (2006) Recovery of heavy metals from metal industry waste waters by chemical precipitation and nanofiltration. J Desalination 200:742–744
4. Verbych S, Hilal N, Sorokin G, Leaper M (2004) Ion exchange extraction of heavy metal ions from wastewater. J Separat Sci Technol 39:2031–2040
5. Sudilovskiy PS, Kagramanov GG, Trushin AM, Kolesnikov VA (2007) Use of membranes for heavy metal cationic wastewater treatment: flotation and membrane filtration. J Clean Technol Environ. Policy 9:189–198
6. Liu L, Li C, Bao C (2012) Preparation and characterization of chitosan/graphene oxide composites for the adsorption of Au(III) and Pd(II). Talanta 93:350–357
7. Erturk U, Yerlikaya C, Sivritepe N (2007) In vitrophytoextraction capacity of blackberry for copper and zinc. J Asian Chem 19:2161–2168
8. Khan NA, Hasan Z, Jhung SH (2013) Adsorptive removal of hazardous materials using metal-organic frameworks (MOFs): a review. J Hazard Mater 244–245:444–456
9. Iijima S (1991) Helical microtubules of graphitic carbon. J Nature 354:56–58
10. Popov VN (2004) Carbon nanotubes: properties and application. J Mater Sci Eng R 43:61–102
11. Endo M, Kroto HW (1992) Formation of carbon nanofibers. J Phys Chem 96:6941–6944
12. Iijima, S, Ichihashi T (1993) Single-shell carbon nanotubes of 1-nm diameter. Nature 363(6430):603–605
13. Bethune DS, Kiang CH, De Vries MS, Gorman G, Savoy R, Vazquez J, Beyers R (1993) Cobalt-catalysed growth of carbon nanotubes with single-atomic-layer walls. Nature 363 (6430):605–607
14. Thostenson ET, Ren ZF, Chou TW (2001) Advances in the science and technology of carbon nanotubes and their composites: a review. J Compos Sci Technol 61:1899–1912
15. Avouris P (2002) Molecular electronics with carbon nanotubes. J Acc Chem Res 35:1026–1034
16. Dai H (2001) Nanotube growth and characterization. J Carbon Nanotubes. Springer, Berlin, Germany
17. Kong J, Soh HT, Cassell, AM, Quate CF, Dai H (1998) Synthesis of individual single-walled carbon nanotubes on patterned silicon wafers. Nature 395(6705):878–881
18. Fan S (1999) Self-Oriented regular arrays of carbon nanotubes and their field emission properties. Sci 283(5401):512–514
19. Agnihotri S, Mota JPB, Rostam-Abadi M, Rood MJ (2006) Theoretical and experimental investigation of morphology and temperature effects on adsorption of organic vapors in single-walled carbon nanotubes. J Phys Chem B 110:7640–7647
20. Agnihotri S, Mota JPB, Rostam-Abadi M, Rood MJ (2005) Structural characterization of single-walled carbon nanotube bundles by experiment and molecular simulation. J Lang 21:896–904
21. Gatica SM, Bojan MJ, Stan G, Cole MW (2001) Quasi-one-dimensional and two-dimensional transitions of gases adsorbed on nanotube bundles. J Chem Phys 114:3765–3769
22. Hayati B, Maleki A, Najafi F, Gharibi F, Mckay G, Gupta VK, Marzban N (2018) Heavy metal adsorption using PAMAM/CNT nanocomposite from aqueous solution in batch and continuous fixed bed systems. J Chem Eng 346:258–270
23. Tawabini BS, Al-Khaldi SF, Khaled MM, Atieh MA (2011) Removal of arsenic from water by iron oxide nanoparticles impregnated on carbon nanotubes. J Environ Sci Health A 46:215–223
24. Alijani H, Shariatinia Z (2017) Effective aqueous arsenic removal using zero valent iron doped MWCNT synthesized by in situ CVD method using natural α-Fe_2O_3 as a precursor. J Chemosphere 171:502–511
25. Chen B, Zhu Z, Ma J, Yang M, Hong J, Hu X, Qiu Y, Chen J (2014a) One-pot, solid-phase synthesis of magnetic multiwalled carbon nanotube/iron oxide composites and their application in arsenic removal. J Colloid Interface Sci 434:9–17

26. Hsieh SH, Horng JJ, Tsai CK (2006) Growth of carbon nanotube on micro-sized Al_2O_3 particle and its application to adsorption of metal ions. J Mater Res 21:1269–1273
27. Li YH, Ding J, Lun Z, Di Z, Zhu Y, Xu C, Wu D, Wei B (2003) Competitive adsorption of Pb^{2+}, Cu^{2+} and Cd^{2+} ions from aqueous solutions by multiwalled carbon nanotubes. Carbon 41:2787–2792
28. Li YH, Wang SW, Luan ZL, Ding JD, Xu C, Wu D (2003) Adsorption of cadmium (II) from aqueous solution by surface oxidized carbon nanotubes. Carbon 41:1057–1062
29. Tofighy MA, Mohammadi T (2011) Adsorption of divalent heavy metal ions from water using carbon nanotube sheets. J Hazard Mater 185:140–147
30. Vukovic GD, Marinkovic AD, Colic M, Ristic MD, Aleksic R, Grujic AAP, Uskokovic PS (2010) Removal of cadmium from aqueous solutions by oxidized and ethylenediamine-functionalized multi-walled carbon nanotubes. J Chem Eng 57:238–324
31. Atieh MA (2011) Removal of chromium (VI) from polluted water using carbon nanotubes supported with activated carbon. J Proc Env Sci 4:281–293
32. Kumar ASK, Jiang S, Tseng W (2015) Effective adsorption of chromium(vi)/Cr(iii) from aqueous solution using ionic liquid functionalized multiwalled carbon nanotubes as a super sorbent. J Mater Chem A 3:7044–7057
33. Di, ZC, Ding J, Peng XJ, Li YH, Luan ZK, Liang, J (2006) Chromium adsorption by aligned carbon nanotubes supported ceria nanoparticles. Chemosphere 62(5):861–865
34. Kumar ASK, Kakan SS, Rajesh N (2013) A novel amine impregnated graphene oxide adsorbent for the removal of hexavalent chromium. J Chem Eng 230:328–337
35. Sankararamakrishnan N, Jaiswal M, Verma N (2014) Composite nanofloral clusters of carbon nanotubes and activated alumina: an efficient sorbent for heavy metal removal. J.Chem Eng 235:1–9
36. Zhan Y, Hai H, Yi H, Long Z, Wan X, Zeng G (2016) Novel amino-functionalized Fe_3O_4/carboxylic multi-walled carbon nanotubes: one-pot synthesis, characterization and removal for Cu(II). J Russ Appl Chem 89:1894–1902
37. Wu CH (2007) Studies of the equilibrium and thermodynamics of the adsorption of Cu^{2+} onto as-produced and modified carbon nanotubes. J Coll Interf Sci 311(2):338–346
38. Ge Y, Li Z, Xiao D, Xiong P, Ye N (2014) Sulfonated multi-walled carbon nanotubes for the removal of copper (II) from aqueous solutions. J Ind Eng Chem 20:1765–1771
39. Rosenzweig S, Sorial GA, Sahle-Demessie E, Mack J (2013) Effect of acid and alcohol network forces within functionalized multiwall carbon nanotubes bundles on adsorption of copper (II) species. J Chemosphere 90:395–402
40. Alomar MK, Alsaadi MA, Hayyan M, Akib S, Ibrahim M, Hashim MA (2017) Allyltriphenylphosphonium bromide based DES-functionalized carbon nanotubes for the removal of mercury from water. J Chemosphere 167:44–52
41. Chen PH, Hsu C, Tsai DD, Lu Y, Huang W (2014) Adsorption of mercury from water by modified multi-walled carbon nanotubes: adsorption behaviour and interference resistance by coexisting anions. J Environ Technol 35:1935–1944
42. Bandaru NM, Reta N, Dalal H, Ellis AV, Shapter J, Voelcker NH (2013) Enhanced adsorption of mercury ions on thiol derivatized single wall carbon nanotubes. J Hazard Mater 261:534–541
43. Gupta A, Vidyarthi SR, Sankararamakrishnan N (2014) Enhanced sorption of mercury from compact fluorescent bulbs and contaminated water streams using functionalized multiwalled carbon nanotubes. J Hazard Mater 274:132–144
44. Moghaddam HK, Pakizeh M (2015) Experimental study on mercury ions removal from aqueous solution by MnO_2/CNTs nanocomposite adsorbent. J Ind Eng Chem 21:221–229
45. Shawky HA, El-Aassar AHM, Abo-Zeid DE (2012) Chitosan/carbon nanotube composite beads: Preparation, characterization, and cost evaluation for mercury removal from wastewater of some industrial cities in Egypt. J Appl Polym Sci 125(S1):E93–E101
46. Zhang C, Sui J, Li J, Tang Y, Cai W (2012) Efficient removal of heavy metal ions by thiol-functionalized superparamagnetic carbon nanotubes. J Chem Eng 210:45–52

47. Yang S, Li J, Shao D, Hu J, Wang X (2009) Adsorption of Ni(II) on oxidized multi-walled carbon nanotubes: effect of contact time, pH, foreign ions and PAA. J Hazard Mater 166:109–116
48. Kandah MI, Meunier JL (2007) Removal of nickel ions from water by multi-walled carbon nanotubes. J Hazard Mater 146:283–288
49. Chen CL, Hu J, Shao DD, Li JX, Wang XK (2009a) Adsorption behavior of multiwall carbon nanotube/iron oxide magnetic composites for Ni(II) and Sr(II). J Hazard Mater 164:923–928
50. Wang H, Zhou A, Peng F, Yu H, Yang, J (2007) Mechanism study on adsorption of acidified multiwalled carbon nanotubes to Pb(II). J Colloid Interface Sci 316(2):277–283
51. Wang HJ, Zhou AL, Peng F, Yu H, Chen LF (2007) Adsorption characteristic of acidified carbon nanotubes for heavy metal Pb(II) in aqueous solution. J Mater Sci Eng A 466(1–2):201–206
52. Zhao X, Jia Q, Song N, Zhou W, Li, Y (2010) Adsorption of Pb(II) from an Aqueous Solution by Titanium Dioxide/Carbon Nanotube Nanocomposites: Kinetics, Thermodynamics, and Isotherms. J Chem Eng Data 55(10):4428–4433
53. Ji L, Zhou L, Bai X, Shao Y, Zhao G, Qu Y, Wang C, Li Y (2012) Facile synthesis of multiwall carbon nanotubes/iron oxides for removal of tetrabromobisphenol A and Pb(ii). J Mater Chem 22:15853–15862
54. Long QR, Yang RT (2001) Carbon nanotubes as superior sorbent for dioxin removal. J Am Chem Soc 123:2058–2059
55. Mubarak NM, Alicia RF, Abdullah EC, Sahu JN, Haslija ABA, Tan J (2013) Statistical optimization and kinetic studies on removal of Zn^{2+} using functionalized carbon nanotubes and magnetic biochar. J Environ Chem Eng 1:486–495
56. Lu C, Chiu H, Liu C (2006) Removal of Zinc(II) from aqueous solution by purified carbon nanotubes: kinetics and equilibrium studies. J Ind Eng Chem Res 45:2850–2855
57. Zhu J, Sadu R, Wei S, Chen DH, Haldolaarachchige N, Guo Z (2012) Magnetic graphene-nanoplatelet composites toward arsenic removal. J ECS Sol Sta Sci Tech 1(1):M1-M5
58. Porwal H, Tatarko P, Grasso S, Hu C, Boccaccini AR, Dlouhý I, Reece MJ (2013) Toughened and machinable glass matrix composites reinforced with graphene and graphene-oxide nano platelets. J Sci Tech Adv Mat 14(5):055007
59. Chen JH, Xing HT, Guo HX (2014) Investigation on the adsorption properties of Cr(VI) ions on a novel graphene oxide (GO) based composite adsorbent. J Mater Chem A 2:12561–12570
60. Namvari M, Namazi H (2015) Preparation of efficient magnetic biosorbents by clicking carbohydrates onto graphene oxide. J Mater Sci 50:5348–5361
61. Hadi Najafabadi H, Irani M, Rad LR (2015) Removal of Cu^{2+}, Pb^{2+} and Cr^{6+} from aqueous solutions using a chitosan/graphene oxide composite nanofibrous adsorbent. J RSC Adv 5:16532–16539
62. Wei H, Zhu J, Wu S (2013) Electrochromicpolyaniline/graphite oxide nanocomposites with endured electro-chemical energy storage. J Polymer (Guildf) 54:1820–1831
63. Chen R, Zhao T, Tian T, Cao S, Coxon PR, Xi K, Cheetham AK (2014) Graphene-wrapped sulfur/metal organic framework-derived microporous carbon composite for lithium sulfur batteries. J APL Mat 2(12):124109
64. Kamali AR, Fray DJ (2013) Molten salt corrosion of graphite as a possible way to make carbon nanostructures. Carbon 56:121–131
65. Parmar KR, Patel I, Basha S, Murthy ZVP (2014) Synthesis of acetone reduced graphene oxide/Fe_3O_4 composite through simple and efficient chemical reduction of exfoliated graphene oxide for removal of dye from aqueous solution. J Mater Sci 49:6772–6783
66. Huang LJ, Wang YX, Tang JG, Wang Y, Liu JX, Huang Z, Belfiroe LA (2015) A new graphene nanocomposite to improve the electrochemical properties of magnesium-based amorphous alloy. J Mat Lett 160:104–108
67. Sitko R, Turek E, Zawisza B, Malicka E, Talik E, Heimann J, Wrzalik R (2013) Adsorption of divalent metal ions from aqueous solutions using graphene oxide. J Dalt Trans 42(16):5682–5689

68. Yang J, Wu J, Lu Q, Lin T (2014) Facile preparation of lignosulfonate–graphene oxide–polyaniline ternary nanocomposite as an effective adsorbent for Pb(II) ions. J ACS Sustain Chem Eng 2:1203–1211
69. Wang Y, He Q, Qu H, Zhang X, Guo J, Zhu J, Bhana S (2014) Magnetic graphene oxide nanocomposites: nanoparticles growth mechanism and property analysis. J Mater Chem C 2(44):9478–9488
70. Brodie BC, Philos BC (1859) On the atomic weight of graphite. Trans R Soc London 149(1859):249
71. Staudenmaier L (1898) Verfahrenzurdarstellung der graphitsäure. Berichte der deutschen-chemischen Gesellschaft 31(2):1481–1487
72. Hummers WS Jr, Offeman RE (1958) Preparation of graphitic oxide. J ACS 80(6):1339
73. Zhu Y, Murali S, Cai W, Li X, Suk JW, Potts JR, Ruoff RS (2010) Graphene and graphene oxide: synthesis, properties, and applications. J Adv Mat 22(35):3906–3924
74. Johnson DW, Dobson, BP, Coleman, KS (2015) A manufacturing perspective on graphene dispersions. Curr Opin Colloid Interface Sci 20(5–6):367–382
75. Kumar S, Nair RR, Pillai PB (2014) Graphene oxide-$MnFe_2O_4$ magnetic nanohybrids for efficient removal of lead and arsenic from water. J ACS Appl Mater Interfaces 6:17426–17436
76. Chandra V, Park J, Chun Y, Lee JW, Hwang IC, Kim KS (2010) Water-Dispersible Magnetite-Reduced Graphene Oxide Composites for Arsenic Removal. ACS Nano 4(7):3979–3986
77. Wen T, Wu X, Tan X, Wang X, Xu A (2013) One-Pot Synthesis of Water-Swellable Mg–Al Layered Double Hydroxides and Graphene Oxide Nanocomposites for Efficient Removal of As(V) from Aqueous Solutions. ACS Appl Mater Interfaces 5(8):3304–3311
78. Chauke VP, Maity A, Chetty A (2015) High-performance towards removal of toxic hexavalent chromium from aqueous solution using graphene oxide-alpha cyclodextrin-poly-pyrrole nanocomposites. J Mol Liq 211:71–77
79. Li S, Lu X, Xue Y (2012) Fabrication of poly-pyrrole/graphene oxide composite nanosheets and their applications for Cr(VI) removal in aqueous solution. J. PLoS ONE 7:43328
80. Najafabadi HH, Irani M, Rad LR, Haratameh, AH, Haririan I (2015) Correction: Removal of Cu, Pb and Cr from aqueous solutions using a chitosan/graphene oxide composite nanofibrous adsorbent. RSC Adv 5(29):22390–22390
81. Lei Y, Chen F, Luo Y, Zhang L (2014) Three-dimensional magnetic graphene oxide foam/Fe_3O_4 nanocomposite as an efficient absorbent for Cr(VI) removal. J Mater Sci 49:4236–4245
82. Kumar R, Ansari MO, Barakat MA (2013) DBSA doped polyaniline/multi-walled carbon nanotubes composite for high efficiency removal of Cr(VI) from aqueous solution. J Chem Eng 228:748–755
83. Ge H, Ma Z (2015) Microwave preparation of tri-ethylenetetramine modified graphene oxide/chitosan composite for adsorption of Cr(VI). J Carbohydr Polym 131:280–287
84. Li L, Luo C, Li X (2014) Preparation of magnetic ionic liquid/chitosan/graphene oxide composite and application for water treatment. J Int J Biol Macromol 66:172–178
85. Li L, Duan H, Wang X, Luo C (2014) Adsorption property of Cr(VI) on magnetic mesoporous titanium dioxide–graphene oxide core–shell microspheres. J New Chem 38:6008–6016
86. Fan L, Luo C, Sun M, Qiu H (2012) Synthesis of graphene oxide decorated with magnetic cyclodextrin for fast chromium removal. J Mater Chem 22:24577–24583
87. Guo F, Liu Y, Wang H (2015) Adsorption behavior of Cr(VI) from aqueous solution onto magnetic graphene oxide functionalized with 1,2-diaminocyclohexanetetraacetic acid. RSC Adv 5:45384–45392
88. Li L, Fan L, Sun M (2013) Adsorbent for hydroquinone removal based on graphene oxide functionalized with magnetic cyclodextrin-chitosan. J Int Biol Macromol 58:169–175
89. Tzu T, Tsuritani T, Sato K (2013) Sorption of Pb(II), Cd(II), and Ni(II) toxic metal ions by alginate-bentonite. J Environ Prot (Irvine, Calif) 4:51–55
90. Tan M, Liu X, Li W, Li H (2015) Enhancing sorption capacities for copper(II) and lead(II) under weakly acidic conditions by L-tryptophan-functionalized graphene oxide. J Chem Eng Data 60:1469–1475

91. Li L, Wang Z, Ma P (2015) Preparation of polyvinyl alcohol/chitosan hydrogel compounded with graphene oxide to enhance the adsorption properties for Cu(II) in aqueous solution. J Polym Res 22:150
92. Xing HT, Chen JH, Su X (2015) NH_2-rich polymer/graphene oxide use as a novel adsorbent for removal of Cu(II) from aqueous solution. J Chem Eng 263:280–289
93. Cui L, Wang Y, Gao L (2015) EDTA functionalized magnetic graphene oxide for removal of Pb(II), Hg(II) and Cu(II) in water treatment: adsorption mechanism and separation property. J Chem Eng 281:1–10
94. Li X, Zhou H, Wu W et al (2015) Studies of heavy metal ion adsorption on chitosan/sulfydryl-functionalized graphene oxide composites. J Colloid Interface Sci 448:389–397
95. Sui N, Wang L, Wu X (2015) Polyethylenimine modified magnetic graphene oxide nanocomposites for Cu^{2+} removal. RSC Adv 5:746–752
96. Wu W, Yang Y, Zhou H (2012) Highly efficient removal of Cu(II) from aqueous solution by using graphene oxide. J Water Air Soil Pollut 224:1372
97. Zhang F, Wang B, He S, Man R (2014) Preparation of graphene-oxide/polyamidoamine dendrimers and their adsorption properties toward some heavy metal ions. J Chem Eng Data 59:1719–1726
98. Hu XJ, Liu YG, Wang H (2013) Removal of Cu(II) ions from aqueous solution using sulfonated magnetic graphene oxide composite. J Sep Purif Technol 108:189–195
99. Algothmi WM, Bandaru NM, Yu Y (2013) Alginate-graphene oxide hybrid gel beads: an efficient copper adsorbent material. J Colloid Interface Sci 397:32–38
100. Wang Y, Liu X, Wang H (2014) Microporous spongy chitosan monoliths doped with graphene oxide as highly effective adsorbent for methyl orange and copper nitrate ($Cu(NO_3)_2$) ions. J Colloid Interface Sci 416:243–251
101. Sitko R, Janik P, Zawisza B, Talik E, Margui E, Queralt I (2015) Green approach for ultratrace determination of divalent metal ions and arsenic species using total-reflection X-ray fluorescence spectrometry and mercapto-modified graphene oxide nanosheets as a novel adsorbent. J Anal Chem 87(6):3535–3542
102. Sitko R, Zawisza B, Talik E, Janik P, Osoba G, Feist B, Malicka E (2014) Spherical silica particles decorated with graphene oxide nanosheets as a new sorbent in inorganic trace analysis. J Anal Chim Acta 834:22–29
103. Jiang T, Liu W, Mao Y (2015) Adsorption behavior of copper ions from aqueous solution onto graphene oxide–CdS composite. J Chem Eng 259:603–610
104. Wang Y, Liang S, Chen B et al (2013) Synergistic removal of Pb(II), Cd(II) and humic acid by Fe_3O_4 @ mesoporous silica–graphene oxide composites. J PLoS ONE 8:2–9
105. Zhao G, Ren X, Gao X (2011) Removal of Pb(II) ions from aqueous solutions on few-layered graphene oxide nanosheets. J Dalt Trans 40:10945–10952
106. Jia W, Lu S (2014) Few-layered graphene oxides as superior adsorbents for the removal of Pb(II) ions from aqueous solutions. J Korean Chem Eng 31:1265–1270
107. Yang X, Chen C, Li J et al (2012) Graphene oxide-iron oxide and reduced graphene oxide-iron oxide hybrid materials for the removal of organic and inorganic pollutants. RSC Adv 2:8821
108. Madadrang CJ, Kim HY, Gao G et al (2012) Adsorption behavior of EDTA-graphene oxide for Pb(II) removal. J ACS Appl Mater Interfaces 4:1186–1193
109. Liu Y, Xu L, Liu J et al (2016) Graphene oxides cross-linked with hyper branched polyethylenimines: preparation, characterization and their potential as recyclable and highly efficient adsorption materials for lead(II) ions. J Chem Eng 285:698–708
110. Gari VRDK, Kim M (2015) Removal of Pb(II) using silver nanoparticles deposited graphene oxide: equilibrium and kinetic studies. J Monatshefte fur Chemie 146:1445–1453
111. Luo S, Xu X, Zhou G et al (2014) Amino siloxane oligomer-linked graphene oxide as an efficient adsorbent for removal of Pb(II) from wastewater. J Hazard Mater 274:145–155
112. Cui L, Wang Y, Hu L et al (2015) Mechanism of Pb(II) and methylene blue adsorption onto magnetic carbonate hydroxyapatite/graphene oxide. RSC Adv 5:9759–9770
113. Zhou G, Liu C, Tang Y et al (2015) Sponge-like polysiloxane-graphene oxide gel as a highly efficient and renewable adsorbent for lead and cadmium metals removal from wastewater. J Chem Eng 280:275–282

114. Yang Y, Wu WQ, Zhou HH (2014) Adsorption behavior of cross-linked chitosan modified by graphene oxide for Cu(II) removal. J Cent South Univ 21:2826–2831
115. Shabnam S, Nematzadeh SSMA, Ashori A (2015) Preparation of graphene oxide/chitosan/FeOOH nanocomposite for the removal of Pb(II) from aqueous solution. J Int Biol Macromol 80:475–480
116. He YQ, Zhang NN, Wang XD (2011) Adsorption of graphene oxide/chitosan porous materials for metal ions. J Chin Chem Lett 22:859–862
117. Sitko R, Janik P, Feist B, Talik E, Gagor A (2014) Suspended aminosilanized graphene oxide nanosheets for selective preconcentration of lead ions and ultrasensitive determination by electrothermal atomic absorption spectrometry. J ACS Appl Mat Int 6(22):20144–20153
118. Wang Y, Yan T, Gao L, Cui L, Hu L, Yan L, Wei Q (2016) Magnetic hydroxypropyl chitosan functionalized graphene oxide as adsorbent for the removal of lead ions from aqueous solution. J Desal Wat Treat 57(9):3975–3984
119. Fan L, Luo C, Sun M, Li X, Qiu H (2013) Highly selective adsorption of lead ions by water-dispersible magnetic chitosan/graphene oxide composites. J Col Surf B Bio 103:523–529
120. Ma S, Zhan S, Jia Y, Zhou Q (2015) Highly efficient antibacterial and Pb(II) removal effects of Ag-CoFeO-GO nanocomposite. ACS Appl Mater Interfaces 7(19):10576–10586

Removal of Arsenic V^+ contaminant by Fixed Bed Column Study by Graphene Oxide Manganese Iron (GO-Mn-Fe) Nano Composite-Coated Sand

Spandan Ghosh, Soumya Kanta Ray, and Chanchal Majumder

1 Introduction

Arsenic-contaminated groundwater is now a severe problem which affected thousands of people across the world. Arsenic is found in both organic and inorganic forms. Arsenic exhibits some toxicological and carcinogenic property in human body [1]. The higher arsenic (0.05–0.3 mg/L) contamination groundwater exists in Bangladesh and West Bengal. Some distinct cases it can reach up to 3 mg/L. It was found that around 60 million people are drinking groundwater containing arsenic more than 0.01 ppm [2]. Long-time intake of highly concentrated water leads to serious health damage like skin cancer, melanosis, keratosis, cardiovascular disease, anaemia, lung cancer, etc. 3–6]. Three basic minerals namely realgar (arsenic disulphide), orpiment (arsenic trisulphide) and arsenopyrite (ferrous arsenic sulphide) are found in the environment. The metalloid of Arsenic is found in valence state of −3, 0, +3 and +5 and are responsible for groundwater arsenic contamination [7]. The groundwater is contaminated with reduced arsenite [As(III)] and oxidized arsenate [As (V)]. The arsenic dose in groundwater was reduced to 0.01 ppm by World Heath Organization (WHO) [8]. Oxyanions of As (V) are found in four different species: H_3AsO_4 at pH <2, $H_2AsO_4^-$ at pH 3–6, $HAsO_4^{2-}$ at pH 8–10 and AsO_4^{3-} at pH >12 [9]. The toxicity of inorganic arsenic is more than 100 times from organic arsenic, and arsenic (III) is more than 60–80 times from arsenic (V) [10]. Many industrial

S. Ghosh (✉) · S. Kanta Ray · C. Majumder
Department of Civil Engineering, Indian Institute of Engineering Science and Technology, Shibpur, Howrah, India
e-mail: sgcoolspandan@gmail.com

S. Kanta Ray
e-mail: ray.soumya5@gmail.com

C. Majumder
e-mail: chanchal@civil.iiests.ac.in

S. Kumar et al. (eds.), *Sustainability in Environmental Engineering and Science*, Lecture Notes in Civil Engineering 93,
https://doi.org/10.1007/978-981-15-6887-9_25

wastewaters contain large amount of arsenic (1000 mg/L) which is a major issue specially in developing country like India. This inorganic arsenic exhibits toxicity due to accumulation in human cell [11]. Numerous methods have been improvised to remove As (V) such as adsorption, oxidation, ion exchange, reverse osmosis and co-precipitation. Out of the process, adsorption is most effective due to its environmentally friendly, low cost and high efficiency. But adsorption process also has some limitations. Adsorption process could not give good status in commercial levels because lack of commercial graded column [12]. Some adsorbents are not suitable for removal of different types of water pollutant. Various researchers are developed many adsorbents such as surfactants, activated carbon and ferrous material [13]. To increase the efficiency of adsorption, nano materials are introduced. Macro particles comprise intra-particle diffusion which reduces adsorption capacity, whereas nanoparticles have small diffusion resistance which increase the adsorption efficiency [14]. Due to some properties of nano materials such as large specific surface area, small size, high reactivity, catalytic potential, easy separation, nano materials are useful for removal of arsenic.

2 Materials and Methods

Synthesis of GO and fRGO: GO was synthesized from graphite powder via Hummers method [15]. Batch synthesis was done by Hummer's method with graphite powder (5.0 g) and $NaNO_3$ (2.5 g). This mixture was poured into a borosil glass beaker of volume 1.2 L and emerged by 120 mL of conc. H_2SO_4 (95%). This suspension stirring for 30 min by magnetic stirrer and put into an ice bath. After homogeneous mixing, potassium permanganate ($KMnO_4$) (15.0 g) was poured to the mixture into beaker very carefully. The overall temperature of mixture is maintained at 20 °C. After 1 h vigorous mixing of the mixture, that solution was turned to light brown colour. After another 1 h. stirring, the temperature of solution becomes raised to 98 °C with external heating arrangement, and 150 mL of H_2O was poured dropwise and observed an effervescence. The fumes inside from solution were stopped, and the temperature was downed to 20 °C in a water bath. The reaction was stopped by 450 mL of H_2O was mixed to stop the oxidation. A 15 mL aliquot of 30% H_2O_2 was mixed to the reaction, and the colour turned into yellow [16]. Iron was added in the GO solution in such a way that C-Mn: Fe 1:3. The pH of the solution is then raised to 7 to form hydroxide precipitate with C-Mn nano composite. The mixture was then filtered, washed several times with DI and dried and kept in vacuum desiccator.

GO-Mn-Fe nano composite is not directly used at field because of its less hydraulic conductivity. Due to its very small size and less porosity, water is not passed through this material. To minimize this problem, supporting material is used which is relatively larger in size. Many researchers use sand as a supporting material because of its relatively high porosity.

Ennore sand with particle size that passing through 2 mm and retained 1 mm is collected and washed with 10% HCL and DI water to remove the impurity. About

150 ml of GO-Mn-Fe solution (concentration 20 mg/ml) is added on 250 gm ennore sand and heated at 400 °C so that H_2SO_4 is decomposed to H_2O and SO_3. It is then cooled into room temperature and stored for further use (Photos 1 and 2).

Photo 1 Fresh ennore sand

Photo 2 Go-Mn-Fe-coated ennore sand

3 Material Characterization

Scanning Electron Microscopy (SEM): Scanning electron microscopy (SEM) (HITACHI S-3400 N) attached with 15 kV power source was used for characterizing the morphology of the GO-Mn-Fe nano composite particles. EDAX facility (EMAX) was mounted with SEM to understand the elemental composition of the material.

Atomic Force Microscopy (AFM): Atomic force microscope (AFM) of VEECO DICP-II model no. AP0100, USA California, is used in air by tapping mode. Ambient surrounding is recording in laboratory of Atomic Force Microscopy (AFM), the temperature ~20–22 °C and relative humidity ~30%. Rectangular Si cantilevers are retained with a spring constant of ~50 N m^{-1} and a resonance frequency of ~200–300 kHz. Spin casting method is performed on a silicon wafer as a substrate for GO-Mn-Fe nano composite dispersion of deionized (DI) water and Dimethylformamide (DMF) co-solvents and is dried at 27 °C for 30 min.

Brunauer–Emmett–Teller (BET): Brunauer–Emmett–Teller (BET) measurement is done by Quantachrome Autosorb 1 instrument at 77 K through N_2 adsorption–desorption method. The pore size and pore structure are analysed by Surface Area Analyzer Beckman Coulter SA 3100.

4 Packed Bed Column Study

Dynamic column studies were done in a glass column of diameter and 15 cm height. The desired flow rate was to maintain by a peristaltic pump. 5 cm thick glass wool was placed in the bottom side to prevent any loss of adsorbent and was to give mechanical support to adsorbent bed. Total experiment was carried out at room temperature. Samples are collected in a gap of every half an hour from the bottom of the column and were determined to know the As (V) concentration. The column performance was investigated by calculating the breakthrough time and adsorption capacity. Adsorption capacity at 15% breakthrough was calculated according to

$$q_B = \frac{X_B}{m_{\text{adsorbent}}} \tag{1}$$

where X_B is mass of As (V) adsorbed in the column at breakthrough (mg), $m_{\text{adsorbent}}$ is mass of adsorbent in column (g).

5 Desorption Study

Regeneration or desorption of adsorbent is very vital to decrease the cost. After the adsorption process, the adsorbent gets exhausted. So, for reuse of adsorbent, regeneration is important. For desorption study, batch experiments were performed at different pH values. To study effect of pH on desorption study, five different solutions of pH values ranging 3–11 are prepared. Then, 5 g of adsorbents are added to 100 mL of distilled water. The samples were then shaken at 150 rpm for 6 h in a shaker. The samples were then filtered, and the arsenic concentration of effluent was measured

6 Results and Discussions

6.1 Material Characterization

6.1.1 Scanning Electron Microscopy (SEM)

The shining image of GO-Mn-Fe nanoparticles is changed to glossy-dull image after enlarging. The surfaces of nanoparticle globules are rough with surface protuberances with the approximate size of five micrometers by scanning electron microscopy (SEM) [1, 16, 17]. The elemental composition shows the presence of carbon (C), oxygen (O) and iron (Fe), manganese (Mn) in GO-Mn-Fe nano material. Remaining amount of iron is leached through washing of nano material by DI water [16] (Fig. 1).

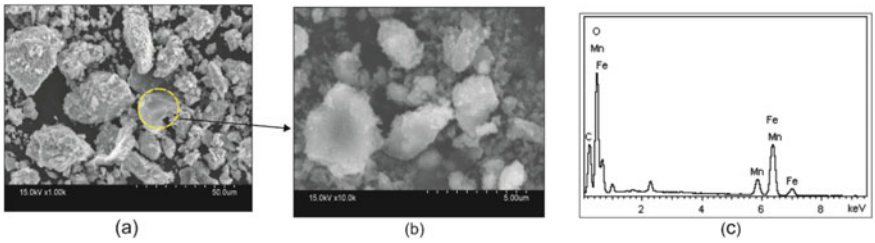

Fig. 1 Scanning electron microscopy (SEM) of and energy-dispersive X-ray spectroscopy (EDX) images: surface of GO-Mn-Fe adsorbent 50 μm (a) 5 μm (b) enlargement, (c) EDX image of GO-Mn-Fe

6.2 *Atomic Force Microscopy (AFM)*

The dispersed molecules of GO-Mn-Fe nanocomposite are aggregated onto silicon wafer as concentrated particle shaped features (Fig. 2a). This particle features are showed like a cotton or cloud shaped configuration at enlarged condition (Fig. 2b). The dimensions offlakes were average ~500–5 μm tightly bounded on the silicon wafer top surface [16, 18, 19]. Whereas for better enlargement of AFM image, the study of depth profile from surface microtopography is depicted in Fig. 2(c). It is found that the vertical height of GO-Mn-Fe nano particles are approximately an average of ~2 to 5 nm [20, 21]. It can be clearly observed in Fig. 2b, c that for the flake marked by the white line in panel (b), the nanoparticle sheets were typically between 1.0 and 2.5 nm thick [18, 19]. This observation is concluded that the 1.0–2.5 nm nano composite sheets presence of single layer GO sheet combined with double layer sheets hold iron and manganese ligand on their surface [16].

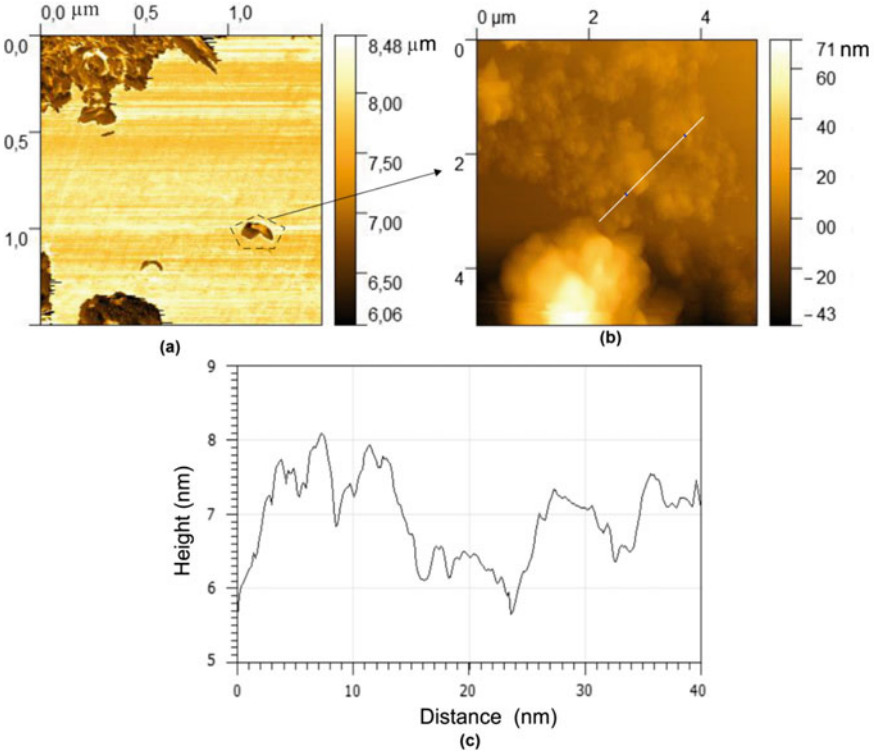

Fig. 2 Atomic force microscopy (AFM) images (a) Surface micrography in micrometer, (b) Enlarged Surface micrography in nanometer, (c) Depth profile

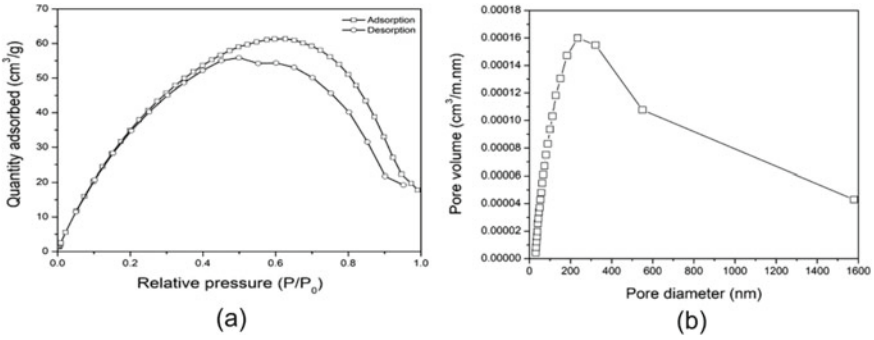

Fig. 3 BET hysteresis loop of GO-Mn-Fe nano composite, (a) BET pattern for adsorption–desorption curve and (b) particles size distribution

6.3 Brunauer–Emmett–Teller (BET)

The surface area and the total pore volume of the GO-Mn-Fe nano material are calculated to be 139.240 m^2/g and 0.07 cm^3/g, respectively. This amount of surface area is adequate in iron functionalized nano material [22, 23]. The large hysteresis loop area indicates the high surface of GO functionalized with Fe and Mn with it mesopores (Fig. 3a) [11, 21]. The average pore diameter is estimated to be 177 Å from (Fig. 3b) [21]. The high surface area enhances the adsorption capability [18], but this is decreasing for more functionalization of iron in GO-Mn-Fe nano material [2].

Packed Bed Column Study: Breakthrough curve is plotted between volume of sample passed and final concentration/initial concentration. From this graph, it is seen that breakthrough is achieved at $C_t/C_0 = 0.15$, and volume of sample passed is 6162 ml (Fig. 4).

Laboratory Scale Data: Flow rate (Q) = 15.8 mL/min, column diameter (d) = 3.5 cm, column depth (D) = 15 cm, weight of GO-Mn-Fe-coated sand = 187 g, volume of packed column = 144.24 cm^3, packed bed density = 1.29 g/cm^3, volume treated at break point (V_b) = 6162 mL, volume treated at exhaustion (V_x) = 18644 mL, adsorption capacity at 15% breakthrough (q_B) = 0.00659 mg/g, adsorption capacity at exhaustion = 0.01994 mg/g, length of mass transfer zone (δ) = 10.04 cm, empty bed contact time (EBCT) = 9.13 min, filtration rate (F_m) = 1.64 cm/min, % saturation of column at break point = 49.40%, total amount of solute accumulated at in the column at complete saturation = 3.71 mg.

For evaluation of breakthrough results, Bohart and Adams model, Thomas model, Yoon and Nelson model are applied.

Bohart and Adams model is applied to check the dynamic behaviour of the column. The Eq. 2 is expressed as

$$\ln\left(\frac{C_t}{C_0}\right) = K_{AB}C_0 t - K_{AB}N_0\left(\frac{Z}{U_0}\right) \tag{2}$$

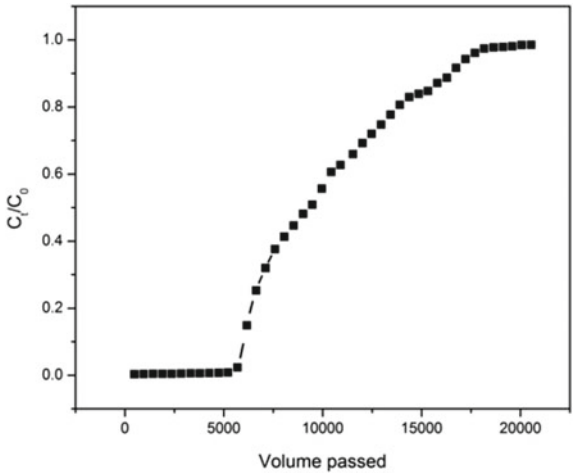

Fig. 4 Breakthrough curve [24–26]

Influent and effluent concentration are denoted as C_0 and C_t. K_{AB} represents kinetic constant (L/mg min), N_0 is the saturation concentration (mg/L), t is the flow time (min), Z stands for bed depth of fixed bed column (cm), and U_0 is superficial velocity (cm/min). A plot of $\ln(C_t/C_0)$ versus t gives the value of correlation coefficient (R^2), K_{AB} and N_0. The values of R^2, K_{AB}, N_0 are given in Table 1; (Fig. 5).

Thomas model is accepted for evaluation of breakthrough results for experimental data of column studies. The linearized form of Thomas model is indicated as

$$\ln\left(\frac{C_0}{C_t} - 1\right) = \frac{K_{Th}q_0m}{Q} - K_{Th}C_0t \tag{3}$$

where K_{Th} is the Thomas kinetic coefficient (mL/min mg), t is the total flow time (min), and Q is the volumetric flow rate (mL/min). Adsorption capacity and mass of the adsorbent are denoted by q_0 (mg/g) and m (g). Plot of $\ln((C_0/C_t) - 1)$ versus time (t) gives the value of K_{Th} and q_0, which are given in Table 1. R^2 value ranging between 0.57 and 0.99 indicates the good fitting of the model with the experimental breakthrough curve (Fig. 6).

Yoon and Nelson model is also applied to check the experimental data which is expressed as

$$\ln\left(\frac{C_t}{C_0 - C_t}\right) = K_{YN} - \tau K_{YN} \tag{4}$$

Table 1 Parameters of Adams–Bohart, Thomas and Yoon–Nelson model

Bohart and Adams model			Thomas Model			Yoon and Nelson model		
R^2	K_{AB}	N_0	R^2	K_{Th}	q_0	R^2	K_{yn}	τ
0.75	0.0251	22.17	0.935	0.042	12.084	0.52	0.034	13.08

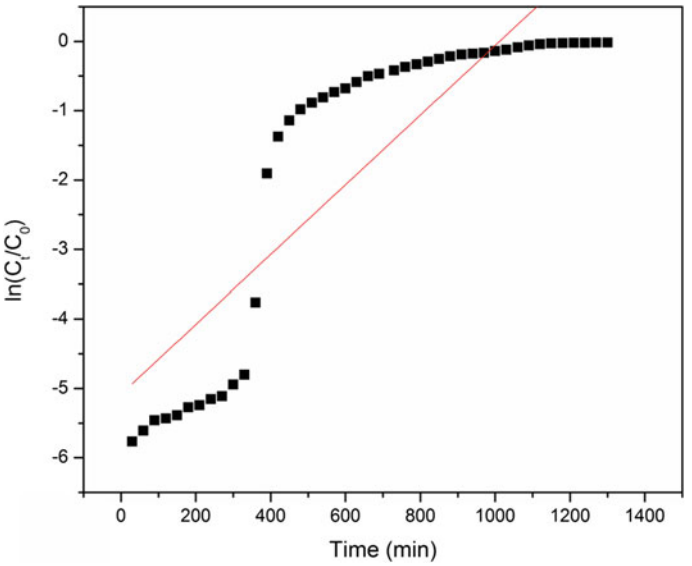

Fig. 5 Bohart and Adams model [24–26]

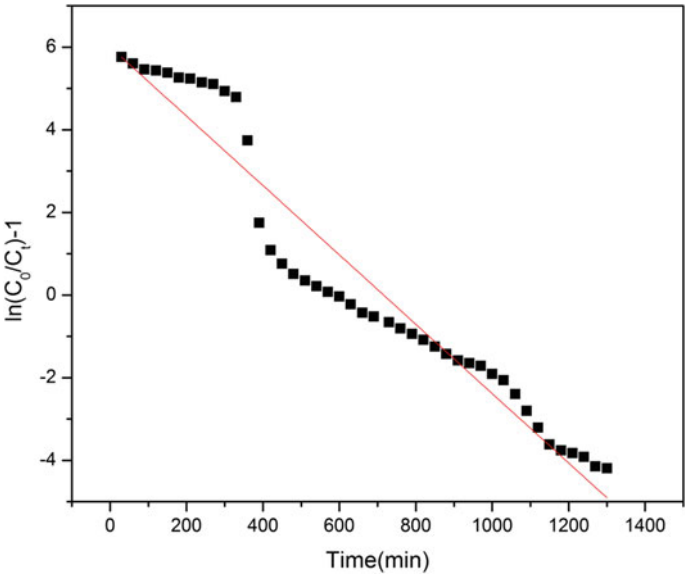

Fig. 6 Thomas model [24–26]

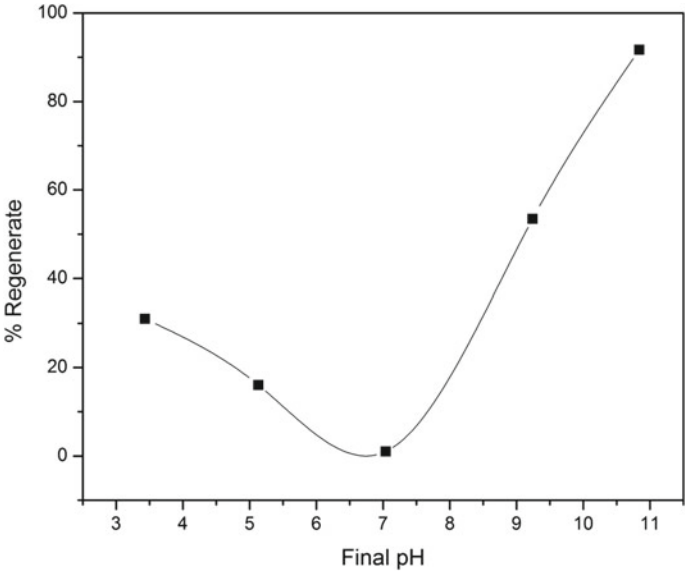

Fig. 7 Desorption study [24–26]

Desorption Study: During desorption study, it is observed that 91% adsorbed As (V) was removed at pH 11 because at high pH values, the surface –OH and –COOH groups undergo deprotonating and become negatively charged, leading to desorption of the negatively charged arsenic ions (Fig. 7).

7 Conclusion

In this study, it was determined that GO-Mn-Fe-coated sand bed could be utilized as an effective adsorbent for the removal of As (V). A cloud-shaped configuration of nano structure is achieved at enlarging circumstance. This nano composite was presenting mesoporous sheet structure of GO holding double layer sheets of ligands as iron and manganese on their surface. This nano composite exhibits superior adsorption capability for the removal of arsenic (V) from potable water contaminant. The prediction of breakthrough curve was obtained by using Adams–Bohart, Thomas and Yoon–Nelson model. However, the entire breakthrough curve is best predicted by Thomas model. By the desorption study, it is shown that this adsorbent can be used in the column operation several times. This will enhance the cost effectiveness of the removal of As (V) by using GO-Mn-Fe-coated sand.

References

1. Zhang K, Dwivedi V, Chi C, Wu J (2010) Graphene oxide/ferric hydroxide composites for efficient arsenate removal from drinking water. J Hazard Mater 182(1–3):162–168
2. Chandra V, Park J, Chun Y, Lee JW, Hwang IC, Kim KS (2010) Water-dispersible magnetite-reduced graphene oxide composites for arsenic removal. ACS Nano 4(7):3979–3986
3. Majumder C (2017) Arsenic (V) removal using activated alumina: kinetics and modeling by response surface. J Environ Eng 144(3):04017115
4. Mazumder DG (2008) Chronic arsenic toxicity and human health. Indian J Med Res 128(4):436–447
5. Mazumder DNG, Haque R, Ghosh N, De BK, Santra A, Chakraborty D, Smith AH (1998) Arsenic levels in drinking water and the prevalence of skin lesions in West Bengal India. Int J Epidemiol 27(5):871–877
6. USEPA (U.S. Environmental Protection Agency) (2000) Regulations on the disposal of arsenic residuals from drinking water treatment plants. EPA/600/R-00/025, Cincinnati
7. Hristovski K, Baumgardner A, Westerhoff P (2007) Selecting metal oxide nanomaterials for arsenic removal in fixed bed columns: from nanopowders to aggregated nanoparticle media. J Hazard Mater 147(1–2):265–274
8. Wang C, Luo H, Zhang Z, Wu Y, Zhang J, Chen S (2014) Removal of As (III) and As (V) from aqueous solutions using nanoscale zero valent iron-reduced graphite oxide modified composites. J Hazard Mater 268:124–131
9. Balasubramanian N, Madhavan K (2001) Arsenic removal from industrial effluent through electrocoagulation. Chem Eng Technol Indl Chem Plant Equipent Process Eng Biotechnol 24(5):519–521
10. Çiftçi TD, Henden E (2015) Nickel/nickel boride nanoparticles coated resin: a novel adsorbent for arsenic (III) and arsenic (V) removal. Powder Technol 269:470–480
11. Mishra AK, Ramaprabhu S (2011) Functionalized graphene sheets for arsenic removal and desalination of sea water. Desalination 282:39–45
12. Grassi M, Kaykioglu G, Belgiorno V, Lofrano G (2012) Removal of emerging contaminants from water and wastewater by adsorption process. In: Emerging compounds removal from wastewater, Springer, Dordrecht, pp 15–37
13. Hashim MA, Mukhopadhyay S, Sahu JN, Sengupta B (2011) Remediation technologies for heavy metal contaminated groundwater. J Environ Manage 92(10):2355–2388
14. Attia TMS, Hu XL (2013) Synthesized magnetic nanoparticles coated zeolite for the adsorption of pharmaceutical compounds from aqueous solution using batch and column studies. Chemosphere 93(9):2076–2085
15. Hummers WS Jr, Offeman RE (1958) Preparation of graphitic oxide. J Am Chem Soc 80(6):1339
16. Ray SK, Majumder C, Saha P (2017) Functionalized reduced graphene oxide (fRGO) for removal of fulvic acid contaminant. RSC Adv 7(35):21768–21779
17. Wang SG, Sun XF, Liu XW, Gong WX, Gao BY, Bao N (2008) Chitosan hydrogel beads for fulvic acid adsorption: behaviors and mechanisms. Chem Eng J 142(3):239–247
18. Kumar S, Nair RR, Pillai PB, Gupta SN, Iyengar MAR, Sood AK (2014) Graphene oxide–$MnFe_2O_4$ magnetic nanohybrids for efficient removal of lead and arsenic from water. ACS Appl Mater Interfaces 6(20):17426–17436
19. Paredes JI, Villar-Rodil S, Martínez-Alonso A, Tascon JMD (2008) Graphene oxide dispersions in organic solvents. Langmuir 24(19):10560–10564
20. Zhang J, Azam MS, Shi C, Huang J, Yan B, Liu Q, Zeng H (2015) Poly (acrylic acid) functionalized magnetic graphene oxide nanocomposite for removal of methylene blue. RSC Adv 5(41):32272–32282
21. Zhao D, Gao X, Wu C, Xie R, Feng S, Chen C (2016) Facile preparation of amino functionalized graphene oxide decorated with Fe_3O_4 nanoparticles for the adsorption of Cr (VI). Appl Surf Sci 384:1–9

22. Qiu J, Liu F, Cheng S, Zong L, Zhu C, Ling C, Li A (2017) Recyclable nanocomposite of flowerlike MoS2@ hybrid acid-doped PANI immobilized on porous PAN nanofibers for the efficient removal of Cr (VI). ACS Sustain Chem Eng 6(1):447–456
23. Wei Z, Xing R, Zhang X, Liu S, Yu H, Li P (2012) Facile template-free fabrication of hollow nestlike α-Fe2O3 nanostructures for water treatment. ACS Appl Mater Interfaces 5:598–604
24. Mishra V, Balomajumder C, Agarwal VK (2013) Adsorption of Cu (II) on the surface of nonconventional biomass: a study on forced convective mass transfer in packed bed column. J Waste Manage
25. Chowdhury ZZ, Abd Hamid SB, Zain SM (2015) Evaluating design parameters for breakthrough curve analysis and kinetics of fixed bed columns for Cu (II) cations using lignocellulosic wastes. Bioresources 10(1):732–749
26. Sana D, Jalila S (2017) A comparative study of adsorption and regeneration with different agricultural wastes as adsorbents for the removal of methylene blue from aqueous solution. Chin J Chem Eng 25(9):1282–1287
27. Han R, Wang Y, Zhao X, Wang Y, Xie F, Cheng J, Tang M (2009) Adsorption of methylene blue by phoenix tree leaf powder in a fixed-bed column: experiments and prediction of breakthrough curves. Desalination 245(1–3):284–297

Water Quality of the Ganges and Brahmaputra Rivers: An Impact Assessment on Socioeconomic Lives at Ganga–Brahmaputra River Basin

Subhankar Dutta and Sumanta Nayek

1 Introduction and Objective

The river water quality of Ganges and Brahmaputra has gradually worsened due to the rising urbanization, industrialization practices, using of agrochemicals, industrial wastes disposal, water tourism activities, etc., over the years. Various studies such as [1–3] etc., had carried out to evaluate the water quality of the Ganges and Brahmaputra rivers. In our study, we consider observed average values of several water quality parameters including pH, DO, BOD, COD, conductivity, TSS and TDS of both the Ganges and Brahmaputra rivers during 2016–17 based on the above-mentioned research studies. All these parameters have been classified under three categories like drinking water, irrigation water and surface water, which actually determine the feasibility of river water for human consumption in terms of health aspect, economic viability for using river water and how river water can impact on social status of people residing in the Ganga–Brahmaputra river basin, respectively. Further, observed average values of all these parameters under three categories have been compared to the Indian Standard values of drinking water, irrigation water and surface water, respectively. Subsequently, the interpretation has been written, analyzing the water quality of both the rivers.

With this analysis, the main objective of the study is to find out whether the river water quality of the Ganges and Brahmaputra is suitable for human consumption, irrigation activities and daily household works within the recommended standards.

S. Dutta (✉)
Maulana Abul Kalam Azad University of Technology, Kolkata, West Bengal, India
e-mail: subhankar.du@gmail.com

S. Nayek
Department of Environmental Science, AIES, Amity University Kolkata, Kolkata, West Bengal 700135, India
e-mail: sumanta.nayek@gmail.com

S. Kumar et al. (eds.), *Sustainability in Environmental Engineering and Science*, Lecture Notes in Civil Engineering 93,
https://doi.org/10.1007/978-981-15-6887-9_26

2 Methodology

The secondary data consisting of observed average values of several water quality parameters including pH, DO, BOD, COD, conductivity, TSS and TDS of both the Ganges and Brahmaputra rivers during 2016–17 have been taken into account for analysis. All the observed average values of water quality parameters and the corresponding Indian Standard values of drinking water, irrigation water and surface water are written in a table. After that, comparative analyses have been carried out, and the final interpretation has been developed. From the interpretation, the results can be validated whether the river water quality of both the Ganges and Brahmaputra is suitable for human consumption, irrigation and daily usages within the suggested standards.

3 Results and Discussion

The comparative analyses have been carried out and reflected in the following table:

From Table 1, it is identified that observed average pH values of Brahmaputra and the Ganges rivers are very much within the recommended standards, which signifies that water of both the rivers can be used for human consumption (drinking purpose). Therefore, human health-related aspects are met with positive note. Similarly, pH values of both the rivers are very much within the recommended standards for irrigation and surface water activities, which determine that water of these two rivers is suitable for irrigation and other daily usages, respectively. Hence, it satisfies the economic and social perspectives in a positive direction.

From Table 1, it is noticed that observed average DO value of Brahmaputra river is above the recommended values for drinking, irrigation and surface water standards. In case of DO, if observed value is higher than standard value, then it signifies good and positive and vice versa. So, in this case, the Brahmaputra river water is suitable for human consumption, irrigation and other usages. Also, it satisfies the health, economic and social perspectives in a positive direction.

On the other hand, the observed average DO value of the Ganges river water is less against the recommended standard for drinking water. So, the Ganges river water is unsuitable for human consumption. Here, the health-related aspect is met with negative in nature. Apart from that, the average DO value of the Ganges river water is higher in both irrigation and surface water standards, respectively, which signify that the water is suitable for irrigation and other usages. Hence, it satisfies the economic and social perspectives in a positive direction.

From Table 1, it is identified that observed average BOD value of Brahmaputra river is less than the recommended values for drinking, irrigation and surface water standards. In case of BOD, if observed value is lesser than standard value, then it signifies good and positive and vice versa. So, in this case, the Brahmaputra river

Table 1 Comparative analyses of water quality parameters of Brahmaputra and the Ganges rivers

Brahmaputra river					The Ganges river				
Parameters (unit)	Average value[a]	Indian standard for drinking Water	Indian standard for irrigation Water	Indian standard for surface water[b]	Parameters (unit)	Average value[a]	Indian standard for drinking Water	Indian standard for irrigation Water	Indian standard for surface water[b]
pH (–)	8.26	8.5	8.5	8.5	pH (–)	7.42	8.5	8.5	8.5
DO (mg/L)	7.86	6	4	4	DO (mg/L)	4.57	6	4	4
BOD (mg/L)	1.73	2	3	3	BOD (mg/L)	2.41	2	3	3
COD (mg/L)	5.48	–	250	250	COD (mg/L)	5.88	–	250	250
Conductivity (S/m)	351.12	250	700	–	Conductivity (S/m)	412.78	250	700	–
TSS (mg/L)	62.20	–	30	–	TSS (mg/L)	75.00	–	30	–
TDS (mg/L)	178.54	500	1500	700	TDS (mg/L)	271.60	500	1500	700

[a]The average values have been taken from various previous research studies, which have been mentioned in References. [b] [4]

water is suitable for human consumption, irrigation and other usages. Also, it satisfies the health, economic and social perspectives in a positive direction.

On the other hand, the observed average BOD value of the Ganges river water is high against the recommended standard for drinking water. So, in this case, the Ganges river water is unsuitable for human consumption. Here, the health-related aspect is satisfied in negative note. Apart from that, the average BOD value of the Ganges river water is lesser in both irrigation and surface water standards, respectively, which signify that the water is suitable for irrigation and other usages. Hence, it satisfies the economic and social perspectives in a positive direction.

From Table 1, it is noted that observed average COD values of Brahmaputra and the Ganges rivers are very less against the recommended standards (excluding the standard values for drinking water, as the values are unavailable), which signifies that water of both the rivers can be used for irrigation and surface water activities. As the drinking water standard values are not available, so it is undecided whether the water is suitable for human consumption and satisfies the health-related aspect. Therefore, in this case, the COD water parameter of two rivers only satisfies the economic and social perspectives in a positive direction.

From Table 1, it is identified that observed average 'conductivity' value of Brahmaputra river is higher than the recommended value for drinking water standard but lower the recommended value for irrigation water standard. However, no recommended value is recorded for surface water standard. In case of 'conductivity,' if observed value is less than the standard value, then it signifies good and positive and vice versa. So, in this case, the Brahmaputra river water is termed as polluted and consequently unsuitable for human consumption. But, irrigation activities can be carried out with the Brahmaputra river water. So, the Brahmaputra river water quality only satisfies the economic perspective in a positive direction.

Similarly, from Table 1, it is identified that observed average 'conductivity' value of the Ganges river is higher than the recommended value for drinking water standard but lower the recommended value for irrigation water standard. However, no recommended value is recorded for surface water standard. Therefore, in this situation, the Ganges river water is polluted and not suitable for human consumption. But, irrigation activities can be performed with the Ganges river water. Hence, the Ganges river water quality only satisfies the economic perspective in a positive direction.

In case of TSS parameter, if the observed average value is less than the standard value, then it is considered as good and positive and vice versa. From Table 1, it is noticed that the observed average values of TSS for both Brahmaputra and the Ganges river water are higher than the irrigation water standard. Hence, the water of these rivers is recognized polluted and unsuitable for irrigation activities. However, no recommended standard has been found for drinking and surface water, respectively, for both the river water. So, in this case, only economic aspect is satisfied in a positive note.

Finally, in case of TDS parameter, if the observed average value is less than the standard value, then it is considered as good and positive and vice versa. From Table 1, it is identified that the observed average values of TDS for both Brahmaputra and the Ganges rivers are less than the standard values for drinking water, irrigation water and

surface water. Hence, water of both the rivers can be used for human consumption, irrigation and other usages. Here, the water quality satisfies health, economic and social perspectives in a positive direction.

4 Conclusion

After obtaining the research findings, it can be said that both the rivers are flowing with polluted substances. Out of total seven water quality parameters, some parameters suit for human consumption, irrigation and other usages but not all parameters satisfy the recommended quality standards. So, it is advised that both the rivers need water quality check before using in reality. Also, the proper implementation of efficient, rational and equitable river water management practices may intensify the socio-economic development in the region.

References

1. Islam MS, Datta T, Ema IJ, Kabir MH Meghla NT (2015) Investigation of water quality from the Brahmaputra River in Sherpur District, Bangladesh J Sci Res 28(1):35–41
2. Kotoky P, Sarma B (2017) Assessment of water quality index of the Brahmaputra River of Guwahati City of Kamrup District of Assam, India. Int J Eng Res Technol (IJERT) 6(03)
3. Kar S, Ghosh I, Ghosh A, Aitch P, Bhandari G (2017) Determination of water quality index (WQI) during mass bathing in different ghats of River Ganga in Howrah and North 24 Parganas District, West Bengal, India. Int J Res Appl Sci Eng Technol (IJRASET) 5(IX)
4. Surface water quality criteria for different uses (specified by CPCB, 1979 and the Bureau of Indian Standards, 1982)

Physico-Chemical and Heavy Metal Analysis of Effluent Wastewater from Rold Gold Jewellery Industries and to Review on Its Safe Disposal Using Phytoremediation Approach with Special Emphasis on *Hydrilla Verticillata*, an Aquatic Plant

Lanka Suseela, M. Swarupa Rani, and Kota Ashok Kumar

1 Effluent Wastewater Rold Gold Jewellery Industries

With increasing industrial development, safe disposal of wastewater is one of the major ecological challenges. Industrial wastewater must be treated before being discharged into the environment to prevent pollution and eutrophication of rivers and other water bodies [1]. Pollution of environment via toxic metals arises as a result of various industrial activities and has turned these metal ions into major health issue [2]. Adjacent areas along with the drain of industrial effluent are highly polluted and represent a sink for heavy metals and a large variety of chemicals [3].

Machilipatnam, the headquarters of Krishna District, is well known for its rold gold jewellery which has a great demand from different parts of the country. The effluent wastewater from rold gold manufacturing industries harbours various toxic materials and heavy metals that are released during the process of electroplating. Metal finishing works usually employ electroplating technique to deposit a fine layer of one metal on another metal involving electrolytic process. This imparts colour, lustre, aesthetics, corrosion protection, value addition, enhanced surface hardness

L. Suseela (✉) · M. Swarupa Rani · K. Ashok Kumar
Department of Biosciences and Biotechnology, Krishna University, Machilipatnam, Andhra Pradesh, India
e-mail: susheelalankaku@gmail.com

M. Swarupa Rani
e-mail: kaushikprem@gmail.com

K. Ashok Kumar
e-mail: ashokkota7@gmail.com

S. Kumar et al. (eds.), *Sustainability in Environmental Engineering and Science*, Lecture Notes in Civil Engineering 93,
https://doi.org/10.1007/978-981-15-6887-9_27

Fig. 1 **a** Jewellery Park Entrance, Pothepally, Machilipatnam. **b** Inlet water tank with screen chamber. **c** Eqilization tank. **d** Outlet store tank. **e** Final disposal outlet tank

and many more. Figure 1 shows the images of inlet and outlet tanks of imitation jewellery effluent treatment plant.

The major problem associated with this industry is the discharge of toxic materials and heavy metals through effluent wastewater. Table 1 shows the physico-chemical parameters and heavy metals (iron, chromium, copper, cyanide and nickel) present in the common effluent treatment plant inlet water. Heavy metals are easily transported, get accumulated in the environment and can cause deleterious effects on living organisms. A number of industries, viz. steel, textile, electroplating, metal producing industries release heavy metals such as copper, cadmium, chromium, lead and nickel in the form of effluent wastewater.

2 Analysis of Effluent Wastewater

Sampling and analysis were done as per the standard methods prescribed by BIS and as per the standards laid by Ministry of Environment and Forests, Government of India for Common Effluent Treatment Plants (CETP) (Government protection rules, 1986).

3 Phytoremediation

The non-biodegradable nature of heavy metals poses a major concern to both humans and ecosystem [4]. Important measures are required to remediate such polluted area. Of all the remediation advancements, phytoremediation has been favoured in light of its cost-adequacy and easy maintenance [5, 6].

Table 1 Analysis of common effluent treatment plant inlet water

S. No.	Parameters	Test method as per BIS	Units	Results	CETP limits	Limits as per CPCB
Physical examination						
1	Colour	IS: 3025 part 4 1983	Hezen	40	–	–
2	pH at 25 °C	IS: 3025 part 11 1983	–	1.67	5.50–9.0	5.50–9.0
3	Temperature	IS: 3025 part 9 1983	°C	25	45	–
4	Total dissolved solids	IS: 3025 part 16 1983	mg/L	8844	5000 max	2100 max
5	Total suspended solids	IS: 3025 part 17 1983	mg/L	34	1000 max	200 max
Chemical examination						
6	Total hardness as $CaCO_3$	IS: 3025 part 21 1983	mg/L	20	–	–
7	Calcium as Ca	IS: 3025 part 40 1983	mg/L	4.0	–	–
8	Magnesium as Mg	IS: 3025 part 46 1983	mg/L	2.4	–	–
9	Alkalinity-Phenolphthalein	IS: 3025 part 22 1983	mg/L	Nil	–	–
10	Alkalinity-Methyl Orange	IS: 3025 part 23 1983	mg/L	Nil	–	–
11	Sulphates as SO_4	IS: 3025 part 24 1983	mg/L	5995.8	1000 max	1000 max
12	Sodium as Na	IS: 3025 part 45 1983	mg/L	3258.6	–	–

(continued)

Table 1 (continued)

S. No.	Parameters	Test method as per BIS	Units	Results	CETP limits	Limits as per CPCB
13	Potassium as K	IS: 3025 part 45 1983	mg/L	9.7	–	–
Organic and nutrient parameters						
14	Biological Oxygen Demand (3 days for 27 °C)	IS: 3025 part 441983	mg/L	874	–	100 max
15	Chemical Oxygen Demand	IS: 3025 part 58 1983	mg/L	4780	15,000 max	–
16	Phosphates PO_4	IS: 3025 part 31 1983	mg/L	1.84	–	–
17	Nitrates as NO_3	IS: 3025 part 34 1983	mg/L	18.9	–	–
Heavy metals						
18	Iron as Fe	IS: 3025 part 53 1983	mg/L	0.24	–	–
19	Chromium as Cr	IS: 3025 part 52 1983	mg/L	1.79	2.0 max	–
20	Copper as Cu	IS: 3025 part 42 1983	mg/L	2.6	3.0 max	–
21	Cyanide as CN	IS: 3025 part 27 1983	mg/L	0.04	2.0 max	0.2
22	Nickel as Ni	IS: 3025 part 54 1983	mg/L	0.19	3.0 max	–

Though various methods are currently available to treat effluent wastewater from industries like electro-dialysis, reverse osmosis and absorption, etc., they are not economical and difficult to get optimum results [7, 8]. Bioremediation, i.e. removal of pollutants or contaminants through biological agents offers one eco-friendly and cost-effective methodology that can be applied for the treatment of heavy metals from wastewater [9]. One of the environmental friendly and economically feasible

techniques is the use of plants to effectively remove the heavy metals from contaminated water. This technique known as phytoremediation is not a new method, and it began 300 years ago in the water treatment processes to treat polluted water [10].

Phytoremediation combines the disciplines of plant physiology, soil and water microbiology, chemistry and hence is an integrated multidisciplinary approach to the cleanup of contaminated soils and water [5, 11, 12]. It is the most applicable among the bioremedial measures and is an emerging technology. The capacity to both endure raised degrees of substantial metals and gather them in extremely high focuses has been advanced both autonomously and together in number of various plant species [13–15]. Figure 2 shows the mechanism of heavy metal uptake by plants through phytoremediation technology. The limit of plants to expel conceivably harmful substantial metals is very much recorded. Aquatic plants can serve as best candidates in alleviating toxic heavy metal of wastewater/contaminated water resource [16]. Plants have the ability to absorb metal ions based on the affinity they will deposit in various parts of the plant [17]. The potentiality of macrophytes in absorption and accumulation of metal ions renders the services of cleaning heavy metal contaminated effluent wastewater.

4 Phytoremediation and Aquatic Plants

Aquatic plants are of special interest because of their ability to bio-accumulate toxic metals and nutrients in large quantities when compared to terrestrial plants [18]. Macrophytes have been found to absorb the pollutants at different rates and efficiencies based on the biochemical composition, habit, species, abundance and environment. Studies have found that during the pollutant stress, plants produce metal-binding cysteine-rich peptides (phytochelatins), which detoxify heavy metals by forming complexes with them [19]. All aquatic plants whether free floating, submerged or emergents that have a fast growth rate are excellent candidates in the removal of heavy metals.

Priyanka et al. [20] showed that *Eichhornia crassipes,* a water hyacinth species, was effective in the removal of hexavalent Cr (Cr (VI)) from the processed water of SCM in 15 days. The plant is also effective in lowering other elements of water, reducing total dissolved solids (TDS), chemical oxygen demand (COD), biological oxygen demand (BOD), etc. Ekta Chaudhary and Praveen Sharma [21] reviewed the efficacy of duckweed (*Lemna minor*, *Lemna gibba*, *S. polyrhiza*) in the removal of heavy metals. *Azolla,* an aquatic pteridophyte used as a bio-fertilizer in agriculture, as green manure, feed for livestock is also found to be a good choice for heavy metal removal from contaminated water [22–25] mainly due to its global distribution, growth habitat, high multiplication rate, high biomass production and high protein content. Biomass of Azolla can be utilized for substantial metal expulsion from wastewater. Chakraborty et al. 2013 [26] showed hexavalent chromium (Cr(VI)) removal by a water lettuce (*Pistia* sp). Shore line plants *Bulrushes* (*Scirpus* sp.) and *rushes* (*Juncus* sp.) are also excellent water purifiers as they remove excess

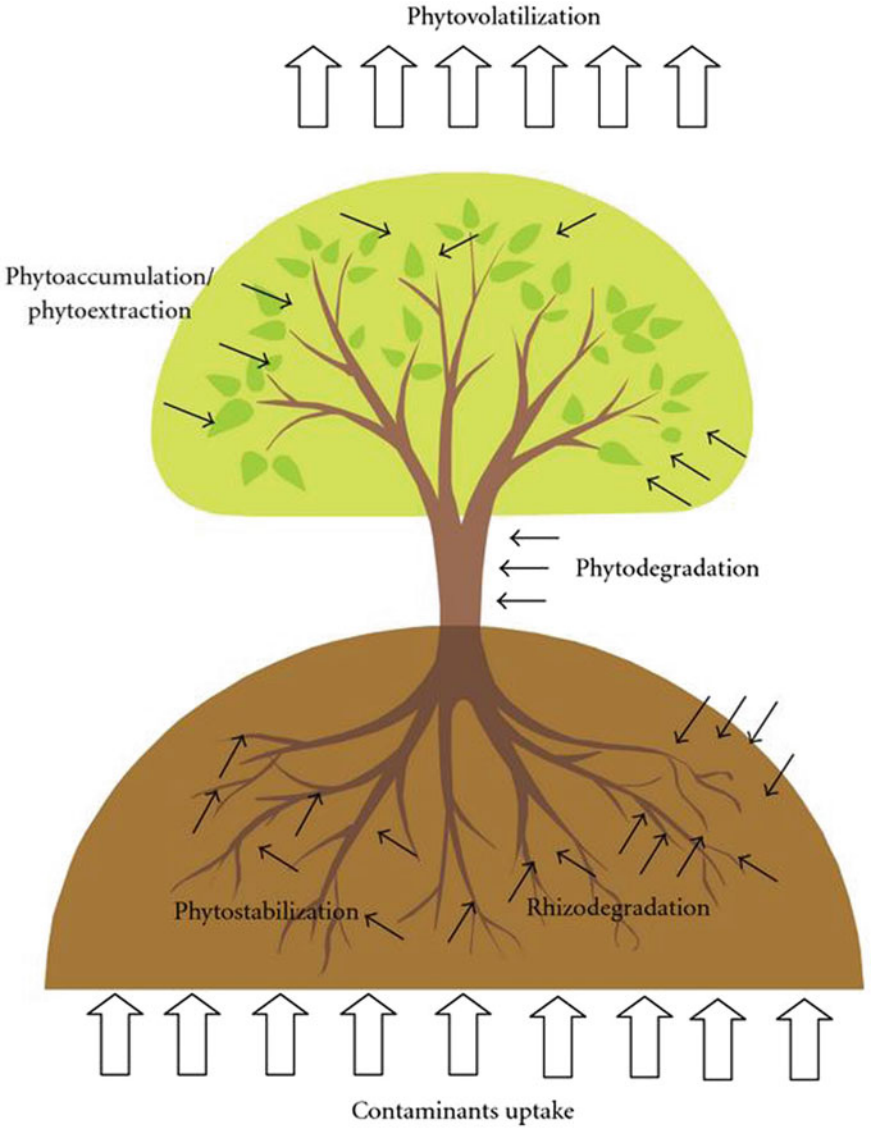

Fig. 2 Mechanism of heavy metal uptake by plants through phytoremediation technology. **Source* Google

nutrients and as well oil from the polluted water. They also play role in the removal of heavy metals such as copper, nickel and zinc.

Table 2 Classification of *Hydrilla verticillata*

Kingdom	Plantae (Plants)
Subkingdom	Tracheobionta (Vascular plants)
Super division	Spermatophyta (Seed plants)
Division	Magnoliophyta (Flowering plants)
Class	Liliopsida (Monocotyledons)
Subclass	Alismatidae
Order	Hydrocharitales
Family	Hydrocharitaceae (Tape-grass family)
Genus	*Hydrilla* Rich. (hydrilla)
Species	*Hydrilla verticillata* (L. f.) Royle (waterthyme)

5 Hydrilla Verticillata

When compared to many other freshwater aquatic plants, *Hydrilla* has high resistance to salinity, hence selected for the current study. *Hydrilla verticillata* (L.f.) Royle is a gregarious, submerged, rooted aquatic plant that forms dense and interwined mats in a variety of freshwater bodies. *It* can grow in a wide variety of ecological habitats but usually in shallow waters. Even the small plant fragments kept in water can quickly generate adventitious roots, thereby producing an entire plant. It tolerates moderate salinity up to 33% of seawater [27, 28]. It likewise develops well in both oligotrophic and eutrophic waters and even endures elevated levels of crude sewage. Hydrilla can grow well on rocky and sandy substrates without nutrient avalability [29]. It has been reported to scavenge Cadmium and Chromium [30]. Table 2 shows the classification of *Hydrilla verticillata.*

Another advantage with *Hydrilla* is it can spread efficiently through both tubers and turions (Ecological impacts). Patel and Kanungo 2012 reported that *Hydrilla verticillata* shows variable tendency in growth and in the generation of biomass [31]. The available literature confirms that it is a hyper accumulator of mercury, chromium, cadmium, copper and lead and can play key role in phytoremediation [32–37]. The plant also finds to have many digestive and health benefits. The plant is also a rich source of minerals (calcium, iron and magnesium), vitamins (vitamin B-12) and antioxidants. So, the plant is extremely popular as "super food" [38]. Figure 3 shows *Hydrilla vercillata* collected from nearby natural pond in Machilipatnam and *Hydrilla vercillata* grown in the effluent wastewater of treatment plant.

6 Conclusion

The effluent wastewater from rold gold jewellery industries is analysed for physico-chemical parameters and for the presence of certain heavy metals. Treatment of effluent wastewater is necessary for its safe disposal. Currently, various chemical treatment methods were being used by the effluent treatment plant of rold gold

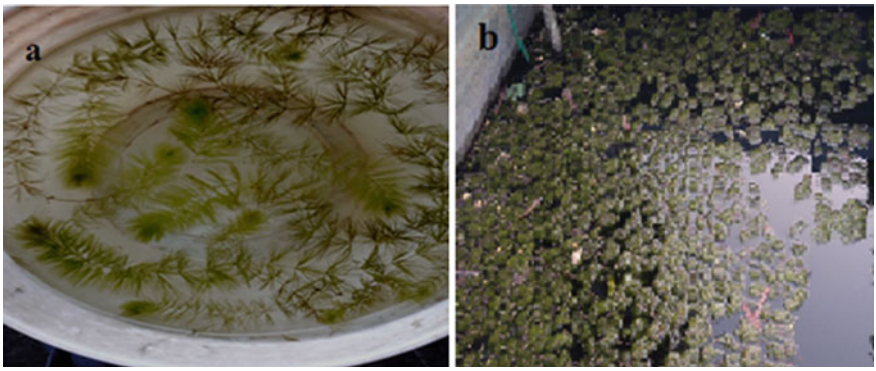

Fig. 3 **a** *Hydrilla vercillata* collected from nearby natural pond, Machilipatnam, and **b** *Hydrilla vercillata* grown in effluent wastewater at jewellery park effluent treatment plant

jewellery park which are very costly and are also not so effective. Hence, Krishna University, located in Machilipatnam, as part of its social responsibility considered the need to remediate effluent wastewaters from the rold gold jewellery industries for its safe discharge using *Hydrilla verticillata.*

Acknowledgements Authors acknowledge the support of Machilipatnam Imitation Jewellery Park Pvt. Ltd. Pothepally, Machilipatnam, Krishna District, Andhra Pradesh, India, for providing us common effluent treatment plant inlet water and for extending their help in the wastewater analysis.

References

1. Ruiz-Martinez A, Martin-Garcia N, Romero I, Seco A, Ferrer J (2012) Microalgae cultivation in wastewater: nutrient removal from anaerobic membrane bioreactor effluent. Bioresour Technol 126:247–253
2. Waisberg M, Joseph P, Hale B, Beyersmann D (2003) Molecular and cellular mechanisms of cadmium carcinogenesis. Toxicol 192:95–117
3. Pandey S, Srivastava VS (2002) Heavy metal accumulation in industrial solid waste amended soils. Nature Environ Pollut Technol 1(1):73–75
4. Kabata-Pendias A (2011) Trace elements in soils and plant. CRC Press, Boca Raton, USA
5. Uqab B, Mudasir S, Sheikh AQ, Nazir R (2016) Bioremediation: a management tool. J Bioremed Biodeg 7:331
6. Kamran MA, Mufti R, Mubariz N, Syed JH, Bano A et al (2014) The potential of the flora from different regions of Pakistan in phytoremediation: a review. Environ Sci Pollut Res 21:801–812
7. Sharma S, Iffat N, Ishtiaq A, Safia A (2011) Monitoring of physico-chemical and microbiological analysis of under ground water samples of district Kallar Syedan, Rawalpindi-Pakistan. Res J Chem Sci 1(8):24–30
8. Deshpande SM, Aher KR (2012) Evaluation of groundwater quality and its suitability for drinking and agriculture use in parts of Vaijapur, District Aurangabad MS. India Res J Chem Sci 2(1):25–31
9. Singh DB, Prasad G, Rupainwar DC (1996)Adsorption technique for the treatment of As (V) rich effluents. Colloids Surf III 49–56

10. Hartman WJ(1975) An evaluation of lead treatment of municipal west water and physical siting of facility installations. US Department of arm, Washington, DC
11. Jadia DC, Fulekar MH (2009) Phytoremediation of heavy metals: recent techniques. African J Biotechnol 8:921–928
12. Sarma H (2011) Metal hyperaccumulation in plants: a review focusing on phytoremediation technology. J Env Sci Tech 4:118–138
13. Abida B, HariKrishna S (2010) Bioaccumulation of trace metals by aquatic plants. Int J Chem Tech Res 2(1):250–254
14. Abida B, Ramaiah M, Harikrishna S, Khan I, Veena K (2009) Heavy metal pollution and chemical profile of Cauvery River water. J Chem 6(1):47–52
15. Abida B, Ramaiah M, Harikrishna S, Khan I, Veena K (2009) Analysis of heavy metals concentration in soil and litchens from various localities of Hosur road. J Chem 6(1):13–22
16. Yaowakhan P, Kruatrachue M, Pokethitiyook P, Soonthornsarathool V (2005) Removal of lead using some aquatic macrophytes. Bull Environ Contam Toxicol 75:723–730
17. Sutton DL, Ornes WL (1975) Phosphorus removal from static sewage effluent. J Environ Quality 4:367–370
18. Pratas J, Favas PJC, Paulo C, Rodrigues N, Prasad MNV (2012) Uranium accumulation by aquatic plants from uranium-contaminated water in Central Portugal. Int J Phytoremed 14:221–234
19. Kinnersely AM (1993) The role of phytochelatins in plant growth and productivity. Plant Growth Regul 12:207–217
20. Priyanka SP, Shinde O, Sarkar S (2017) Phytoremediation of Industrial mines waste water using Water hyacinth. Int J Phytorem 19(1):87–96
21. Chaudhary E, Sharma P (2014) Duckweed as ecofriendly tool for phytoremediation. Int J Sci Res (IJSR) 3(6)
22. Naghipour D, Ashrafi SD, Gholamzadeh M, Taghavi K, Naimi-Joubani M (2018) Phytoremediation of heavy metals (Ni, Cd, Pb) by *Azolla filiculoides* from aqueous solution: a dataset. Data Brief 21:1409–1414
23. Sood A, Uniyal PL, Prasanna R, Ahluwalia AS (2012) Phytoremediation potential of aquatic macrophyte, Azolla. AMBIO 41:122–137
24. Mandakini LLU, Bandara NJGJ, Gunawardana D, A Study on the phytoremediation potential of azolla pinnata under laboratory conditions. Department of Forestry and Environmental Science, University of Sri Jayewardenepura, Sri Lanka, Department of Botany, University of Sri Jayewardenepura, Sri Lanka
25. Tangahu BV, Sheikh Abdullah SR, Hassan B, Idris M, Anuar N, Mukhlisin M (2011) Review on heavy metals (As, Pb, and Hg) uptake by plants through phytoremediation. Int J Chem Eng Article ID 939161
26. Chakraborty R, Mitra AK, Mukherjee S (2013) Synergistic chromium bioremediation by water lettuce (Pistia) and Bacteria (*Bacillus cereus* GXBC-1) Interaction. J Biol Chem Research 30(2)421-431
27. Reddy CS, Reddy KVR, Humane SK, Damodaram B (2012) Accumulation of chromium in certain plant species growing on mine dump from Byrapur, Karnataka, India. Res J Chem Sci 2(12):17–20
28. Haller WT, Sutton DL (1975) Community structure and competition between *Hydrilla* and *Vallisneria.* Hyacinth Control J 13:48–50
29. Mahler MJ (1979) *Hydrilla,* the number one problem. Aquatics 1:56
30. Rai UN, Tripathi RD, Sinha S, Chandra P (1995) Chromium and Cadmium bioaccumulation and toxicity in *Hydrilla verticillata* (l.f.) Royle and *Chara corallina* Wildenow. J Environ Sci Health Part A 30(3):537–551
31. Patel DK, Kanungo VK (2012) Study on growth, potential utility and N.P.P. of a submerged aquatic plant *Hydrilla verticillata Casp.* J Exp Sci 3:48–50
32. Mc Cutcheon CS, Schnoor JL (2004) Phytoremediation: transformation and control of contaminants. Wiley, vol 898. ISBN 978-0-471-45932-3

33. Abdul A, Aldhamin AS (2016) Phytoremediation of chromium and copper from aqueous solutions using *Hydrilla verticillata.* Iraqi J Sci 57(1):78–86
34. Hassan NA, Al-Kubaisi ARA, Al-Obiadi AHM (2016) Phytoremediation of lead by *Hydrilla verticellata* Lab. Work Int J Curr Microbiol App Sci 5(6):271–278
35. Phukan P, Phukan R, Phukan SN (2015) Heavy metal uptake capacity of *Hydrilla verticillata*: a commonly available aquatic plant. Int Res J Environment Sci 4(3):35–40
36. Kameswaran S, Vatsala TM (2017) Efficacy of bioaccumulation of heavy metals by Aquatic Plant *Hydrilla verticillata* royle. Int J Sci Res (IJSR) 6(9):535–538
37. Xue PY, Li GX, Liu WJ, Yan CZ (2010) Copper uptake and translocation in a submerged aquatic plant *Hydrilla verticillata* (L.f.) Royle. Chemosphere 81(9):1098–103
38. https://pdfs.semanticscholar.org/f9e6/bfe0fd70ae33b69d88ffa4d44a42c9cc3b0c.pdfn

Monitoring of Land Use/Land Cover Changes by the Application of GIS for Disposal of Solid Waste: A Case Study of Proposed Smart Cities in Bihar

Aman Kumar, Ekta Singh, Rahul Mishra, and Sunil Kumar

1 Introduction

The Eleventh Five-Year Plan under Indian Government encouraged urbanization with the determination to promote economic development in India. This idea automatically put immense pressure on all the available public services such as sanitation, lodging, safety and energy [1, 2]. Approximately, 31% Indians live in the urban areas. It was also projected that this would rise to approximately 40.8% by the end of year 2030 [3].

Such severe changes lead to new human, social and infrastructural development in order to improve the quality of life and draw the citizens. Natural resource use is very rapid with the increasing population levels that is about to get depleted quickly. Scientists are improvising studies to understand the adverse effects of human waste on the atmosphere [4]. Consequently, in every part of the globe, the appropriate waste management method is practiced in sustainable way for the use of waste as resources by material recovery.

Indian government's smart cities initiative has powered several innovations and concepts for various human, social, socio-economic and infrastructural changes. These consist of good solid waste disposal and general cleanliness. Key challenges occurring in the field of solid waste management (SWM) in India comprise inappropriate waste collection, accumulation, lack of appropriate treatment and disposal systems [5–7].

A. Kumar · E. Singh · S. Kumar (✉)
CSIR-National Environmental and Engineering Research Institute (CSIR-NEERI), Nagpur 440020, India
e-mail: s_kumar@neeri.res.in

R. Mishra
Banaras Hindu University, Varanasi 221005, India

S. Kumar et al. (eds.), *Sustainability in Environmental Engineering and Science*, Lecture Notes in Civil Engineering 93,
https://doi.org/10.1007/978-981-15-6887-9_28

Solid waste is one of the major challenges occurring in the development of the smart cities. This study advances towards the evaluation of solutions for SWM-related issues and recommending a proper solution to the prevailing SWM issues of the proposed smart cities in Bihar.

While selecting the solid waste disposal site, various factors need to be properly analysed which should be integrated into one system. Geographic information system (GIS) is one such technique. It is capable of handling the required data collected from different sources properly. GIS combines the geographical data available with quantitative, qualitative and descriptive sources that support a large number of spatial inquiries. All these render GIS as an essential resource for various location specific setups, landfill siting being one of them [8, 9].

Remote sensing is also an effective method for observing the world and usable resources because of its remarkable capacity to offer a synoptic vision of a huge range of Earth's surface and its repeated ability to cover it.

Its multispectral capability offers an effective comparison between different natural characteristics, whereas the repeated scope makes available information on the dynamic changes happening over the earth's surface and its environment [10].

GIS has a significant role in the field of solid waste management since many planning and operations elements are extremely dependent on spatial details. In addition, GIS plays an important role to managing the account data for optimizing the inventory activities.

In this way, aspects such as customer service are important; study of suitable locations for transfer stations; preparing routes for vehicles carrying garbage, location of new landfills and monitoring them. GIS is a method that reduces times and expenses for site selection as well as gives a digital archive for future site monitoring [11]. GIS can easily manage larger spatial data from various sources which makes it effective during site selection. Kao et al. [12] found that GIS can analyse large amounts of spatial data, thus saving time which would otherwise be spent choosing a suitable location.

While Daneshvar et al. [13] concluded that GIS is the ultimate preliminary tool for site selection since it efficiently stores, retrieves, analyses and shows user-defined specification details.

2 Study Area

Bihar Sharif: The municipal area of Bihar Sharif is approximately 23.50 km^2 and is located at latitude 25° 07′ N and longitude 85° 31′ E [14]. As headquarters of the district, it provides a population of over 28 lakhs including its own population of 296,889 [15]. Biharsharif generates an average of 50 MT of solid waste per day and collects this waste with the assistance of 200 Safai Karmachari [16]. The current productivity in collecting solid waste is only 32%, leading to city-wide garbage dumps [16]. The collected waste is neither isolated nor scientifically disposed of,

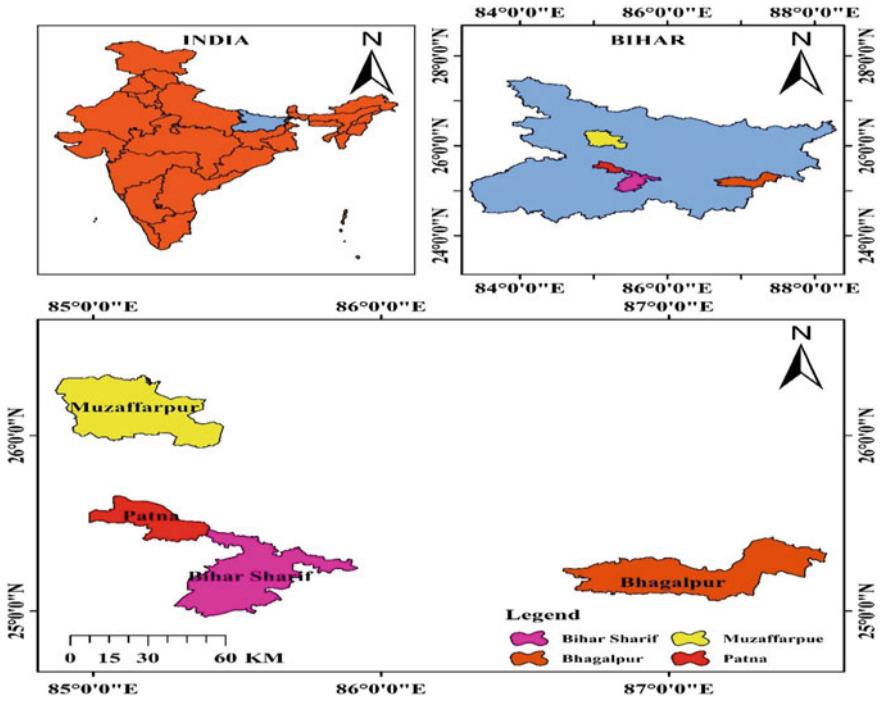

Fig. 1 Location map of study area

and all waste is discarded majorly in four open locations in the city [17]. Figure 1 shows the location map of the Biharsharif study area.

Patna: Patna is one of the country's oldest surviving towns. It is the state capital of Bihar and represents a flourishing centre of political, economic and educational activities in recent years. Located between 25° 30–26° 45′ N latitude and 85° 0–85° 15′ E longitude, it is on the southern bank of the Ganga River [18]. The western boundary of the Patna Urban Area is bounded by River Son [18]. The Hajipur and Sonepur urban areas are located on the northern banks of River Ganges. Its location is between Delhi and Kolkata, in the eastern part of India. The town has limited scope for geographical growth due to the presence of large perennial rivers on three sides. Patna has grown as a linear city as a result of this restriction, which has its bearings on municipal sanitation employments. Solid waste management is the corporation's overall responsibility according to Bihar Municipal Act 2007 and MSW (management and handling) rules 2000 [18]. Patna Municipal Corporation (PMC) is a mission city under the Government of India's Jawaharlal Nehru National Urban Renewal Mission (JNNURM) and smart cities. It is also eligible for grants under various schemes from the central/state government [18].

Muzaffarpur: Fig. 1 shows the location map of Muzaffarpur study area. Muzaffarpur Municipal Corporation, with a population of approximately 3.5 lakh, is the only municipal corporation in Musahri sub-district of Muzaffarpur district in Bihar

state, India. Muzaffarpur municipal corporation has a total geographical area of 26 km^2 [19]. City population density is 13,411 individuals per square kilometre. There are 49 wards in the district, among them Muzaffarpur Ward No 49 is the most populated ward with population of about 10,000 and Muzaffarpur Ward No 05 is the least populated ward with population of 5252 [19]. Muzaffarpur produces about 170 metric tons of waste every day, with approximately 300 g of per capita daily waste generation. The per capital waste production is between 600 and 800 g, according to CSE figures. Muzaffarpur is located in India in the city region with 26° 7′ 17.3028″ N and 85° 22′ 7.5072″ E gps coordinates [19].

Bhagalpur: Bhagalpur lies 220 km east of Patna and 410 km northwest of Kolkata. Geographically, it is located on the southern alluvial plains of River Ganga at 25° 15′ 0″ North latitude and 87° 0′ 0″ East longitude [20]. Through rail and road networks, Bhagalpur is well connected to the rest of the country. The town consists of 51 wards. The town's population as per Census 2001 was 3.40 lakhs. This was 14% of the district population. The average town population density is 113 people per hectare. Bhagalpur is the state's third-largest urban centre. Bhagalpur is estimated to generate about 225 tons of waste per day, of which 87% (196 tonnes) are collected [20]. The municipal corporation has implemented door-to-door collection and transportation in the last year, road sweeping and drain cleaning through a private operator in ten city wards. The organization has minimal solid waste management equipment—12 tractors, 1 JCB, 1 road roller and 220 carts. The garbage is not handled until disposal. The waste is actually deposited on vacant open spaces. The CDP is predicting that by 2030, Bhagalpur will produce 321,62 tons of garbage per day [20].

3 Methodology

Effective use of GIS depends on the appropriate quantity and quality of data accessibility, reflecting complex layers for reconstructing the applicable real-world conditions. The quality and consistency of the data will alter the probable results of any study done. Extensive effort needs to be made to regularly revise the required datasets which is to be used in GIS. This approach is further sub-divided in two sub-methodologies namely land use and land cover as well as site selection criteria with the help of GIS.

3.1 Land Use/Land Cover Map Creation

Figure 2 (A to D) indicates a subset of Landsat ETM^+ and Landsat-TM, acquired during February 1989, March 1999 and January 2009, respectively. Such photos help in creating maps of land use/cover and track urban expansion and related changes. The images were further georeferenced to a projection of Universal Transverse Mercator (UTM). One classification system was introduced using the classifier of maximum

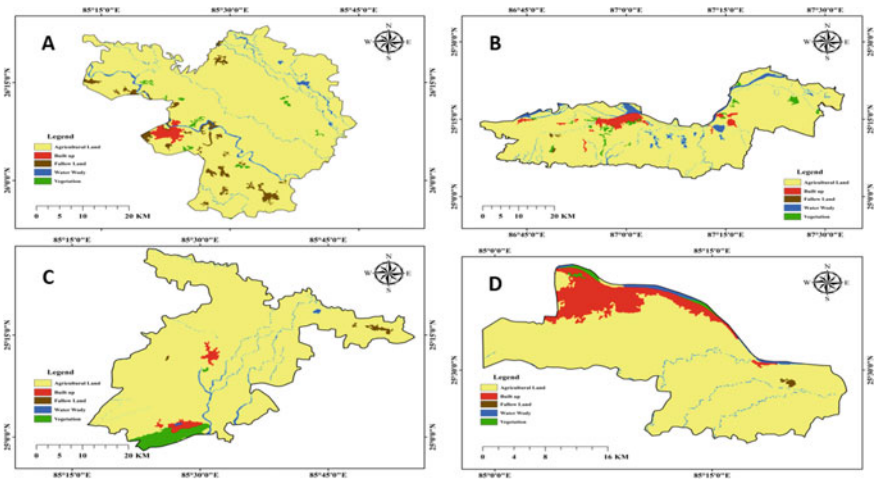

Fig. 2 LULC map of **a** Muzaffarpur. **b** Bhagalpur. **c** Biharsharif. **d** Patna

likelihood. Highest probability assumes that the statistics are normally distributed for each class in each category and estimate the possibility of a given pixel belongs to a particular class. The images obtained from Landsat were divided into three groups of land use and land cover patterns, namely urban, agricultural and bare ground. For every Landsat image, a minimum of 150 pixels were picked. These pixels were tested against topographic maps of 1:50,000 and 1:10,000 and with an understanding of in situ power.

3.2 Criteria of Site Selection Using WLC and GIS

Using the WLC model, a GIS-based MCE methodology explores various solutions for siting any problem, and various parameters and competing objectives are also taken into account. Data is processed in the GIS program to be used for site selection and is collected from different sources.

ArcGIS software package and its extensions were used for practical application of the WLC research. A weighted sum function is used by ArcGIS software, serves as an interpretation of the WLC. A weighed analysis includes the integration of several contributions to construct a combined analysis where it integrates multiple inputs that reflect numerous factors. It is one of the standard methods used in particular for the selection of sites suitable for disposing solid waste.

Here, the approach was used for site selection criteria, with some differences in the chosen parameters depending on the research area's local conditions [21]. This offers decision-makers with numerous choices regarding suitable landfill site locations as this approach, and the final production map can vary from "the most

appropriate" to "not suitable". All input data attributes had scores given. The scores reflect land constraints from 0 to 10 for sitting a landfill. 0 shows no limitation, while a score of 10 shows an overall limit. Such maps were usually given weights to reflect the relative significance. To make the performance map meaningful and accurate, the overall weight should be added up to 100%, and the values should be selected using such a system that remains similar for each map. These maps were not given equal importance in this analysis, as some of the considerations are more important in comparison with others while selecting sites for landfills. In addition, the value of each factor may vary on the basis of the prevailing conditions of one study area from that of another. So, the range of relative importance should be compatible with the research area's local conditions.

The standards in this analysis are based on measures used in U.S. EPA and other literature review [22]. This research used nine parameters for suitability which were the distance from urban areas, agricultural land, roads, aquifer media, streams and slopes. In compliance with a particular scheme, each requirement was reclassified, and then, rankings were issued based on that. A final composite map was then drawn up using WLC. In addition to the literature surveys done on the study area, the weights and scores were allocated after consulting local experts. Higher weights were given to factors that directly affect the environment, such as distance from urban areas, distance from agricultural land and distance from wells, while lower scores were given to the other factors that have lower impacts on the community or can be modified through engineering processes.

3.3 Distance from Urban Areas

As discussed in several studies that, the landfill site being chosen should not be too close to the urban settlements [23, 24]. Due to public issues such as aesthetics, odour, noise and health concerns, it is more suitable to construct it at a considerable distance from the urban areas. Using spatial analysis, buffer zones 1000 m away around urban areas were built. Baban and Flannagan [21] proposed that landfill sites should be within 10 km of an urban area. A distance lesser than 1000 m and greater than 10 km was given value of 10 [21]. This was allocated a high weight of 0.15 because it impacts the community directly, which should be given priority in the landfill site selection planning.

3.4 Distance from Agricultural Lands

In order to avoid declaring landfill sites in the agricultural areas, it is very crucial to determine the major boundaries of the agricultural fields [21]. Furthermore, it is not advised to position these sites near the agricultural lands, due to the odour and insects related issues, which can adversely affect farming activities. These lands were

mapped using the 1999 and 2009 Landsat photos [21]. Using GIS spatial analysis, a buffer of 500 m distance was generated around agricultural land after which a score of 10 was given at a distance less than 500 m and 0 for over 1000 m. This aspect has also been assigned a 0.15 which is very significant when identifying a landfill site [23, 24].

3.5 Distance from Roads

No particular rules are available for the identification of optimal distance to landfill site should be. Most research indicated that a 1 km buffer from the roads should be situated within the landfill site [21, 23]. Nonetheless, when determining a landfill site venue, makers prefer to give an aesthetic view a prior consideration. These sites should also not be located far away from roads. This in turn would reduce the transportation costs. A buffer was generated around the road network at specific distances using spatial analysis from GIS. Taking into account the enormous transport costs, it was decided to give a score in between 0 and 10. If the distance ranged from 200 to 1000 m, it would be given 0 score, while a score value of 10 would be assigned if it was more than 10 km and less than 200 m. This gives a weight of 0.1 because the engineers can change this factor depending on the project conditions [21].

4 Result and Discussion

The most suitable locations in this study included overlay operations, and the multi-criteria evaluation was identified by GIS analysis and operations. The following factors are taken for making final chart of suitability. These are type of land use or land cover, proximity to urban areas, distance from the surface waters, distance from the study area to transport road, geology and soil type.

4.1 Land Use or Land Cover Maps

Figure 2a–d shows land use and land cover maps by organizing the Landsat images of proposed smart cities. Figure 2a shows the land use or land cover map of Muzaffarpur. Over 10% is covered by urbanized area, while over 20% is bareland or vegetation, about 70% of the land cover is used for agriculture. Figure 2b shows the land use or land cover map of the Bhagalpur. Over 10% is covered by urbanized area and 10% covered by water body, while over 20% area is covered by bareland or vegetation, over 60% of the land cover is used for agriculture. Figure 2c shows the land use or land cover map of the Biharsharif study area. Over 10% area is covered by bareland or vegetation, while only about 20% is covered as urbanized area, over 70% of the

land cover is used for agriculture. Figure 2d shows the land use or land cover map of the Patna study area. Over 60% of the land cover use is for agriculture, while over 10% is covered by bareland or vegetation only about 30% is covered by urbanized area.

4.2 Landfill Site Selection

Figure 2a–d shows the land cover map within the study area which is suitable for the best possible solid waste disposal sites. For the landfill, two sites have been proposed. All belong to very high suitability category. The appearance of a dump from the villages was also taken into account. Given the weights, it can be inferred that the distance from the surface flows is an important criterion. Also, the distance from the road network, the height, slope and the length have a minimum weight because they do not have any significant impact on the environment but are taken into account as they measure the construction costs.

The conditions of the suggested alternative sites were checked by conducting a field survey. All the suggested sites were found to be suitable from environmental point. But, when public opinion was considered, there might be the need to consider more detailed investigation regarding hydrogeological, engineered as well as geotechnical points.

5 Conclusions and Recommendations

This study observed the issues of disposal sites in Bihar and their consequences for the town's residents. The study revealed that, over the years, Bihar has grown significantly in both population and spatial extent. As a result, the waste generation has gone up tremendously. These phenomena with some other factors have led to many urban issues including generation of waste. This research used digitized data layers using GIS consisting of minor roads, major roads, soil, streams, geology, land use or land cover and wards for find out the most suitable location of waste disposal site in the proposed smart cities of Bihar. GIS results showed that there are few suitable areas, and adequate sites have been selected under predefined parameters. All chosen sites are situated far from any areas of environmental significance, lakes, urban areas where population is strongly concentrated, thus reducing social tension and environmental impacts.

Rautiniya in Muzaffarpur and Ramachak-Bairiya in Patna are the most suitable sites, with significance of these given points, i.e. plain ground, close to the urbanized area, within the vegetative areas and also geologically appropriate. The suggestions were proposed for appropriate waste management and disposal systems to be implemented in the area. The planning and implementation of solid waste management should involve public awareness and participation. The Government should explore

various avenues such as media, school symposia, workshops and seminars. The involvement of private sector is not a panacea and hence Government should participate and follow policies that will help in encouraging private operators. GIS approach has proved to be a powerful tool in the field of site selection, waste disposal and enhance the process of siting. It is an important instrument for locating appropriate waste disposal sites.

References

1. Franco S, Mandla VR, Rao KRM (2017a) Urbanization, energy consumption and emissions in the Indian context: a review. Renew Sustain Energy Rev 71:898–907
2. Franco S, Mandla VR, Rao KRM (2017b) Trajectory of urban growth and its socioeconomic impact on a rapidly emerging megacity. J Urban Planning Dev 143(3)
3. Lellaa J, Mandlab VR, Zhuc X (2017) Solid waste collection/transport optimization and vegetation land cover estimation using geographic information system (GIS): a case study of a proposed smart-city. Sustain Cities Soc 35:336–349
4. Raghavan K, Mandla VR, Franco S (2015) Influence of urban areas on environment: special reference to building materials and temperature anomalies using geospatial technology. Sustain Cities Soc 19:349–358
5. Ghatak TK (2016) Municipal solid waste management in India: a few unaddressed issues. Procedia Soc Behav Sci 35:169–175
6. Rajput R, Prasad G, Chopra AK (2009) Scenario of solid waste management in present Indian context, Caspian. J Environ Sci 45–53
7. Urban solid waste management in Indian cities, PEARL, national institute of urban affairs (2015)
8. Church RL (2002) Geographical information systems and location science. Comput Oper Res 29(6):541–562
9. Murray A (2010) Advances in location modeling: GIS linkages and contributions. J Geogr Syst 12(3):335–354
10. Navalgund RR, Kasturirangan K (1983) The remote sensing satellite—a programme overview. In: Proceedings of the Indian academy of sciences section c: engineering sciences—remote sensing–III, 6, 313–336
11. Tomlison RF(1990) Current and potential uses of geographic information systems: the North American experience. In: Peuquet D, Marble D (eds) introductory readings in geographic information systems. Taylor and Francis, New York
12. Kao J, Chen W, Lin H, Guo S (1996) Network expert geographic information system for landfill siting. J Comput Civil Eng 122(10):307–317
13. Daneshvar R, Fernandes L, Warith M, Daneshfar B (2005) Customizing arcmap interface to generate a user- friendly landfill site selection GIS tool. J Solid Waste Technol Manag 31(1):1–12
14. Nalanda District, Bihar.com, last modified 2014. http://www.bihar.com/dist_nalanda.aspx
15. Directorate of census operations, Bihar, District census handbook- Nalanda, Series-11, Part XII-B, Patna, 13, 2011
16. Urban development and housing department government of bihar, City development plan (2010–30) Bihar Sharif: executive summary, Patna, 9, 2015
17. Tripathi KP, Birds fly away from dry Giddhi, the Telegraph, Wednesday, 24 Aug 2011. http://www.telegraphindia.com/1110824/jsp/bihar/story_14398436.jsp. Accessed on 3 Mar 2016
18. Pandey MK, Solid waste management Patna (2014) http://www.nswai.com/docs/swm%20patna%201.pdf

19. Decentralized solid waste management in Muzaffarpur, Bihar. https://www.cseindia.org/muzaffarpur-8962
20. City Development Plan (2010–30) Bhagalpur CDP prepared by: LEA associates south asia Pvt. Ltd., New Delhi, 2010
21. Baban SJ, Flannagan J (1998) Developing and implementing gis-assisted constraints criteria for planning landfill sites in the UK. Planning Pract Res 13(2):139–151
22. Epa US (1993) Solid waste disposal facility criteria, EPA530-R-93-017, US EPA. DC, Washington
23. Tagaris E, Sotiropoulou RE, Pilinis C, Halvadakis CP (2003) A methodology to estimate odors around landfill sites: the use of methane as an odor index and its utility in landfill siting. J Air Waste Manag Assoc 53(5):629–634
24. Chang NB, Parvathinathan G, Breeden JB (2008) Combining gis with fuzzy multicriteria decision- making for landfill siting in a fast-growing urban region. J Environ Manag 87(1):139–153

Eco-efficiency Tool for Urban Solid Waste Management System: A Case Study of Mumbai, India

Ekta Singh, Aman Kumar, Rahul Mishra, and Sunil Kumar

1 Introduction

The waste management sector contributes relatively less towards global greenhouse gas (GHG) emissions which were estimated to be about 3–5% of gross anthropogenic emissions in 2005 [1]. Although waste processing and recycling produce low emission levels, waste management such as the reuse of secondary contents or energy in all other sectors of the economy has prevented additional emissions [1]. Because of population growth, economic development, rapid urbanization and the local management of solid waste (MSWM), it has become one of the major challenge for India. The overall production of MSW is expected to rise to 165 million tonnes by the end of year 2031. Current stocks contain just 70–80% of MSW, of which 28% will be collected by towns and others will be discarded without additional treatment [2], which increases the risk for fires at landfill sites. As per the World Health Organization (WHO), 22 diseases are stated to decrease if MSW management in India is strengthened [2]. A recent study shows that 8% of Indian pollution is directly caused due to particulate matter (PM) which is added just by burning MSW [3].

While various governmental NGOs (e.g. OECD [4]; UN [5]) varied from the eco-efficiency concept, World Business Council for Sustainable Development (WBCSD) offered the most common interpretation which was that "Eco-efficiency is reached by the delivery of competitively priced goods and services that satisfy human needs and bring quality of life, while progressively reducing environmental impacts and resource intensity throughout the life cycle, to a level at least in line with the Earth's

E. Singh · A. Kumar · S. Kumar (✉)
CSIR-National Environmental and Engineering Research Institute (CSIR-NEERI), Nagpur 440020, India
e-mail: s_kumar@neeri.res.in

R. Mishra
Banaras Hindu University, Varanasi 221005, India

S. Kumar et al. (eds.), *Sustainability in Environmental Engineering and Science*, Lecture Notes in Civil Engineering 93,
https://doi.org/10.1007/978-981-15-6887-9_29

estimated carrying capacity" [6]. This can be defined as minimizing the output of solid waste at lower cost or a better added value in the region of waste management. Huppes et al. [7] suggested a mathematical model for estimation of eco-efficiencies. To measure this fraction, information of various units, for example financial and non-financial, has to be calculated. Nevertheless, the value added is showed up in financial units, whereas the impacts are primarily determined in physical units. At the theoretical and practical stage, many accounting methods are given to provide information required in relation to solid waste. Such approaches included tools for tracking and disclosing information regarding cost behind managing solid waste, potential liabilities and other relevant information. However, these approaches were heavily criticized.

Life cycle analysis accounting methods (LCAAMs) document details in physical units throughout the lifespan of the product. However, it should be noted that the methods are not uniform even in those situations where eco-efficiency is measured. There are some guidelines that give the structure for noting down both financial as well as non-financial data, and they do not undergo the general accepted accounting principles (GAAPs) reporting requirements. The paper seeks to provide an integrated approach for assessing the eco-efficiency of solid waste.

2 Study Area

The study area i.e. Mumbai (Maharashtra, India) currently produces around 9000 tons of municipal solid waste per day. Most collected MSW is transported within the city limits to one of three dumping grounds, namely Mulund, Deonar and Kanjurmarg. All of these have either reached their maximum capacity to collect garbage or are about to hit it soon. Consequently, the long-term handling of waste is also a major concern. Data related to Greater Mumbai city have been obtained from various sources. Based on 2011 census data, Greater Mumbai was estimated to be have a population of about 12.47 million. The overall annual growth rate was found to be 0.41% between year 2001 to 2011 [8]. In the current study, the available disposal options for the municipal solid waste were looked for the final 20 years (2016–2035). For these years, the overall increasing growth of population was considered to be stable at 0.41%. In Mumbai, the production rate of municipal solid waste per capita is 0.36 kg day^{-1} with an annual increment by 1.3% [9]. Since the efficiency of MSW collection for Mumbai is 90% [2], the total amount of collection was 4124 t day^{-1} for the year 2016. Figure 1 shows the location map of the study area.

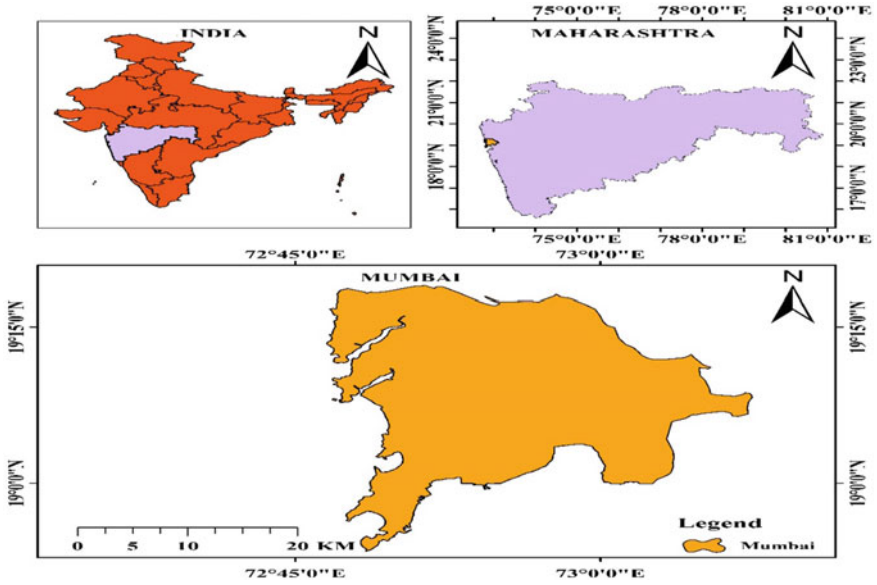

Fig. 1 Location map of study area

3 Conceptual LCA Model for Measuring Solid Waste Eco-efficiency Performance

This section of the paper indicates the description of key environmental measures applicable to the system, which consists of an environmental input and performance database [10]. All the data that have been used in this analysis were obtained from Gabi database 8.5.0.79. Figure 2 shows the process boundary that further separates into foreground system integrating emissions from treatment plants included during analysis, i.e. materials recovery facility, composting, anaerobic digestion and landfilling, and the context system incorporating energy, electricity and diesel requirements into the foreground system, as well as mineral fertilizer output.

3.1 Life Cycle Assessment (LCA)

LCA is a tool of environmental management utilized for the evaluation of any product, service or process at all stages of a material during its life cycle right from the procurement of raw material through extraction, production, delivery, usage, reuse or recycling, final waste management to its disposal [11].

LCA consists of four phases, i.e. target and scope description; analysis of resource; impact evaluation and interpretation, all of which have been consolidated into this study. Depending on its use, LCA has been a commonly established tool that can

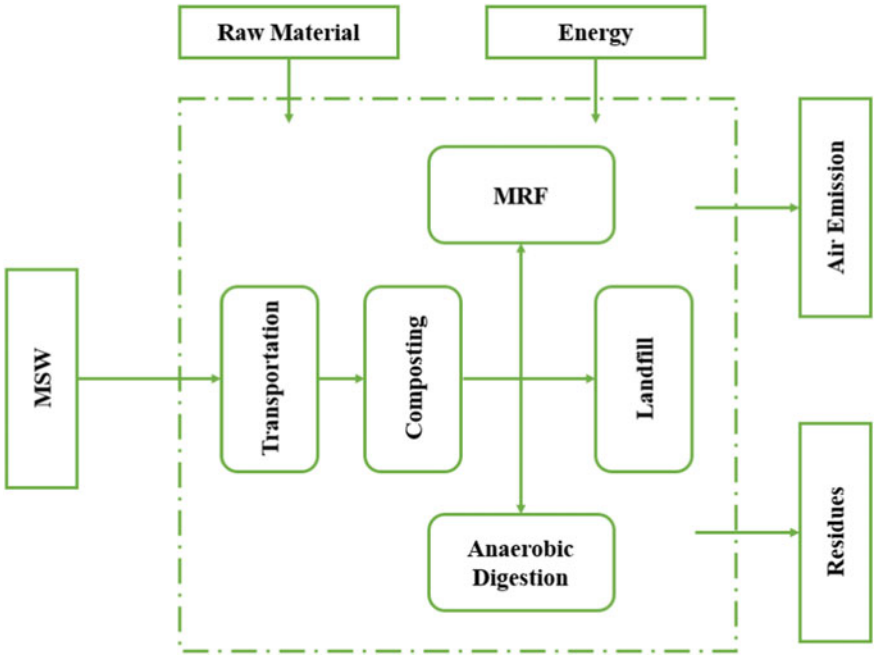

Fig. 2 System boundary of LCA study

allow for a fairer and more comprehensive environmental evaluation to determine the processes for waste management [12]. Throughout the process, LCA approaches the potential environmental impacts of whole life cycle of the waste.

3.2 Scenarios

Baseline scenario (BAU): The current MSW management practice in Mumbai is represented by Business as Usual (BAU). In Mumbai, approximately 31% of the total 9000 metric tons of MSW produced are handled using BLF and the remaining are dumped into open dumps (ODs).

Scenario 1 (SLF MRF): Conversion of open dumps into landfills would be the best solution in future. The scenario assumes that 30% of the materials are recovered by recycling, while the residual waste is disposed into sanitary landfill instead of the open disposal. The estimated levels of recycling are focused on recycling rate in Pune, India. The scenario also suggests that it would capture 60% of the biogas emitted from the landfill and then use biogas to generate electricity, and the remainder will escape in the atmosphere.

Scenario 2 (SLF MRF COM): The major focus of this scenario relies on biodegradation of Municipal Solid Waste. The scenario assumes that the MRF recovers 30%

of recycled materials and that 50% is COM, while the residual amount is finally disposed of in the sanitary landfills.

Scenario 3 (SLF MRF AD): This scenario indicates that 70% of the biodegradable waste is digested by anaerobic digestion (AD) and 30% of the recycled materials are treated rather than composting, while the remaining is landfilled. The biogas generated from these landfill sites is then used for the generation of electricity.

Scenario 4 (SLF MRF AD COM): Fourth scenario indicates that 30% of recycled materials are processed and that 40% of biodegradable materials are composted while the remaining 30% are anaerobically digested. Residual waste is then landfilled.

Scenario 5 (SLF MRF INC): This scenario combines composting, recycling and incineration, in which only 20% of biodegradable materials are composted and 30% of recycled materials are recycled while the remaining are finally incinerated.

Scenario 6 (MRF INC): The sixth scenario assumes recycling 30% of the waste and incinerating the remaining.

4 Results

All three compositions of solid waste collected were assessed for the environmental impacts, and the outcomes were found to be below 5%. When MSW is sent to landfill because of partial anaerobic conditions at the landfill, methane is emitted by the biodegradable portion. A large amount of phosphorous and nitrogenic compounds are also produced during this process. Yet due to the underlying landfill conditions, it is not possible to collect all the gases. A significant amount is thereby released to the atmosphere from landfill that contributes to global warming, human toxicity and acidification. A considerable reduction in environmental impacts is found while composting or anaerobic processing of biodegradable waste is treated and any other waste is transported to the landfill.

BAU scenario shows the highest eutrophication impact of 0.59 kg PO_4^{-3} eq t^{-1} due to the absence of a lining material in open dumps. Also, the release of high amounts of total N and P during the process is responsible for the arising situation.

Scenario 2: This scenario comprising of MRF COM SLF shows the lowest eutrophication of 0.00706 kg PO_4^{-3} eq t^{-1} because of the existence of impermeable plastic foundation as lining material in the landfills.

Scenario 3: This scenario comprising of MRF AD and SLF showed a eutrophication of 0.00917 kg PO_4^{-3} eq t^{-1} that was found to be more than Scenario 2 but lesser when compared to that of Scenario 1.

Scenario 4: The MRF COM AD SLF scenario showed an average eutrophication impact of 0.00792 kg PO_4^{-3} eq t^{-1} that was less than that of Scenario 1 and 3 but more than Scenario 2.

Various toxins such as SO_2, NO_x, PM, cadmium, mercury are responsible for human toxicity. The incineration scenario (MRF INC) resulted in maximum impact in human toxicity (719.90 kg 1,4-DB eq t^{-1}) due to SO_2 and NO_x, heavy metal, NH_3 emissions. Composting provides other advantages on condition of the combined

composting and incineration scenario (situation: MRF COM INC). Consequently, for exclusive incineration, the overall impact of this case is less than that.

The results show that the greatest pressures prevented are the situations based on incineration. Net emissions among all scenarios are low, as these scenarios generate considerably higher amount of energy than the other scenarios. The emissions prevented are large, considering that the power sector of India is largely dependent on coal. The overall influence of scenarios based on incineration on eutrophication and acidification is negative due to the large pollution avoided. Nevertheless, the impact of scenarios focused on incineration on human toxicity is considerably high in comparison with other scenarios based on biological processes. Mumbai currently produces around 9000 t daily of MSW [13]. It would contribute towards approximately 2.9 mt CO_2 eq y^{-1} global warming, 398 t SO_2 eq y^{-1} to acidification, 1618 t PO_4^{-3} eq y^{-1} to eutrophication, and 1390 t 1,4-DB eq y^{-1} to human toxicity [13]. In replacing the current system of accessible disposal with composting and sanitary landfilling, human toxicity could be cut down by almost 7%, global warming by 9% and eutrophication by 92%.

The recycling rates could have a significant impact on the pollution during the entire life cycle of management system for MSW. The effect of various rates of recycling on the life cycle emissions was also analysed for in this study. Products including pulp, fabric, leather materials and bottles are claimed to be recycled here. The recycling levels in this sample ranged from 10 to 90%. As the amount of recycling goes up, it is obvious that the potential environmental benefits would increase. There is a linear relationship between the environmental benefits and the recycling levels in subject to global warming. The trend lines differ in subject to eutrophication and acidification. This ensures that recycling of resources adds enormously to the environmental benefits.

4.1 Economic Analysis

Open dumping-based scenarios showed minimum anticipated cost (INR344 t^{-1}), as it included only MSW's land acquisition and transportation costs [14]. Furthermore, landfill and LFG recovery expenses were included in the SL LFG case, and for 1 t of MSW INR397 was more than that of OD. The expense of INR1023 t^{-1} to this situation was more than OD. The second lowest expense was for the CO SL scenario, and INR187 t^{-1} exceeds OD [14].

Mehta et al. [14] gave a detailed analysis for the cost of constructing a sanitary landfill including the operating costs and capital investment for each portion. A sanitary landfill received INR59 t^{-1} for a greater area of 241 ha. Landfill building and operating costs added 17% of the total expense, and Mehta et al. [14] calls for further separation of that expense into its subcomponents.

5 Conclusion

SWM strategies are extreme on the environmental sustainability agenda. Organizations have adopted many tools to cope with their waste output, such as solid waste minimization techniques and cleaner manufacturing practices. These methods aim to expand the organisation's production in solid waste eco-efficiency. Nevertheless, the robust application of these methods requires precise knowledge provided by environmental solid waste accounting methodologies. It provides an innovative and intangible outline for assessing the success of solid waste organisations in terms of eco-efficiency. This approach is important for trustworthy and reliable estimation of the effects of eco-efficiency, as well as for achieving certain accounting characteristics. The paper would further help connect solid waste accounting methods to eco-efficiency indicators, which illustrate the importance of knowledge on financial and non-financial success assessment.

References

1. UNEP (United Nations Environment Programme) (2010) Waste and climate change: global trends and strategy framework. http://www.unep.or.jp/ietc/Publications/spc/Waste&ClimateChange/Waste&ClimateChange
2. Commission Planning (2014) Report of the task force on waste to energy, vol 1. New Delhi, Government of India
3. Nagpure AS, Ramaswami A, Russell A (2015) Characterizing the spatial and temporal patterns of open burning of Municipal Solid Waste (MSW) in Indian cities. Environ Sci Technol 49(21):12904–12912
4. OECD eco-efficiency (1998) Organisation for Economic Co-operation and Development, Paris
5. UN (2003) A manual for the preparers and users of eco-efficiency indicators. United Nations Publication UNCTAD/ITE/IPC/2003/7, Prepared by Andreas Strum, Kaspar Muller and Suji Upasena
6. DeSimone LD, Popoff F (2000) Eco-efficiency: the business link to sustainable development. MIT Press, Cambridge, MA
7. Huppes G, Dardson MD, Kuyper J, Van Oers L, Udo de Haes HA, Warringa G (2007) Eco-efficient environmental policy in oil and gas production in the Netherlands. Ecol Econ 61:43–51
8. Bhagat RB, Jones GW (2013) Population change and migration in Mumbai metropolitan region: implications for planning and governance. Working paper series no 201, Asia Research Institute, National University of Singapore, Singapore
9. Narain S, Sambyal SS (2016) Not in my backyard: solid waste management in Indian cities. Centre for Science and Environment (CSE), New Delhi
10. Song Q, Wang Z, Li J (2013) Environmental performance of municipal solid waste strategies based on LCA method: a case study of Macau. J Clean Prod 57:92–100
11. Rajaeifar MA, Tabatabaei M, Ghanavati H, Khoshnevisan B, Rafiee S (2015) Comparative life cycle assessment of different municipal solid waste management scenarios in Iran. Renew Sustain Energy Rev 51:886–898
12. Edwards J, Othman M, Crossin E, Burn S (2017) Life cycle assessment to compare the environmental impact of seven contemporary food waste management systems. Bioresour Technol

13. Maharashtra Pollution Control Board (2013) Maharashtra Pollution Control Board annual report on implementation of municipal solid waste (management & handling) rules, 2000
14. Mehta Y, Joseph B, Shastri Y (2018) Economic analysis and life cycle impact assessment of Municipal Solid Waste (MSW) disposal: a case study of Mumbai, India: supplementary information